ΕΘΝΙΚΟ ΜΕΤΣΟΒΙΟ ΠΟΛΥΤΕΧΝΕΙΟ

ΣΧΟΛΗ ΕΦΑΡΜΟΣΜΕΝΩΝ ΜΑΘΗΜΑΤΙΚΩΝ & ΦΥΣΙΚΩΝ ΕΠΙΣΤΗΜΩΝ

ΤΟΜΕΑΣ ΜΗΧΑΝΙΚΗΣ

ΔΙΔΑΚΤΟΡΙΚΗ ΔΙΑΤΡΙΒΗ

«Αριθμητική Μοντελοποίηση, Πειραματική Μελέτη και Πρόβλεψη της Αντοχής των Αεροκατασκευών από Σύνθετα Υλικά»

«Numerical Modelling, Testing and Strength Prediction of Composite Material Airframe Structures»

Ιωάννης Κ. Γιαννόπουλος

Επιβλέπων: Ευστάθιος Ε. Θεοτόκογλου, Καθηγητής Ε.Μ.Π.

Αθήνα, 2016

ΕΘΝΙΚΟ ΜΕΤΣΟΒΙΟ ΠΟΛΥΤΕΧΝΕΙΟ

ΣΧΟΛΗ ΕΦΑΡΜΟΣΜΕΝΩΝ ΜΑΘΗΜΑΤΙΚΩΝ & ΦΥΣΙΚΩΝ ΕΠΙΣΤΗΜΩΝ

ΤΟΜΕΑΣ ΜΗΧΑΝΙΚΗΣ

ΔΙΔΑΚΤΟΡΙΚΗ ΔΙΑΤΡΙΒΗ

«Αριθμητική Μοντελοποίηση, Πειραματική Μελέτη και Πρόβλεψη της Αντοχής των Αεροκατασκευών από Σύνθετα Υλικά»

«Numerical Modelling, Testing and Strength Prediction of Composite Material Airframe Structures»

Ιωάννης Κ. Γιαννόπουλος

Η Εξεταστική Επιτροπή

Θεοτόκογλου Ευστάθιος Ε.	**Κοντού – Δρούγκα Ευαγγελία**	**Σπαθής Γεράσιμος**
Καθηγητής ΕΜΠ	*Καθηγήτρια ΕΜΠ*	*Καθηγητής ΕΜΠ*
(Επιβλέπων)	*(Μέλος Τριμελούς Συμβουλευτικής Επιτροπής)*	*(Μέλος Τριμελούς Συμβουλευτικής Επιτροπής)*

Κυτόπουλος Βίκτωρ	**Μανωλάκος Δημήτριος**	**Προβατίδης Χριστόφορος**	**Smith Howard**
Αν. Καθηγητής ΕΜΠ	*Καθηγητής ΕΜΠ*	*Καθηγητής ΕΜΠ*	*Professor Cranfield University*

Αθήνα, 2016

<*Page intentionally left blank* >

Στις οικογένειες μας που μας στηρίζουν,
στην γυναίκα μου που με υπομένει,
στην κόρη μου που με περιμένει,
στην μητέρα μου που με καθοδηγεί,
στον πατέρα μου που θα χαρεί,
στην αδερφή που μεγαλώσαμε μαζί
και στην άλλη την μικρή

Ευχαριστίες

Με την ολοκλήρωση της παρούσας διδακτορικής διατριβής, θα ήθελα να ευχαριστήσω θερμά τον επιβλέποντα καθηγητή μου κύριο Ευστάθιο Θεοτόκογλου, που ανέλαβε την υποχρέωση και τα καθήκοντα του επιβλέποντα, για την βοήθεια του στους τομείς της διεξαγωγής της διατριβής και ειδικότερα στο κομμάτι που έλαβε χώρα στο εξωτερικό καθώς και για τον τρόπο με τον οποίο βοήθησε στην μετεξέλιξή μου από μηχανικό σε ερευνητή. Θα ήθελα επίσης να ευχαριστήσω θερμά τα μέλη της τριμελούς επιτροπής κύριο Σπαθή Γεράσιμο και κυρία Κοντού-Δρούγκα Ευαγγελία για την εποικοδομητική συνεργασία μας. Τέλος, θα ήθελα να ευχαριστήσω και τον καθηγητή κύριο Τσαμασφύρο Γεώργιο και τα υπόλοιπα μέλη της επιτροπής επιλογής υποψήφιων διδακτόρων, που μου έδωσαν την ευκαιρία να εγγραφώ στο μεταπτυχιακό πρόγραμμα σπουδών και να καταφέρω με αυτόν τον τρόπο να διεκδικήσω τον τίτλο του διδάκτορα Ε.Μ.Π.

Περίληψη

Το αντικείμενο της διατριβής αφορά στην α) επισκόπηση και κριτική αξιολόγηση της εφαρμογής της μεθόδου των πεπερασμένων στοιχείων (ΠΣ) στην πρόβλεψη της αντοχής των αεροκατασκεών από σύνθετα υλικά, β) στην διερεύνηση της ωριμότητας των αριθμητικών εφαρμογών με ΠΣ στην πιστοποίηση της Αξιοπλοϊας των αεροκατασκευών και γ) στην πρόβλεψη μελλοντικών τάσεων στην περαιτέρω εφαρμογή της μεθόδου των ΠΣ στον τομέα των αεροκατασκευών. Η επισκόπηση λαμβάνει χώρα μέσω επιλεγμένων και αντιπροσωπευτικών αριθμητικών και πειραματικών μελετών των οποίων η κλίμακα μοντελοποίησης κυμαίνεται από μεγάλα συναρμολογήματα έως την μικροκλίμακα των ινωδών σύνθετων πολυμερών υλικών.

Summary

The objective of the thesis is a) to provide with an overview and a critical evaluation in the application of the finite element analysis in the strength prediction of airframe structures made of composite materials, b) to explore the maturity in the application of finite element method to certification of airframe structures according to the relevant airworthiness regulations and c) to predict future trends in the further application of the finite element method in the airframe sector. The overview is performed through the presentation of representative numerical and testing examples at different modelling scales ranging from large structural assemblies, down to the micro scale level of fibre reinforced polymers.

Περιεχόμενα / Contents

Εισαγωγή ***και Σύνοψη Διατριβής***

Η παρούσα διδακτορική διατριβή με θέμα «Αριθμητική Μοντελοποίηση, Πειραματική Μελέτη και Πρόβλεψη Αντοχής Αεροκατασκευών από Σύνθετα Υλικά» παρουσιάζεται εντός του κυρίως σώματος της διατριβής και εν συνεχεία του παρόντος εισαγωγικού κεφαλαίου, στην Αγγλική γλώσσα. Οι λόγοι που οδήγησαν στην υποβολή της διατριβής στην Αγγλική είναι αφενός ότι ο υποψήφιος διδάκτορας διαμένει μόνιμα στο εξωτερικό, είναι μέλος του ακαδημαϊκού προσωπικού σε Πανεπιστήμιο του Ηνωμένου Βασιλείου της Αγγλίας (Cranfield University), αφετέρου για την εκπόνηση τμήματος της εργασίας υπήρξε συνεργασία και με καθηγητή του Πανεπιστημίου του Cranfield. Η υποβολή του κυρίως σώματος στην Αγγλική γλώσσα στοχεύει στην διευκόλυνση πρόσβασης της διατριβής από την διεθνή συναδελφική επιστημονική κοινότητα.

Η ερευνητική δραστηριότητα που έλαβε χώρα κατά την διάρκεια εκπόνησης της διδακτορικής μελέτης, αποτυπώθηκε μέσω δημοσιεύσεων, ανακοινώσεων και εργασιών σε διεθνή επιστημονικά περιοδικά του χώρου [1-6]. Η διατριβή αποτελείται από την συρραφή αυτών των εργασιών και την γεφύρωση των μέσω συζήτησης και επεξηγηματικών σχολιασμών.

Ακολουθεί η συνοπτική περιγραφή των κεφαλαίων στα Ελληνικά, η οποία έχει σαν σκοπό να παραθέσει συνοπτικά και να επεξηγήσει τον ρόλο των επιμέρους κεφαλαίων στην δημιουργία της συνολικής διδακτορικής διατριβής καθώς και στην ερευνητική δραστηριότητα που έλαβε χώρα σε καθεμία από τις θεματικές ενότητες που παρατίθενται εν συνεχεία. Εντός του κυρίως σώματος της διατριβής, παρατίθενται τα αποτελέσματα της έρευνας ανά κεφάλαιο, η σημασία αυτών και η σύγκριση τους με αποτελέσματα άλλων επιστημονικών εργασιών του χώρου. Σε συγκεκριμένες περιπτώσεις συζητούνται και οι επιπτώσεις των αποτελεσμάτων επί του σχεδιασμού των αεροκατασκευών.

Εισ.1) Εισαγωγή, σκοπός και αντικείμενο διατριβής

Το αντικείμενο και ο σκοπός της διατριβής αφορούν στην προσφορά στη γνώση και στην εξαγωγή συμπερασμάτων στους ακόλουθους τομείς:

- Στην αντοχή των αεροκατασκευών από πολυμερή ινώδη σύνθετα υλικά και στην πρόβλεψη αυτής μέσω αναλυτικών προσεγγίσεων, πειραματικών μελετών και αριθμητικών αναλύσεων. Οι αναλύσεις είναι βασισμένες στις πιο χαρακτηριστικές εφαρμογές του χώρου των αεροκατασκευών.

- Στην κριτική αξιολόγηση της εφαρμογής της αριθμητικής μεθόδου των πεπερασμένων στοιχείων (ΠΣ) ως προς την πρόβλεψη της αντοχής των αεροκατασκευών από σύνθετα υλικά και στην διερεύνηση της 'ωριμότητας' των αριθμητικών εφαρμογών με ΠΣ για την πιστοποίηση της Αξιοπλοΐας των αεροκατασκευών.

Η αξιολόγηση των μεθόδων για την πρόβλεψη της αντοχής λαμβάνει χώρα μέσω ***επιλεγμένων*** και ***αντιπροσωπευτικών*** αριθμητικών και πειραματικών μελετών των οποίων η κλίμακα μοντελοποίησης κυμαίνεται από μεγάλα δομικά συναρμολογήματα έως την μικροκλίμακα των ινωδών σύνθετων πολυμερών υλικών.

Επιγραμματικά, το περιεχόμενο των επιμέρους κεφαλαίων στο εισαγωγικό και στο κυρίως σώμα της διατριβής:

- Το πρώτο κεφάλαιο, παραθέτει το σκοπό και το αντικείμενο της διατριβής
- Στο δεύτερο κεφάλαιο, παρατίθενται ο ορισμός της Αξιοπλοΐας (Airworthiness) των αεροπορικών κατασκευών, όπως διατυπώνεται από τον Ευρωπαϊκό Οργανισμό Επιστασίας της Ασφάλειας πτήσεων (European Aviation Safety Authority - EASA) και της αντοχής αυτών μέσα από το πρίσμα των προδιαγραφών Αξιοπλοΐας
- Το τρίτο κεφάλαιο παρουσιάζει μελέτη επί της εφαρμογής των ΠΣ στο σχεδιασμό της συνδεσμολογίας διαφράγματος (bulkhead) της ουραίας ατράκτου (empenage) αεροσκάφους από σύνθετα υλικά. Η μελέτη συγκρίνεται με επιστημονική εργασία του χώρου, συσχετίζεται με σχετική αναφορά αεροπορικού ατυχήματος και επεξηγείται πρόταση για τον σχεδιαστικό ανασχεδιασμό της κατασκευής, ο οποίος έγινε αποδεκτός από εταιρία σχεδιασμού αεροπορικού υλικού (Alenia-Aermacchi)

- Στο τέταρτο κεφάλαιο περιγράφεται μελέτη διερεύνησης της απόκρισης και αντοχής λεπτότοιχου νευρωμένου κελύφους από σύνθετα υλικά υπό θλιπτικό φορτίο. Η μελέτη έλαβε χώρα με ΠΣ και τα αποτελέσματα εν συνεχεία συγκρίθηκαν με αποτελέσματα πειραματικής διάταξης
- Το πέμπτο κεφάλαιο παρουσιάζει το φαινόμενο της κρούσης ξένων σωματιδίων επί των κατασκευών από σύνθετα υλικά, μέσω πειραματικής μελέτης που έλαβε χώρα σε στρωσιγενείς πλάκες από σύνθετα υλικά
- Η θεματολογία του έκτου κεφαλαίου περιστρέφεται γύρω από τη μικρομηχανική των ινωδών συνθέτων υλικών και τον ρόλο αυτών στην πρόβλεψη της αντοχής των κατασκευών
- Το έβδομο κεφάλαιο συνοψίζει τα αποτελέσματα της διατριβής συνολικά και παραθέτει προτάσεις για την περαιτέρω έρευνα επί του αντικειμένου της πρόβλεψης της αντοχής των αεροκατασκευών από σύνθετα υλικά

Η ανάπτυξη της επιμέρους θεματολογίας αποτυπώνεται σχηματικά ανά κεφάλαιο στο σχήμα ε.1.

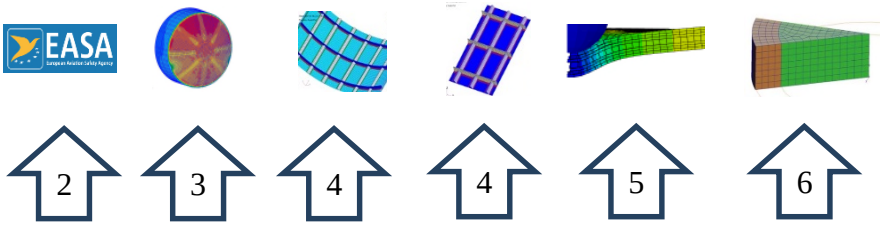

Σχήμα ε.1.1: Ανάπτυξη θεματολογίας ανά κεφάλαιο

Επίσης, η διατριβή προσπαθεί να συνεισφέρει στην:

- Πρόβλεψη των μελλοντικών τάσεων σε ότι αφορά την εφαρμογή της μεθόδου των ΠΣ στον τομέα της πρόβλεψης της αντοχής των αεροκατασκευών και της πιστοποίησης της Αξιοπλοΐας αυτών.

Στο σχήμα ε.1.2, αποτυπώνεται η σχέση των επιμέρους μελετών που παρουσιάζονται ανά κεφάλαιο, σε αντιπαράθεση με μια τυπική σειρά πειραματικών διατάξεων που απαιτούνται για την απόδειξη συμμόρφωσης με τα πρότυπα πιστοποίησης της αντοχής κατά EASA [7, 8].

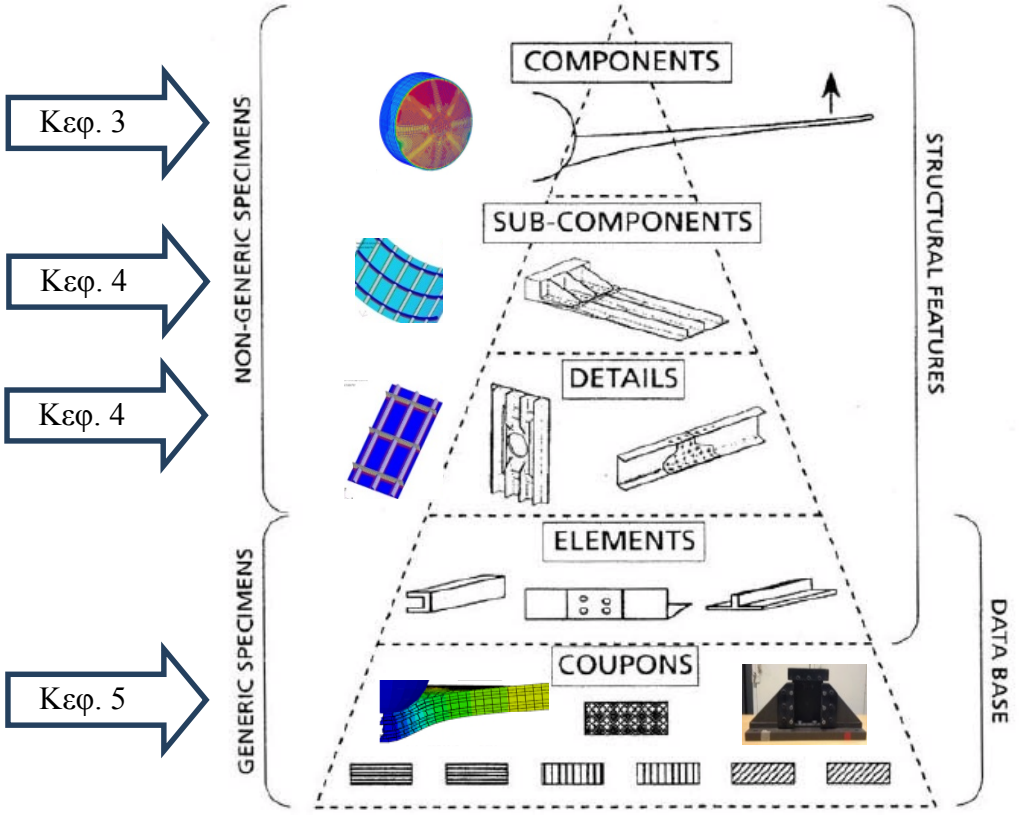

Σχήμαε.1.2: Πειραματικές δοκιμές για την πλήρωση των απαιτήσεων επίδειξης συμμόρφωσης της αντοχής των αεροκατασκευών από σύνθετα υλικά [8]

Το αντικείμενο που περιγράφεται από τον τίτλο της διατριβής αφορά σε ένα ευρύ γνωστικό φάσμα και δεν είναι εφικτή η αναφορά σε όλα τα επιμέρους εδάφια του φάσματος αυτού. Για τον λόγο αυτό, επί του αντικείμενου εφαρμόζονται περιορισμοί σε ότι αφορά την εξωτερική φόρτιση και την επακόλουθη απόκριση της κατασκευής, σε ότι αφορά τα υλικά αυτής, καθώς και στις αριθμητικές μεθόδους πρόβλεψης.

- Σχετικά με την εξωτερική φόρτιση, το αντικείμενο της διατριβής διερευνά στην απόκριση της κατασκευής υπό στατική φόρτιση και επακόλουθη στατική

απόκριση. Η αντοχή σε δυναμική φόρτιση εξετάζεται μερικώς ενώ η αντοχή σε φορτία κόπωσης δεν εξετάζεται στην παρούσα διατριβή.

- Σε σχέση με τα υλικά της κατασκευής, η διατριβή ενασχολείται με τα ινώδη πολυμερή που χρησιμοποιούνται στις αεροκατασκευές
- Επίσης, περιορισμοί εφαρμόζονται και επί του επιπέδου πολυπλοκότητας και ωριμότητας των αριθμητικών μεθόδων και αναλύσεων που λαμβάνουν χώρα για την επίδειξη των εφαρμογών στην πρόβλεψη αντοχής. Εντός της διατριβής γίνεται μόνο αναφορά σε αριθμητικά μοντέλα και μεθόδους επίλυσης προβλημάτων απί της αντοχής των κατασκευών τα οποία είναι ευρέως αποδεκτά ως προς τα αποτελέσματα που παράγουν και εφαρμόζονται στη βιομηχανία

Εισ.2) Ο ορισμός της αντοχής των αεροκατασκευών και οι προδιαγραφές Αξιοπλοΐας

Το δεύτερο κεφάλαιο της διατριβής αναφέρεται σε μια περιοχή εφαρμοσμένων πρακτικών γύρω από την *Αξιοπλοΐα* (Airworthiness) των αεροκατασκευών. Επεξηγήσεις ως προς τον ορισμό της Αξιοπλοΐας των αεροκατασκευών και ποιά η σχέση της με την παρούσα διατριβή αναφέρονται στις ακόλουθες παραγράφους, και αναπτύσσονται εκτενώς στο δεύτερο κεφάλαιο του κυρίως σώματος της διατριβής. Η έννοια της Αξιοπλοΐας και η εφαρμογή αυτής στις αεροκατασκευές είναι ο *ακρογωνιαίος λίθος* σε ότι αφορά την ασφάλεια αυτών και πιο συγκεκριμένα στην δομική αντοχή της κατασκευής, αντικείμενο το οποίο πραγματεύεται η παρούσα διατριβή.

Για την διερεύνηση των ιδιοτήτων των υλικών και πιο συγκεκριμένα των μηχανικών τους ιδιοτήτων, χρησιμοποιούνται πειραματικές διατάξεις και δοκιμές σε δοκίμια των υλικών αυτών. Για την πειραματική διερεύνηση και εξαγωγή των διαφόρων ιδιοτήτων έχουν συνταχθεί προδιαγραφές από διάφορους ανεξάρτητους οργανισμούς, όπως για παράδειγμα: ASTM –American Society for Testing and Materials, ISO –International Standardization Organization, DIN – Deutsches Institut für Normung και άλλους. Οι προδιαγραφές αυτές αποτυπώνουν τις καλύτερες πρακτικές σε όλο το φάσμα της διεξαγωγής των πειραματικών δοκιμών και της επακόλουθης εξαγωγής των ιδιοτήτων στις οποίες αναφέρονται. Η πληροφορία σχετικά με τις ιδιότητες και πιο συγκεκριμένα της αντοχής μεταλλικών ή συνθέτων υλικών που αποκομίζεται από μια πειραματική δοκιμή, *δεν είναι αρκετή* για τον ορισμό της αντοχής των αεροκατασκευών.

Οι προδιαγραφές Αξιοπλοΐας, σε μια προσπάθεια απλοϊκού ορισμού αυτών, είναι ένα σύνολο διατυπώσεων που αφορούν στην λειτουργία και την συμπεριφορά των αεροσκαφών κατά την διάρκεια της ζωής αυτών, η συμμόρφωση με τις οποίες πρέπει να αποδειχθεί σε ανεξάρτητους φορείς/οργανισμούς από αυτούς που σχεδίασαν, κατασκεύασαν, λειτουργούν και συντηρούν την αεροκατασκευή. Οι ανεξάρτητοι φορείς αυτοί, είναι υπεύθυνοι για την ασφάλεια των αεροσκαφών και γενικότερα με ότι

σχετίζεται με την ασφάλεια πτήσεων. Στη Ευρώπη, αυτός ο οργανισμός είναι η EASA (European Aviation Safety Authority). Συνοπτικά:

- Η EASA είναι ο υπεύθυνος οργανισμός επιστασίας της διαχείρισης της ασφάλειας της αεροπλοΐας του πολιτικού νηολογίου. Η απόδειξη της Αξιοπλοΐας των αεροκατασκευών γίνεται βάσει προδιαγραφών πιστοποίησης από την EASA (στην Ευρώπη).

- Οι αεροκατασκευές πρέπει να αποδείξουν συμμόρφωση με τις προδιαγραφές Αξιοπλοΐας. Στην περίπτωση των αεροκατασκευών, μερικές από τις απαιτήσεις σχετίζονται με την αντοχή σε στατική φόρτιση.

- Η απόδειξη συμμόρφωσης των αεροκατασκευών με τις προδιαγραφές Αξιοπλοΐας μπορεί να επιτευχθεί είτε με πειραματικές δοκιμές, είτε με αναλυτικούς / αριθμητικούς υπολογισμούς είτε με συνδυασμό και των δύο μεθόδων.

Οι προδιαγραφές αξιοπλοΐας δεν προϋπήρξαν/προπορεύθηκαν των πρώτων προσπαθειών του ανθρώπου για πτήση με πτητικές μηχανές. Δημιουργήθηκαν σαν αποτέλεσμα της εμπειρίας και των πειραματισμών επί των πτητικών μηχανών με σκοπό να προλαμβάνουν πιθανά ατυχήματα κατά την λειτουργία των. Μπορεί να υποτεθεί ότι οι προδιαγραφές της αξιοπλοΐας είναι *η κληρονομία* των επί σειρά ετών εφαρμογής ορθών σχεδιαστικών πρακτικών. Σε παγκόσμιο επίπεδο, υπάρχει η τάση ενοποίησης αυτών των προδιαγραφών ασφαλείας. Στην παρούσα διατριβή, χρησιμοποιούνται οι προδιαγραφές πιστοποίησης κατά EASA CS-25 [7].

Στο δεύτερο κεφάλαιο του κυρίως σώματος της διατριβής (Chapter 2), αναφέρεται η διατύπωση της αντοχής των αεροκατασκευών όπως αυτή έχει αναπτυχθεί μέσα από χρόνια σχεδιασμού και διερεύνησης αστοχιών κατά την λειτουργία των πτητικών μηχανών και σαν αποτέλεσμα διασφάλισης έναντι αεροπορικών ατυχημάτων που έλαβαν χώρα στο παρελθόν.

Οι σημαντικές παράμετροι για την διατύπωση της αντοχής των αεροκατασκευών σε στατική φόρτιση είναι ο ορισμός της οριακής φόρτισης, ο ορισμός της μέγιστης φόρτισης μαζί με τον αντίστοιχο συντελεστή ασφαλείας και ο ορισμός της αποδεκτής κατάστασης των υλικών και της κατασκευής εν γένει υπό την στατική φόρτιση σε

οριακό ή μέγιστο επίπεδο. Κάτωθι, παρατίθενται επιγραμματικά, ο ορισμός της αντοχής των αεροκατασκευών μέσα από τις προδιαγραφές πιστοποίησης, ανά εδάφιο εντός των προδιαγραφών κατά EASA CS-25 [7]:

- Εδάφιο CS-25.301: Οριακή φόρτιση, είναι η φόρτιση με την οποία θα φορτιστεί η κατασκευή κατά την διάρκεια της λειτουργίας/ζωής της.
- Εδάφιο CS-25.303: Μέγιστη φόρτιση, είναι η οριακή φόρτιση πολλαπλασιασμένη με συντελεστή ασφαλείας ίσο με 1.5.
- Εδάφιο CS-25.305: Η αεροκατασκευή πρέπει να υποστηρίξει την οριακή στατικώς επιβαλλόμενη φόρτιση χωρίς να επιδείξει ***επιβλαβή μόνιμη παραμόρφωση***. Επίσης πρέπει να αντέξει την μέγιστη, στατικώς επιβαλλόμενη φόρτιση χωρίς να ***αστοχήσει καθολικά.***
- Εδάφιο CS-25.307: Συμμόρφωση με τα παραπάνω αναφερόμενα εδάφια, πρέπει να αποδειχθεί με πειραματικές δοκιμές ή με αναλυτικές / αριθμητικές μεθόδους και υποστήριξη / συσχέτιση αυτών με αποτελέσματα από πειραματικές δοκιμές.

Οι απαιτήσεις για την πιστοποίηση των αεροκατασκευών μπορούν σε ορισμένες περιπτώσεις να εκπληρωθούν από αναλυτικές / αριθμητικές μεθόδους πρόβλεψης της αντοχής. Τα χαρακτηριστικά των μεθόδων για την απόδειξη της αντοχής σύμφωνα με τις απαιτήσεις πιστοποίησης είναι η αποδεδειγμένη εμπειρία στην εφαρμογή και στα αποτελέσματα των μεθόδων αυτών. Οι αναλυτικές/αριθμητικές μέθοδοι για την απόδειξη της αντοχής των αεροκατασκευών έχουν σαν στόχο:

- Την μείωση των απαιτήσεων των προδιαγραφών σε πειραματικές δοκιμές.
- Την διεξαγωγή παραμετρικών μελετών χωρίς ιδιαίτερο κόστος.
- Την εκτίμηση της αντοχής των αεροκατασκευών εν ενεργεία, που υπέστησαν ζημιά.

Η έννοια της Αξιοπλοΐας, οι προδιαγραφές και η εφαρμογή αυτών στις αεροκατασκευές είναι θεμελιώδης και διαδραματίζει πρωταρχικό ρόλο στην επιχειρηματολογία εντός της διατριβής. Τα βασικά σημεία του πρώτου κεφαλαίου αναφέρονται κάτωθι επιγραμματικά:

- Εντός των προδιαγραφών πιστοποίησης, βρίσκεται ο σαφής ορισμός της αντοχής των αεροκατασκευών και η μετάφραση αυτού στην γλώσσα των αεροκατασκευών.
- Οι προδιαγραφές της αξιοπλοΐας είναι το ‘αποτύπωμα’ της συσσωρευμένης γνώσης γύρω από την ασφάλεια των αεροκατασκευών, γνώση η οποία έχει δημιουργηθεί κατά κύριο λόγο από την εφαρμογή υλικών διαφορετικών των ινωδών πολυμερών.
- Υπάρχουν αναλυτικές/αριθμητικές μέθοδοι που συμβάλλουν στην πρόβλεψη αντοχής οι οποίες έχουν χαρακτηριστεί αξιόπιστες. Με την εισαγωγή νέων υλικών στον κύκλο ζωής των αεροκατασκευών, οι μέθοδοι πρέπει να επανεξετάζονται ως προς την αξιοπιστία τους.

Εισ.3) Η εφαρμογή των μεθόδων καθολικής/ τοπικής μοντελοποίησης με ΠΣ στις αεροκατασκευές από σύνθετα υλικά

Το τρίτο κεφάλαιο της διατριβής αφορά στις πιο κλασσικές εφαρμογές της μεθόδου των πεπερασμένων στοιχείων (ΠΣ) αεροκατασκευές οι οποίες συμβάλλουν στην διαδικασία πρόβλεψης της αντοχής. Οι μέθοδοι αυτές αφορούν στην αναγωγή της εξωτερικής φόρτισης της κατασκευής στην επιμέρους φόρτιση των απαρτίων αυτής (καθολική μοντελοποίηση με ΠΣ = global FE modelling) και στην αριθμητική προσέγγιση του πεδίου τάσεων της κατασκευής (τοπική μοντελοποίηση με ΠΣ = local FE modelling).

Η καθολική μοντελοποίηση με ΠΣ (global FE modelling) χρησιμοποιείται ευρέως στον κλάδο των αεροκατασκευών. Με τον όρο 'καθολική' εννοείται η μοντελοποίηση της δομής του αεροσκάφους συνολικά. Το καθολικό μοντέλο της αεροκατασκευής υπόκειται στην εξωτερική φόρτιση η οποία απαρτίζεται από τα συνολικά αεροδυναμικά φορτία πτήσης και τα αδρανειακά λόγω ελιγμών. Το μοντέλο χρησιμοποιείται για την αναγωγή της εξωτερικής φόρτισης σε εσωτερική δηλαδή στον επιμερισμό των εξωτερικών φορτίων εσωτερικά στα επιμέρους δομικά τμήματα της κατασκευής. Ουσιαστικά το αριθμητικό μοντέλο αφορά στην επίλυση ενός αόριστου στατικού προβλήματος. Τα αποτελέσματα που επιζητούνται κατά την επίλυση ενός καθολικού μοντέλου είναι η εσωτερική φόρτιση στους κόμβους των στοιχείων του αριθμητικού πλέγματος με την μορφή δυνάμεων και ροπών και όχι με την μορφή τάσεων ή τροπών στους κόμβους ή στα στοιχεία. Εν συνεχεία, η κατανεμημένη εσωτερική φόρτιση στα επιμέρους τμήματα θα τροφοδοτηθεί σε αναλυτικές μεθόδους και πρακτικές για τις οποίες έχει αποδειχθεί, βάσει εμπειρίας και πειραματικών δοκιμών, ότι περιγράφουν ικανοποιητικά την επιμέρους δομική φόρτιση και παράγουν συντηρητικά αποτελέσματα έναντι της δομικής αστοχίας.

Ο στόχος της καθολικής μοντελοποίησης είναι να μοντελοποιήσει την απόκριση της κατασκευής στο σύνολό της και λόγω του μεγέθους αυτής, η προσπάθεια επικεντρώνεται στην δημιουργία ενός αριθμητικού μοντέλου με τις λιγότερες δυνατές υπολογιστικές απαιτήσεις. Τα στοιχεία που χρησιμοποιούνται στην πράξη είναι γραμμικά για την συρρίκνωση του υπολογιστικού κόστους. Για αυτόν τον λόγο, η

αποτύπωση του πεδίου των τάσεων δεν είναι ακριβής. Παράδειγμα καθολικού μοντέλου με ΠΣ παρατίθεται κάτωθι, στο σχήμα ε.3.1:

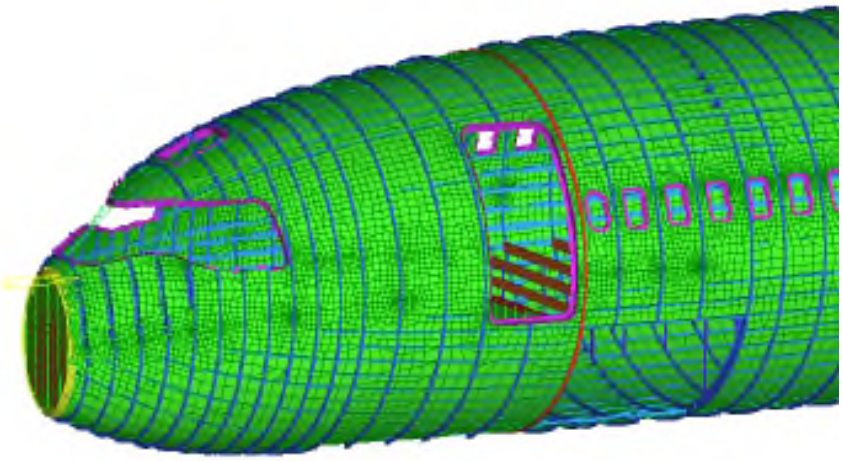

Σχήμα ε.3.1: Παράδειγμα αριθμητικού μοντέλου πεπερασμένων στοιχείων καθολικής μοντελοποίησης

Η τοπική μοντελοποίηση με πεπερασμένα στοιχεία (local FE modelling) χρησιμοποιείται όταν επιζητείται η επίλυση του πεδίου των τάσεων / τροπών. Όταν χρησιμοποιείται η μέθοδος της τοπικής μοντελοποίησης υπάρχει η δυνατότητα ορθής αποτύπωσης του πεδίου των τάσεων της κατασκευής με την εφαρμογή περισσότερων στοιχείων ανά περιοχή ή στοιχείων με πιο μεγάλο βαθμό συνάρτησης σχήματος επί των στοιχείων. Οι αναλύσεις αυτές δεν μπορούν να εφαρμοστούν για την μοντελοποίηση της απόκρισης της κατασκευής συνολικά λόγω αδυναμίας υπολογιστικής ισχύος και μεγάλου υπολογιστικού κόστους. Στην πράξη, εφαρμόζονται σε συγκεκριμένα σημεία της κατασκευής για τα οποία επιβάλλεται η συλλογή πληροφοριών γύρω από το πεδίο των τάσεων.

Ο αριθμός και το είδος των στοιχείων που χρησιμοποιούνται σε ένα μοντέλο, εξαρτάται από τον ρυθμό μεταβολής του πεδίου των μετατοπίσεων που επιλύεται. Στο σχήμα ε.3.2, επιδεικνύεται η αναγωγή μοντέλου πεπερασμένων στοιχείων σε μοντέλο με περισσότερα αριθμητικά στοιχεία, πράξη η οποία οδηγεί αυτόματα στην

μοντελοποίηση ενός μόνο τομέα της αρχικής κατασκευής για τον περιορισμό του υπολογιστικού κόστους.

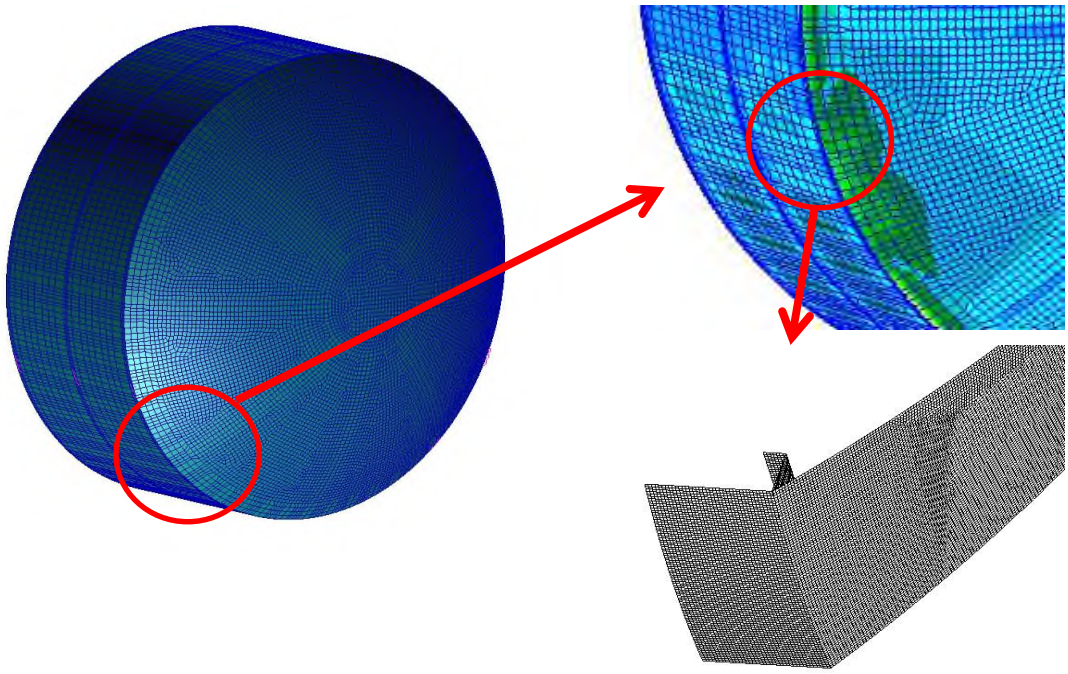

Σχήμα ε.3.2: Παράδειγμα μοντέλων πεπερασμένων στοιχείων τοπικής μοντελοποίησης διαφόρων επιπέδων. Μετάβαση από ένα τοπικό μοντέλο διαφράγματος (bulkhead) ουραίας ατράκτου (empennage) αεροσκάφους, σε μοντέλο με πύκνωση του αριθμητικού πλέγματος ικανής για την ορθή αποτύπωση του πεδίου των τάσεων

Η μέθοδος της καθολικής/τοπικής μοντελοποίησης ανήκει στην ομάδα των υπολογιστικών μεθόδων οι οποίες έχουν θεωρηθεί ότι παράγουν ικανοποιητικά αποτελέσματα. Το αντικείμενο που πραγματεύεται το τρίτο κεφάλαιο της διατριβής σχετίζεται με την τοπική μοντελοποίηση της σύνδεσης του διαφράγματος της ουραίας ατράκτου με την άτρακτο του αεροσκάφους, βλέπε σχήμα ε.3.3. Περιγράφει το σφάλμα που δημιουργείται στην επίλυση του τασικού πεδίου της εν λόγω περιοχής χρησιμοποιώντας την μέθοδο τοπικής μοντελοποίησης και εξηγεί γιατί αυτό το σφάλμα είναι πιο σοβαρό στην περίπτωση κατασκευών από σύνθετα υλικά.

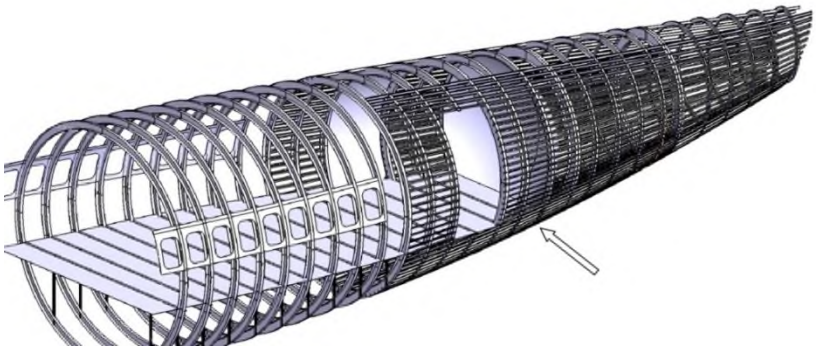

Σχήμα ε.3.3: Η εφαρμογή της τοπικής μοντελοποίησης της κατασκευής του συνδέσμου του διαφράγματος με την άτρακτο, ως το κυρίως θέμα του τρίτου κεφαλαίου [1]

Το πεδίο των τάσεων στην εγγύς περιοχή του συνδέσμου του διαφράγματος στην ουραία άτρακτο, μεταβάλλεται σημαντικά. Ο σκοπός της μοντελοποίησης με ΠΣ είναι να γίνει σωστή επιλογή του μεγέθους και του είδους των ΠΣ έτσι ώστε τα μεγέθη του πεδίου που μεταβάλλονται να επιλυθούν σωστά. Στο σχήμα ε.3.4, παρατίθεται σχηματικά παράσταση της παραμόρφωσης του διαφράγματος υπό εσωτερική πίεση, η οποία υποδεικνύει την μεταβολή στην εσωτερική φόρτιση της κατασκευής.

.

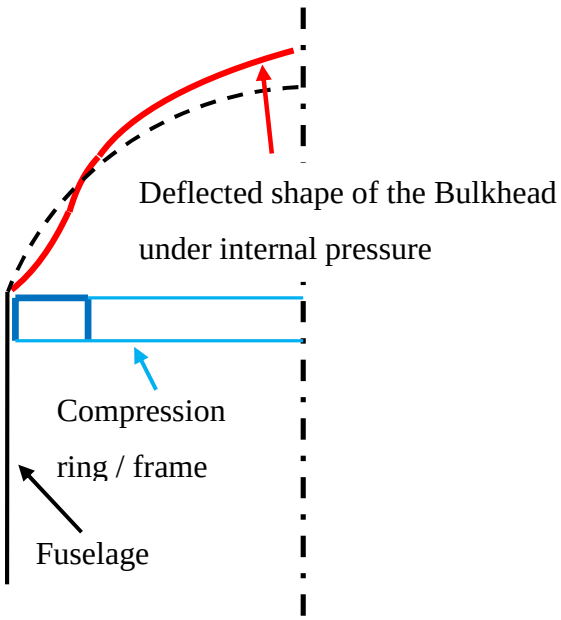

Σχήμα ε.3.4: Παραμόρφωση του διαφράγματος σε συνθήκες εσωτερικής πίεσης [1]

Η καθολική μοντελοποίηση δεν μπορεί να παραστήσει ικανοποιητικά το πεδίο των τάσεων στην περιοχή της συνδεσμολογίας. Πειραματισμοί με την τοπική πύκνωση του αριθμητικού πλέγματος, βλέπε σχήμα ε.3.5, και σύγκριση με την λύση από αναλυτικές μεθόδους έλαβε χώρα.

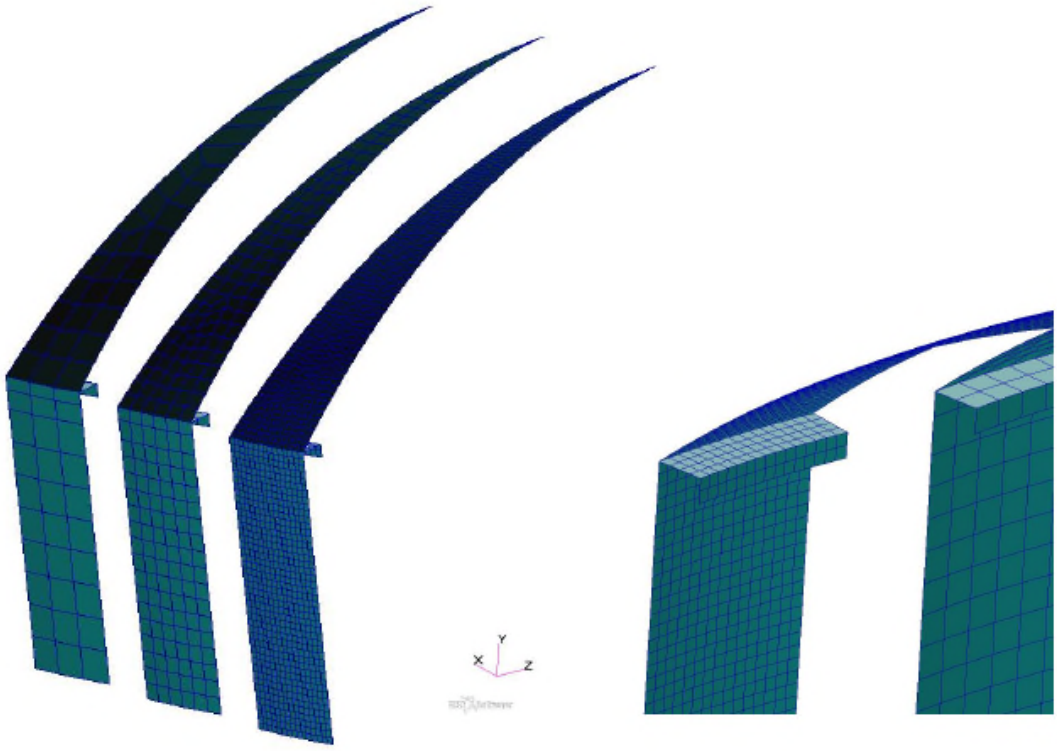

Σχήμα ε.3.5: Τοπική πύκνωση του αριθμητικού πλέγματος για την διερεύνηση του σφάλματος της αριθμητικής λύσης σχετικά με αντίστοιχες αναλυτικής μορφής

Η μελέτη τοπικής πύκνωση του πλέγματος των ΠΣ, οδήγησε στην δημιουργία του μοντέλου που απεικονίζεται στο σχήμα ε.3.6. Στο σχήμα ε.3.7 διευκρινίζονται οι δυνάμεις και οι ροπές ανά μοναδιαίο μήκος που επιζητούνται και στο σχήμα ε.3.8 αποτυπώνεται η λύση με τη μορφή διαγραμμάτων των δυνάμεων και ροπών από το σημείο τομής του σφαιρικού διαφράγματος με την κυλινδρική άτρακτο έως 300mm προς τον άξονα της κατασκευής (βλέπε σχήμα ε.3.6)

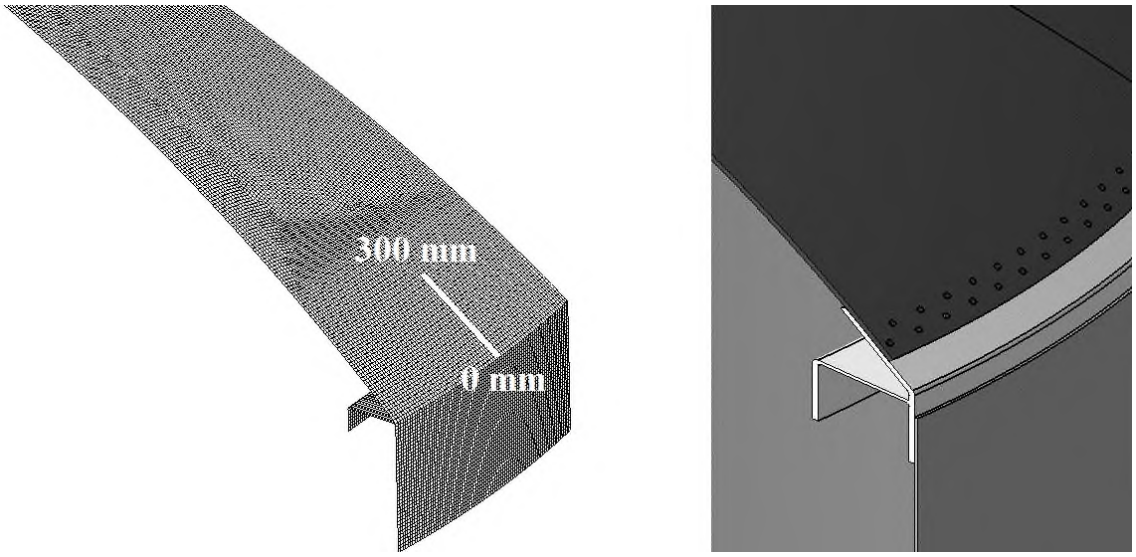

Σχήμα ε.3.6: Μοντέλο ΠΣ με την κατάλληλη πύκνωση πλέγματος για την μείωση του αριθμητικού σφάλματος [1]. Η αριθμητική λύση εστιάζεται σε απόσταση από το σημείο τομής του διαφράγματος με την άτρακτο (0mm) και για 300mm προς τον άξονα της κατασκευής.

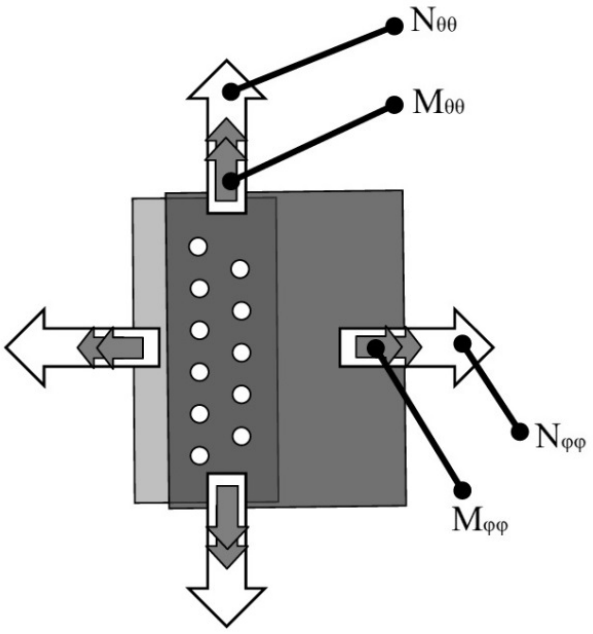

Σχήμα ε.3.7: Ονοματολογία μοναδιαίων (ανά μήκος) δυνάμεων και ροπών επί του κελύφους [1].

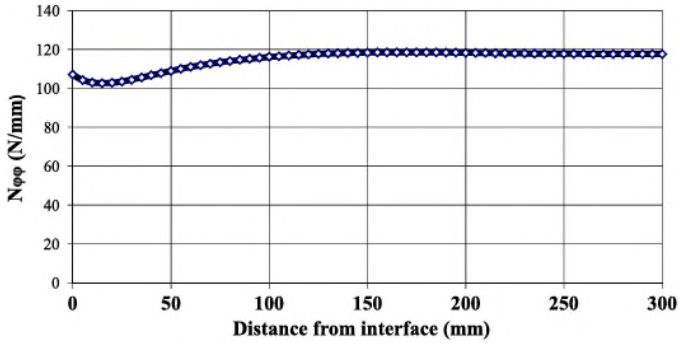

a) Unit force tangent to meridian curves, Nφφ

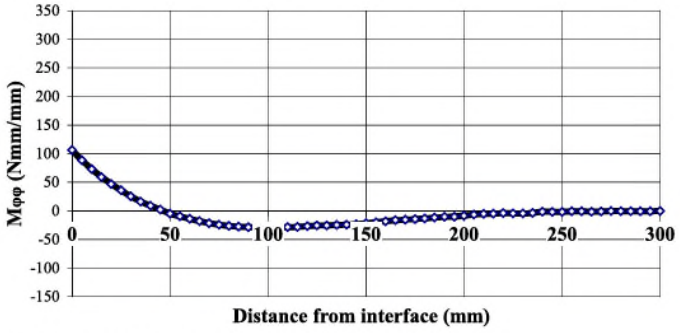

b) Unit moment tangent to meridian curves, Mφφ

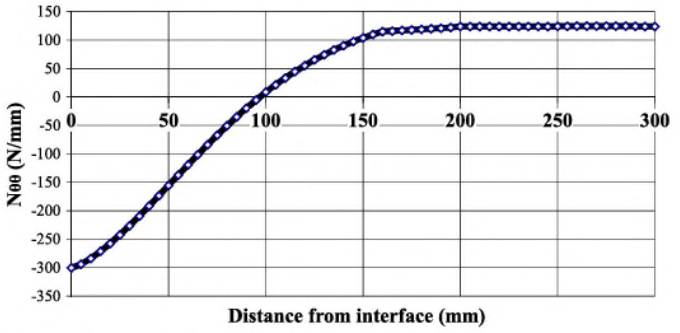

c) Unit force tangent to equatorial curves, Nθθ

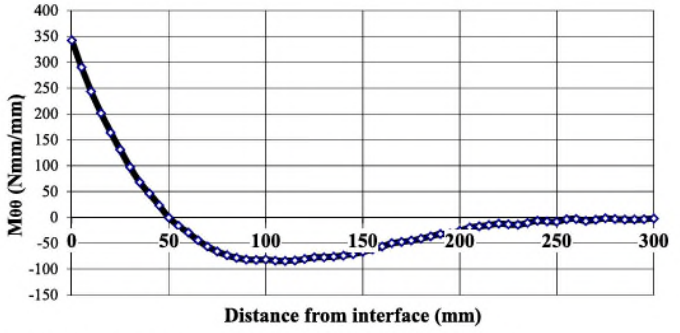

d) Unit moment tangent to equatorial curves, Mθθ

Σχήμα ε.3.8: Αποτελέσματα αριθμητικής επίλυσης ως προς τις μοναδιαίες δυνάμεις και ροπές επί του κελύφους [1]

Στον αεροκατασκευαστικό σχεδιαστικό κλάδο, υπάρχει η γνωση ότι το πεδίο των τάσεων επιλύεται πιο σωστά αναλόγως των μεταβολών του πεδίου του αντίστοιχου μεγέθους του αριθμητικού πλέγματος και των συναρτήσεων σχήματος των ΠΣ. Η περιοχή της συνδεσμολογίας του διαφράγματος της ουριαίας ατράκτου είναι μια από τις περιοχές που παρουσιάζουν μεγάλες μεταβολές στο τασικό πεδίο στην περιοχή σύζευξης με την άτρακτο, όπως αναπτύσσεται στο τρίτο κεφάλαιο . Η μέθοδος της καθολικής μοντελοποίησης δεν είναι ικανή για την ορθή αποτύπωση του τασικού πεδιού λόγω του μεγέθους και του είδους των αριθμητικών στοιχείων που χρησιμοποιούνται στο πλέγμα αλλά και λόγω της γεωμετρικής ιδιομορφίας της σύζευξης ενός κυλινδρικού (άτρακτος) με ένα σφαιρικό δομικό απάρτιο (διάφραγμα). Η αεροκατασκευαστική βιομηχανία, τις περισσότερες φορές μεταπηδά στην ανάλυση των φορτίων στους κόμβους για την αποφυγή δημιουργίας αριθμητικών μοντέλων τοπικής μοντελοποίησης αλλά για την παρούσα σχεδιαστική λεπτομέρεια και αυτή η μέθοδος δεν αποφέρει σωστά αποτελέσματα εάν δεν χρησιμοποιηθούν αρκετά στοιχεία. Ένα σχετικό παράδειγμα μη ορθής μοντελοποίησης και εξαγωγής εσφαλμένων συμπερασμάτων λόγω συτής σε παρεμφερή σχεδιαστική λεπτομέρειας παρουσιάζεται στο σχήμα ε.3.9 και σχολιάζεται εκτενώς εντός του τρίτου κεφαλαίου.

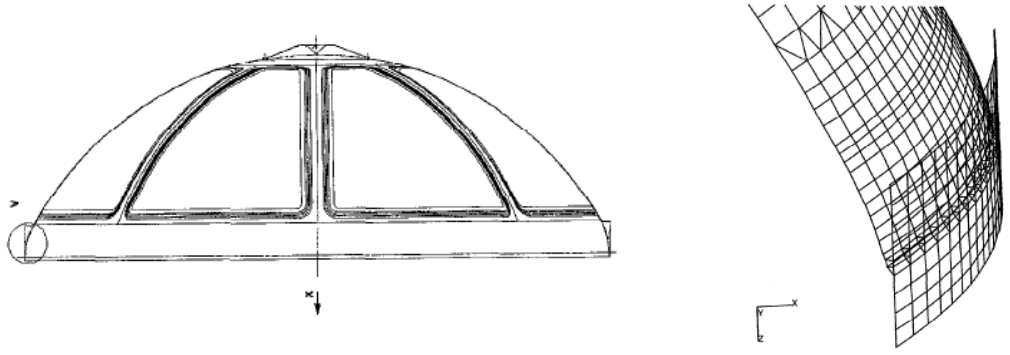

Σχήμα ε.3.9: Αριθμητική μοντελοποίηση στην περιοχή της συναρμογής σφαιρικού διαφράγματος με κυλινδρική κατασκευή στην περίπτωση του πυραύλου Arianne 5 [9]

Η σημασία της περιοχής της συναρμογής του διαφράγματος με την άτρακτο, αποτυπώνεται σε σχετική αναφορά αεροπορικού ατυχήματος/συμβάντος όπως παρατίθεται στο σχήμα ε.3.10. Η σχετική συζήτηση λαμβάνει χώρα επίσης εντός του

τρίτου κεφαλαίου. Πιθανές αιτίες που ενδεχομένως να μπορούν να συσχετιστούν με τις αστοχίες της αναφοράς, είναι και η μη ορθή πρόβλεψη του είδους και μεγέθους της φόρτισης της περιοχής τοπικά.

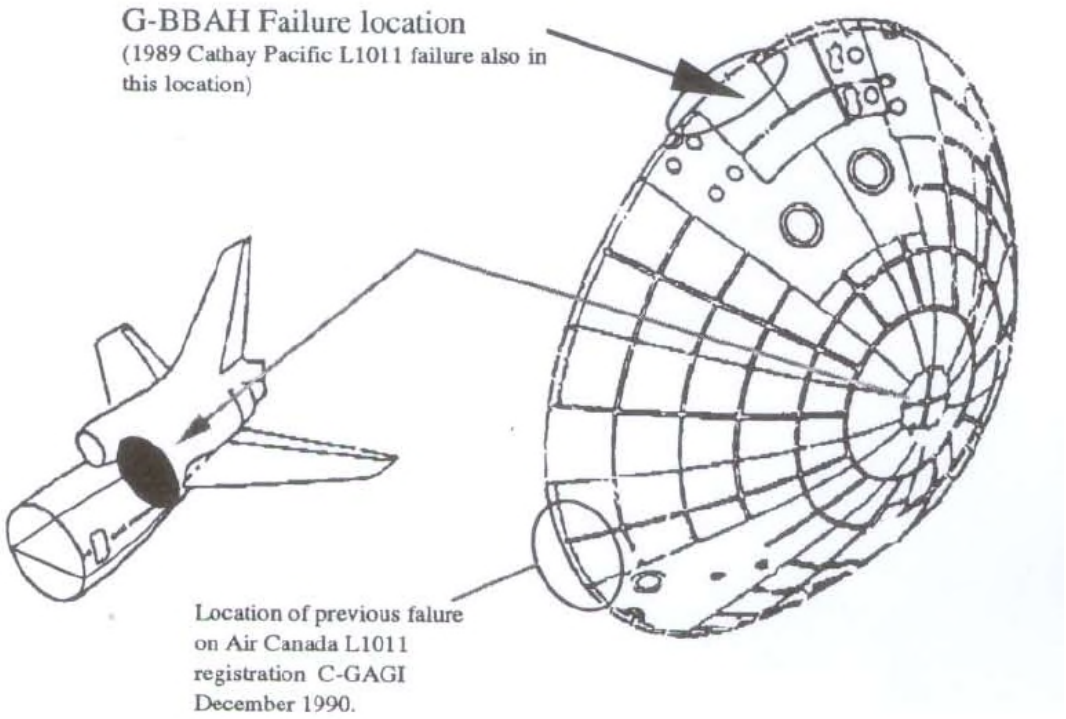

Σχήμα ε.3.10: Έκθεση αεροπορικών ατυχημάτων στην συμβολή του διαφράγματος με την άτρακτο [10]

Βάσει των αναλύσεων που έλαβαν χώρα για την δομική φόρτιση της περιοχής και λαμβάνοντας υπόψη την κρισιμότητα της θλιπτικής φόρτισης στην περίπτωση που το διάφραγμα κατασκευαστεί από σύνθετα στρωσιγενή υλικά σε αντίθεση με τις υφιστάμενες κατασκευές από κράματα αλουμινίου, υποβλήθηκε σχετική πρόταση ανασχεδιασμού σε εταιρία κατασκευής αεροπορικού υλικού η οποία και έγινε αποδεκτή. Ο αρχικός σχεδιασμός της συνδεσμολογίας φαίνεται στο σχήμα ε.3.11, ενώ η σχεδιαστική αναπροσαρμογή αποτυπώνεται στο σχήμα ε.3.6. Η διαφορά μεταξύ των δύο σχεδιαστικών προσεγγίσεων εστιάζεται στην δημιουργία μεγαλύτερης συνδετικής

φλάντζας (interface ring) από μεταλλικό υλικό στην περιοχή υψηλής μεταβολής των δομικών φορτίων.

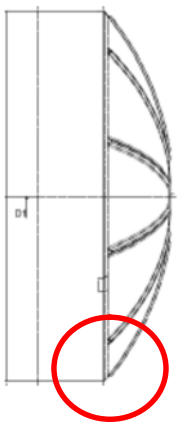

A1-A1

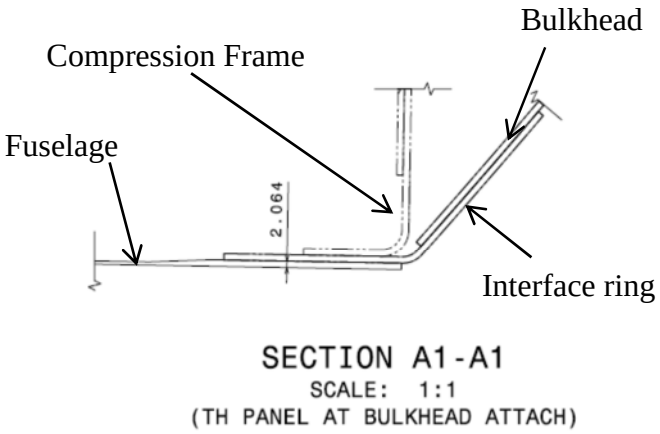

Σχήμα ε.3.11: Αρχικός σχεδιασμός συνδεσμολογίας διαφράγματος για την σύνδεση διαφράγματος με την άτρακτο σε κατασκευή της Alenia-Aermacchi

Επιγραμματικά, τα κύρια σημεία και τα συμπεράσματα του τρίτου κεφαλαίου, παρατίθενται κάτωθι. Για την πιο ορθή κατανόηση των συμπερασμάτων, θα πρέπει να γίνει ανάγνωση του αντίστοιχου κεφαλαίου του κυρίως σώματος της διατριβής και ενδεχομένως ανάγνωση μερικών αναφορών του κεφαλαίου αυτού.

- Ο κλάδος των αεροκατασκευών, χρησιμοποιεί την καθολική μοντελοποίηση με ΠΣ για την εξεύρεση των φορτίων στους κόμβους του αριθμητικού πλέγματος και στην συνέχεια χρησιμοποιεί αναλυτικούς υπολογισμούς για τον υπολογισμό τάσεων και την πλήρωση των απαιτήσεων σε αντοχή. Αυτή η μεθοδολογία, όταν συνδυάζεται με πειραματικές δοκιμές έχει θεωρηθεί ***αξιόπιστη*** και ικανή για την πλήρωση των απαιτήσεων συμμόρφωσης με τις προδιαγραφές αντοχής.
- Η αξιοπιστία αυτής της μεθοδολογίας έχει αποδειχτεί σε αεροκατασκευές κατασκευασμένες κατά κύριο λόγο από ισότροπα μεταλλικά υλικά.

- Οι τοποθεσίες συνδέσμων σε μία άτρακτο είναι κρίσιμες καθότι είναι περιοχές με υψηλές διακυμάνσεις του πεδίου τάσεων. Το αντικείμενο της εργασίας έχει απασχολήσει τους υπεύθυνους οργανισμούς ασφάλειας πτήσεων και στο παρελθόν. Παρουσιάζεται σχετική αναφορά αεροπορικών ατυχημάτων.
- Διαφράγματα από μεταλλικά υλικά συμπεριφέρονται διαφορετικά σε συνθήκες υπερφόρτισης και αστοχίας και πιο ειδικά σε θλιπτικά φορτία. Παρουσιάζεται δημοσιευμένη έρευνα παρεμφερούς κατασκευής από μεταλλικά υλικά.
- Παρουσιάζεται σχεδιαστική πρόταση για την περίπτωση διαφράγματος από ινώδη στρωσιγενή πολυμερή σύνθετα.

Εισ.4) Η εφαρμογή των Π.Σ. στην βελτιστοποίηση και αντοχή των αεροκατασκευών. Συσχέτιση πρόβλεψης με πειραματικά αποτελέσματα

Τα δομικά συναρμολογήματα που αποτελούνται από λεπτά κελύφη ενισχυμένα με δοκούς (stiffened panels), είναι από τις πιο χαρακτηριστικές σχεδιαστικές διατάξεις στις αεροναυπηγικές κατασκευές. Οι *ελαφριές* αυτές κατασκευές που αποτελούν την πιο συνήθη σχεδιαστική λύση για την άτρακτο και τις πτέρυγες των αεροκατασκευών, πάσχουν κυρίως από αστοχία σε λυγισμό υπό θλιπτική φόρτιση. Οι μελέτες για την απόδειξη αντοχής σε λυγισμό είναι από τις πιο χαρακτηριστικές στον αερο-κατασκευαστικό τομέα. Είναι σημαντικό να επιδειχθεί η δυνατότητα πρόβλεψης της αντοχής αυτών με αριθμητικές μεθόδους όπως αυτές εφαρμόζονται σήμερα.

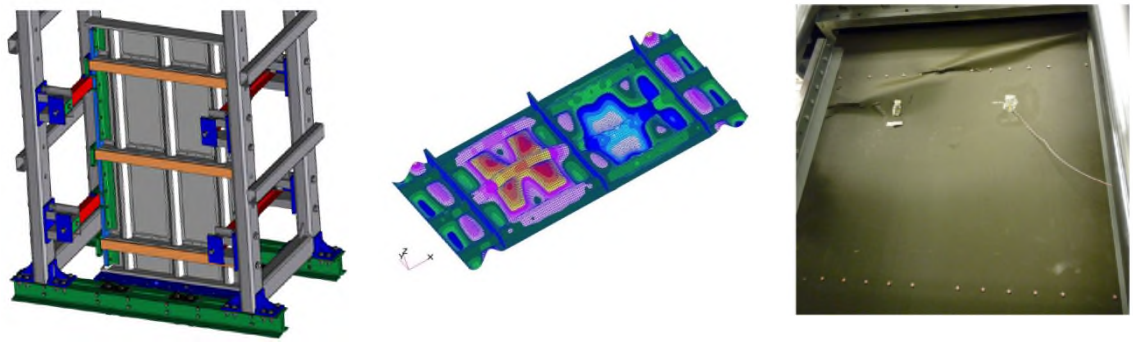

Σχήμα ε.4.1: Η εφαρμογή των πεπερασμένων στοιχείων στην βελτιστοποίηση και πρόβλεψη αντοχής νευρωμένου κελύφους σε θλιπτικά φορτία, ως το κυρίως θέμα του τέταρτου κεφαλαίου

Στο τέταρτο κεφάλαιο της διατριβής παρουσιάζεται μία μελέτη γύρω από την αντοχή σε θλιπτικά φορτία λεπτότοιχου νευρωμένου κελύφους (stiffened panel) από σύνθετα υλικά. Η μελέτη αυτή πραγματοποιήθηκε με αριθμητική ανάλυση και επακόλουθη πειραματική δοκιμή. Η αριθμητική μεθοδολογία αποτελείτο από ένα κομμάτι μη γραμμικής αριθμητικής ανάλυσης με ΠΣ σε ότι αφορά την πρόβλεψη της απόκρισης της κατασκευής σε θλιπτική φόρτιση και στην πρόβλεψη της αντοχής αυτής

καθώς και από ένα κομμάτι αριθμητικής βελτιστοποίησης της κατασκευής το οποίο έλαβε χώρα επίσης με την μέθοδο των ΠΣ. Στο σχήμα ε.4.2, αποτυπώνεται η αριθμητική πρόβλεψη της απόκρισης του νευρωμένου κελύφους υπό θλιπτική φόρτιση.

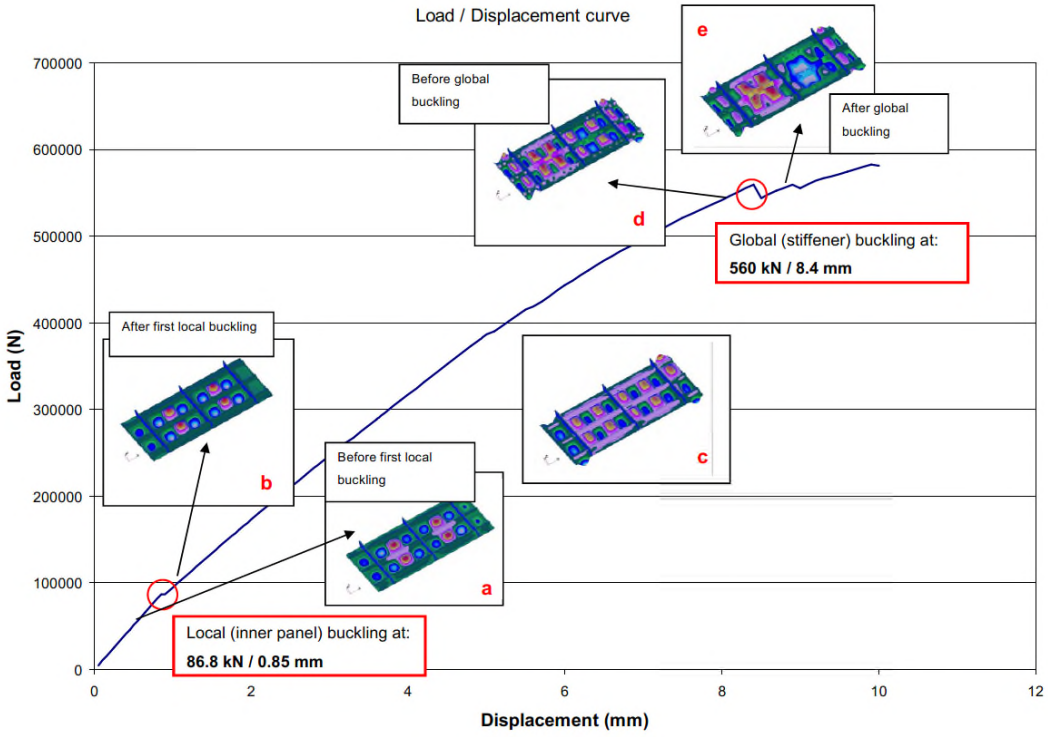

Σχήμα ε.4.2: Μη γραμμική αριθμητική ανάλυση και πρόβλεψη της απόκρισης νευρωμένου κελύφους υπό θλιπτικά φορτία

Η αριθμητική προσομοίωση της απόκρισης της κατασκευής χρησιμοποιήθηκε σε αρχικό στάδιο για την εξεύρεση της μέγιστης φόρτισης έτσι ώστε τα συναρμολογήματα που κατασκευάστηκαν βάσει του βέλτιστου σχεδιασμού να δοκιμαστούν σε κατάλληλη πειραματική διάταξη. Επίσης, είχαν σαν σκοπό τη συσχέτιση των φαινομένων αστοχίας μεταξύ αριθμητικής και πειραματικής μελέτης, ως προς το είδος των αστοχιών που εμφανίζονται κατά την διαδικασία, την αλληλουχία αυτών και του επιπέδου της φόρτισης που εμφανίζονται. Στο σχήμα ε.4.3, παρατίθεται η συσχέτιση της αριθμητικής προσομοίωσης με την πειραματική μελέτη.

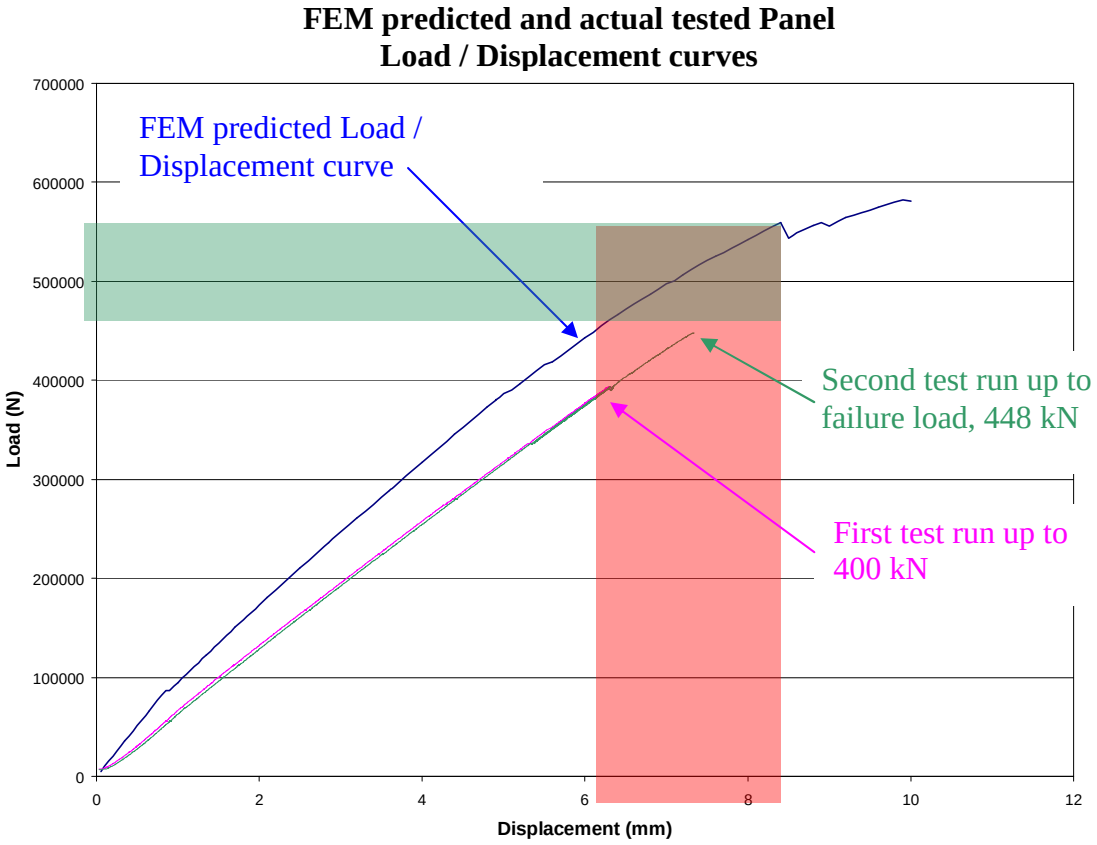

Σχήμα ε.4.3: Διάγραμμα θλιπτική φόρτισης/απομάκρυνσης. Συσχέτιση αριθμητικής προσομοίωσης και πειραματικής δοκιμής νευρωμένης πλάκας υπό θλιπτική φόρτιση

Στο τέταρτο κεφάλαιο της διατριβής, παρατίθεται εκτεταμένη συζήτηση επί των αποτελεσμάτων της συσχέτισης των αριθμητικών με τα πειραματικά. Λαμβάνει χώρα εκτενής συζήτηση ως προς την ικανότητα πρόβλεψης της αντοχής της κατασκευής με αριθμητικές μεθόδους. Επίσης, παραθέτει και επεξηγεί τους τρόπους με τους οποίους η ερευνητική κοινότητα προσπαθεί να συνεισφέρει στην πιο σωστή προσομοίωση παρεμφερών σεναρίων και κατά πόσο αυτό είναι εφικτό με τα πιο σύγχρονα υπολογιστικά μέσα. Στο σχήμα ε4.4, παρουσιάζεται συσχέτιση μεταξύ αριθμητικής λύσης και πειράματος ως προς την εξεύρεση πιθανών περιοχών εκκίνησης της αστοχίας.

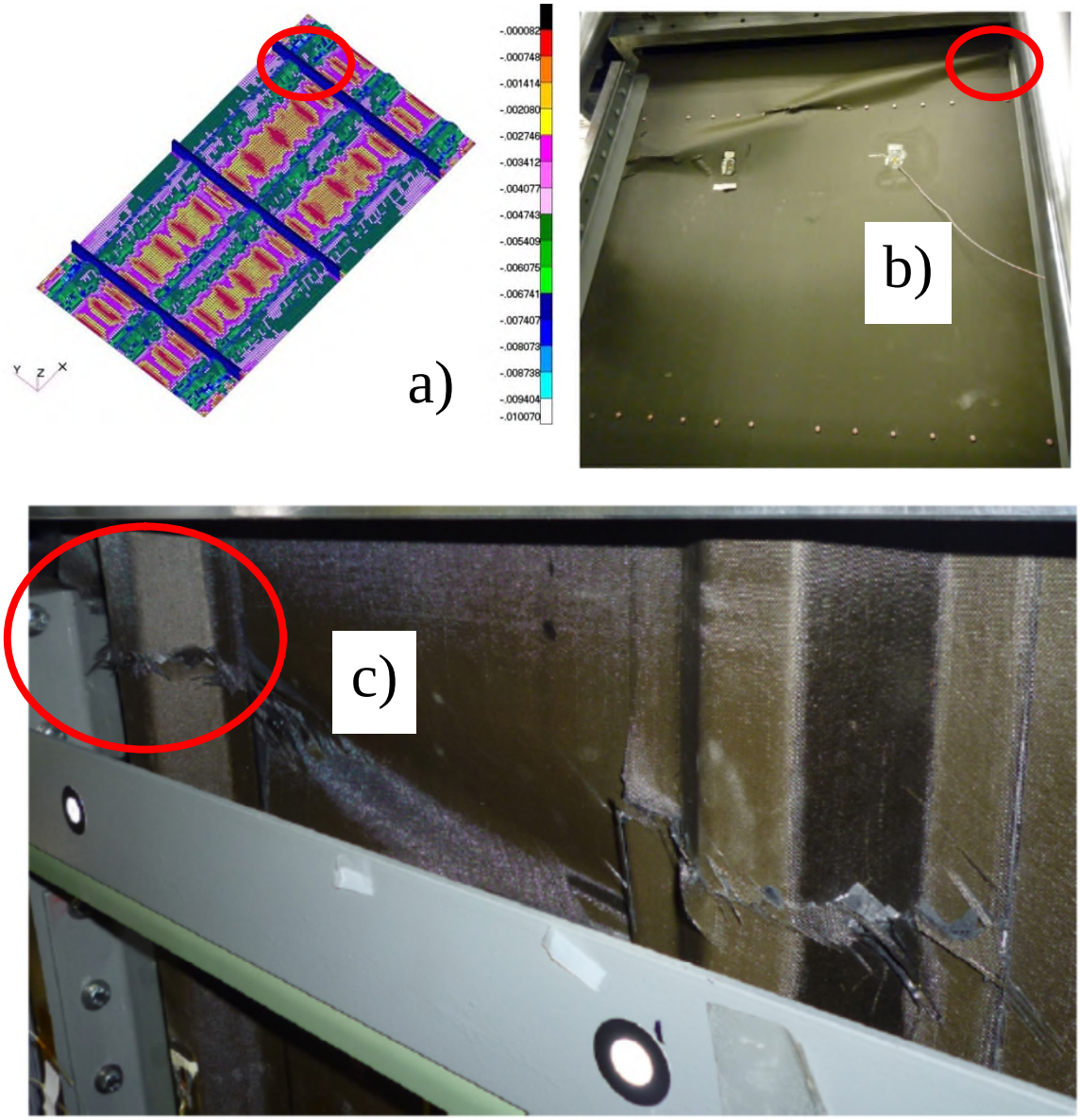

Σχήμα ε.4.4: Η αριθμητική λύση επέδειξε σημείο επί της κατασκευής όπου τοπικά οι εν λόγω τροπές πλησίασαν την τροπή αστοχίας υπό θλίψη

Επιγραμματικά, τα κύρια σημεία και τα συμπεράσματα του τέταρτου κεφαλαίου, παρατίθενται κάτωθι. Για την πιο ορθή κατανόηση των συμπερασμάτων, θα πρέπει να γίνει ανάγνωση του αντίστοιχου κεφαλαίου του κυρίως σώματος της διατριβής και ενδεχομένως ανάγνωση μερικών αναφορών του κεφαλαίου αυτού.

- Με την εφαρμογή ινωδών πολυμερών υλικών στις αεροκατασκευές, η βελτιστοποίηση της φέρουσας κατασκευής, βρέθηκε στο επίκεντρο του σχεδιασμού κατασκευών από σύνθετα υλικά. Η δυνατότητα σχεδιασμού δομής μικρότερου συνολικού βάρους με την ίδια ή καλύτερη απόδοση σε αντοχή και κατασκευαστική συμπεριφορά είναι ιδιαίτερα ελκυστική από την βιομηχανία των αεροκατασκευών. Εντός του κεφαλαίου, παρουσιάζεται η μελέτη βελτιστοποίησης νευρωμένου κελύφους υπό θλίψη.
- Εν συνεχεία, η συσχέτιση των πειραματικών και αριθμητικών αποτελεσμάτων σε λεπτότοιχο ενισχυμένο κέλυφος υπό θλιπτικά φορτία λαμβάνει χώρα σε κατασκευή η οποία δεν περιέχει δομικές αστοχίες πριν την επιβολή φόρτισης.
- Βάσει των προδιαγραφών Αξιοπλοΐας, οι αεροκατασκευές από σύνθετα πολυμερή υλικά, θα πρέπει να επιδείξουν συμμόρφωση με τα πρότυπα αντοχής σε στατική φόρτιση υπό συνθήκες ύπαρξης δομικών βλαβών. Η πρόβλεψη της αντοχής λεπτότοιχων ενισχυμένων κελυφών μεγάλων συναρμολογημάτων τα οποία έχουν υποστεί και εμπεριέχουν δομικές βλάβες, δεν ανήκουν προς στιγμήν στις εφαρμοσμένες αριθμητικές μεθόδους για την απόδειξη της αντοχής. Η μοντελοποίηση αστοχιών σε σύνθετα υλικά μαζί με την προοδευτική εξέλιξη αυτών είναι αντικείμενο ευρείας ερευνητικής δραστηριότητας σήμερα και η προσπάθεια έγκειται στην ορθή αποτύπωση της προόδου της αστοχίας και στην ορθή πρόβλεψη της εναπομείνασας αντοχής. Οι μέθοδοι αυτές είναι υπό εξέλιξη και δεν μπορούν να θεωρηθούν αποδεκτές μέθοδοι για την αξιόπιστη και συντηρητική πρόβλεψη της αντοχής την παρούσα χρονική στιγμή.

Εισ.5) Δομικές βλάβες και αντοχή αεροκατασκευών από στρωσιγενή σύνθετα τα οποία υπέστησαν ζημιά από κρούση

Βάσει των προδιαγραφών Αξιοπλοΐας [7, 8], οι αεροκατασκευές από σύνθετα πολυμερή υλικά, θα πρέπει να επιδείξουν συμμόρφωση με τις προδιαγραφές αντοχής βάσει προτύπου, σε στατική φόρτιση και υπό συνθήκες ύπαρξης δομικών βλαβών στην κατασκευή. Οι βλάβες αυτές θα πρέπει να είναι χαρακτηριστικές αυτών που θα δημιουργηθούν κατά την διάρκεια της ζωής και του περιβάλλοντος λειτουργίας της κατασκευής. Τα λεπτότοιχα κελύφη και γενικότερα τα δομικά μέρη κατασκευών από σύνθετα ινώδη στρωσιγενή πολυμερή υλικά είναι ιδιαίτερα ευπαθή σε δομικές αστοχίες μετά από πρόσκρουση με ξένα σώματα. Η συχνότητα των φαινομένων κρούσης, της ενέργειας κρούσης και των μαζών των ξένων σωματιδίων που θα έρθουν σε επαφή με την κατασκευή εξαρτώνται από διάφορους παράγοντες όπως ο ρόλος του αεροσκάφους και η αποστολή που θα διατελέσει, το σημείο επί της κατασκευής, ο τρόπος που θα συντηρηθεί και διάφοροι άλλοι.

Οι κατασκευές από μεταλλικά υλικά με αντίστοιχες από ινώδη πολυμερή σύνθετα συμπεριφέρονται διαφορετικά σε φαινόμενα κρούσης από ξένα σώματα σε ότι αφορά την δημιουργία ζημιάς αλλά και πιο σημαντικά σε ότι αφορά στην *εναπομένουσα αντοχή* της κατασκευής. Συγκρίνοντας μια κατασκευή από μεταλλικά υλικά και παρεμφερούς συνολικού δομικού βάρους και σχεδιαστικών λεπτομερειών με μία αντίστοιχη από ινώδη στρωσιγενή, η *εναπομένουσα μετά από κρούση* αντοχή της κατασκευής, στις περισσότερες περιπτώσεις, είναι μεγαλύτερη στην περίπτωση της μεταλλικής κατασκευής. Αυτό οφείλεται κυρίως στην ικανότητα της πλαστικής παραμόρφωσης των μεταλλικών υλικών η οποία μπορεί να αποσβέσει μεγάλο κομμάτι της ενέργειας πρόσκρουσης.

Για την μελέτη φαινομένων κρούσης, δύο είναι οι βασικές παράμετροι για την ποσοτικοποίηση της εναπομένουσας αντοχής: το συνολικό εύρος της δομικής ζημιάς και η εναπομένουσα αντοχή της κατασκευής σε θλιπτικά φορτία. Το αντικείμενο του πέμπτου κεφαλαίου, παρουσιάζει το φαινόμενο της κρούσης και τις επιπτώσεις αυτού σε κατασκευές από σύνθετα υλικά μέσω εξειδικευμένης πειραματικής μελέτης κρούσης και αντοχής σε θλίψη που διεξήχθη σε δοκίμια κατασκευής. Στο κάτωθι σχήμα ε.5.1.α) απεικονίζεται ένας πύργος ρίψης μαζών όπου επίπεδα δοκίμια συγκεκριμένων

διαστάσεων εισάγονται στο χαμηλότερο σημείο της πειραματικής διάταξης και μάζα με τη μορφή εμβόλου ρίπτεται από συγκεκριμένο ύψος για να εξομοιώσει κρούση σε συγκεκριμένο επίπεδο ενέργειας. Στο σχήμα ε.5.1.β), απεικονίζεται μια μηχανή θλίψεως δοκιμίων όπου μετράται η εναπομένουσα αντοχή των δοκιμίων που υπέστησαν κρούση.

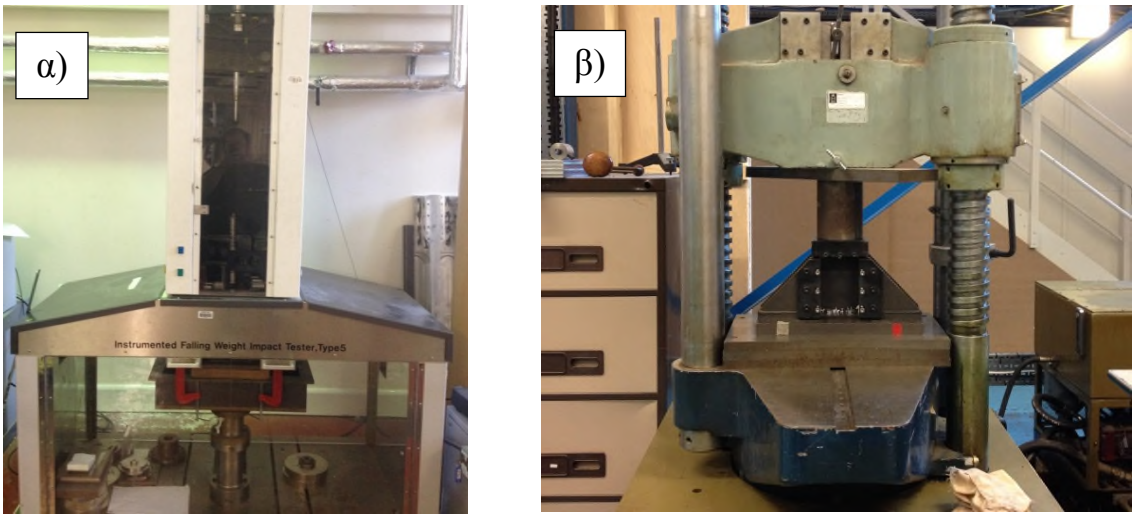

Σχήμα ε.5.1: α) Πειραματική δοκιμή κρούσης σε πύργο ρίψεως μαζών από ύψος σε δοκίμια από στρωσιγενή σύνθετα και β) επακόλουθη δοκιμή αντοχής σε θλίψη

Οι αριθμητικές μέθοδοι προσέγγισης του φαινομένου της κρούσης που λαμβάνουν χώρα σήμερα είναι αρκετά εξελιγμένες. Διάφορες μέθοδοι αριθμητικής μοντελοποίησης, είδη πεπερασμένων στοιχείων, αριθμητικοί επιλυτές και άλλα, συμβάλουν με διαφορετικό τρόπο και σε διαφορετικό βαθμό στην προσομοίωση του φαινομένου της κρούσης με αριθμητική προσομοίωση. Διαφορετικά σενάρια, απαιτούν διαφορετική μεθοδολογία προσέγγισης και μοντελοποίησης για την επίτευξη του στόχου της ορθής προσομοίωσης. Σήμερα, η ερευνητική κοινότητα διερευνά την πιστότητα και συσχέτιση των αριθμητικών αποτελεσμάτων με τα πειραματικά. Οι περισσότερες μελέτες στην βιβλιογραφία επιζητούν την ορθότερη αποτύπωση του φαινομένου από πλευράς έκτασης της ζημιάς και από πλευράς εναπομένουσας αντοχής στης κατασκευή. Παρόλο το πλήθος των αριθμητικών μελετών και προσομοιώσεων στην βιβλιογραφία σήμερα, για τα αποτελέσματα αριθμητικών μοντέλων προσομοίωσης κρούσης απαιτείται περαιτέρω ωρίμανση πριν θεωρηθούν ικανά για την παραγωγή αποτελεσμάτων προς αντικατάσταση των πειραματικών έστω και έως κάποιο

βαθμό. Η βιομηχανία σήμερα στηρίζεται και χρησιμοποιεί πειραματικές μεθόδους για την διερεύνηση της συμπεριφοράς και της αντοχής κατασκευών από κρούση.

Η μελέτη που εκπονήθηκε γύρω από το φαινόμενο της κρούσης αφορούσε στην διερεύνηση της συμπεριφοράς στρωσιγενούς συνθέτου υλικού το οποίο αποτελούταν από μήτρα που εμπεριείχε διασπορά σωματιδίων που προσέδιδαν χαρακτηριστικά καταστολής της αυτανάφλεξης του υλικού. Δύο διαφορετικές διαστρωματώσεις διερευνήθηκαν κάτω από συνθήκες κρούσης σε πέντε διαφορετικά επίπεδα ενέργειας. Η έκταση ζημιά που προκλήθηκε στα δοκίμια, παρουσιάζεται στο σχήμα ε.5.2, όπως αποτυπώθηκε με μεθόδους μη καταστροφικού ελέγχου (C-Scan).

Impact Energy (J)	8	15	25	35	50
Configuration C1 [+/-, 0/90, -/+, 90/0]s	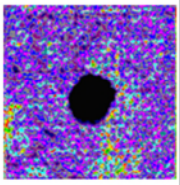	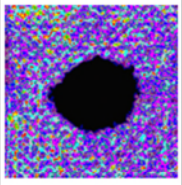	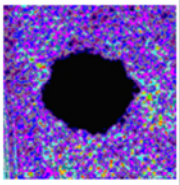	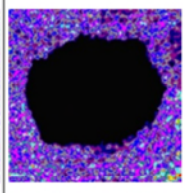	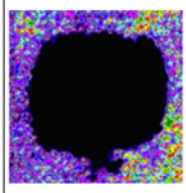
Max Diameter (mm)	30	57	59	85	89
Area (mm²)	688 (circular)	2122 (oval)	2346 (oval)	4504 (oval)	5767 (oval)
Configuration C2 [+/-, 0/90, 90/0, 0/90]s	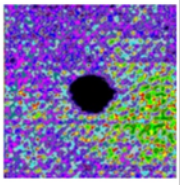	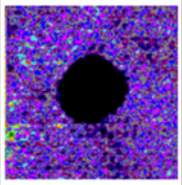	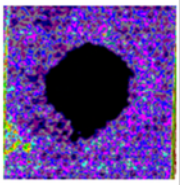	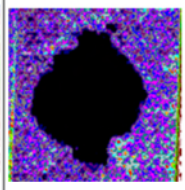	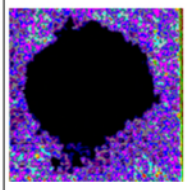
Max Diameter (mm)	29	45	56	79	87
Area (mm²)	550 (oval)	1523 (oval)	2028 (diamond)	3904 (diamond)	4288 (diamond)

Σχήμα ε.5.2: Μη καταστροφικός έλεγχος της ζημιάς που προκλήθηκε σε δοκίμια δύο διαφορετικών διαστρωματώσεων, σε πέντε επίπεδα ενέργειας κρούσης

Τα αποτελέσματα της πειραματικής μελέτης σε ότι αφορά την κρούση, αποδίδονται σε μορφή διαγραμμάτων δύναμης αντίδρασης από την επαφή του κρουστικού εμβόλου με το δοκίμιο ως προς το χρόνο, δύναμης αντίδρασης ως προς την μετακίνηση του δοκιμίου στο σημείο κρούσης και άλλες μορφές, βλέπε σχήμα ε.5.3 και ε.5.4

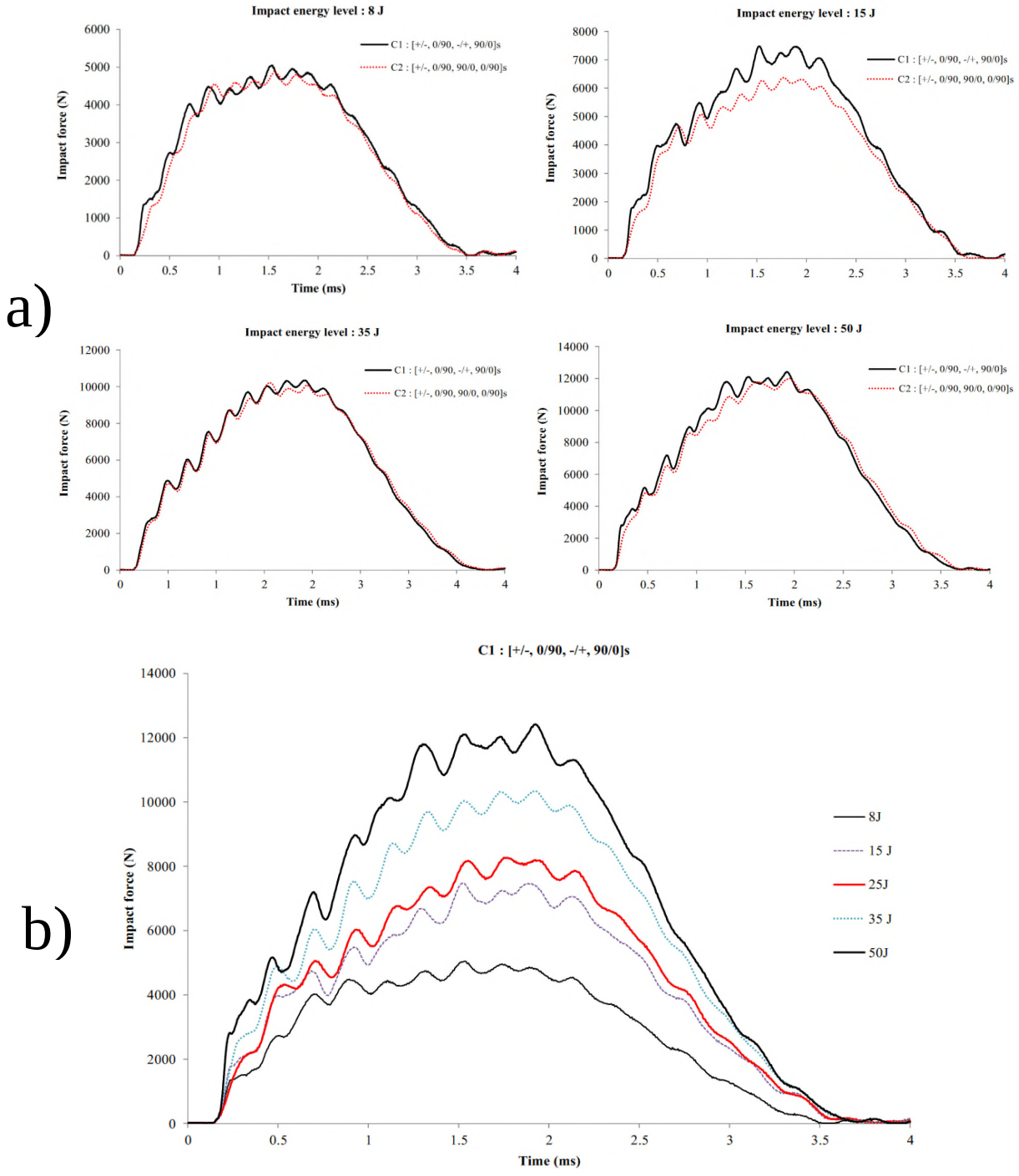

Σχήμαε.5.3: a) Δύναμη κρούσης ως προς το χρόνο για τα δοκίμια των δύο διαστρωματώσεων και για επίπεδα ενέργειας: 8 J, 15 J, 35 Jκαι 50 J. b) Δύναμη κρούσης ως προς το χρόνο για την διαστρωμάτωση C1 σε όλα τα επίπεδα ενέργειας της μελέτης

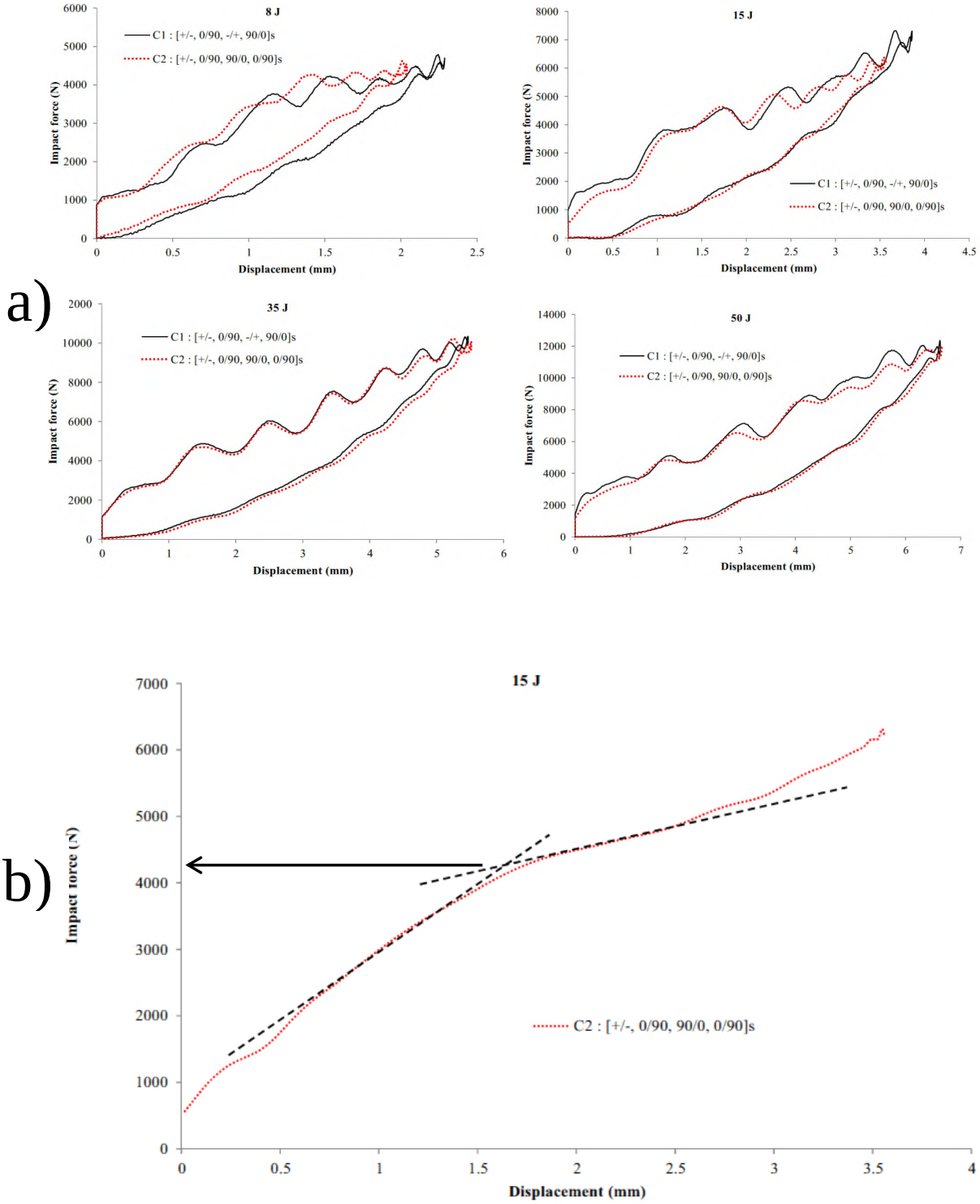

Σχήμαε.5.4: a) Δύναμη κρούσης ως προς την απομάκρυνση για τα δοκίμια των δύο διαστρωματώσεων και για επίπεδα ενέργειας: 8 J, 15 J, 35 Jκαι 50 J. b) Σημείο μεταβολής της ελαστικότητας του δοκιμίου που υποδηλώνει έναρξη της ζημιάς

Αποτελέσματα από την πειραματική μελέτη κρούσης, μπορούν να παρουσιαστούν σε διάγραμμα που αποτυπώνεται η συνολικής επιφάνειας ζημιάς ως προς τα επίπεδα ενέργειας κρούσης (σχήμα ε.5.5) και σε διάγραμμα αντοχής σε θλιπτική φόρτιση κατόπιν κρούσης ως προς τα επίπεδα ενέργειας κρούσης (σχήμα ε.5.6)

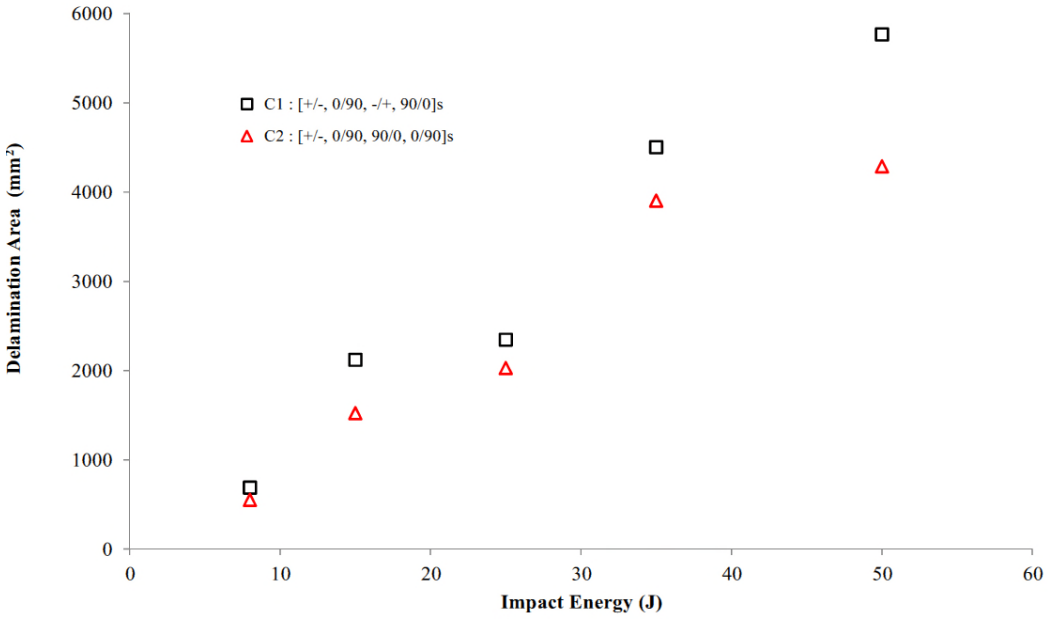

Σχήμα ε.5.5: Συνολική επιφάνεια ζημιάς επί του δοκιμίου ως προς τα επίπεδα ενέργειας κρούσης

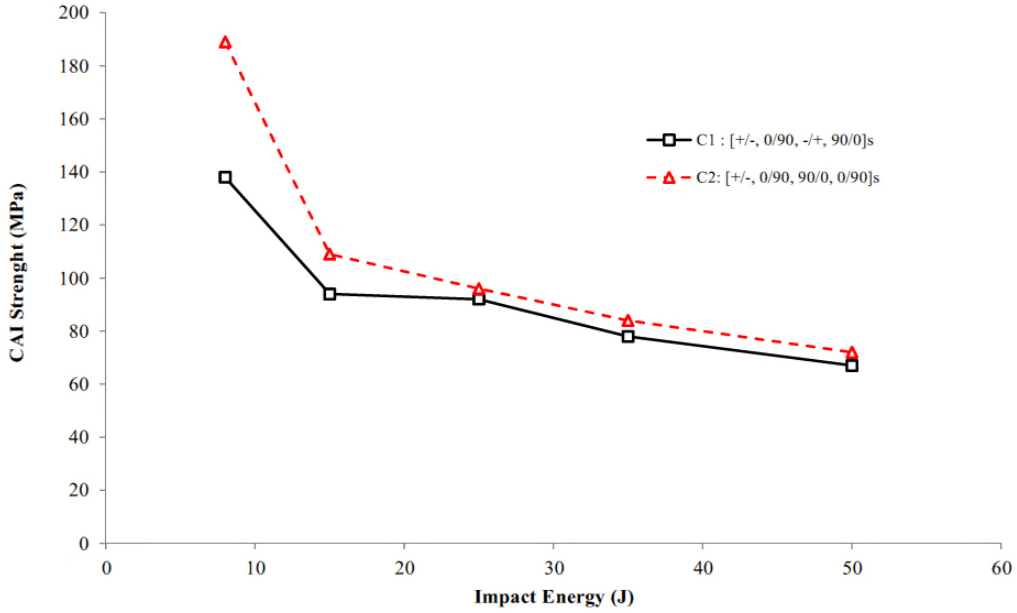

Σχήμαε.5.6: Αντοχής σε θλιπτική φόρτιση κατόπιν κρούσης ως προς τα επίπεδα ενέργειας κρούσης

Επιγραμματικά, τα κύρια σημεία και τα συμπεράσματα του πέμπτου κεφαλαίου, παρατίθενται κάτωθι. Για την πιο ορθή κατανόηση των συμπερασμάτων, θα πρέπει να γίνει ανάγνωση του αντίστοιχου κεφαλαίου του κυρίως σώματος της διατριβής και ενδεχομένως ανάγνωση μερικών αναφορών του κεφαλαίου αυτού.

- Αντιμετωπίζεται το φαινόμενο της κρούσης σε σύνθετα υλικά, η ζημιά που δημιουργείται και οι σημαντικές παράμετροι και ιδιότητες του υλικού που συμβάλουν στην μεγαλύτερη αντοχή έναντι της κρούσης.
- Παρουσιάζεται πειραματική μελέτη κρούσης σε δοκίμια από σύνθετα υλικά τα οποία έχουν την ιδιότητα επιβράδυνσης σε ανάφλεξη. Για να επιτευχτεί η επιβράδυνση αυτή, η μήτρα εμπεριέχει σωματίδια σε μορφή διασποράς τα οποία επιφέρουν επιπτώσεις στην αντοχή και την ευθραυστότητα μεταξύ των στρώσεων του συνθέτου. Επεξηγείται ο τρόπος με τον οποίο τα αποτελέσματα χρησιμοποιήθηκαν σε επιλογή σχεδιασμού της κατασκευής.

Εισ.6) Μικρομηχανικές αριθμητικές αναλύσεις και ο ρόλος αυτών στην πρόβλεψη της αντοχής των κατασκευών

Στις επιμέρους μελέτες που παρουσιάστηκαν εντός των προηγούμενων κεφαλαίων και βάσει των αποτελεσμάτων και συζητήσεων που διατυπώνονται στο κυρίως σώμα της διατριβής, διαφαίνεται η εξελικτική ερευνητική πορεία προς την αριθμητική μοντελοποίηση της ζημιάς και της αριθμητικής μοντελοποίησης της προοδευτικής ανάπτυξης αυτής υπό αυξανόμενη φόρτιση μέχρι του σημείου της καθολικής αστοχίας της κατασκευής. Όπως έχει ήδη διατυπωθεί στο δεύτερο κεφάλαιο, βάσει των προδιαγραφών αξιοπλοΐας [7,8], οι αεροκατασκευές από σύνθετα πολυμερή υλικά, θα πρέπει να επιδείξουν συμμόρφωση με τα πρότυπα αντοχής σε στατική φόρτιση υπό συνθήκες ύπαρξης δομικών ζημιών. Αριθμητικά εργαλεία προσομοίωσης της έναρξης της ζημιάς/φθοράς και της επακόλουθης ανάπτυξης αυτής υπάρχουν διαθέσιμα σήμερα σε εμπορικά πακέτα πεπερασμένων στοιχείων. Στην παρούσα χρονική στιγμή, η ερευνητική κοινότητα σε διεθνές επίπεδο, βρίσκεται στο στάδιο διερεύνησης της συσχέτισης των αριθμητικών αποτελεσμάτων προσομοιώσεων προοδευτικής αστοχίας με αντίστοιχα πειραματικών διατάξεων. Για την επίτευξη του στόχου της πιο πιστής μοντελοποίησης της αστοχίας των αεροκατασκευών από σύνθετα υλικά, πρέπει να μοντελοποιηθεί ορθότερα η αστοχία στην μικροκλίμακα του υλικού. Αυτή η διαπίστωση έχει επιφέρει την ώθηση στην ανάπτυξη διαφόρων μικρομηχανικών μοντέλων και αριθμητικών αναλύσεων, χαρακτηριστικά παραδείγματα των οποίων παρατίθενται και συζητούνται στο κυρίως σώμα της διατριβής .

Το θέμα του έκτου κεφαλαίου, αφορά σε αριθμητικές μικρομηχανικές αναλύσεις. Οι αναλυτικές και αριθμητικές μελέτες που έλαβαν χώρα στο πλαίσιο της διατριβής, συσχετίστηκαν με πειραματικά δεδομένα από την βιβλιογραφία και αφορούν στην διερεύνηση των ελαστο-στατικών ιδιοτήτων μικρομηχανικού μοντέλου με την υπόθεση ύπαρξης ενδιάμεσης φάσης [4,6], καθώς και στην διερεύνηση ελαστο-δυναμικών ιδιοτήτων μικρομηχανικού μοντέλου [5].

Η ενδιάμεση φάση των ινωδών συνθέτων, περιγράφει την περιοχή της μήτρας γύρω από την ίνα του σύνθετου υλικού. Η περιοχή αυτή είναι εξίσου σημαντική με αυτήν της ίνας και της μήτρα μιας και είναι υπεύθυνη για την μεταφορά της εσωτερικής

φόρτισης στο υλικό από την μία φάση στη άλλη. Έχει αποδειχθεί ότι οι μηχανικές ιδιότητες αντοχής των συνθέτων υλικών εξαρτώνται σε πολύ μεγάλο βαθμό από την συνοχή που προσδίδει η ενδιάμεση φάση στο σύνθετο υλικό. Οι μικρομηχανικές αναλύσεις έχουν σαν αφετηρία την θεώρηση μικρομηχανικών μοντέλων (Representative Volumetric Elements–RVEs) τα οποία έχουν σαν σκοπό να αντιπροσωπεύσουν/αναπαραστήσουν το υλικό συνολικά με μια πιο απλουστευμένη γεωμετρική αναπαράσταση. Το μικρομηχανικό μοντέλο που χρησιμοποιήθηκε στην ελαστο-στατική μελέτη [4,6], απεικονίζεται στο σχήμα ε.6.1.

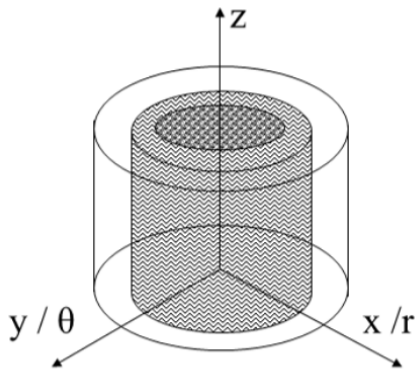

Σχήμα ε.6.1:Το μικρομηχανικό μοντέλο τριών φάσεων σε καρτεσιανές και κυλινδρικές συντεταγμένες που μελετήθηκε αριθμητικά στις ελαστοστατικές αναλύσεις με την υπόθεση της ενδιάμεσης φάσης [4,6]

Οι ελαστο-στατικές ιδιότητες του μοντέλου που απεικονίζεται στο σχήμα ε.6.1 και ειδικότερα η θεώρηση της μεταβολής των ιδιοτήτων της ενδιάμεσης φάσης με βάση την απόσταση από την επιφάνεια της ίνας, αποτυπώνονται στο σχήμα ε.6.2. Στο σχήμα ε.6.3 παρουσιάζεται το αριθμητικό χωρίο/τομέας που χρησιμοποιήθηκε για την αριθμητική μοντελοποίηση του αντιπροσωπευτικού χωρίου του σχήματος ε.6.1. Η μεταβολή της συνολικής επιφάνειας της ενδιάμεσης φάσης σε σχέση με την κατ' όγκο συγκέντρωση των ινών αποτυπώνεται στο σχήμα ε.6.4. Τα σχήματα ε.6.5 και ε.6.6, παρουσιάζουν σε μορφή διαγραμμάτων τη σύγκριση μεταξύ αναλυτικών, αριθμητικών και πειραματικών αποτελεσμάτων ως προς τα κύρια ελαστο-στατικά μεγέθη υπό μελέτη, το διάμηκες και εγκάρσιο μέτρο ελαστικότητας του συνθέτου [4].

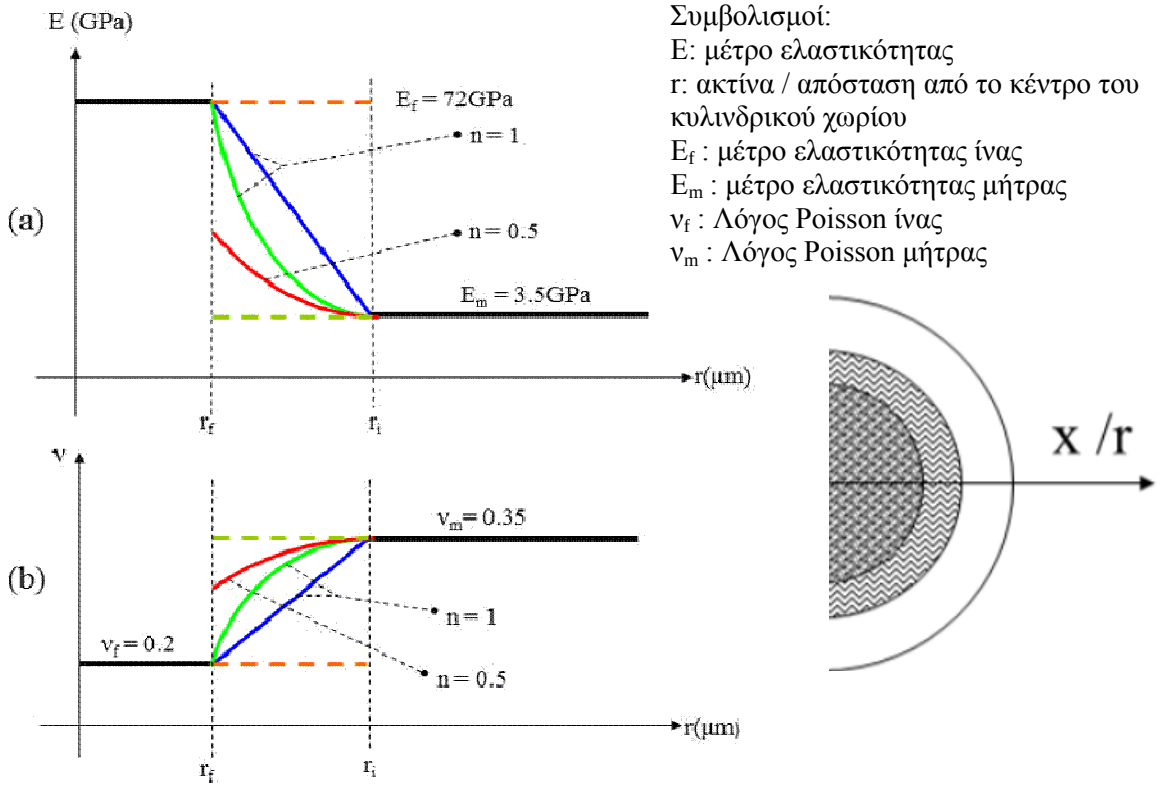

Σχήμα ε.6.2: Μεταβολή μέτρου ελαστικότητας και λόγου του Poisson στο χωρίο της ενδιάμεσης φάσης [4]

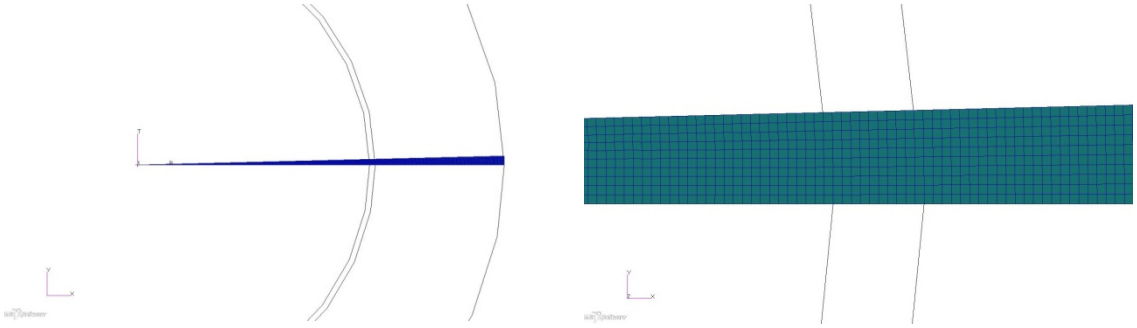

Σχήμα ε.6.3: Τομέας αριθμητικού πλέγματος ΠΣ [4]

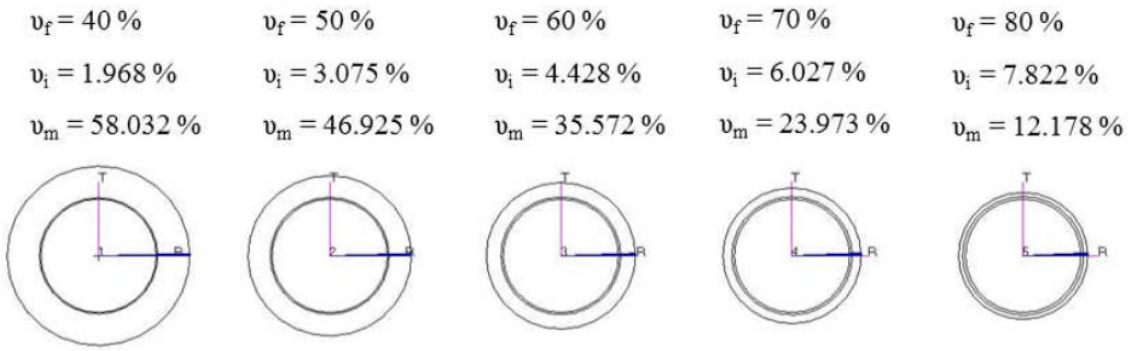

Σχήμα ε.6.4: Μεταβολή της συνολικής επιφάνειας που καταλαμβάνει η ενδιάμεση φάση σε σχέση με την κατ' όγκο συγκέντρωση των ινών σε σύνθετο υλικό από ίνες υάλου σε εποξειδική μήτρα [4]

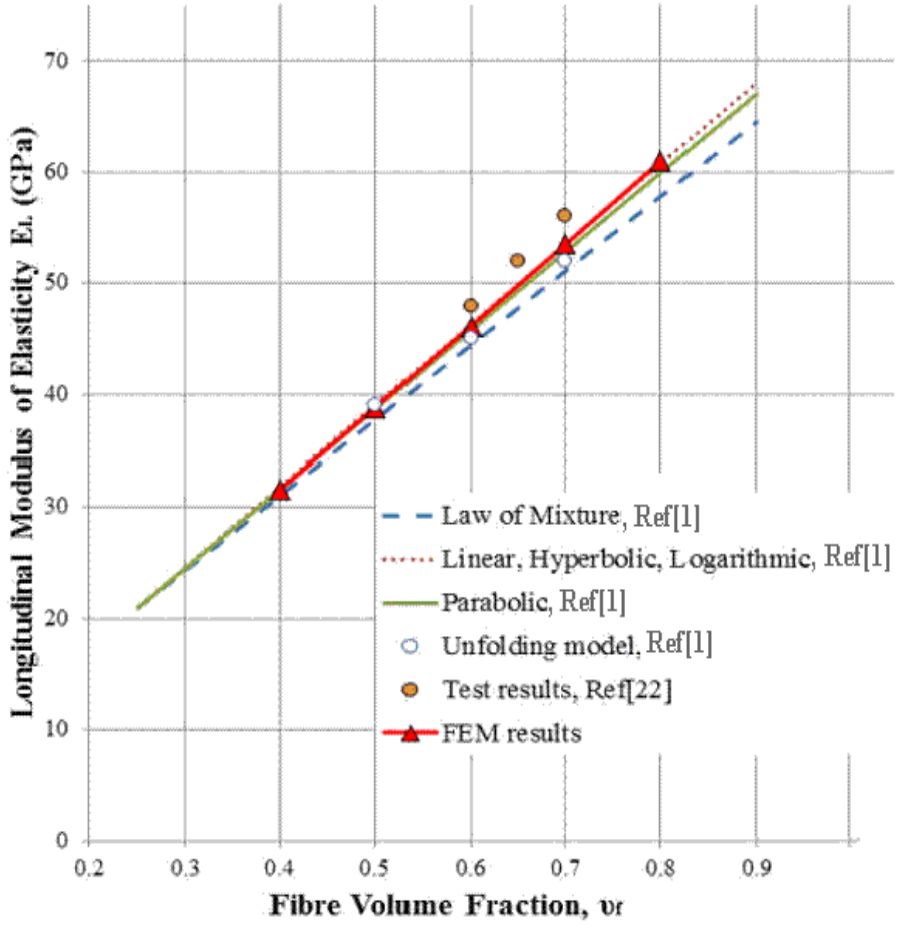

Σχήμα ε.6.5: Μεταβολή του διάμηκες μέτρου ελαστικότητας, E_L(longitudinal modulus of elasticity) ως προς την συγκέντρωση των ινών κατ' όγκο, υ_f (fibre volume ratio), σε μικρομηχανική ανάλυση που προϋποθέτει την ύπαρξη ενδιάμεσης φάσης, [4]

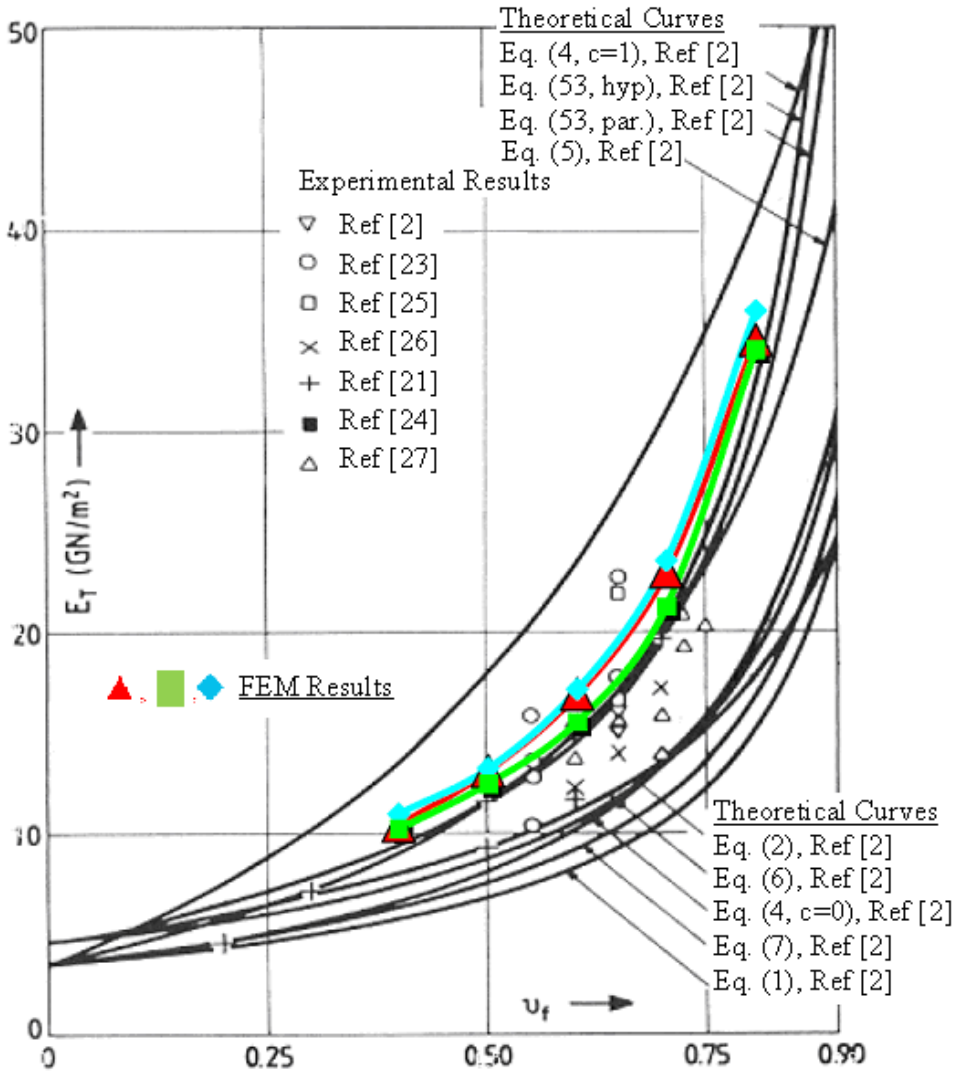

Σχήμα ε.6.6: Μεταβολή του εγκάρσιου μέτρου ελαστικότητας, E_T (transverse modulus of elasticity) ως προς την συγκέντρωση των ινών κατ' όγκο, υ_f (fibre volume ratio), σε μικρομηχανική ανάλυση που προϋποθέτει την ύπαρξη ενδιάμεσης φάσης, [4]

Πέραν των ελαστο-στατικών μικρομηχανικών αναλύσεων που έλαβαν χώρα, έγινε σχετική προσπάθεια για προσφορά στη γνώση και στο χώρο των ελαστο-δυναμικών μικρομηχανικών αναλύσεων. Το μικρομηχανικό μοντέλο που χρησιμοποιήθηκε σε αυτές τις αναλύσεις, παρουσιάζεται στο σχήμα ε.6.7. Λόγω της πολυπλοκότητας του αριθμητικού σχήματος επίλυσης, η μοντελοποίηση έλαβε χώρα με την υπόθεση της μη ύπαρξης ενδιάμεσης φάσης. Η μελέτη είχε σαν σκοπό να διερευνήσει την απόκριση του μικρομηχανικού μοντέλου σε συνθήκες δυναμικής φόρτισης κατά την εγκάρσια διεύθυνση όπου οι ιδιότητες της μήτρας έχουν σημαντική προσφορά στην απόσβεση των δονήσεων. Τα μέτρα ελαστικότητας του υλικού που μετρούν την διατήρηση και την απώλειας της ελαστικότητας (storage E’ and loss E’’ modulus) κατά την εγκάρσια διεύθυνση, E'_T και E''_T αντίστοιχα, είναι χαρακτηριστικά μεγέθη για την ποσοτικοποίηση της απόσβεσης του υλικού σε δυναμική φόρτιση.

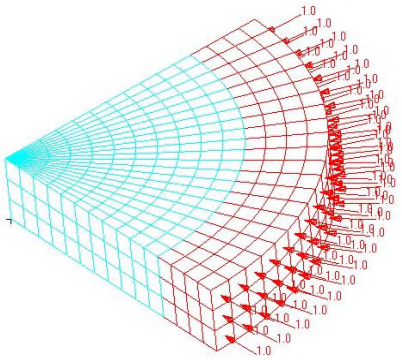

Σχήμα ε.6.7: Μικρομηχανικό μοντέλο σε εγκάρσια φόρτιση για την δυναμική μελέτη [5]

Οι ελαστο-δυναμικές ιδιότητες της μήτρας και της ίνας αντίστοιχα είχαν θεωρηθεί δεδομένες για την ανάλυση. Η υπόθεση ήταν ότι η ίνα δεν θα επιδείξει ποσοστό απώλειας της ελαστικότητας και η περιγραφή της μεταβολής των μεγεθών για την μήτρα, παρατίθενται στο σχήμα ε.6.8.

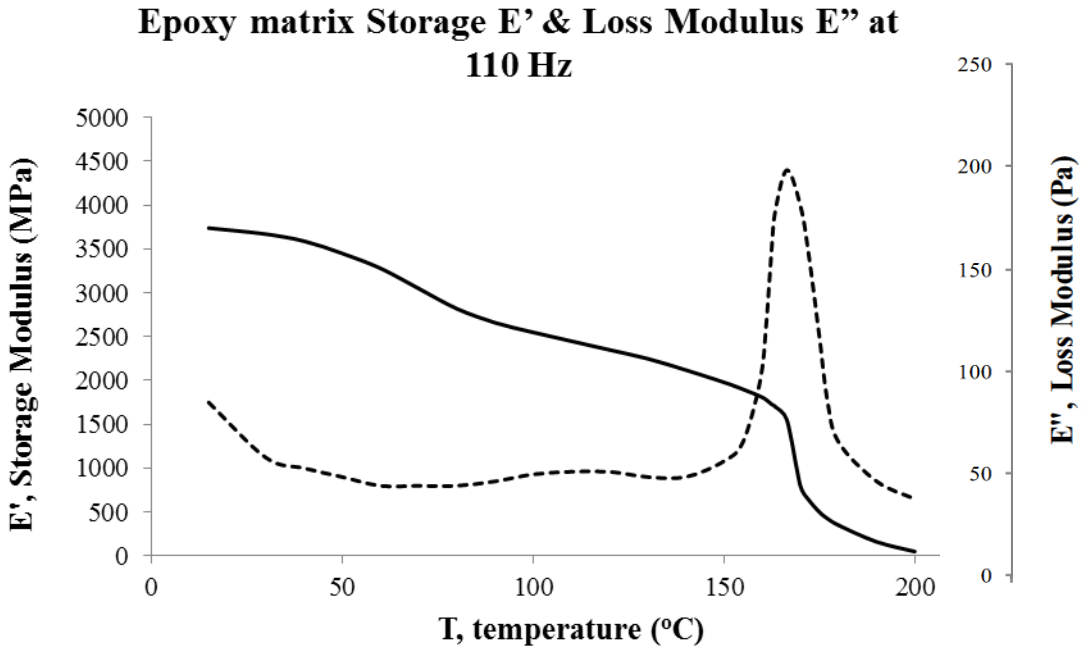

Σχήμα ε.6.8: Μεταβολή μέτρων ελαστικότητας της μήτρα υπό δυναμικό φορτίο με συχνότητα 100Hz, σε σχέση με την θερμοκρασία [5]

Η αναλυτική και πειραματική επίλυση του προβλήματος οι οποίες είχαν δημοσιευθεί σε προηγούμενες εργασίες του χώρου, συσχετίστηκαν με τα αριθμητικά αποτελέσματα σε ικανοποιητικό βαθμό. Τα παρακάτω σχήματα ε.6.9 και ε.6.10, παρουσιάζουν την εν λόγω συσχέτιση.

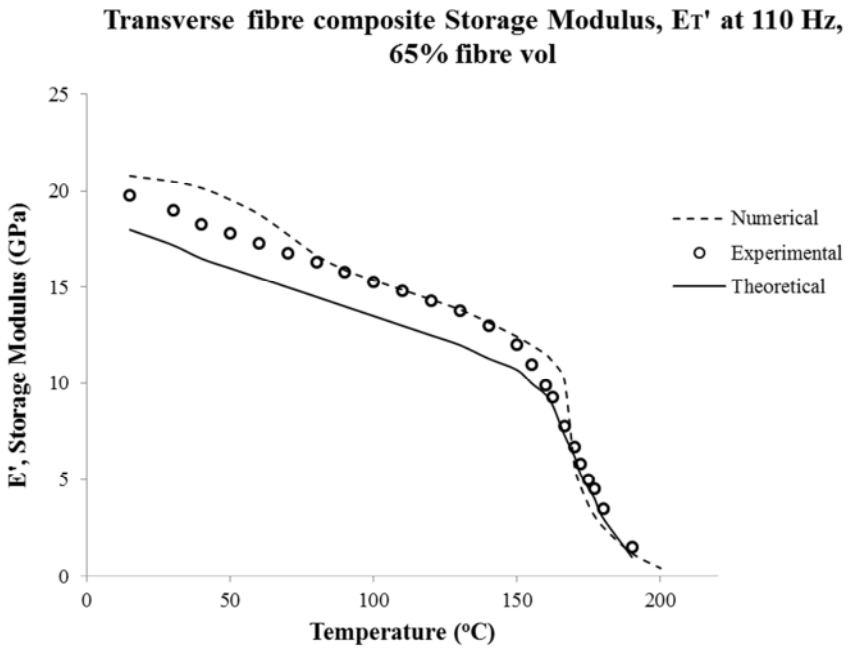

Σχήμα ε.6.9: Συσχέτιση του εγκάρσιου μέτρου διατήρησης της ελαστικότητας των αριθμητικών αποτελεσμάτων με αναλυτικά και πειραματικά από άλλες εργασίες του χώρου

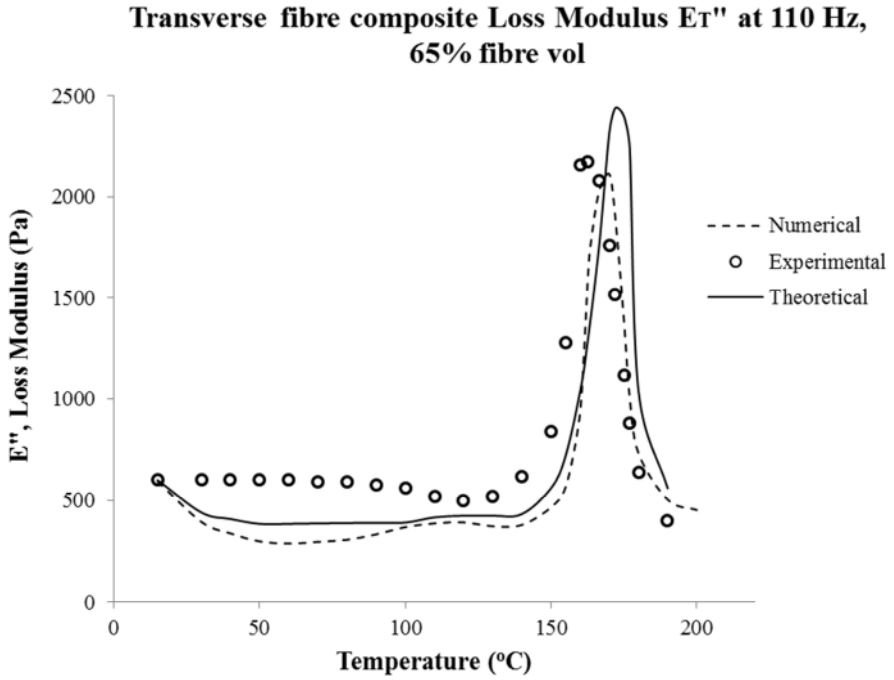

Σχήμα ε.6.9: Συσχέτιση του εγκάρσιου μέτρου απώλειας της ελαστικότητας των αριθμητικών αποτελεσμάτων με αναλυτικά και πειραματικά από άλλες εργασίες του χώρου

Στο κυρίως σώμα της διατριβής, παρουσιάζονται και ορισμένες επιλεγμένες και αντιπροσωπευτικές μελέτες από άλλους ερευνητές του χώρου, με σκοπό την πιο ολοκληρωμένη παρουσίαση του ρόλου της μικρομηχανικής στον χώρο της ανάλυσης των ιδιοτήτων των συνθέτων υλικών και πιο ειδικά των μηχανικών ιδιοτήτων που σχετίζονται με την αντοχή.

Επιγραμματικά, τα κύρια σημεία και τα συμπεράσματα του έκτου κεφαλαίου, παρατίθενται κάτωθι. Για την πιο ορθή κατανόηση των συμπερασμάτων, θα πρέπει να γίνει ανάγνωση του έκτου κεφαλαίου του κυρίως σώματος της διατριβής και ενδεχομένως ανάγνωση μερικών από τις αναφορές του κεφαλαίου αυτού.

- Οι μικρομηχανικές αναλύσεις είναι μια σημαντική περιοχή ευρέως αναπτυσσόμενη και πολλά υποσχόμενη ως προς την μοντελοποίηση των ιδιοτήτων των υλικών σε μικρομηχανική κλίμακα. Διαφαίνεται ότι θα αποτελέσουν τον συνδετικό κρίκο μεταξύ μικροκλίμακας και μακροκλίμακας μοντελοποίησης, μιας και τα αποτελέσματα της συμπεριφοράς από μικρομηχανικές αναλύσεις μπορούν να αποτυπωθούν και να ορίσουν την συμπεριφορά αριθμητικών στοιχείων μεγαλύτερης κλίμακας.
- Οι υπολογιστικές απαιτήσεις μικρομηχανικών αναλύσεων είναι μεγάλες και για αυτό η μοντελοποίηση είναι δύσκολο να επεκταθεί σε μεγαλύτερα χωρία από αυτών που εμπεριέχουν μερικές δεκάδες ίνες.
- Για να γίνει σωστή συσχέτιση πειραματικών και υπολογιστικών μοντέλων θα πρέπει να γίνει και η αντιπαραβολή τους στην μικρομηχανική κλίμακα πράγμα που είναι περίπλοκο σε ότι αφορά τις πειραματικές διατάξεις και σε κάποιες περιπτώσεις ακόμα και αδύνατο.

Εισ.7) Συμπεράσματα διατριβής και μελλοντική έρευνα

Εντός του κυρίως σώματος της διατριβής και στο τέλος των επιμέρους κεφαλαίων, αναφέρονται τα κύρια σημεία και συμπεράσματα ανά κεφάλαιο. Στο έβδομο κεφάλαιο της διατριβής, παρατίθενται μια συνοπτική εικόνα των ιδίων συμπερασμάτων μαζί με προτάσεις για μελλοντική έρευνα:

- Η απόδειξη συμμόρφωσης με τις προδιαγραφές Αξιοπλοΐας αποτελεί μεγάλο μέρος του κόστους σχεδιασμού των αεροκατασκευών. Η βιομηχανία των αεροκατασκευών στην προσπάθεια για την μείωση αυτού του κόστους, προσπαθεί να χρησιμοποιήσει αριθμητικές μεθόδους για την εκπλήρωση των προδιαγραφών αντοχής. Οι αριθμητικές μέθοδοι πρέπει να ωριμάσουν περισσότερο ως προς τον τρόπο περιγραφής της δημιουργίας αστοχιών και της εξελικτικής τους πορείας μέχρι την τελική έτσι ώστε τα αποτελέσματα αυτών να χρησιμοποιηθούν να γίνει περαιτέρω συρρίκνωση αυτού του κόστους. Σήμερα, οι αεροκατασκευές δεν μπορούν να πιστοποιηθούν βάσει αριθμητικών αναλύσεων ή άλλων αναλυτικών μεθόδων μόνο.

- Οι απαιτήσεις συμμόρφωσης των αεροκατασκευών ως προς την αντοχή τους βάσει των προτύπων Αξιοπλοΐας, δεν θα απαλλαγούν από την απαίτηση για την απόδειξη αυτής με πειραματικές διατάξεις. Υπάρχουν όμως δυνατότητες συρρίκνωσης των απαιτήσεων και συνεπακόλουθα του κόστους των πειραματικών δοκιμών με την αντικατάσταση αυτών από πιο πιστές αριθμητικές προσομοιώσεις. Σημαντικό ρόλο σε αυτόν το τομέα θα παίξει η συσσώρευση εμπειρίας της επιστημονικής κοινότητας γύρω από την εφαρμογή των αριθμητικών μεθόδων και την επιτυχή συσχέτιση αυτών με πειραματικές δοκιμές.

- Εγκεκριμένες αναλύσεις και μεθοδολογίες που χρησιμοποιούνται για την απόδειξη της αντοχής των αεροκατασκευών από σύνθετα υλικά οι οποίες οι οποίες έχουν αξιολογηθεί και πιστοποιηθεί επί των μεταλλικών κατασκευών, θα πρέπει να επανεξετάζονται

- Η μέθοδος των πεπερασμένων στοιχείων έχει εφαρμοστεί με επιτυχία στον παραμετρικό σχεδιασμό των αεροκατασκευών, στην εφαρμογή της για την εξαγωγή

εσωτερικών φορτίων στην κατασκευή και για την προσομοίωση της απόκρισης αυτής σε φόρτιση έως του σημείου εμφάνισης των αρχικών αστοχιών. Για την περαιτέρω εφαρμογή της μεθόδου των πεπερασμένων στοιχείων σε φόρτιση της κατασκευής στην οποία έχει δημιουργηθεί η προϋπήρχε ζημιά, θα πρέπει να μοντελοποιηθούν η έναρξη και η εξέλιξη της ζημιάς. Αυτές οι αριθμητικές διατυπώσεις δημιουργούν υψηλό υπολογιστικό κόστος ειδικά σε κατασκευές μεγάλης κλίμακας με ζημιές στο επίπεδο μικρο-κλίμακας. Η μοντελοποίηση κατασκευών μεγάλης κλίμακας με ατέλειες γεωμετρικές, υλικού ή άλλες, μαζί με την μοντελοποίηση της έναρξης της αστοχίας και της προοδευτικής εξέλιξης αυτής και απόδειξη καλού συσχετισμού με πειραματικές δοκιμές θα αποτελέσουν το κλειδί για την περαιτέρω εφαρμογή της μεθόδου των ΠΣ στην διαδικασία σχεδιασμού και πιστοποίησης.

- Είναι αναπόφευκτο γεγονός ότι οι αεροπορικές κατασκευές θα δεχθούν κρούσεις από ξένα σωματίδια κατά την διάρκεια της ζωής τους. Οι κρούσεις αυτές είναι πιο κρίσιμες και επιβλαβής στις κατασκευές από σύνθετα υλικά. Το κόστος πιστοποίησης της αντοχής των κατασκευών είναι μεγαλύτερο σε πειραματικές διατάξεις μεγάλων κατασκευαστικών συναρμολογημάτων. Οι αριθμητικές αναλύσεις σε επίπεδο μικρών δοκιμίων έχουν αναπτυχθεί όμως απαιτούν αρκετή υπολογιστική ισχύ. Αντίστοιχες μελέτες σε κατασκευές μεγάλης κλίμακας, χρειάζονται περαιτέρω μελέτη.

- Οι μικρο-μηχανικές αναλύσεις έχουν επιδείξει καλά αποτελέσματα στην ανάλυση της προοδευτικής αστοχίας στα σύνθετα υλικά και στο επίπεδο της μικρο-κλίμακας. Αποτελέσματα από τις αναλύσεις αυτού του είδους μπορούν να τροφοδοτηθούν σε μοντέλα μεσο-κλίμακας και με αυτόν τον τρόπο να επιτευχθούν πιο πιστές αριθμητικές προσομοιώσεις σε κατασκευαστικά συναρμολογήματα. Οι μικρο-μηχανικές αριθμητικές αναλύσεις πρέπει να τροφοδοτηθούν με τις ιδιότητες αντοχής στην θραύση των επιμέρους φάσεων του συνθέτου, τις ιδιότητες της αντοχής στην θραύση της ενδιάμεσης φάσης, τις ιδιότητες τις πλαστικής απόκρισης της μήτρας κ.α. Για μερικές από αυτές δεν υπάρχει τρόπος εξεύρεσης αυτών σήμερα. Η καλή συσχέτιση μεταξύ αριθμητικών προσομοιώσεων και πειραματικών δοκιμών

μοντέλων που χρησιμοποιούν ιδιότητες από την μικρο-κλίμακα, επίσης δεν έχουν αναπτυχθεί.

Αναφορές εισαγωγικού κεφαλαίου

[1] Ioannis K. Giannopoulos, Efstathios E. Theotokoglou and Xiang Zhang. Design and numerical modelling of a pressurized airframe bulkhead joint. AIAA, Journal of Aircraft, Vol.52, No 6, pg. 1729-1735, Nov-Dec 2015

[2] K.I. Tserpes, V. Karachalios, I. Giannopoulos, V. Prentzias, R. Ruzek Strain and damage monitoring in CFRP fuselage panels using fiber Bragg grating sensors. Part I: Design, manufacturing and impact testing. Composite Structures 107 (2014) 726–736

[3] Ioannis K. Giannopoulos, Efstathios E. Theotokoglou, Xiang Zhang. Impact damage and CAI strength of a woven CFRP material with fire retardant properties. Composites Part B: 91 2016, 8-17

[4] E. Sideridis, E.E. Theotokoglou & I. Giannopoulos: Analytical and computational study of the moduli of fiber-reinforced composites and comparison with experiments, Composite Interfaces, 2015, Vol 22, Issue 7, pg. 563-578

[5] Efstathios E. Theotokoglou, Emilio Sideridis, Ioannis Giannopoulos. Analytical and computational solution of moduli and fracture of fiber reinforced composites. 20th European Conference on Fracture (ECF20).Procedia Materials Science 3 (2014) 880 – 885

[6] Efstathios E. Theotokoglou, Ioannis Giannopoulos, Emilio Sideridis. Analytical, experimental and numerical approach of storage and loss moduli of fibre reinforced epoxy composites. 20th International Conference on Composite Materials Copenhagen, 19-24th July 2015

[7] European Aviation Safety Authority (2015). CS-25: Certification Specification and Acceptable Means of Compliance for Large Aeroplanes, Amendment 17. EASA, Germany.

[8] EASA, European Aviation Safety Authority (2010). AMC 20-29: Acceptable Means of Compliance - Composite Aircraft Structure. EASA, Germany.

[9] Becker, W., and Wacker, T., “Comparison Between Test and Analysis of a Tank Bulkhead Loaded in the Plastic Range,” Aerospace Science and Technology, Vol. 1, No. 1, 1997, pp. 77–81.

[10] https://www.gov.uk/aaib-reports/lockheed-l1011-385-1-14-g-bbaf-19-july-1998

Chapter 1

"Introduction to the subject"

1.1 Objective of the thesis

The objective of the thesis is to provide with an overview and a critical evaluation in the strength prediction of composite material airframe structures via testing and numerical computational methods. The demonstration will be performed through the presentation of representative application examples at different modelling levels / scales where the author of the thesis contributed to the knowledge in the respective field through published work. It is of great importance to explore the maturity and reliability levels of the existing numerical analyses methods used for strength prediction today and to assess whether enough experience exist in their utilization in order to be used for showing compliance to airworthiness requirements, effectively substantiating a large portion of compliance verification testing.

1.2 Thesis scope: Applied loading, materials studied and applicable numerical methods

The subject of *numerical modelling and testing in the strength prediction of fibre reinforced polymer airframe structures* is a vast area of previous and current ongoing research. The scope of the thesis was limited form the start in terms of the *external applied loading* and in terms of the composite *materials* employed in the studies.

In terms of the *applied structural loading*, the scope of the study is limited to assuming the structural strength under *quasi statically* applied *mechanical* loading. Structural behaviour under foreign object low velocity impact events are discussed as well for generating an understanding of the damage inflicted and to further explore the fracture processes under quasi static applied compression loading. Structural response under fatigue loading is not a part of the study presented herein.

In terms of *fibre reinforced polymer materials, mainly* unidirectional and woven carbon fibre reinforced plastic material systems used in the aerospace sector primary and secondary structures are mentioned within the thesis.

In terms of *numerical models analyses and methods*, the ones applicable to large scale structural strength prediction and are currently utilized in the industry on large scale models are discussed.

1.3 Thesis structure

The thesis comprises of chapters highlighting the findings / contributions of the published work. The chapters are sequenced in a way to provide the reader with a smooth transition for better understanding of the work done and not according to the publication date of the accepted article manuscripts. At the end of each section and according to the author's opinion, the importance of the published research is presented and the impact of the results to the scientific community is discussed.

Since it was not possible to make a contribution to knowledge at every single thematic area, on occasions, where there is no contribution from the author, other research in the field is presented instead, for the sake of generating a coherent document structure. In such occasions nevertheless, the importance of the presented research is evaluated and its relation to the author's findings is explained.

1.4 References to other research in the field

Within each chapter reference to other research studies in the field are quoted and presented. These studies are by no means an exhaustive list of the active research currently taking place in that particular field of knowledge. They represent a selection of publications which according to the author's opinion are representative and more properly address the point that need to be made.

References cited in the discussion within the chapters are cited at the end of the chapters.

1.5 Thesis structure

The thesis content is structured around the published work from the author and his co-authors. Figure 1.1 presents the information flow within the manuscript and figure 1.2 shows the relation of *some* of the items with the airframe certification process.

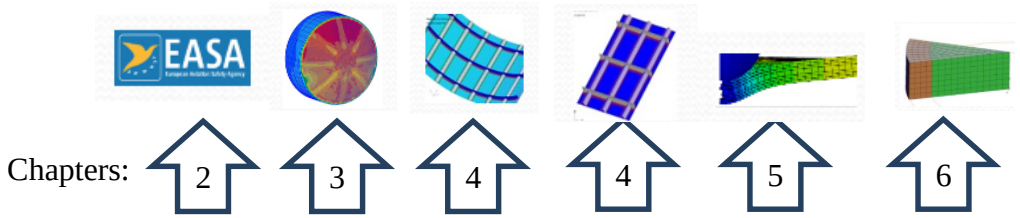

Figure 1.1: Information presented within the thesis:

Overview (short description) of the thesis contents:

- In chapter one, a short introduction to the subject is presented along with the thesis aims and objectives
- In chapter two, the definition of structural strength of airframe structures according to Airworthiness certification specification requirements is described and the relation of the certification requirements to the numerical analysis methods
- In chapter three, a design case numerical finite element study on a composite material bulkhead joint is presented as the primary application of numerical methods in the field of structural analysis
- In chapter four, the numerical analysis of a stiffened panel under compression is shown. The analysis is benchmarked against test results
- In chapter five, the topic of foreign object low velocity impact damage and the compression after impact strength is described by means of a testing research study
- Chapter six discusses the current advances in the field of micromechanical numerical modelling and paves the way to future numerical prediction trends
- In chapter seven, although summaries and conclusions to a specific subject area are presented in each of the previous chapters, the overall top level summary and conclusions of the thesis is presented.

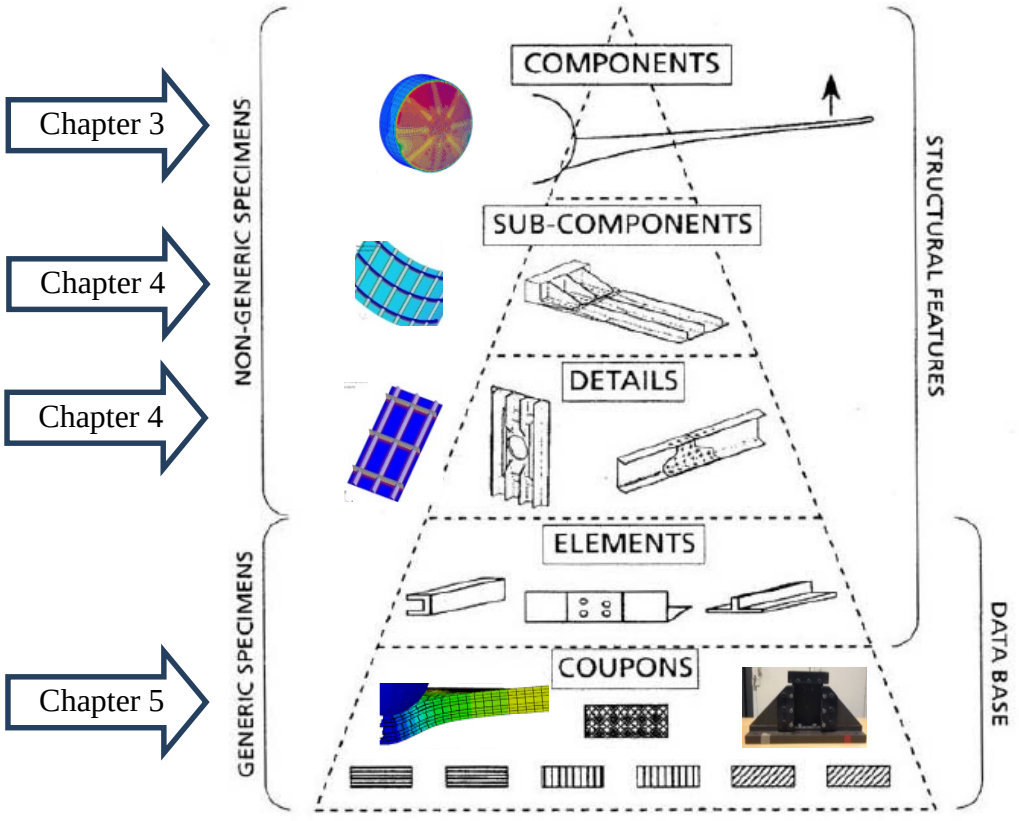

Figure 1.2: Relation of the work presented within the thesis, overlaid to the airworthiness certification test pyramid [1]

Figure 1.2 graphically presents the relation of the numerical examples work presented within the thesis, in an effort to correlate the modelling application areas with the certification requirements testing pyramid.

1.6 References to chapter one

[1] EASA, European Aviation Safety Authority (2010). AMC 20-29: Acceptable Means of Compliance - Composite Aircraft Structure. EASA, Germany.

< *Page intentionally left blank* >

Chapter 2

"Definition of Strength of Airframe Structures"

The chapter aims at providing the engineering and non-engineering audience with an understanding to the meaning of "Structural Strength", when an airframe structure is loaded under quasi static loading conditions. The indirect explanation provided to the term is the result of the discussion presented in the chapter of the respective specification clauses within EASA's CS-25 Airworthiness Certification Specifications which are used as examples. The resulted definition of structural strength is the engineering community's perception to the meaning of strength in the airframe industry.

< *Page intentionally left blank* >

2.1 Introduction to the strength analysis of airframe components

The definition of "Structural Strength" which in a simple format can be stated as "*the ability of the structure to withstand loading without failure"* is more properly stated and more thoroughly explained within the respective regulations/directives provided from the Airworthiness authorities. More specifically within this thesis, reference to strength will be regarded in accordance to the *Proof of Compliance clauses* as dictated in the relevant airworthiness specifications, adherence to which will assure the adequacy of the airframe strength-wise and will certify the airframe product to the relevant certification specifications. Within the thesis context, strength will be implied as the ability of the structure to resist quasi statically externally applied mechanical loading. Dynamic and Fatigue loading and their effects are not considered.

Following the discussion in the definition of structural strength, certain parts embedded within the specification will be highlighted, where the engineering community's perception of strength and in depth understanding of the response of the structure is distilled into a few specifications-statements. Those statements have been derived from years of designing and operating aircraft structures and they can be sought as being the engineering "*heritage*" in the understanding of the airframe structural response and in terms of safeguarding against failure. Also, a hint in the "*bias*" embedded into the certification specifications towards the more traditional aluminium airframe structural design will be discussed.

The discussion in this chapter will be the demonstration of problems that could be the result of *not properly adapt* the knowledge and understanding in the structural response to analyse and certify airframe structures made of composite materials, knowledge which has been generated through years of using the more traditional aluminium materials.

2.2 Structural strength definition; Regulatory and certification authorities

Airframe structures are built by design organizations that have been certified by regulating authorities to design and manufacture airframe components. Certification is

sought by appropriate regulatory and certification authorities and will provide the design organization the ability to commercialize its manufactured products.

With the exception of the military sector, nowadays, airworthiness regulations seem to, *roughly, converge* into a common set of rules. Within this thesis, demonstrations using a set from European Aviation Safety Agency (EASA) certification specifications will be the basis. Since elementary specifications are referenced, there are practically minor differences between the certification specifications from different regulatory authorities.

2.3 European Aviation Safety agency (EASA)

Quoting from https://easa.europa.eu/the-agency : *"EASA is the European Union Authority for aviation safety. The main activities of the organization include the strategy and safety management,* ***the certification of aviation products*** *and the* ***oversight of approved organizations*** *and EU Member States.*

EASA enjoys technical, financial and legal autonomy to ensure the highest common level of safety protection for EU citizens within the EU and worldwide, to ensure the highest common level of environmental protection, ***to avoid duplication in the regulatory and certification processes among Member States*** *and to facilitate the creation of an internal EU aviation market.*

EASA also plays a leading role within the EU External Aviation Policy: the Agency is ***a strong counterpart of other Aviation Authorities outside the EU*** *(e.g. USA, Canada, Brazil) and a major contributor to the export of the EU aviation standards worldwide, in order to promote the* ***free movement of EU aeronautical products****, professionals and services throughout the world."*

The certification of the aviation products is ensured through directives called "Airworthiness Certification Specifications" and they can refer to the so called "initial airworthiness" meaning to the design of a new aircraft, or to "continuing airworthiness requirements" where the requirements for maintaining already existing aircraft platforms are dictated. Depending on the actual aircraft design type, the specifications vary. As an example, if a design organization would like to design a large passenger aircraft, then the CS-25 specifications have to be followed [1].

2.4 EASA Airworthiness Certification Specifications

Although a structural component must be proven capable of withstanding dynamic and fatigue loading as well, in the paragraphs that follow, for the sake of simplicity and in order to remain within the domain of interest, the specifications that relate to the strength requirements under quasi statically external applied loading will be presented and discussed.

According to the author's opinion and on certain occasions, the parts of the specifications that were needed for the discussion were presented and not the full description of each specification. Wherever this is the case, it is clearly underlined. In order to avoid misunderstanding that could be the result of this truncation, the readers of the thesis are advised to refer to [1] for the complete description of the specifications in question.

2.4.1 EASACS-25: Specifications for static strength

Directly quoting from reference [1], the parts of each of the specifications were discussion will take place upon:

*"**CS 25.301 Loads***

*Strength requirements are specified in terms of **limit loads** (the maximum loads to be expected in service) and **ultimate loads** (limit loads multiplied by prescribed factors of safety). Unless otherwise provided, prescribed loads are limit loads. (Continues but not shown here)*

CS 25.303 Factor of safety

*Unless otherwise specified, **a factor of safety of 1.5** must be applied to the prescribed limit loads which are considered external loads on the structure. When loading condition is prescribed in terms of ultimate loads, a factor of safety need not be applied unless otherwise specified.*

CS 25.305 Strength and deformation

(a) The structure must be able to ***support limit loads without detrimental permanent*** *deformation. At any load up to limit loads, the deformation may not interfere with safe operation.*

(b) The structure must be able to ***support ultimate loads without failure*** *for at least 3 seconds. (Continues but not shown here)*

CS 25.307 Proof of structure

Compliance with the strength and deformation requirements of this Subpart must be shown for each critical loading condition. ***Structural analysis may be used*** *only if the structure conforms to that for which* ***experience has shown*** *this method to be* ***reliable****. In other cases,* ***substantiating tests*** *must be made to load levels that are sufficient to verify structural behaviour up to loads specified in CS 25.305. (Continues but not shown here)"*

2.4.2 EASA Acceptable Means of Compliance (AMC) to CS-25

The certification specifications are accompanied by the so called Acceptable Means of Compliance (AMC) documentation, which basically sets the foundation in terms of the proof needed to certify according to each separate specification.

Continuing to quote from reference [1] and under **AMC25.307** which is basically the acceptable means of showing compliance to CS 25.307, *"CS 25.307 requires compliance for each critical loading condition. Compliance can be shown* ***by analysis supported by previous test evidence, analysis supported by new test evidence or by test only.*** *As compliance by test only is impractical in most cases, a large portion of the substantiating data will be based on analysis.*

There are a number of standard engineering methods and formulas which are known to produce acceptable, often conservative results *especially for structures where load paths are well defined. Those standard methods and formulas, applied with a good understanding of their limitations, are* ***considered reliable analyses*** *when showing compliance with CS 25.307. Conservative assumptions may be considered in assessing whether or not an analysis may be accepted without test substantiation.*

The application of methods such as Finite Element Method or engineering formulas to complex structures in modern aircraft is considered reliable only when validated by full scale tests (ground and/or flight tests). Experience relevant to the product in the utilisation of such methods should be considered."

This last requirement is going to be the focus of the investigation within the thesis. The main outcome of the thesis is to explore the maturity of the numerical analyses methods as of today and whether they can be reliable enough or whether enough experience has been built round them so that they could be used for compliance to the requirements and substantiate a large portion of testing.

The approach to certifying a structural component is present below. Quoting from CS 25 certification specifications, AMC 25.307:

"*7. CERTIFICATION APPROACHES*

The following certification approaches may be selected:

a) Analysis, supported by new strength testing of the structure to limit and ultimate load. This is typically the case for New Structure.

Substantiation of the strength and deformation requirements up to limit and ultimate loads normally requires testing of sub-components, full scale components or full scale tests of assembled components (such as a nearly complete airframe). The entire test program should be considered in detail to assure the requirements for strength and deformation can be met up to limit load levels as well as ultimate load levels.

Sufficient limit load test conditions should be performed to verify that the structure meets the deformation requirements of CS 25.305(a) and to provide validation of internal load distribution and analysis predictions for all critical loading conditions.

Because ultimate load tests often result in significant permanent deformation, choices will have to be made with respect to the load conditions applied. This is usually based on the number of test specimens available, the analytical static strength margins of safety of the structure and the range of supporting detail or sub-component tests. An envelope approach may be taken, where a combination of different load cases is applied, each one critical for a different section of the structure.

These limit and ultimate load tests may be supported by detail and sub-component tests that verify the design allowables (tension, shear, compression) of the structure and often provide some degree of validation for ultimate strength.

b) Analysis validated by previous test evidence and supported with additional limited testing. This is typically the case for Similar New Structure.

The extent of additional limited testing (number of specimens, load levels, etc.) will depend upon the degree of change, relative to the elements of paragraphs 5(b)(i) and (ii).

For example, if the changes to an existing design and analysis necessitate extensive changes to an existing test-validated finite element model (e.g. different rib spacing) additional testing may be needed. Previous test evidence can be relied upon whenever practical.

These additional limited tests may be further supported by detail and sub-component tests that verify the design allowables (tension, shear, compression) of the structure and often provide some degree of validation for ultimate strength.

c) Analysis, supported by previous test evidence. This is typically the case for Derivative/ Similar Structure.

Justification should be provided for this approach by demonstrating how the previous static test evidence validates the analysis and supports showing compliance for the structure under investigation. Elements that need to be considered are those defined in paragraphs 5(b)(i) and (ii).

For example, if the changes to the existing design and test-validated analysis are evaluated to assure they are relatively minor and the effects of the changes are well understood, the original tests may provide sufficient validation of the analysis and further testing may not be necessary. For example, if a weight increase results in higher loads along with a corresponding increase in some of the element thickness and fastener sizes, and materials and geometry (overall configuration, spacing of structural members, etc.) remain generally the same, the revised analysis could be considered reliable based on the previous validation.

d) Test only.

Sometimes no reliable analytical method exists, and testing must be used to show compliance with the strength and deformation requirements. In other cases it may be elected to show compliance solely by tests even if there are acceptable analytical methods. In either case, testing by itself can be used to show compliance with the strength and deformation requirements of CS-25 Subpart C. In such cases, the test load conditions should be selected to assure all critical design loads are encompassed.

If tests only are used to show compliance with the strength and deformation requirements for single load path structure which carries flight loads (including pressurisation loads), the test loads must be increased to account for variability in material properties, as required by CS 25.307(d). In lieu of a rational analysis, for metallic materials, a factor of 1.15 applied to the limit and ultimate flight loads may be used. If the structure has multiple load paths, no material correction factor is required."

2.4.3 Discussion on the EASA CS 25 and respective AMCs

Externally applied static loading does not represent, in most of the cases, the actual loading that the structure will be exposed to during service. In nature, loads are time dependant which can greatly affect the structural response. Yet, proving the proof of the structural capability to withstand quasi-statically applied loads is a specification requirement. Within the certification specifications, requirements also describe the need to address other types of loads like dynamic, fatigue, impact and others, but conformance to the strength requirements from externally applied quasi-statically applied loading can be regarded as the cornerstone check in the design process.

Per **CS 25.301** [1], there are two distinctive sets of static loading that the airframe structures have to be designed for and be proven capable to withstand and operate under: limit loads and ultimate loads. Limit loading is the actual loading to be carried during service and ultimate loading is the limit multiplied by a factor of 1.5, according to **CS 25.303** [1].

Airframe industry is striving to create the lightest possible structure. A lighter structure means less fuel needed for operation hence the design is more eco-friendly and

it can also mean less loading on the structure which in its turn can lead into an even lighter aircraft. The design loop explained in the previous sentence is a simplistic approach to the airframe design process. A certain mass is initially assumed for a new aircraft design based on experience, the loads are worked according to the missions of the aircraft, process which then leads into the design of the structure. If the structure is found to be lighter or heavier, then the loading is re-iterated to give a new structure and so on. The ultimate load factor is a detrimental quantity into this process since it enhances the loading to which the structure must show compliance to in terms of strength requirements.

The **ultimate factor,** or in a more general approach, the engineering concept of the application of safety factors, is the common engineer's approach to meet the design requirements at an enhanced loading environment in order to cater for the uncertainty in the predictions and the unpredictability in the natural events. The smaller the ultimate factor, the lighter the resulted engineering design will be. The reason for the **ultimate factor being set to 1.5** in the airframe industry is due to the *legacy*, the *tradition* in the airframe design. This factor has been distilled through the years of airframe design and operating experience. The safety factor used to be larger and gradually through the years has reached the level of 1.5 when the design and analysis process became more reliable. On occasions and for some military projects only, this factor has been set to 1.4. It could be the case that for certain aircraft vehicles and certain specific missions and aircraft utilization, special certifications specifications have been tailored suggesting different safety factors. In such cases, the authority providing with that set of specifications would the responsible body for ensuring safety in a wider sense. This is the reason why deviations from the widely accepted specifications are met only in the military sector and prototype air vehicle designs.

Per **CS 25.305** [1], the structure has to carry limit loading without any *detrimental permanent deformation* taking place. The term *detrimental permanent deformation* has been inherited by the extensive metallic material usage in the airframes. It can certainly adapt to the new era of composite materials but it is worthwhile suggesting that for composites structures, *detrimental permanent deformation* is much closer to *ultimate material failure* in terms of loading than for metallic materials. **CS 25.305** [1] specification practically allows the structure to yield locally on occasions as long as

these local effects are not going to be detrimental for the airframe system operation. This is one of the areas where the translation of the specifications to airframes made of fibre reinforced polymers should be regarded differently. For the metallic materials, local yielding and the subsequent local hardening of the area under yield and the redistribution of load to other parts of the structure could be allowed. For the case of composite materials, the slightest permanent deformation can potentially be detrimental to safety.

Ultimate loading, the multiplication of the limit loading by the safety factor, is a concept engulfing the uncertainty and the unpredictability in the design process. Ultimate loads are not supposed to be met during service, yet the requirements suggest that the structure has to be proven to be able to withstand that loading for at least 3 seconds prior to failure, see **CS 25.305** (b) [1].

Engineering analysis methods provide the means to analyse the structural loading within the various structural components, action which in its turn provide the means to decide on whether the respective structure is going to be capable of bearing the respective loading. Quoting from **C.S. 25.307 Proof of structure [1]**, *"Structural analysis may be used only if the structure conforms to that for which* ***experience has shown this method to be reliable****."*

For the above mentioned certification specification, in the Acceptable Means of Compliance section (A.M.C) of the documentation, the following is stated:

A.M.C to C.S. 25.307 [1]:*"…..There are a number of standard engineering methods and formulas which are known to produce acceptable, often conservative results especially for structures where load paths are well defined. Those standard methods and formulas, applied with a good understanding of their limitations, are considered reliable analyses when showing compliance with CS 25.307…", "……The application of methods such as Finite Element Method or engineering formulas to complex structures in modern aircraft is considered reliable only when validated by full scale tests (ground and/or flight tests). Experience relevant to the product in the utilisation of such methods should be considered."*

Capturing the essence in the above mentioned statements:

- There are engineering methods which can be considered to provide with reliable analyses. These have resulted from experience. They have been proven in practice. They constitute our "heritage" in the understanding of the structural response. They have emerged through the previous years of airframe design where the dominant materials in the primary components where mostly metallic (*Definition of primary structural component: a major load carrying structural part whose failure can cause the loss of aircraft, as for example the fuselage skin*)
- Unless performing full scale testing Finite Element Method or engineering formulas to complex structures in modern aircraft are generally ***not*** considered reliable analyses, hence are not considered acceptable means for compliance.

The discussion above was aimed at highlighting the following:

- Up to date, the engineering community has learned to design, analyse and certify airframe structures which were mainly made of metallic materials, mostly made of aluminium materials. The levels of uncertainty and unpredictability in the design and analysis process have been field tested on such metallic structures. One of the reasons that have led to the reduction of the ultimate factor to 1.5 on occasions and for military projects was the effect of the growing reliance on the analysis/test prediction methods. Quoting from CS 25.307 [1]. ***There are a number of standard engineering methods and formulas which are known to produce acceptable results***. So the engineering community has learned to rely on analyses methodologies were appropriate, which were later on tested on metallic airframes. This is the main reason why novel structures employing fibre reinforced composite materials will require extensive testing.

It is evident from the above mentioned paragraphs, that testing plays a very important role in the certification process and it hardly the case where a structural component can be certified based solely on analysis tools.

Quoting from AMC 20-29 ref [2], specification which specifically targets composite material structures: "*The strength of the composite structure should be reliably*

established, incrementally, through a programme of analysis and a series of tests conducted using specimens of varying levels of complexity. Often referred to in industry as the "building block" approach, these tests and analyses at the coupon, element, details, and sub-component levels can be used to address the issues of variability, environment, structural discontinuity (e.g., joints, cut-outs or other stress risers), damage, manufacturing defects, and design or process-specific details. Typically testing progresses from simple specimens to more complex elements and details over time. This approach allows the data collected for sufficient analysis correlation and the necessary replicates to quantify variations occurring at the larger structural scales to be economically obtained. The lessons learned from initial tests also help avoid early failures in more complex full-scale tests, which are more costly to conduct and often occur later in a certification programme schedule"

Hence, new development programs will involve testing for certification. Numerical analysis can help in that regards indirectly, for example by evaluating the effect of various design parameters and help with downsizing the testing program. In figure 2.1, a testing certification pyramid example is presented aimed at certifying a military airframe Cargo Door.

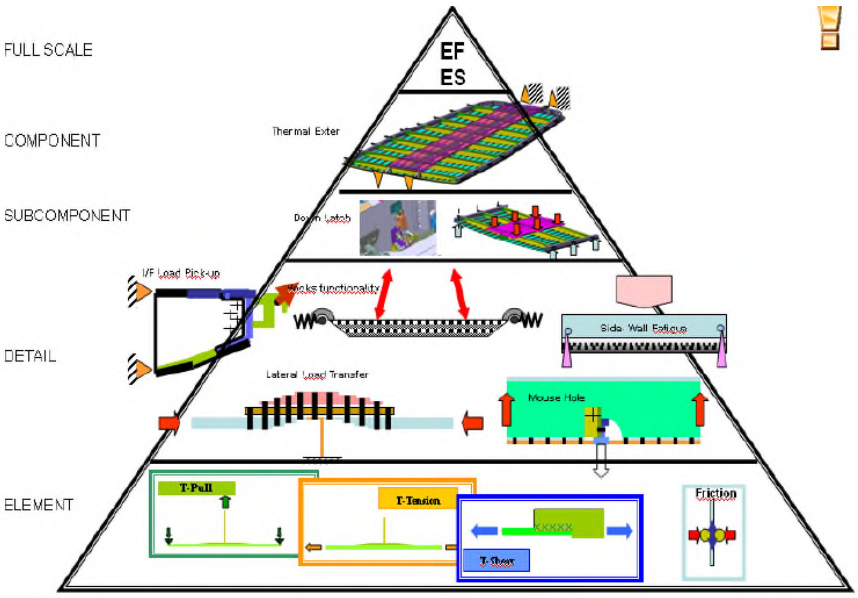

Figure 2.1: Certification testing pyramid. Simpler specimens and conceptual studies reside at the bottom of the pyramid, with higher volume of test articles for validations. Larger component situated towards the top with fewer test articles to be tested.

A similar information presentation flow with the airworthiness specification testing pyramid will be used as a guideline to the presentation of the chapters in the thesis as already explained and also shown in figure 2.2. The information in the chapters has been derived from different components and different composite materials used but the aim is to present examples of applied numerical analysis in representative structural items ranging from large components to coupons. Only a representative number of analyses are shown in order to limit the scope of the thesis. The overall aim it to explore the application field of the FE analysis methods into the strength prediction and to assess the maturity and the role it can play to future certification testing substantiation.

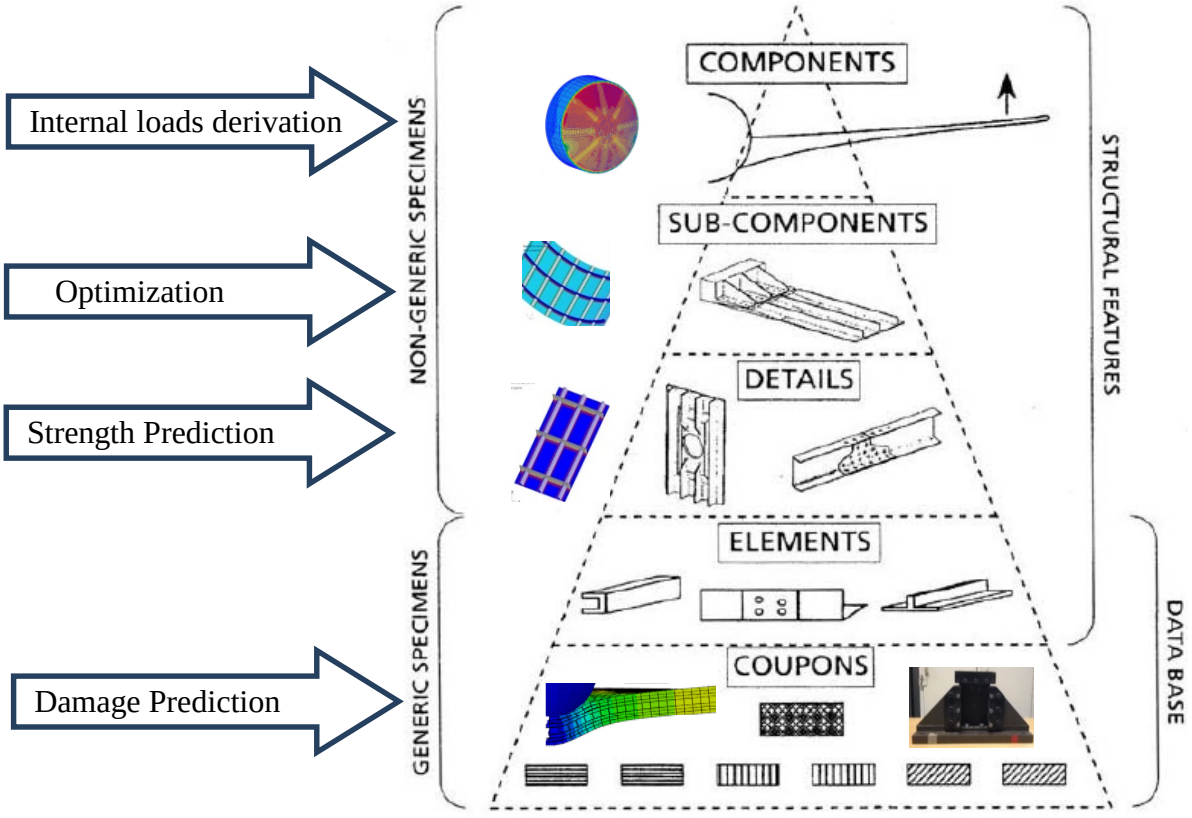

Figure 2.2: Certification testing pyramid from ref [2]. Analyses / testing cases presented within the thesis

2.5 Summary and key points of chapter two

- The explicit definition of structural strength along with its translation in the airframe industrial sector, is provided within the Airworthiness certification specifications
- The Airworthiness certification specifications encompass the consolidated experience gained from all the previous years to date in aircraft design, manufacturing and utilization. Being as such, this experience has resulted from years of exposing structures to service, made mostly of aluminium materials
- Proof of strength, on occasions, can rely on methods that are known to produce acceptable results. With the introduction of fibrous polymer composite materials in the airframe structures, these methods need to be revisited and re-evaluated. Certification for fibrous composite structures will rely heavily on a testing certification programme
- There are engineering methods which can be considered to provide with reliable analyses. These have resulted from experience. They have been proven in practice mostly on structures made of metallic materials, mainly aluminium
- Unless performing full scale testing, applying Finite Element modelling or engineering formulas to complex structures for strength substantiation are generally ***not*** considered reliable analyses, hence are not considered acceptable means for showing compliance to the respective Airworthiness specifications.

2.6 References in chapter two

[1] European Aviation Safety Authority (2015). CS-25: Certification Specification and Acceptable Means of Compliance for Large Aeroplanes, Amendment 17. EASA, Germany.

[2] EASA, European Aviation Safety Authority (2010). AMC 20-29: Acceptable Means of Compliance - Composite Aircraft Structure. EASA, Germany.

Chapter 3

"Application of finite element analysis for internal structural loading derivation"

Airframe industry has implemented Finite Element analyses based procedures for structural strength substantiation quite successfully. In the global structural scale, models for nodal equilibrium loading interrogation are mostly used.

The study presented in this chapter is a Finite Element Analysis where nodal equilibrium loading at structural cross section of interest is interrogated. This study is aimed at exposing the loading in the vicinity of a bulkhead joint in order to provide with an insight as to why the resulted information should be viewed differently when using composite materials.

Following the study presentation, an example from other researchers in the field in a similar study performed is exposed and critiqued in order to present the difference in the behaviour between metallic and composite materials and to expose the reasons for the analyses methods that used to generate acceptable results for metallic structures, care must be taken upon the application to fibre polymer structures.

Finally, an aircraft accident investigation report is presented, to highlight the importance of the numerical study and its results.

<*Page intentionally left blank* >

3.1 Introduction to the strength analysis of a composite bulkhead joint

Current practice in the airframe design sector is using global finite element models to derive internal to the structure member loading. The term “global” analysis relates to the size of the FE model generated which is usually the complete aircraft, and to the analysis studied were loading and response to loading is analysed at the complete aircraft scale. Computational processing power limitations in the size of the model result in a coarse mesh. The coarsely meshed global models serve the purpose of distributing the applied pressure and inertial loading, internally to the nodes of the FE model. From that point onwards, analytical calculations methods are employed for assessing the strength of components. If better fidelity is required, part of the structure is locally modelled in a refined mesh.

Applied stress analysis methodology for aircraft design is based on the elementary theory of structural mechanics. From an airworthiness point of view, the strongest argument for relying upon the results of analytical calculations for structural sizing is the integrity and durability of the components designed that has been validated in service. Metallic materials have been used extensively in the airframe manufacturing for some decades. Most of the today’s existing stress analysis methods have emerged through that era. It can be argued that stress analysis methods have been proven airworthy by taking advantage of the specific attributes of the metallic materials, with plasticity being one of them. Currently, there is an increased usage of carbon fibre reinforced plastic (CFRP) materials for aircraft structural primary load-carrying members where the existing methodologies for component sizing have not yet been extensively validated in service. Thus, a question is posed as to whether the same methods of the past can be assumed reliable for using on structures made of CFRP materials.

Before the extensive finite element modelling for structural analysis, design office procedures for initially assessing the strength of a structural part would primarily rely on analytical methods. The final clearance of the structure would then be justified by a part, a component, and/or by a full-scale structural test. For some decades now, the usage of computational tools provides a discrete, “nodal” loading pattern derived from a “global aircraft finite element (FE) model,” which is basically the means for coarsely

distributing the flight and inertial loading to the various structural elements according to their relative stiffness. Rules for the parameters of the numerical model generation are described in company design manuals. Solutions of the numerical global FE model generated under the application of loading cases are in the form of sets of “nodal equilibrium loads.” From that point onward, simplified mechanics would be used to give a representation of the internal structural loading in terms of local stress distributions. Stress analysis in most of the cases relies upon the output nodal loading from a global FE model to further analytically process the applied stress field and evaluate the integrity of the structure. This general aerospace standardized procedure is not a valid one for the structural application under investigation, as will be shown in the following sections.

When greater fidelity in the numerical results is requested, refined finite element models are generated, using more computational nodes. Due to the high computational costs and the limitations in computational power, these models reflect only a smaller part of the complete structure. The study herein is a refined finite element model numerical investigation at the lap joint location between the empennage fuselage structure and a domed end-pressure bulkhead, shown in Figs. 3.1 and 3.2. The aim of the study is to provide a better understanding of the structural response and the loading levels at the joint location through the proposed numerical analysis procedure, as well as to provide some context for the implications caused by using CFRP materials for the design of similar structural parts as in contrast to using the more traditional metallic materials.

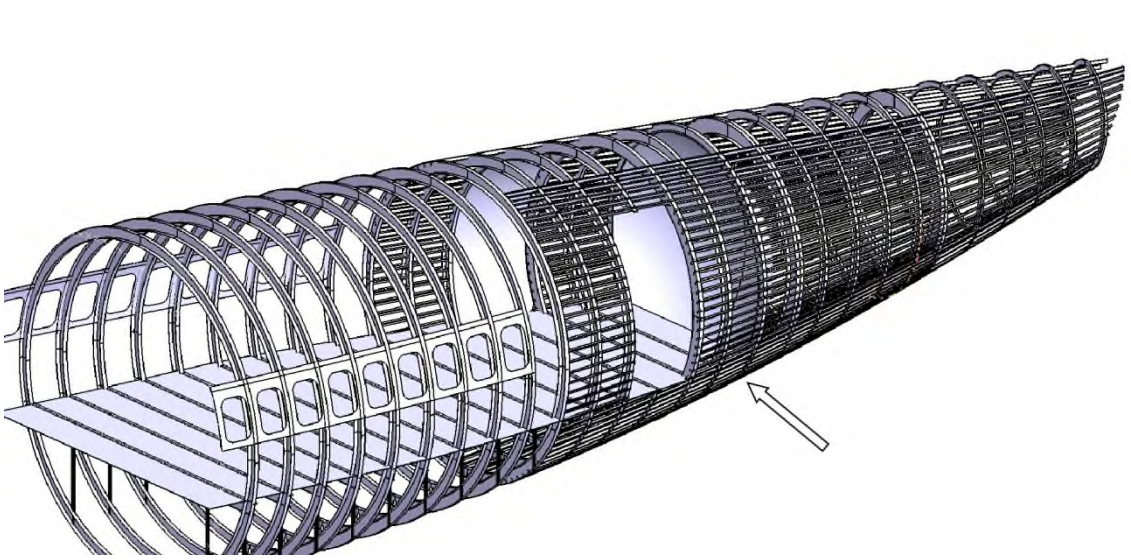

Figure 3.1 Conceptual design of an aircraft empennage structure. The airframe location under investigation is indicated.

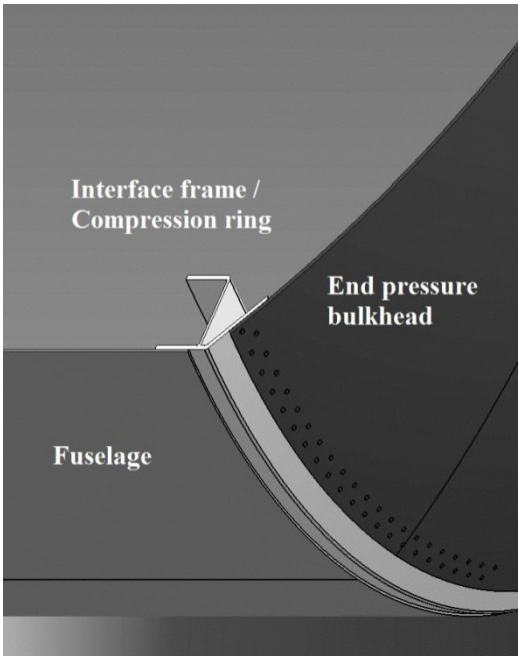

Figure3.2 Enlarged view of the joint between the end-pressure bulkhead dome and the cylindrical fuselage via a frame-type interface structure (compression ring).

Pressurized aircraft vehicle end-fuselage bulkheads are designed either as flat stiffened structures or as dome-shaped ones, stiffened or unstiffened [1]. The dome-shaped structures are usually subjected to limited space requirements. For that reason, they are shaped as part-spherical or part-elliptical ones [2]. These bulkheads are often attached by fasteners to the rest of the structure. The most advantageous stress distribution for an end-pressure bulkhead connected to a cylindrical fuselage under positive internal pressure differential is achieved when the dome is of a half-spherical shape [2]. The biaxial stress in pressurized dome structures is known and documented in the literature.

The scenario of the case study herein investigates the conceptual joint in the empennage of an airframe, shown in Fig. 3.1. It is assumed that the bulkhead is joined by mechanical fasteners to the last frame (compression ring) of a cylindrical fuselage, shown in Fig. 3.2. The area under investigation does not take into account possible bulkhead frames along the meridian direction of the hemisphere that could be joined with fuselage longerons. It addresses the loading of the skin-to-skin lap joint over the bulkhead surface.

Similar studies are not available in the public domain, and some of them are protected by intellectual property rights. A relevant study by Becker and Wacker [3] was performed in the pressure bulkhead of the Ariane-5 tank structure. The bulkhead was made of metallic materials. The focus of the study was the nonlinear numerical investigation including the metallic material plasticity effects. An older and more relevant analytical investigation by Williams [4] highlighted some of the problems of the aircraft pressure cabins. The lack of today's numerical tools provided limited insight to more complex designs. There are various studies [5–13] that considered the analytical and numerical approaches of stresses in vessel-type CFRP structures under pressure. The context of those studies was derived from the aftermath of a different industrial sector and deviates from the one herein, mainly due to considering the vessel-type structures as being monocoque types, which are not implicated by the localized effects of assembled parts with fasteners. The current study is mainly informed from standard airframe design textbooks [1, 2, 14–16].

3.2 Approach Methodology

3.2.1 Deviations from the Elementary Structural Mechanics Theory

Initial structural sizing formulas for pressure dome sizing are found within the literature of structural mechanics [17,18] and are extensively quoted in airframe structural analysis textbooks [14,16]. The stress solution on a pressurized dome surface involves hoop membrane stresses along the meridian and equatorial directions of the spherical surface of equal magnitude. The structural part of the investigation is a part of a spherical dome under internal pressure. Acceptable stress results are anticipated and compared to the elementary theory ones as long as the parameters of the problem represent the real structure, especially the boundary conditions of it. Figure 3.3 serves as a demonstration to the aforementioned statement by using the displacement results from FE analysis on a quarter of a dome structure. The pressurized part-semi spherical dome in Fig. 3.3 has its planar periphery constrained in translation along the direction of its axis of revolution and is not tangent to the edge of the surface, as in the elementary problem formulation. The structure under these boundary conditions has a tendency to shrink along its major diameter when pressurized because it is only a part of a hemisphere and not a full one. The result of it is the generation of a complex stress pattern at the boundary of the structure.

A more complicated problem is formulated when the natural tendency of the dome to shrink is internally constrained by assembling it to an elastic fuselage structure, thus incurring reactions perpendicular to the surface. An approximation to the deflected shape of the bulkhead in such a case is depicted in Fig. 3.4. From the deflected shape, the existence of internal moment loading on the structure laminate is presumed, provided that it has a relative substantial thickness to resist that loading.

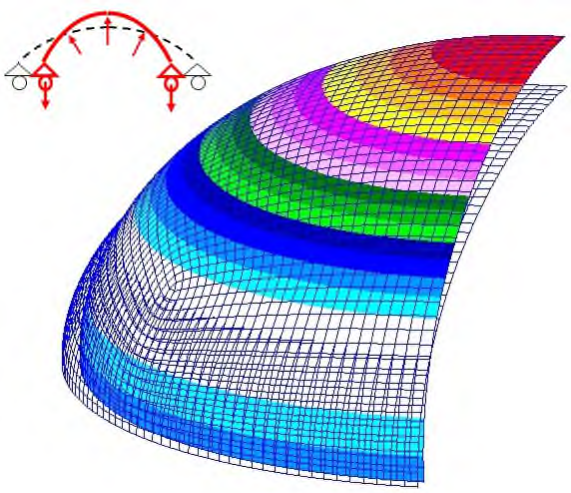

Figure 3.3 FE model of a part-hemispherical bulkhead under internal pressure showing the tendency of shrinkage along its major diameter (axis) when the translational degree of freedom along the revolution axis is constrained.

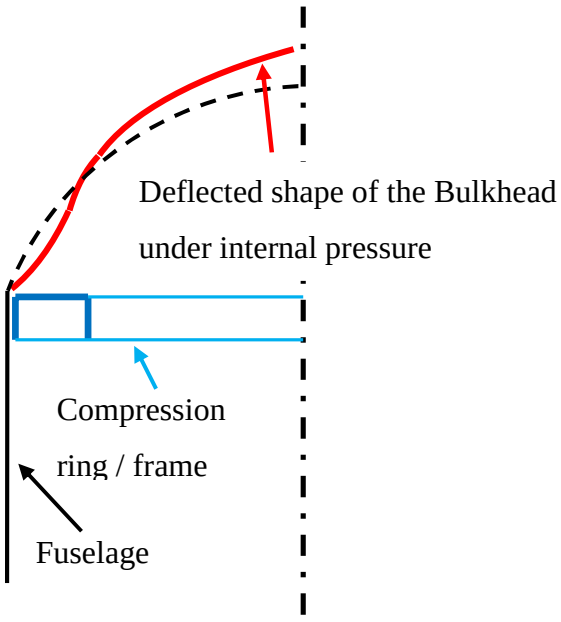

Figure 3.4 Sectional representation of the deflected shape of a bulkhead dome under pressure.

The structural reaction to positive pressure differential is represented by unit loading vectors in a spherical coordinate system, shown in Fig. 3.5. The loading vectors on the bulkhead structure are tangent to the bulkhead surface along the meridian and equatorial curves. The focus of the investigation lies in the vicinity of the geometrical intersection of the fuselage and the bulkhead, shown in Fig. 3.2.

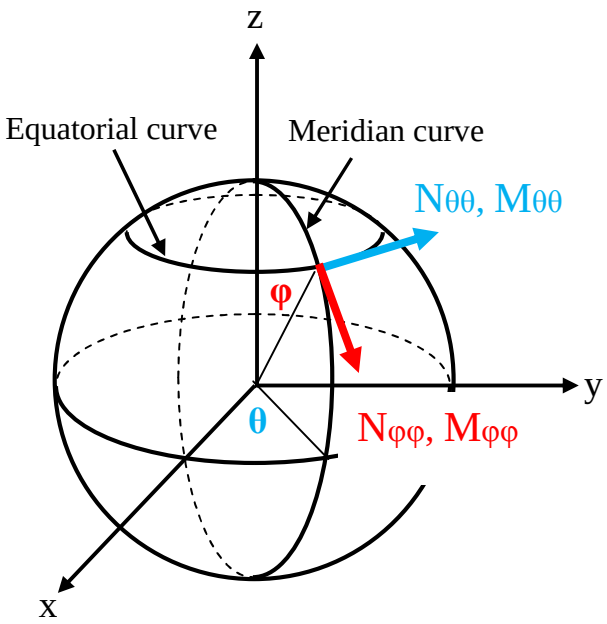

Figure 3.5 Spherical coordinate system for vector internal loading representation.

Along the spherical surface equatorial curves and tangent to those, the structural internal loading in terms of force and moment are represented by $N_{\theta\theta}$ and $M_{\theta\theta}$, respectively. $N_{\theta\theta}$ is the hoop reaction to internal pressurization which is tensile for the bigger part of the structure. Approaching the geometrical intersection, it becomes compressive due to the equator's shrinkage effect, as illustrated in Fig. 3.3. The unit moment load $M_{\theta\theta}$ can be evidenced from the shape of the deflected structure depicted in Fig. 3.4. The cause for the structural response of Fig. 3.4 is the counteraction of the fuselage with the compression ring frame to the shrinking effect of the bulkhead along its major diameter. Tracing the spherical surface meridian curves and tangent to those, the internal force and moment loading are represented as $N_{\varphi\varphi}$ and $M_{\varphi\varphi}$, respectively. Unit load $N_{\varphi\varphi}$ is the anticipated tensile hoop reaction to pressure. The unit moment load

$M_{\varphi\varphi}$ is the most unobvious loading component and relatively difficult to visualize. It is the result of the axisymmetric pattern of the deflected pattern shown in Fig.3.4.

3.2.2 Benchmark Test and Comparison of Analytic with FE Results

Modelling a flat plate under pressure, where standard shell-type finite elements (CQUAD4, PSHELL, [19]) are typically and currently used by the airframe design industry, is an element mesh-size-dependent solution [19,14]. A bypass method used to overcome the mesh size dependency in similar problems is to acquire the nodal built in constraint reaction force and moment values from the numerical solution rather than requesting the shell elements stress output from the numerical solver. Consequently, by applying those loads in an analytical fashion at the boundary of the structure, better approximated stress results are generated. When applying this numerical procedure at the case of a cylindrical fuselage joined to a part-hemispherical dome, the aim of it would be to retrieve the nodal equilibrium force $N_{\varphi\varphi}$ and moment $M_{\theta\theta}$ loading along the intersection curve of the two surfaces. The abrupt change, though, of the surface smoothness at the interface location which joints the geometrical shapes of two different curvatures causes the nodal equilibrium loads at the interface to be element size dependent as well. To study the deviation between the analytic problem formulations of a cylinder connected to a part sphere [17] at the location of the geometrical interface, a series of FE models with variable mesh sizes were constructed and benchmarked against the solution of [17]. Shown in Fig. 3.6, are three of the variable mesh-sized FE models built in NASTRAN [19] that were used for benchmarking. The benchmark took place on the simpler geometrical model of a cylindrical surface connected to the part-spherical dome for the reason that the analytic solution of it is available in the literature. That model does not contain the complication of an additional circumferential frame along the intersection of the surfaces, which is present in the actual airframe structure under investigation. The benchmark showed a difference of 40% in the magnitude $M_{\theta\theta}$ between the coarse and the refined models of Fig.3.6 a). This result led to the conclusion that the only way of resolving the true loading state at that interface in terms of $M_{\theta\theta}$ was through extrapolation of the nodal results from models of varied element sizes. Summarizing, by using the currently aerospace standard finite element formulations at the intersection curve

of a cylinder to a part-spherical surface, not only stress output results are element size dependent but nodal moment $M\theta\theta$ loads as well.

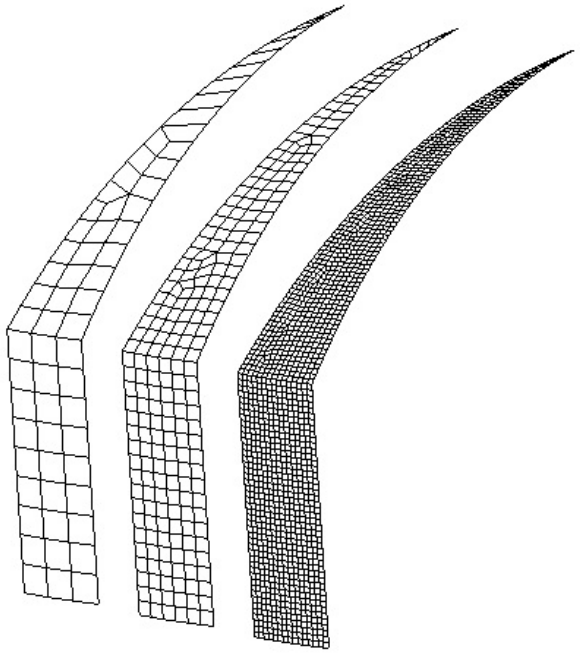

Figure 3.6 a) Models of various refinements for comparison with the analytical solution of the nodal equilibrium force and moment at the intersection curve between the cylindrical and dome structure.

The results of the benchmark numerical studies shown in figures 3.6 b) and 3.6 c), showed that a good correlation existed between the axial and radial loading at the interface location, but the edge moment loading deviated almost 40% for the coarser mesh size.

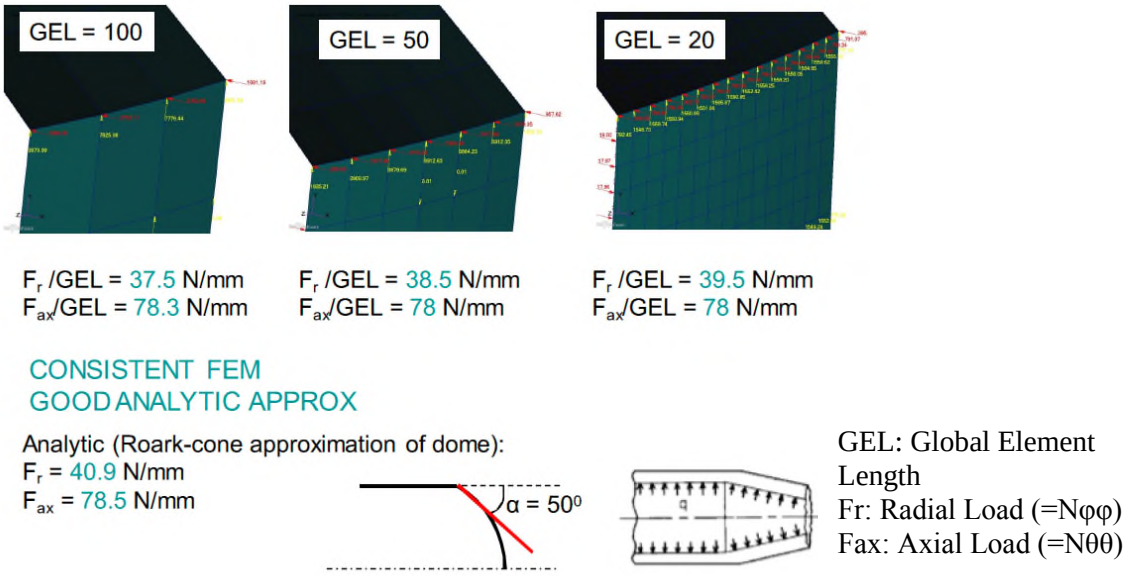

Figure 3.6 b): Models of various refinements for comparison with the analytical solution [17] of the nodal equilibrium force at the intersection curve between the cylindrical and dome structure

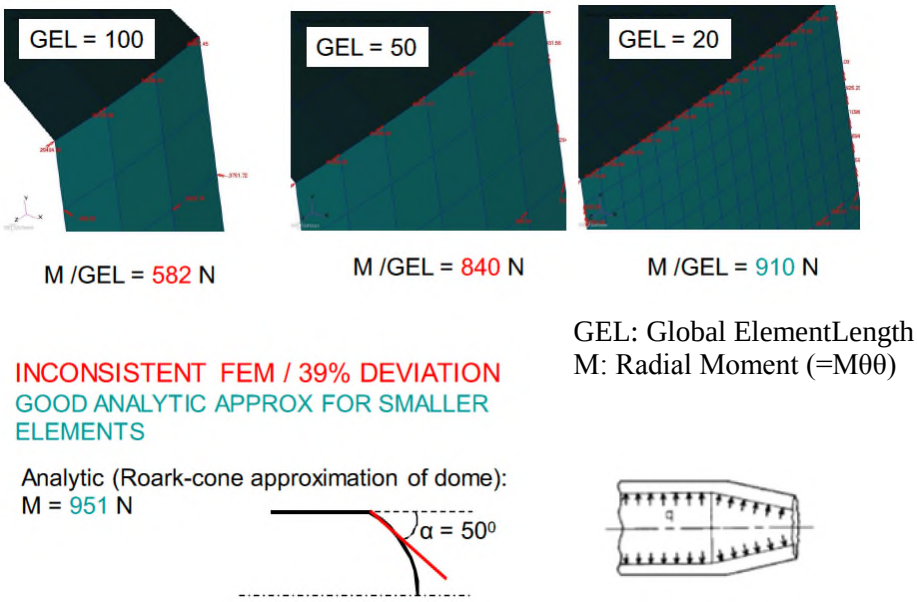

Fig. 3.6 c): Models of various refinements for comparison with the analytical solution of the nodal equilibrium force at the intersection curve between the cylindrical and dome structure

Having generated some confidence into the numerical procedures, models with the end frame were constructed shown in figure 3.6 d). These models would be benchmarked against each other since there was not reference available for the implications caused by the additional structural element.

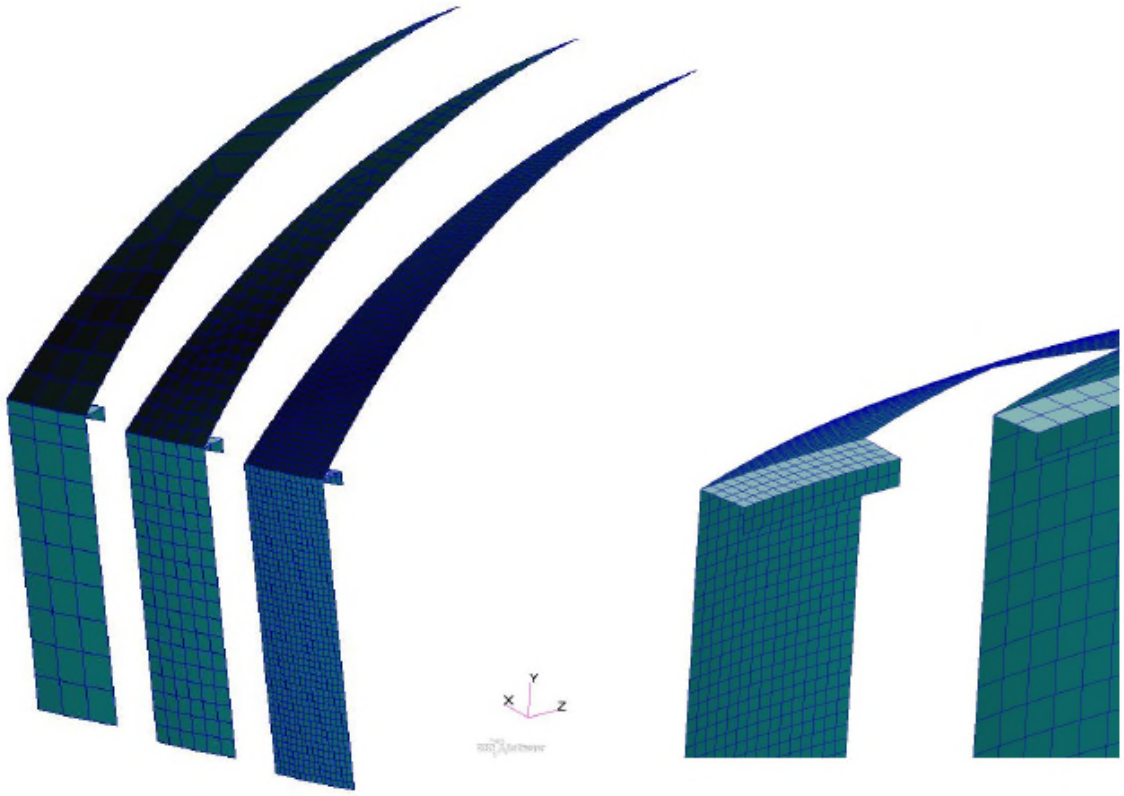

Figure 3.6 d): Models of various refinements containing a compression ring – end frame.

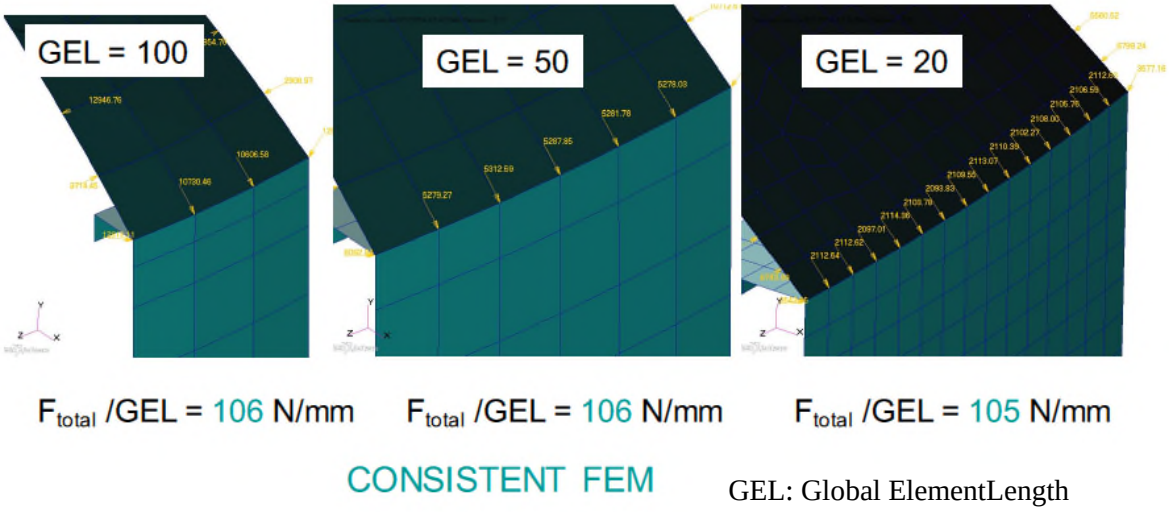

Figure 3.6 e): Models of various refinements for comparison with one another in terms of the nodal equilibrium force at the intersection curve between the cylindrical and dome structure

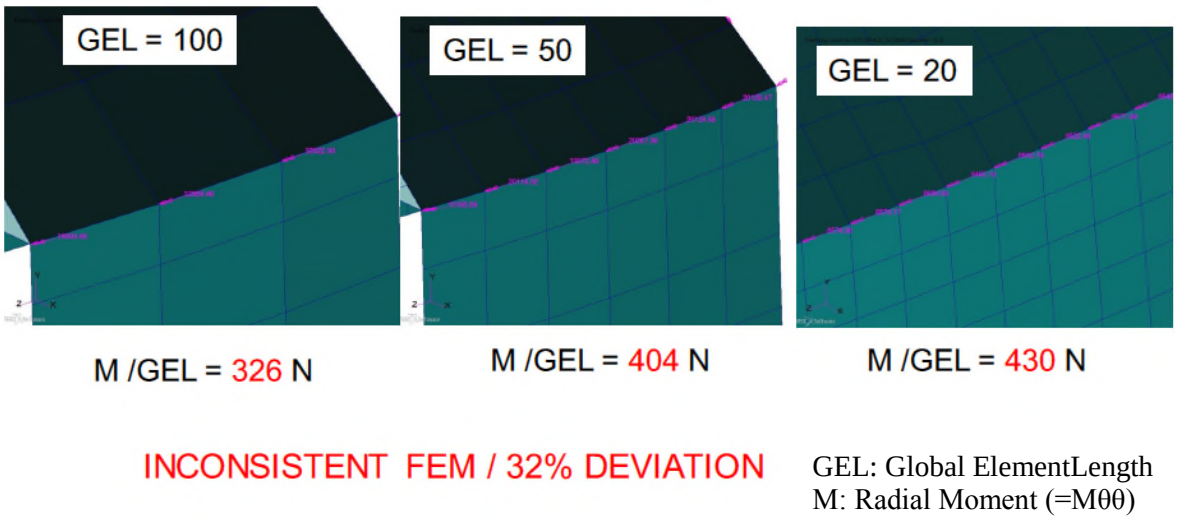

Figure 3.6 f): Models of various refinements for comparison with one another in terms of the nodal equilibrium moment at the intersection curve between the cylindrical and dome structure

3.2.3 Case Study Conceptual Structure and Finite Element Model

The conceptual structure of the investigation consisted of a part-hemispherical bulkhead shell of 2.5 m radius, attached to a 3-m-diam fuselage using an interface frame. In this study, there were no supporting frames to the bulkhead skin along the meridian direction. Alternatively, in the case where the conceptual design incorporated frames along the meridian direction, these would prevent excessive skin distortion at the frame support location and maximum skin distortion would be present in the unsupported region in between the frames.

Both the fuselage and the bulkhead structures were assumed to be made of CFRP materials. The interface compression ring frame, shown in Fig. 3.2, was made of aluminium. The CFRP material system was Tenax-J HTS40 E13 3K 200 TEX woven fibres impregnated with MTM45-1 resin with a cured ply thickness of 0.2 mm. Elastic moduli along the principle directions were assumed identical and equal to 60 GPa. The bulkhead laminate had a quasi-isotropic layup configuration of 2.4 mm total thickness. The manufacturing layup process is shown in Fig. 3.7, where, basically, ply stripes were laid over the bulkhead surface. The layer stripe width had been calculated for avoiding excessive fibre direction deviation due to draping. The internal pressure differential was 0.09 MPa.

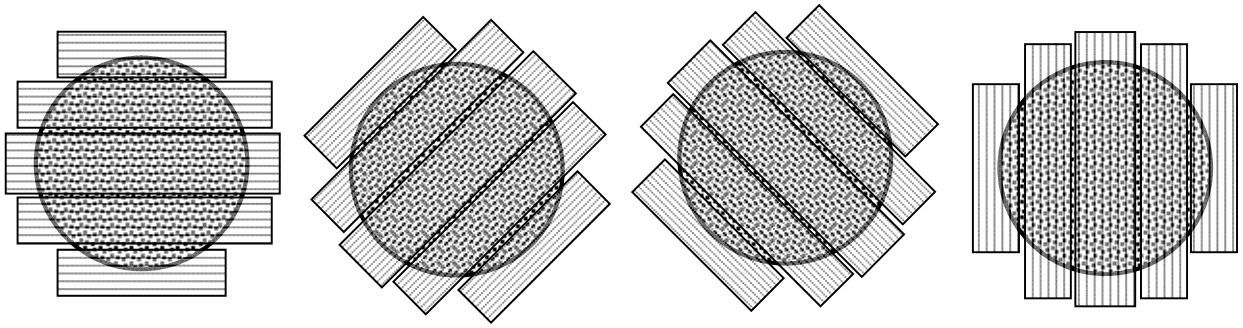

Fig. 3.7 Domed skin surface layup from pre-impregnated CFRP layers.

The local model of the joint generated in NASTRAN [19] is shown in Fig. 3.8. Shell elements (CQUAD4, MAT8, PCOMP [19]) were chosen to represent the thin-walled shell structure. This element technology is currently the aerospace standard for global FE aircraft numerical modelling. The benchmarking, explained previously, was performed in order to assess the finite element output result accuracy in terms of unit nodal force and unit moment equilibrium loading. The result of the benchmarking dictated the appropriate element size needed for the case study to achieve satisfactory results within a specified tolerance. Only a sector of the fuselage was modelled, as shown in Fig. 3.8. Axisymmetric boundary conditions were defined along the section boundary, and internal pressure was applied on the shell elements. Results are drawn in terms of loading from the intersection curve with the cylindrical part and for 300 mm inboard along the bulkhead surface; see Fig. 3.8. The numerical analysis performed was nonlinear static (SOL400 [19]).

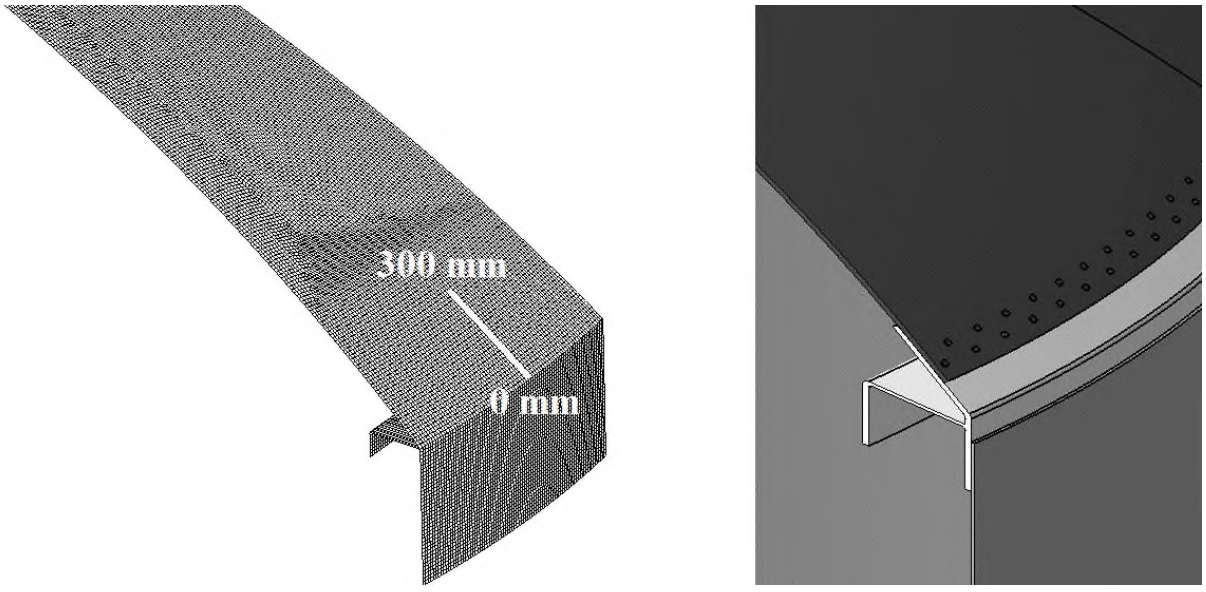

Fig. 3.8 FE model mesh used for deriving the loading in the vicinity of the interface for the case study. Loading results are analysed for the distance shown (0–300 mm).

3.2.4 Results

In Fig. 3.9, a pictorial representation of the defined unit force and moment loading is shown. In Fig. 3.10, the resulting internal loading from the FE calculation is presented for a distance of 300 mm from the geometrical intersection as per Fig.3.8.

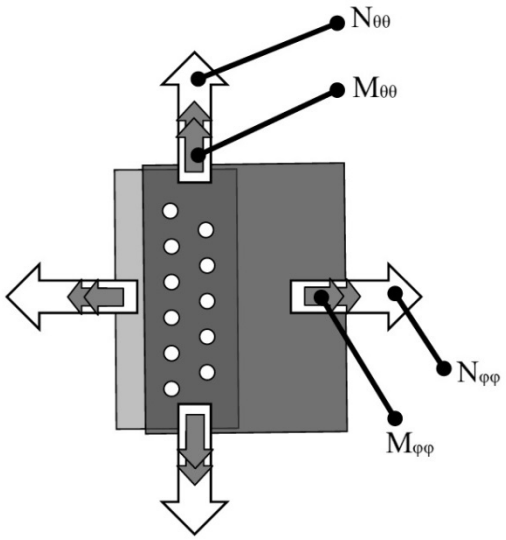

Fig. 3.9 Definition of the force and moment unit loading vectors on an elementary sector of the bulkhead interface lap joint.

The meridian unit force loading $N_{\varphi\varphi}$ (Fig. 3.10a) after 250 mm from the geometrical intersection attained the anticipated magnitude from the initial sizing analysis of spherical domes under pressure [17]. For the structure under study, the variation of the magnitude of the meridian force was less than 15% for the complete analysis length. The loading remained tensile for the whole region under investigation.

Moment unit loading $M_{\varphi\varphi}$ (Fig. 3.10b) could not be predicted from elementary theory of spherical domes under pressure. For the case study, the magnitude of the vector had a peak at the surface intersection location. After approximately 250 mm, it diminished to zero; whereas past 150 mm from the intersection, it was less than 15% of the maximum value. The sign of the moment shifted from positive to negative at around

50 mm from the interface, following the change in the dome's deflected shape, shown in Fig.3.4.

The tangential-force unit loading $N_{\theta\theta}$ (Fig. 3.10c) was initially negative until 100 mm from the geometrical intersection. Following that distance and after 150 mm approximately, it gradually rises to the anticipated elementary theory value.

The tangential moment unit loading $M_{\theta\theta}$ (Fig. 3.10d) changes its sign from positive to negative at approximately 50 mm from the interface location, following a similar change to the meridian moment. After 250 mm, the magnitude of the moment is practically zero, whereas at 150 mm, its value has diminished to more than 15% of the maximum at the interface location.

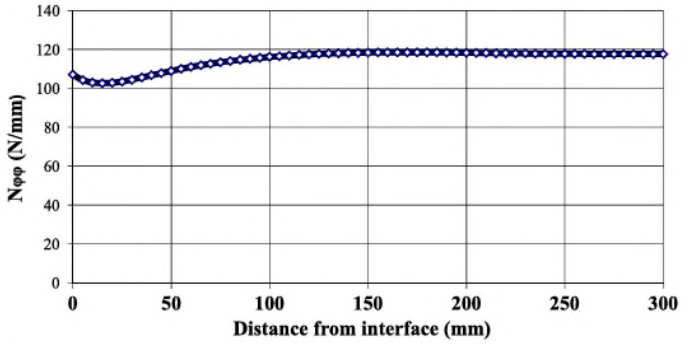

a) Unit force tangent to meridian curves, $N_{\varphi\varphi}$

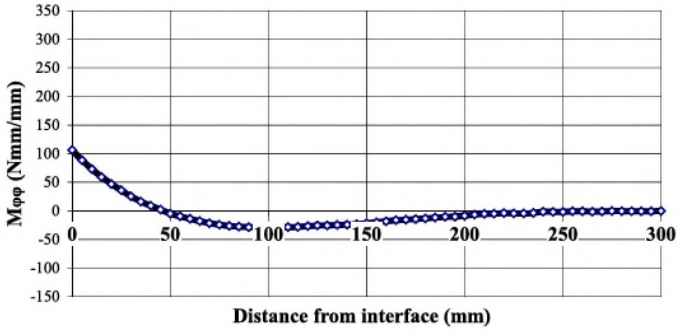

b) Unit moment tangent to meridian curves, $M_{\varphi\varphi}$

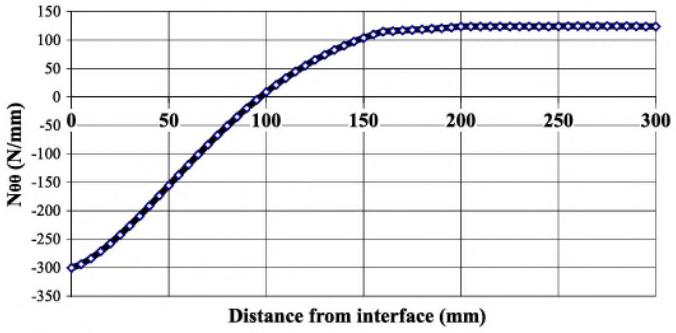

c) Unit force tangent to equatorial curves, $N_{\theta\theta}$

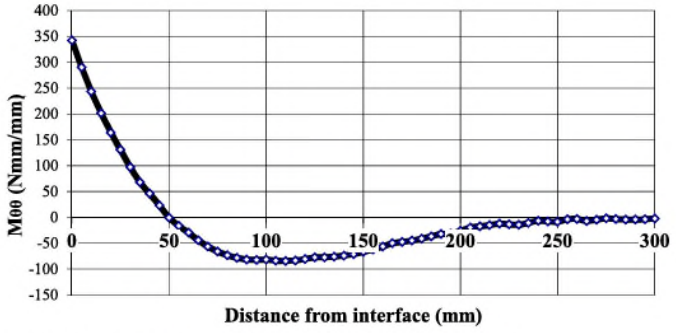

d) Unit moment tangent to equatorial curves, $M_{\theta\theta}$

Fig. 3.10 Internal unit force and moment loading along a meridian curve over the bulkhead skin surface from the interface position to 300 mm towards the apex of the bulkhead dome (Fig. 3.8).

Practically, approximately past the 250 mm distance from the geometrical intersection of the bulkhead with the fuselage surface, the internal loading stress tensor was described by tensile hoop stresses along the meridian and equatorial directions, and tangent to those. Before that distance, which is considered to be the vicinity to the geometrical intersection, high compressive loads existed along the equatorial direction and there was an equally alarming increase in the moment loading in both principle directions as well. Loading vectors $N_{\varphi\varphi}$ and $M_{\theta\theta}$ along the intersection curve were benchmarked and results can be regarded as acceptable for the FE mesh size generated. The rest of the results are finite element technology dependent, and thus could only be verified by real-life testing.

Evaluation of the stresses on the lamina level was performed following the assumptions of the classical lamination theory (CLT) [20,21], making use of the unit loading state of Fig. 3.10. One thing to point out is that there is a variance in the perception of the laminate's layup configuration, depending on the location of the observer around the structure's periphery, shown in Fig. 3.11. To illustrate the previous statement with an example, the CFRP layer shown in Fig.3.11 includes the black- and white-striped blocks laid over the top view of the domed bulkhead, and it is supposed to have its principle fiber direction parallel to the stripes. While moving around the periphery of the bulkhead, this same layer is perceived as a 0 deg layer at position a, as a 45 deg layer at position *b*, and as a 90 deg layer at position *c*. Stresses resulting from unit force and moment loading are affected by this variable layup perception.

To generate the resulting laminate stresses upon the application of the unit loading of Fig. 3.10, a simple demonstration follows by applying the loading over a homogeneous isotropic material with an elasticity modulus of E = 60 GPa and a Poisson ration of $\nu = 0.3$. Results at three different locations on the bulkhead surface at the vicinity of the joint are displayed in the following:

Past a distance of 250 mm from the geometrical intersection, moments $M_{\theta\theta}$ and $M_{\varphi\varphi}$ were equal to zero (Figs. 3.10b and 3.10d). The supposed isotropic bulkhead shell reacted to the internal pressurization with bidirectional hoop stresses:

$N_{\varphi\varphi} = N_{\theta\theta} = 118$ N/mm (Figs. 3.10a and 3.10c) =>

$\sigma_{\varphi\varphi} = \sigma_{\theta\theta} = 50$ MPa

Neglecting the bidirectional moment and assuming the worst compressive $_{N\theta\theta}$ superimposed by $N_{\varphi\varphi}$ loading, then the maximum stresses on the assumed isotropic bulkhead skin at the edge of the skin were the following (Figs. 3.10a and 3.10c):

$N_{\varphi\varphi} = 107$ N/mm, $N_{\theta\theta} = -300$ N/mm =>

$\sigma_{\varphi\varphi} = 45$ MPa, $\sigma_{\theta\theta} = -125$ MPa

Summing the effect of the bidirectional unit loading with the bidirectional moment vectors at the edge of the assumed isotropic skin (Figs. 3.10a–3.10d),

$N\varphi\varphi = 107$ N/mm, $N\theta\theta = -300$ N/mm,

$M\varphi\varphi = 110$ N, $M\theta\theta = 350$ N =>

$\sigma_{\varphi\varphi max} = 160$ MPa, $\sigma_{\varphi\varphi min} = -70$ MPa,

$\sigma_{\theta\theta max} = 239$ MPa, $\sigma_{\theta\theta min} = -490$ MPa

Following the preceding simple demonstration, we applied the last, which is worst-case loading scenario on the CFRP laminate of our case study. The layup configuration, taking into account Fig. 11, is perceived as $[0/90, +/-, 90/0, 0/90, +/-, -/+]_s$ at position a and as $[+/-, 90/0, -/+, +/-, 90/0, 0/90]_s$ at position b. The maximum results were calculated at the midply position of each layer:

At position a of Fig.3.11, along the periphery and at the tip of the intersection,

$N\varphi\varphi = 107$ N/mm, $N\theta\theta = -300$ N/mm,

$M\varphi\varphi = 110$ N, $M\theta\theta = 350$ N =>

$\sigma_{\varphi\varphi max} = 170$ MPa, $\sigma_{\varphi\varphi min} = -182$ MPa,

$\sigma_{\theta\theta max} = 188$ MPa, $\sigma_{\theta\theta min} = -567$ MPa

At position b of Fig.3.11, along the periphery and at the tip of the intersection,

$N\varphi\varphi$ = 107 N/mm, $N\theta\theta$ = -300 N/mm,

$M\varphi\varphi$ = 110 N, $M\theta\theta$ = 350 N =>

$\sigma_{\varphi\varphi max}$ = 162 MPa, $\sigma_{\varphi\varphi min}$ = -202 MPa,

$\sigma_{\theta\theta max}$ = 218 MPa, $\sigma_{\theta\theta min}$ = -597 MPa

From the preceding shown stress evaluations, it is evident that the numerically calculated loading state can be underestimated if the effects of the boundary conditions are not taken properly into account.

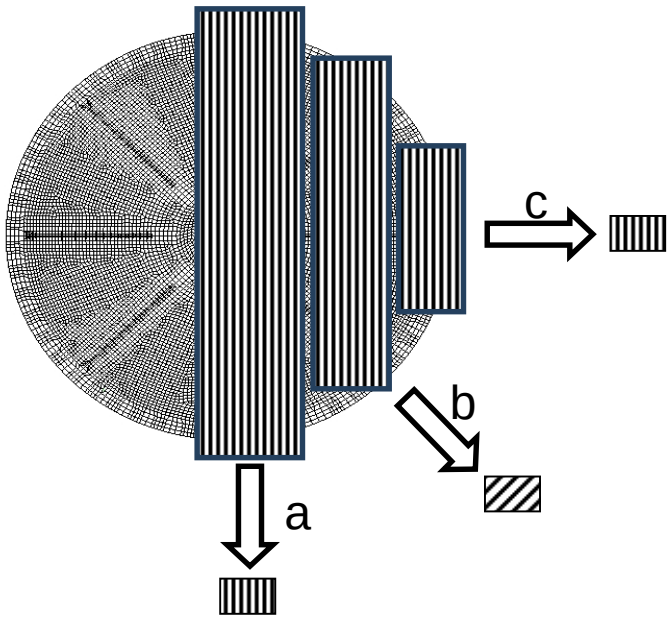

Fig. 3.11 Variance in the perception of the bulkhead laminate layup configuration depending on the observer location around the periphery.

3.2.5 Discussion

Depending on the specific design, materials, and geometric configuration, there is a specific distance from the geometrical intersection between a cylindrical fuselage

and a part-semispherical dome, where the loading is variable to the distance and is far greater than the bidirectional hoop stresses on a pressurized sphere. The severity of the results of such a loading condition could be overshadowed since, most of the time, the connection between the compression ring frame and the pressure bulkhead is more complicated in terms of structural arrangement, creating a secure distance between the bulkhead and the geometrical inflection point of the interface [13,16].

One of the major differences in the airworthiness structural clearance approach between a metallic and a CFRP structure is the structural testing evidence required. This mainly results from the relatively smaller existing field experience and strength validation of the CFRP structures as opposed to the metallic ones. Clearance directives dictate that the strength and fatigue life of the CFRP structure in a damaged state has to be verified by testing. Composite laminated structures containing damage in the form of interlaminar delaminated regions are susceptible to failure under compression loads. Our analysis has indicated the existence of high compressive loading in the vicinity of the joint. In such cases, besides the elastic instability problems that could arise in thin-walled structures irrespective of the material used, the CFRP laminate also has to be sized against its compression after impact (CAI) strength [15]. CAI strength depends on numerous factors and effectively results from component tests, which have to be performed early in the design stage for use in material selection and qualification.

In the case study, the compression ring was designed by metallic materials. In such a scenario, the designer could avoid the area of high-intensity loading by effectively offsetting the CFRP bulkhead structure further inboard. The advantage of such a design was to expose the metallic part of the lap joint to the transitional high loading area, which is easier to inspect and has a more extensively validated and documented strength, fatigue, and damage-tolerance properties.

There is also an opportunity to place the fastener arrays within the region of the tangential-force loading sign change, and thus decrease the effect of the biaxial loaded laminate in case it is found that most favourable strength results can result. The lap joint assembly with fasteners is shown in Fig.3. 2. At a distance of approximately 100 mm from the intersection, as shown in Fig.3.10c, the compressive load equals to zero. Effectively, at the region of the tangential-force loading sign change, the lap joint laminate is almost

uniaxially loaded with relatively reduced biaxial moment vector magnitudes. A typical lap joint test specimen could be used for substantiating the structural strength at that location, provided that the applied loading besides the unidirectional tension along the meridian is assumed negligible; else, the loading on the transitional area has to be assessed by a fine finite element mesh in a conservative manner and the effects of the biaxially loaded fastener holes and the fastener bearing have to be superimposed on the laminate loading.

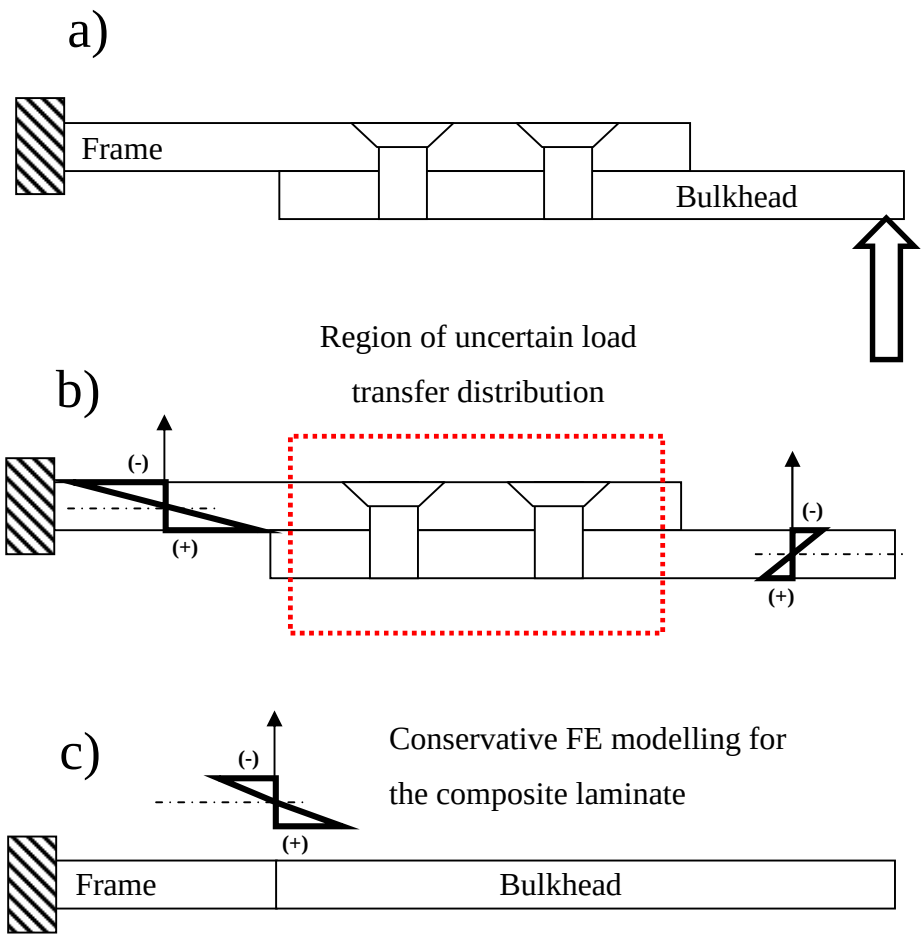

Fig. 3.12 a) Beam model lap joint, b) region of uncertain laminate loading transfer, and c) exposure of the structure to a lengthier and a more severe end loading.

For sizing the lap joint effectively, the bidirectional force and moment loading of the area under investigation need to be evaluated. A conservative FE modelling approach to that shown in Fig.3.12 would be to assume that the CFRP laminate is

modelled to the edge of the structure, thus being exposed to the complete variation of the loading field. That elementary loading in terms of unit force and moment, shown in Fig.3.10, applied on a laminate section following the CLT assumptions would result in the loading of the individual composite material layers [20,21]. It is usual for the finite element modelling practice to exclude the presence of fasteners in the idealization of joints in order to avoid unnecessary modelling effort spent on fastener hole stress concentrations, fastener fits and pre-tightening, contact, three-dimensional effects of laminates, etc. A usual and preferred approach is to solve for the laminate loading and superimpose on top of it the stress field caused by the presence of holes and fastener bearing loads. Another perspective for the modelling approach of Fig. 3.12 is the exposure of the edge of the laminate to higher-intensity loading, in order to assess the through-the-thickness edge stresses caused by the in-plane loading in a more conservative manner.

Full-scale testing is used for satisfying the airworthiness structural clearance procedures. Only full-scale testing can generate the actual loading situation and assess the structural integrity of the joint. Ideally, correlation with full-scale test results from structural testing could verify or amend the aforementioned case study numerical results. Testing data of full-scale pressure bulkhead tests are difficult to come across. If, in the future test, data become available in the public domain, the present study can further progress. Nonetheless, the previously proposed numerical modelling approach, which is based on the currently standard FE technology used in the aerospace industry along with the discussed design complications, can provide designers of similar structural interfaces with an insight to the complications that arise and attain a better initial estimation of the expected structural response.

3.2.6 Conclusions

The numerical investigation of the conceptual joint between a fuselage and a pressure bulkhead has revealed the following:

- Numerical results from coarse FE analysis in terms of loading should not be used for sizing in similar structural arrangements, unless the finite element formulation provides acceptable results in a benchmarking procedure similar to the one shown

herein. Refined mesh FE results can be employed for deriving the applied loading for initial design purposes, but attention has to be drawn to the fact that not only the stress results along the geometrical interface are mesh size dependent but also the force and moment nodal values.

- High-intensity loading exists in the vicinity of the geometrical intersection where the joint was assumed; see Fig. 3.10. The existing force and moment loading magnitudes, as calculated by the FE analysis, cannot be predicted by the use of elementary structural analysis or coarse meshed FE models. The structural response responsible for the high-intensity loading in the vicinity of the joint is attributed to the fact that the major diameter of the bulkhead has a tendency to shrink upon pressure under the boundary conditions imposed by the rest of the structure; see Fig.3.4.
- The numerical analysis has shown the existence of high compressive loading in the vicinity of the joint: a loading mode that affects CFRP structures more than structures made of metallic materials. Besides the elastic instability considerations, the compression after impact strength has to be taken into account.
- Stress results are affected by the stress concentrations of the fastener holes and the edge stress raising effects of the CFRP laminate. In the vicinity of the tangential load, with $N_{\theta\theta}$ being close to zero (Fig.3.10, where the bidirectional moments are reduced as well), opportunities for optimal placement of the fastener pattern and/or the edge of the bulkhead on the assembly exist. This design option can be achieved by a wider interface frame flange and a smaller peripheral radius bulkhead; see Fig. 3.2.
- There are various design and analysis challenges posed by the application of CFRP materials, and they need to be faced until a final airworthiness structural qualification is achieved. By the aforementioned numerical procedure, better approximated stress results could be incorporated earlier within the design cycle of the product and provide the insight needed for decision making in terms of material selection and structural design configuration.

3.3 Results from other researchers in the field: improper use of FEA

Similar numerical analysis to the one presented, has been performed in the past [3]. The comparison between test and analysis and test of a metallic bulkhead is presented, shown also below in figure 3.13. It was mentioned that his metallic bulkhead was a part of the Arianne 5 space shuttle. The aim of the analysis was to simulate the bulkhead under pressurization taking into account the geometrically non-linear effects arising from the shell deformation as well as to incorporate plastic analysis in the regime of ultimate loading.

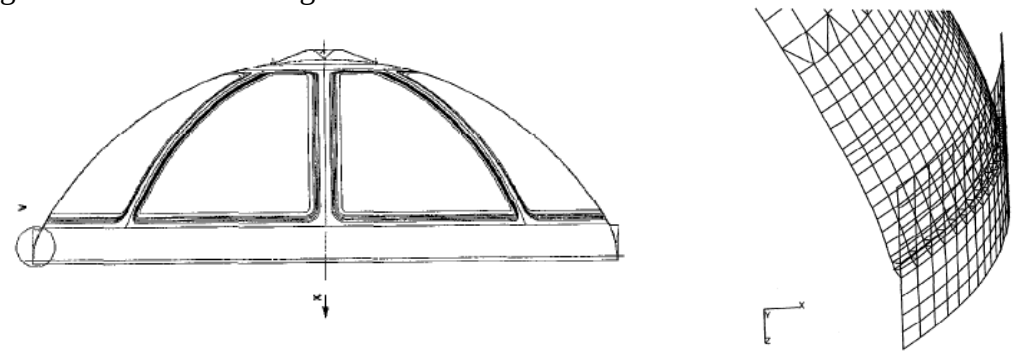

Figure 3.13: Side view of the metallic pressure bulkhead and finite element mesh, reference [3]

The article authors suggest that the full scale test performed and the numerical analysis results showed a very good correlation. In figures 3.14 and 3.15, fringe results in terms of deformation and Von Mises stress were presented. Correlation with the test results is shown in figure 3.16 and it was assumed only in terms of strain measurements.

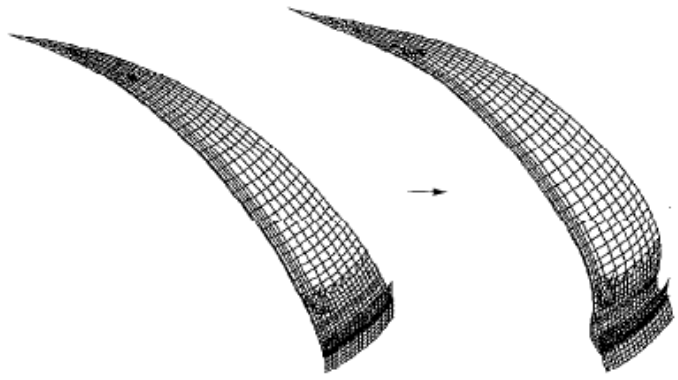

Figure 3.14: Deformation results at a 4.88 bars internal pressure as presented in reference [3]

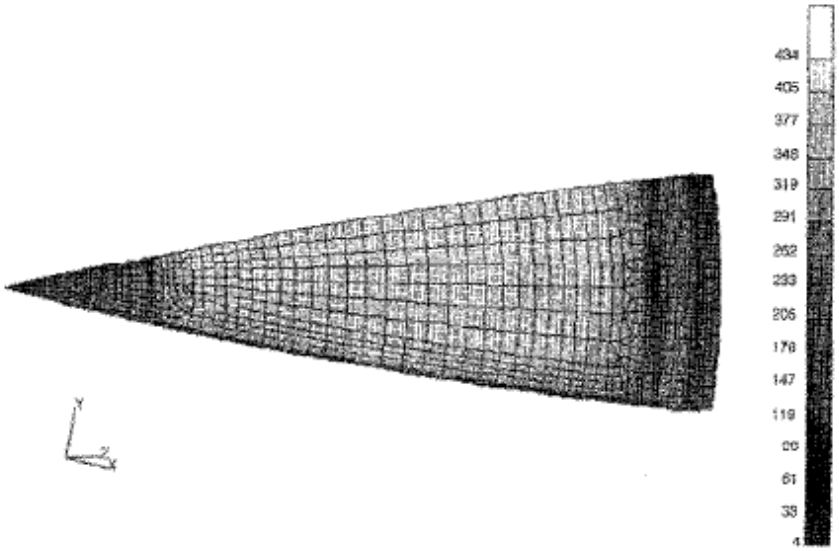

Figure 3.15: Calculated Von Mises stress results at a 6.83 bars internal pressure as presented in reference [3]

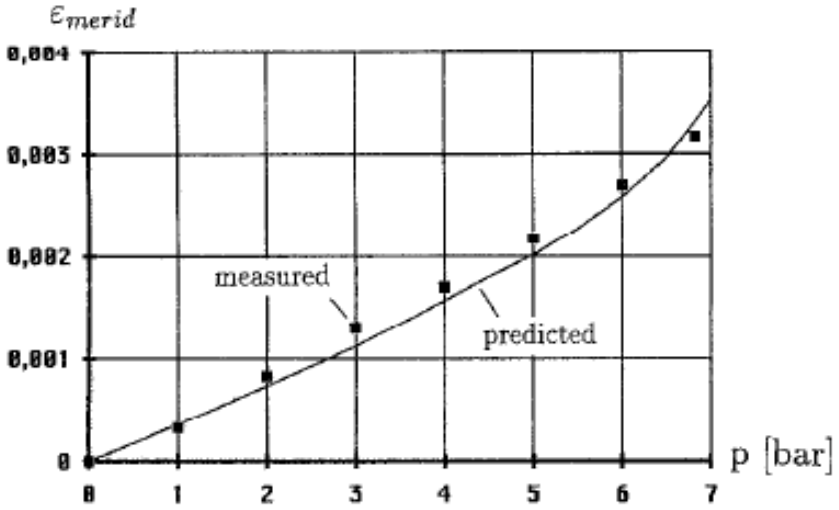

Figure 3.16: Correlation between meridional strains from the test and the numerical simulation [3]. The location of the strain gauge was close to the intersection with the fuselage. The results presented in the our study showed that meridian direction is not affected so much (figure 3.10 a) and it is not the most critical direction of strain measuring (figures 3.10 b, c and d)

3.3.1 Discussion and comments

Extrapolating the results of our analysis, deviations in the loading could be as high as 10% in terms of the circumferential internal loading. A finer mesh from the Arianne 5 article authors could have provided with better numerical results. In the main body of the article, the authors suggest that *"the resultant local strains were recorded through strain gauges at various locations of the bulkhead"*. Unfortunately, the exact positions were the measurements took place were not clearly identified on a drawing only a suggestion of one of these gauges being close to the T joint. Our bulkhead joint analysis has shown that the exact intersection position of the joint is the most critical. Stresses change from extremely negative to positive (besides the meridian stress) within a length of 150 mm from the intersection location, fig.3.10. Beyond the critical stripe of this change in internal loading, stresses and strains can be well approximated by the basic theory of mechanics, of shells under internal pressure, e.g. ref [17].

It has to be mentioned that the authors of [3] implied that the numerical analysis was performed for *qualification and verification* purposes. The author of this thesis agreed with the *verification* component of the study but second thoughts were generated in terms of the *qualification* part, refer to chapter two of this thesis. It was also implied in the article that the results of this study, *qualified the corresponding numerical procedure used as a very good dimensioning tool for highly stresses thin-walled structures*. According to the author's opinion this generalization shouldn't have been drawn just from the agreement between some test results and a numerical investigation.

Summarizing the above comments, the finite element mesh of the numerical study was not proper, results drawn in the vicinity of the joint and correlated between testing and analysis cannot suggest that the stress field is correctly depicted in figure 3.15 for example. The fact that the bulkhead structure survived the full scale test cannot imply that the numerical analysis provided with the correct stress field. Metallic materials possess the "fail safety" characteristic of plastically deforming and subsequently hardening followed by load redistribution. According to the author's opinion, the fact that the bulkhead survived the test and that strain measurements at some arbitrary locations correlated well with the test results does not render this numerical method, the model mesh generated and analysis procedure followed, a proper tool for qualification.

3.4 Importance of the study: Aircraft Accident Investigation Reports

Structural joints are always critical locations and sources of problems in airframe structures. Accident investigation reports have been generated in the past in relation to the joint between a pressurized fuselage and the bulkhead structure. Shown in figures 3.17, 3.18 and 3.19, the location of damages reported in two separate occasions in the vicinity of the bulkhead joint. The accident investigation report is referenced in [22]

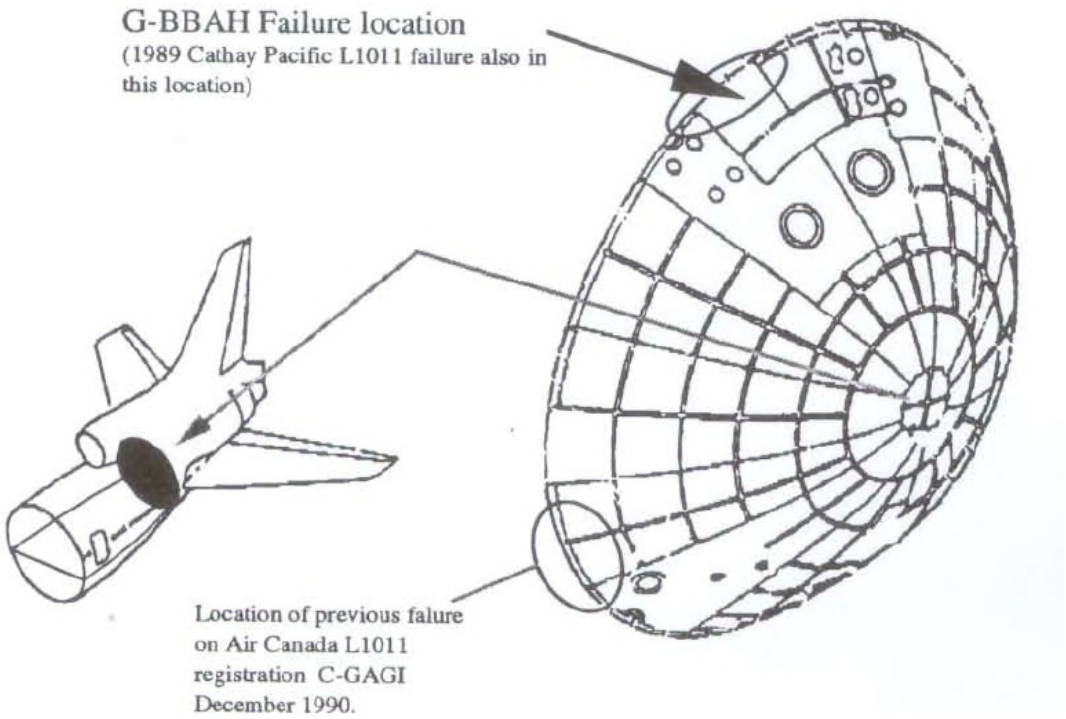

Figure 3.17: Failure positions in Lockheed's L1011 (ref: https://www.gov.uk/aaib-reports/lockheed-l1011-385-1-14-g-bbaf-19-july-1998), [22]

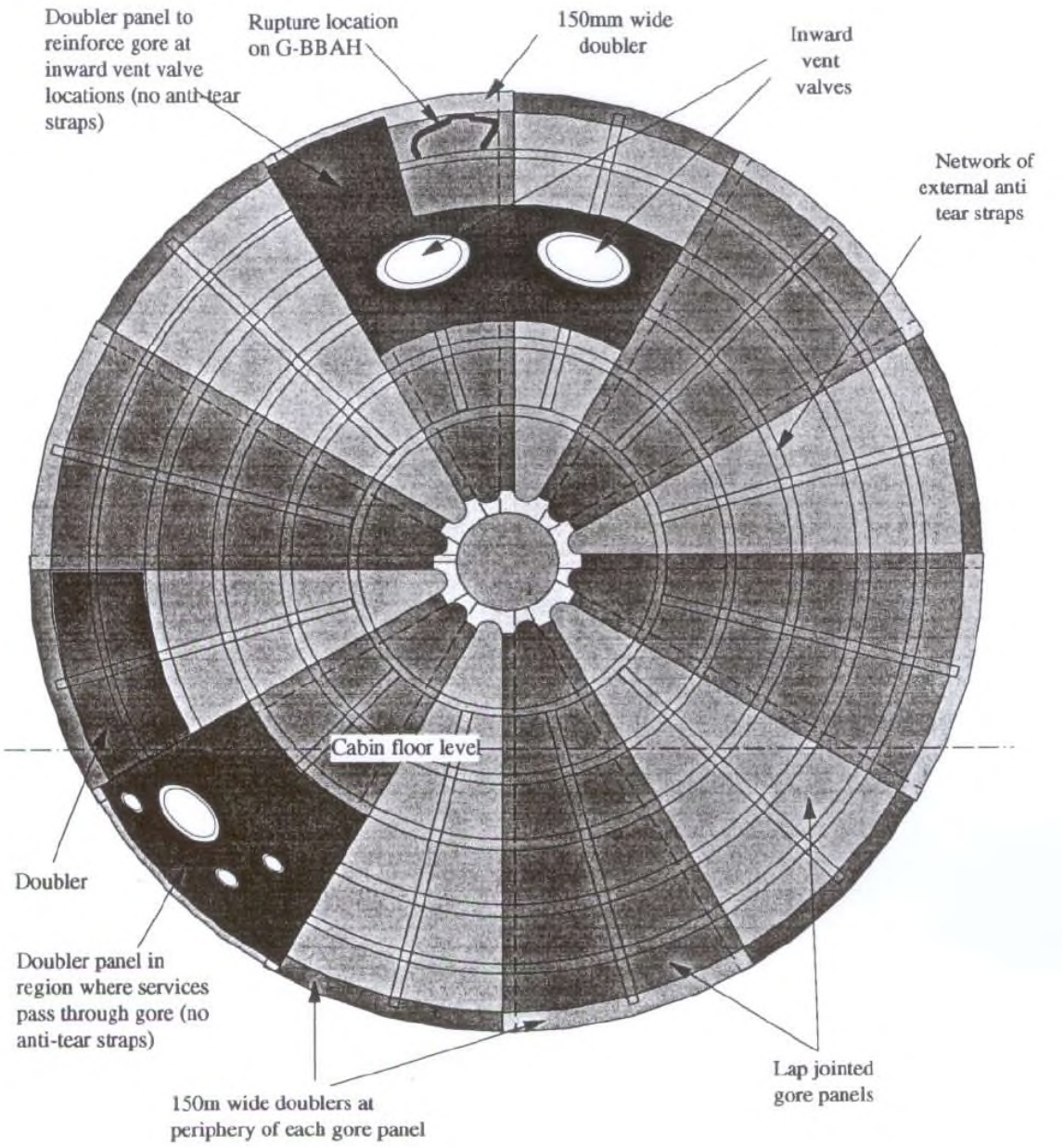

Figure 3.18: Failure positions in Lockheed's L1011 (ref: https://www.gov.uk/aaib-reports/lockheed-l1011-385-1-14-g-bbaf-19-july-1998), [22]

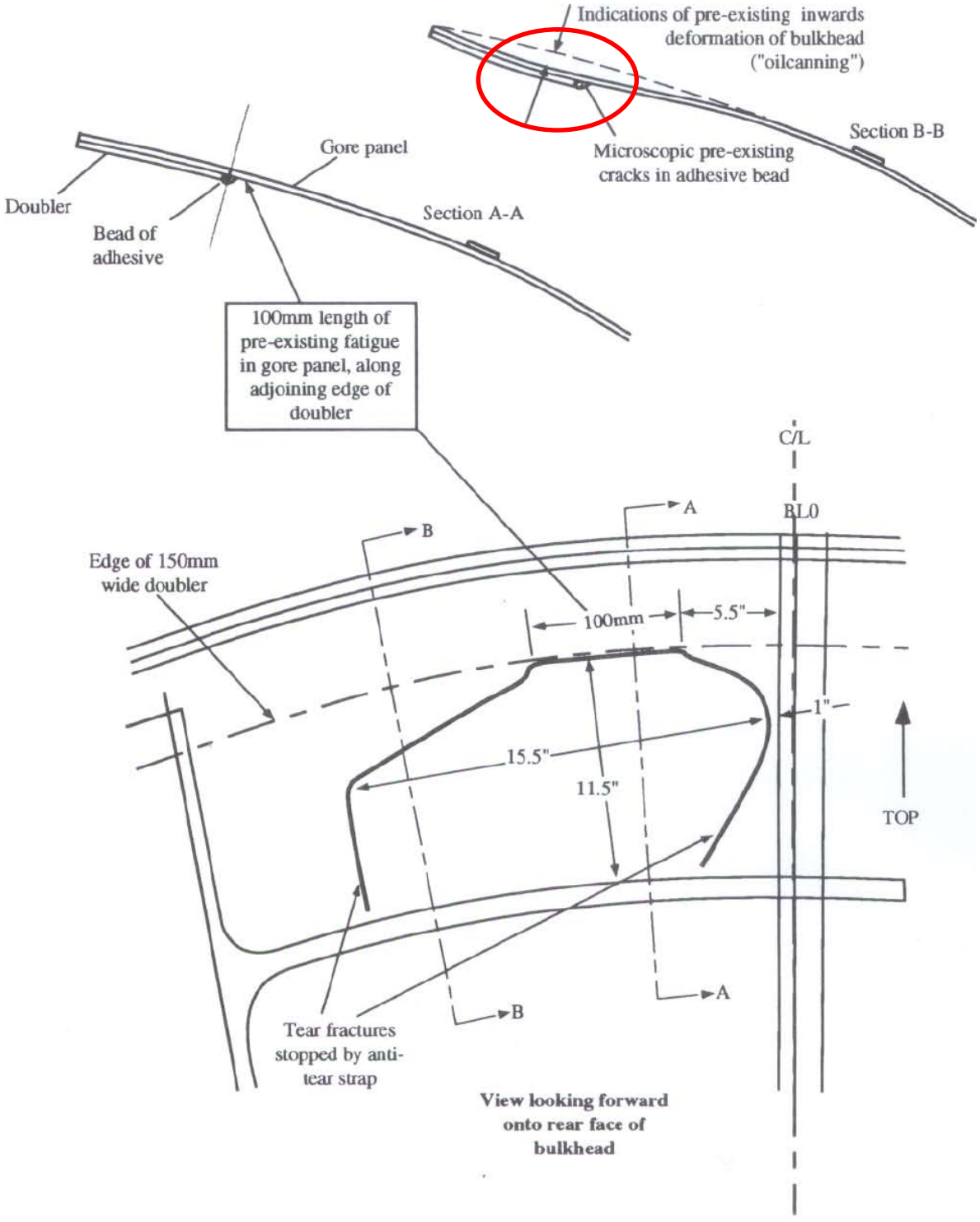

Figure 3.19: Failure positions in Lockheed's L1011 (ref: https://www.gov.uk/aaib-reports/lockheed-l1011-385-1-14-g-bbaf-19-july-1998), [22]

3.4.1 Discussion on the Aircraft Accident Investigation report and comments

Joints in airframes are critical spots of damage initiation and propagation. The specific location of the intersection between the fuselage and the bulkhead is a critical one since de-pressurization or rapid decompression effects can be the result of damage in that part of the pressurized fuselage. Accidents related to that structural area have been reported in the past. The structural failure reported in the accident investigation document [22], related to a metallic material structural failure. The way it was presented, fatigue failure seemed to be the cause. For fatigue cracks to propagate, tension stresses have to be present. Tension loading is shown in figure 3.10a. Some comment that relate with the thesis findings:

- This permanent deformation shape highlighted in figure 3.19 could have been the result of high compressive tangential stresses similar to the ones shown in figure 3.10c. The deformation shape correlates well with the representation shown in figure 3.4. In the report [22], the deformation was reported as permanent therefore local buckling with subsequent plastic deformation could be experienced by the structure and the material.
- The superimposed results from the damage mechanisms mentioned above along with the constant action of a tensile meridian loading and a slight augmentation by corrosion could have caused the crack initiation shown in figure 3.19. So even in a metallic structure, the prediction of such a damage initiation and propagation mechanism wouldn't have been assessed with a global FE model or by the use of classic analytical methods. Only in a refined FE analysis, the correct stress field can be represented in such a case.
- In the case that the certification of the airframe took place in a similar form like the certification presented in [3] and discussed in the previous section, i.e. using an incorrect FE model to account for the stresses followed by a successful full scale test, the severity of the stress distribution in the vicinity are not accounted for.
- The material response to the succession of damage mechanism did not cause catastrophic results, due to the ability of the structure to absorb compressive loading by plastic buckling / deformation. That may not be the case of a composite material bulkhead.

- Measures safeguarding against incidents of the sort most probably have acquired the necessary level of maturity related to metallic materials and design. As a result of this investigation manufacturers might know about the incident and may have addressed this in their design process. Nevertheless, using composite materials, the location has to be designed more carefully paying more attention to the stress levels experienced by the structure since composite structures, reduce their allowable compression load and the results from compression are catastrophic and not plastic deformation.

3.5 Impact of the article: proposed design change

The case study under investigation was proposed as a design change to Alenia-Aermacchi, certified manufacturer of airframe structures. The proposed initial design from Alenia-Aermacchi is shown in figure 3.20.

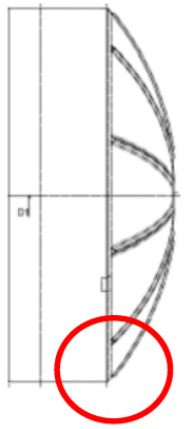

A1-A1

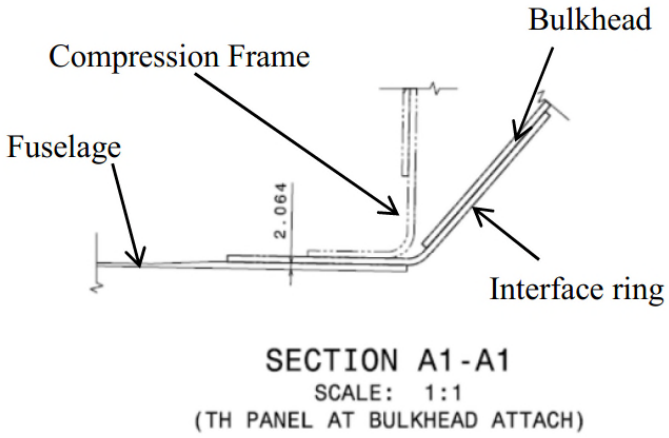

Figure 3.20: Proposed initial design

After communicating the results also contained in this chapter, the company agreed to change their original design concept to the one shown in figure 3.2. The bulkheads' outer diameter was designed slightly smaller in an effort not to expose the composite material into the sever stress intensity field close to the vicinity of the intersection with the fuselage. The interface ring was then made of traditional metallic materials thus making use of the confidence already accumulated in the usage of such materials in similar airframe locations.

3.6 Summary and key points of chapter three

- Global FE method is widely used in the aerospace industry. It is mainly used for internal loading distribution onto structural sub-elements. Provided that approved analytical methods exist for assessing the stress levels locally from the load distribution resulted from the global FE model, this can form an approved method for structural certification. Global FE modelling, due to the FE mesh coarseness, cannot correctly represent local stress raisers.
- Local refined FE modelling can provide with a better stress field depiction.
- In order to simulate structural strength until collapse and not just retrieving loads and stresses as was done in this chapter, damage modelling has to be implemented in the numerical simulation.
- High compressive stresses can be more detrimental in a composite material bulkhead than for a metallic one, due to the different allowable levels (CAI strength) and due to the different structural response until structural collapse (plastic behaviour for metals vs fracture for composites)

3.7 References in chapter three

[1] Howe, D., Aircraft Loading and Structural Layout, AIAA Educational Series, AIAA, Reston, VA, 2004, p. 457.

[2] Niu, M. C. Y., Airframe Structural Design, Hong Kong Conmilit Press, Hong Kong, 1995, pp. 398–402

[3] Becker, W., and Wacker, T., "Comparison Between Test and Analysis of a Tank Bulkhead Loaded in the Plastic Range," Aerospace Science and Technology, Vol. 1, No. 1, 1997, pp. 77–81. doi:10.1016/S1270-9638(97)90025-0

[4] Williams, D., "Structural Problems of Aircraft Pressure Cabins," Progress in Aeronautical Sciences, Vol. 1, Pergamon, New York, 1961, pp. 206–237.

[5] Hyer, M. W., and McMurray, J. M., "Internally Pressurized Elliptical Composite Cylinders," Composite Structures, Vol. 46, No. 1, 1999, pp. 17–31.doi:10.1016/S0263-8223(99)00038-0

[6] Krikanov, A. A., "Composite Pressure Vessels with Higher Stiffness," Composite Structures, Vol. 48, Nos. 1–3, 2000, pp. 119–127. doi:10.1016/S0263-8223(99)00083-5

[7] Kabir, M. Z., "Finite Element Analysis of Composite Pressure Vessels with a Load Sharing Metallic Liner," Composite Structures, Vol. 49, No. 3, July 2000, pp. 247–255.doi:10.1016/S0263-8223(99)00044-6

[8] Onder, A., Sayman, O., Dogan, T., and Tarakcioglu, N., "Burst Failure Load of Composite Pressure Vessels," Composite Structures, Vol. 89, No. 1, 2009, pp. 159–166.doi:1016/j.compstruct.2008.06.021

[9] Vasiliev, V. V., Krikanov, A. A., and Razin, A. F., "New Generation of Filament Wound Composite Pressure Vessels for Commercial Applications," Composite Structures, Vol.62, Nos. 3–4,2003, pp. 449–459.

[10] Hyer, M. W., and Vogl, G. A., "Response of Elliptical Composite Cylinders to a Spatially Uniform Temperature Change," Composite Structures, Vol. 51, No. 2, 2001, pp. 169–179. doi:10.1016/S0263-8223(00)00142-2

[11] Zhang, Q., Wang, Z. W., Tang, C. Y., Hu, D. P., Liu, P. Q., and Xia, L. Z., "Analytical Solution of the Thermo-Mechanical Stresses in a Multi-Layered Composite Pressure Vessel Considering the Influence of the Closed Ends,"

International Journal of Pressure Vessels and Piping, Vol. 98, Oct. 2012, pp. 102–110.doi:10.1016/j.ijpvp.2012.07.009

[12] Wang, Y., Zheng, Z., Sun, M., and Zhu, S, "Finite Element Modelling of Carbon Fibre Reinforced Polymer Pressure Vessel," International Conference on Educational and Network Technology (ICENT), IEEE Publ., Piscataway, NJ, 2010, pp. 259–262. doi:10.1109/ICENT.2010.5532177

[13] Adali, S., Summers, E. B., and Verijenko, V. E., "Optimization of Laminated Cylindrical Pressure Vessels Under the Strength Criterion," Composite Structures, Vol. 25, Nos. 3–4, 1993, pp. 305–312. doi:10.1016/0263-8223(93)90177-R

[14] Niu, M. C. Y., Airframe Stress Analysis and Sizing, 2nd ed., Hong Kong Conmilit Press, Hong Kong, 1999, pp. 181–203.

[15] Niu, M. C. Y., Composite Airframe Structures, Hong Kong Conmilit Press, Hong Kong, 1995, pp. 424–429.

[16] Bruhn, E. F., Analysis and Design of Flight Vehicle Structures, Tri-State Offset, Steubenville, OH, 1973, pp. A16.1–A16.10.

[17] Young, C. Y., and Budynas, G. R., Roark's Formulas for Stress and Strain, 7th ed., McGraw–Hill, New York, 2002, pp. 553–591, 643–644.

[18] Timoshenko, S., Strength of Materials Part II, 2nd ed., D. Van Nostrand Company, Inc., New York, 1947, pp. 159–173.

[19] NASTRAN Quick Reference Guide, MSC Software Corp., Newport Beach, CA, 2012.

[20] Reddy, J. N., Mechanics of Laminated Composites Plates and Shells: Theory and Analysis, 2nd ed., CRC Press, London, 2004, pp. 112–129.

[21] Daniel, I., and Ishai, O., Engineering Mechanics of Composite Materials, Oxford Univ. Press, New York, 1994, pp. 142–181.

[22] https://www.gov.uk/aaib-reports/lockheed-l1011-385-1-14-g-bbaf-19-july-1998

[23] Ioannis K. Giannopoulos, Efstathios E. Theotokoglou and Xiang Zhang.Design and numerical modelling of a pressurized airframe bulkhead joint. AIAA, JOURNAL OF AIRCRAFT, Vol.52, No 6, pg. 1729-1735, Nov-Dec 2015

Chapter 4

"Buckling of stiffened, thin walled fibre polymer shell structures"

Structural subassemblies made of thin shells stiffened by beam elements along the longitudinal and/or transverse direction is the most common structural design concept utilized in major airframe components like the wing and fuselage structures. These structural arrangements are called thin walled structures in the aerospace terms since the members comprising the assembly are made of thin sheets of metallic or fibre polymer composite materials. The structural sizing of these thin walled members is driven mainly from the assembly's resistance to compressive loading. Thin walled structures are susceptible to elastic or elastoplastic buckling instabilities which act as the major driver to the structure's overall weight and hence aircraft performance.

With the introduction of composite layered materials and substitution of their mostly aluminium counterparts, opportunities in terms of weight saving arose by proper tailoring of the composite material properties in terms of composite material system fibre and matrix, number and direction of layers and other design parameters, in order to design lighter and more efficient assemblies.

The fourth chapter presents a study where a numerical optimization methodology was utilized for generating the most efficient stiffened panel for a certain compression loading scenario along with the subsequent manufacturing and testing of the stiffened panel. Nonlinear finite element analysis was used in an effort to virtually represent the testing phase. Discussion is initiated related to airworthiness requirements and the need for showing structural compliance with the strength requirements when the stiffened panel contains damage.

<*Page intentionally left blank* >

4.1 Introduction to the Analysis of strength of Stiffened Panels

Structural components need to be certified either through reliable and proven analyses or via testing or both. Airworthiness certification of a structural assembly is performed in various hierarchical steps, from minor test articles to large assembled components. The aim of the chapter is to demonstrate the application of numerical analysis in the optimization of a stiffened panel design and its subsequent strength prediction which is going to be correlated with tests.

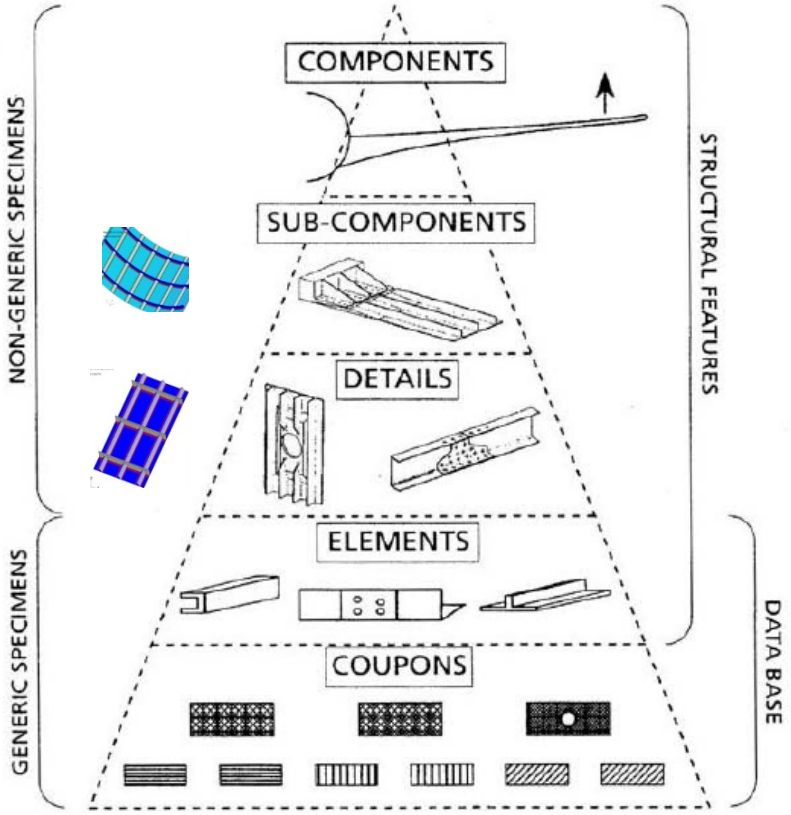

Figure 4.1: Relation of the work presented within chapter four, overlaid to the airworthiness certification test pyramid shown in ref [1]

Numerical finite element analysis applied in a stiffened panel will be presented and the limitations in the method capability for strength prediction discussed. From this testing / numerical evaluation and correlation survey, the importance of the impact damage will be highlighted and its threat to composite material airframes. Examples in

the numerical predictions from other sources will be shown and a relevant research case study will expose the limitation in the usage on numerical prediction tools. The publication related to this study is shown in reference [2]. Within the main body of the thesis, the author's contribution to the work is presented and discussed.

4.2 Description of the research project on stiffened panels

The project in ref [2] was set around the ability of various damage sensing techniques and architectures. In the context of assessing the damage sensing techniques, three identical composite stiffened panels were manufactured. All of them would be compression tested until failure. One of the panels was undamaged; the others were artificially damaged to contain barely visible damages (BVID) visible damages (VID) and artificial delamination. In the thesis context, the numerical simulation of the compression test until failure of the undamaged panel will be exhibited, work which was contributed by the author of the thesis.

More specifically, the performed tasks by the author of the thesis and its contribution to the project and to the subsequent journal publication were:

- To perform an optimization design study for designing the stronger/lighter compression stiffened panel by the variation in some of the design parameters such as number of stiffeners and the layup for the skin and stiffeners
- To evaluate/predict the failure load of the undamaged pristine composite panel. Geometrically non-linear analysis was used for fulfilling the task

4.2.1 Design case study: Optimization of a composite stiffened panel design parameters

The design organization where the author of this thesis was a part of, was tasked to design and manufacture the optimum stiffened panel that would be assumed to be a part of a fuselage. A numerical representation of the structure is shown in figure 4.2. Bending and torsional loads were assumed with respect to the fuselage cylindrical axis. The structure would have to be designed to carry a prescribed level of combined

bending and torsional loads without failure. Simulations were generated and performed with NASTRAN commercial software [3].

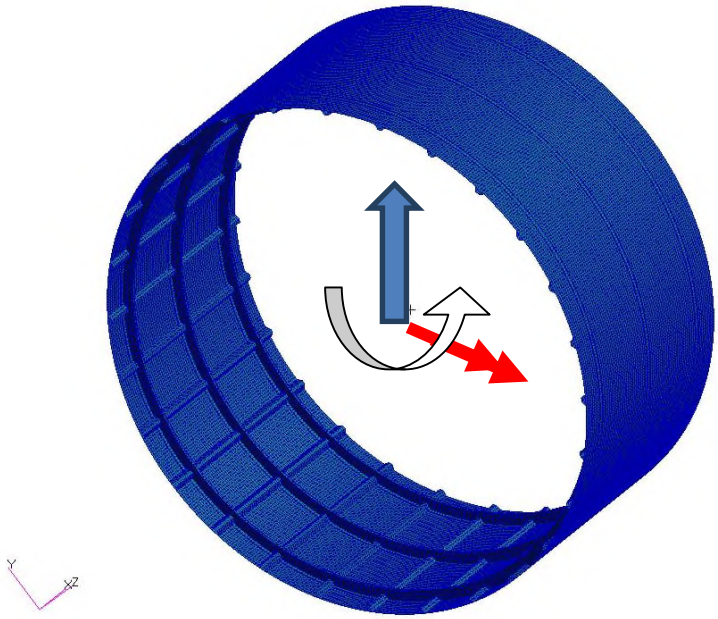

Figure 4.2: Numerical FE representation of an airframe fuselage section. FE full barrel geometry, adopted for correct combined compression and shear loading application

It was anticipated that the structure would be susceptible to buckling instabilities. Hence for the sake of simplicity, resistance to combined compression and shear loading were the criteria set for optimum design. In order to resolve the problem, various FE models were generated with the following varying parameters:

- pitch of stringers
- laminate layup of skin and
- laminate layup of stringers

The aim of the structural optimization was to create the lightest possible panel that fulfils the structural design criteria set, along with any other type of constraints need to be met by the structure.

The particular structural optimization problem was described by a number of design variables and design constraints. A multi variable optimization problem is strongly affected by the solution strategy and algorithm considered, can be time consuming and the final design solution set achieved can be questioned if it is indeed the “global” optimum variables set or not. For this reason, there has been an effort to diminish the number of design variables and constraints in this problem.

Other peculiarities of similar types of optimization problems are that most of the design variables are discrete, i.e. not continuously ranging inside a real number range, meaning, that the optimized number of applied stiffeners, for example must be an integer value e.g. 4, 5, 12 stiffeners etc. and not a real one e.g. 7.56 stiffeners. The same holds for most of the design variables considered.

Apart from being a discrete variable optimization problem, there were also certain manufacturing and design constraint rules that need to be fulfilled which rules are specific to the product realization and are not relevant to the optimization algorithm itself. These constraints are transformed into design value space boundaries for the design variables.

For the specific curved stiffened panel to be designed, the panel combined compression and shear loading was given. The structural design criteria were:

- The panel has to endure ultimate loading without failure
- The panel should not fail due to global buckling instability at limit loading. Local buckling is permitted as long as the post buckled shape does not induce failure strains

There has been a great effort in trying to reduce the number of design variables. By the aid of literature [4], [5], [6] and [7] for similar stiffened panel geometries, some of the variables and constraints were predefined; the shape of the omega stiffeners (total height, angle of the webs, upper cap width, lower feet width)

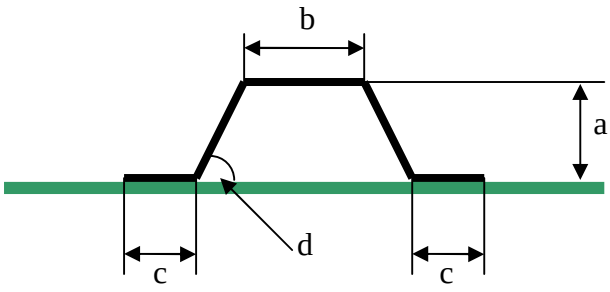

a: stiffener height

b: stiffener upper cap width

c: stiffener lower feet width

d: angle of the stiffener webs

Figure 4.3: Predefined design variables

The range of the skin thicknesses for the bays or the omega stiffeners has been pre-set to range from 1mm to 2.5mm. These configurations follow the rules of a symmetrical and balanced layup.

The applicable layup configurations for the above mentioned range and specifically for the stiffeners has been divided to three categories, stiff – medium – soft layup. These layups are characterized as such, depending on the 0^o ply content, the more zero degree plys applied, the stiffer the layup. These configurations also follow the rules of a symmetrical and balanced layups.

The application of the predetermined constraints onto the problem is to effectively bind the design variables into a series of applicable layup configurations ranging from 1mm-2.5mm thicknesses and a stiff-medium-soft categorization in respect to the longitudinal E11 modulus property for the stiffeners.

The final optimization variables and the respective constraints chosen for the algorithm are:

- Number of stiffeners used (ranging from 24 to 40 for the FEM full barrel geometry)
- The layup configuration of the stiffeners (stiff – medium – soft)
- The skin thickness of the stiffeners (1mm – 2.5mm)

- The skin thickness of the bays (1mm – 2.5mm)

For the algorithm, a steepest descent scheme is adopted: for a given set of design variables, the effect upon the structural response is evaluated via FEM considering also the mass of the part that corresponds to the specific set of variables. For the neighbouring set of variables the response is also evaluated via FEM and the route to optimization is decided upon the effectiveness of the response correlated to the mass of the part.

4.2.2 FEM evaluation

Representative fuselage sections that would carry the prescribed loading (figure 4.2) were generated in NASTRAN virtual environment and their response to the loading is evaluated. The measured responses were:

- Linear analysis strain behaviour to ultimate loading,
- Non-linear analysis of buckling behaviour to limit loading,
- Non-linear analysis strain behaviour to limit loading.

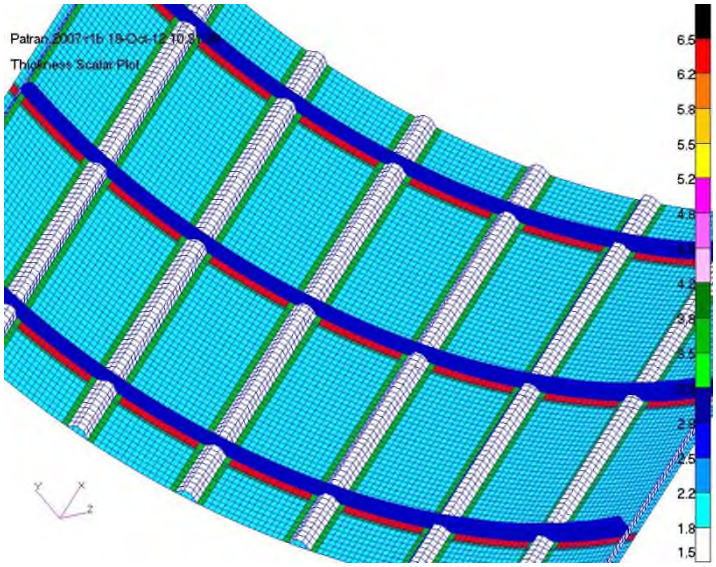

Figure 4.4: Finite FEM membrane thickness plot of the curved panel geometry. Number of stiffeners, stiffener and skin thickness and layup are design variables, constrained accordingly

4.2.3 Results

The optimization algorithm resulted in the number of stiffeners required and the layup of the skins and stiffeners for the lightest panel to fulfil the loading requirements. The FE models used for the optimization were curved. Since curved panels are more difficult to manufacture than straight ones due to the tooling and since the application of combined compression the actual testing survey was then performed on straight panels with the same design parameters as the curved ones. The resulted panel is shown in figure 4.5 in a layer thickness fringe plot. Also since the application of combined compression and shear loading is difficult to apply in a normal testing facility, the panel was tested under compression only.

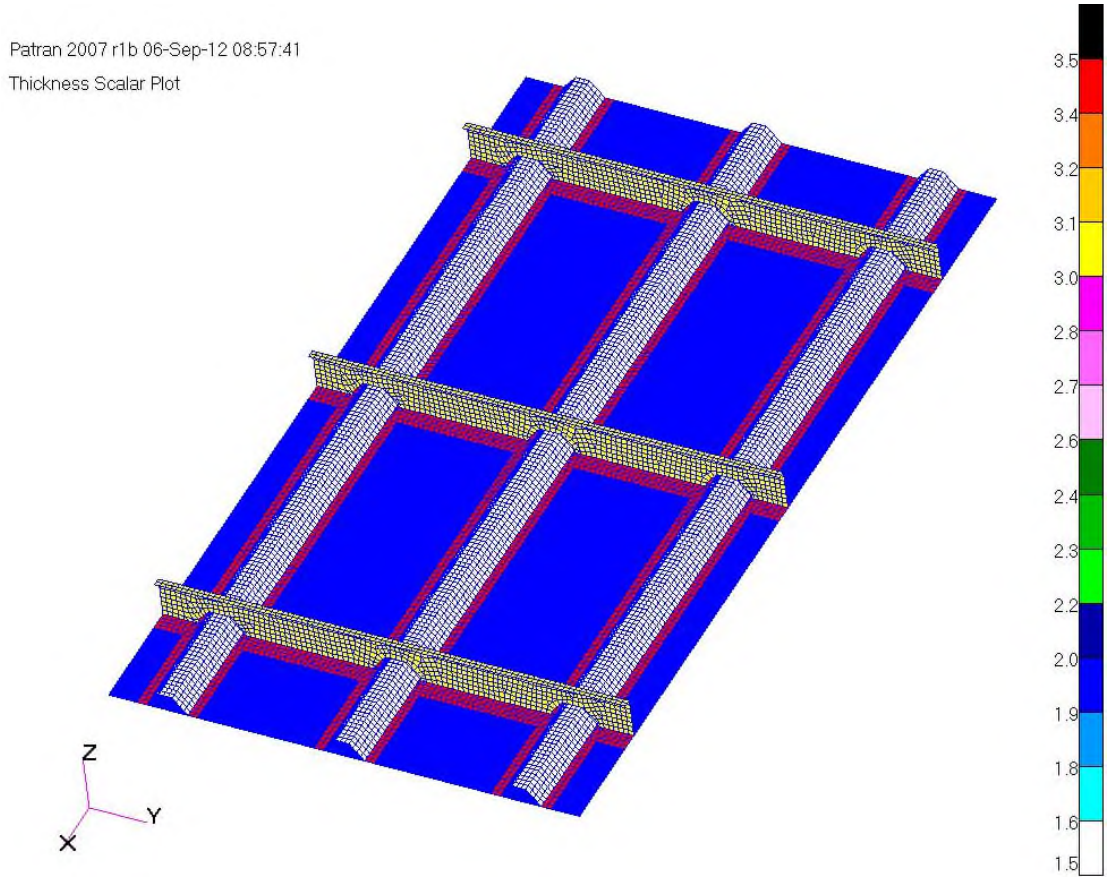

Figure 4.5: Finite element model of the pristine/undamaged composite material stiffened panel. Fringe plot shows the thickness of the resulted shell element thickness in millimetres, after the optimization cycles

4.3 Numerical verification of a test case study: Compression test of a stiffened panel

The aim of this section is to present the numerical analysis performed for evaluating and correlating the strength of the composite material stiffened panel with tests. The design parameters of the panel had been dictated by the previous optimization study. According to the author, a panel of minimum weight with maximum load bearing capacity in combined compression and shear loading was the outcome of the optimization study.

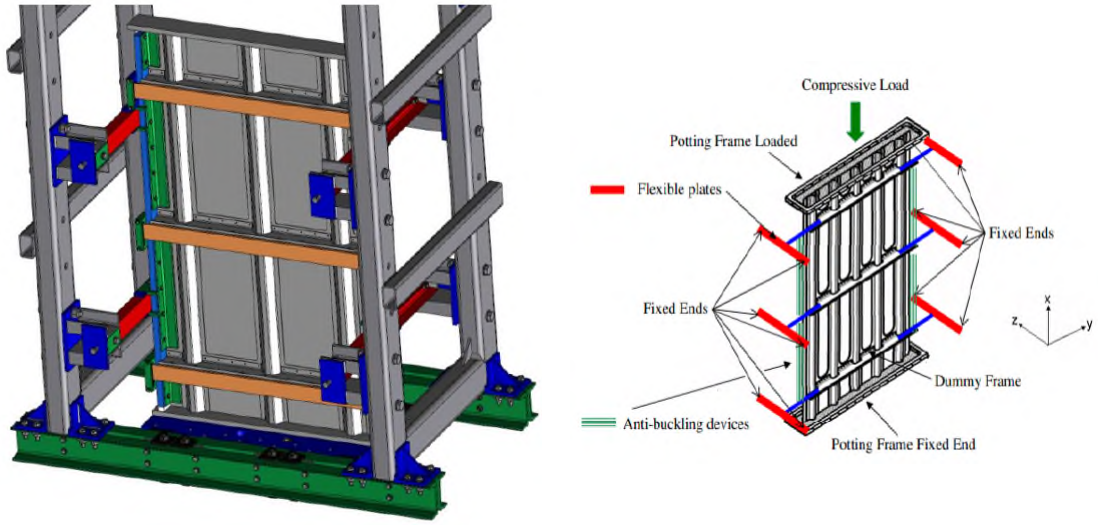

Figure 4.6: CAD representation of the panel under compression, the testing fixtures and boundary conditions. The boundary conditions were simulated in the FEA

4.3.1 Numerical analysis setup and results

To simulate compression testing and since local and global buckling instabilities were expected to take place, the simulation was modelled by the aid of geometrically nonlinear numerical subroutines. NASTRAN commercial software package was used [3]. The aim was to model the force displacement curve with FE analysis and monitor local buckling behaviour as well as predict the ultimate failure if possible. Ultimate failure was expected to be either in the form of global buckling or in the form of local material failure. Maximum strain failure criterion was also implemented in the solver

and was monitored in that respect in order to be aware at which part of the force displacement curve, material failure was predicted.

Prior to analyzing a model with geometrically non-linear solvers, it is a good practice to perform an eigenvalue analysis. The results of such an analysis are presented below.

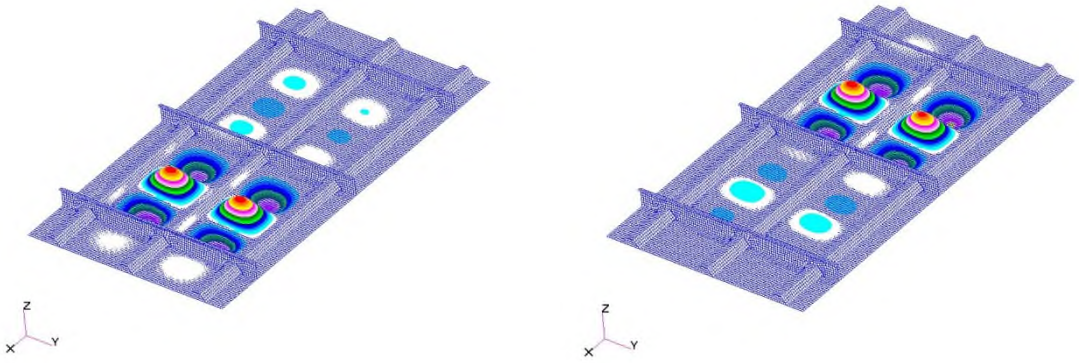

a) First buckling shape 58.4 kN b) Second buckling shape 58.5 kN

Figure 4.7: The first two eigen modes and eigenvalues of the stiffened panel under compression

The resulted eigen values / eigen modes shown in the figure 4.7, having not a great difference between them, indicate that the structure will be very susceptible to initial imperfections, ref [8]

The geometrically non-linear solution, revealed the following load displacement curve, shown in figures 4.8, 4.9 and commented below:

- Starting from 0 kN / 0.0 mm up to the point of approximately 86.8kN / 0.85mm, the panel exhibited a close to linear behavior. Visible deformational distortions in the z-direction appeared as the load built up. The local pre-buckling shape is shown in also in 4.9 (a).
- Approximately at 86.8kN / 0.85mm, local buckling of the panels in between the frames and the stiffeners to took place. This is shown also in 4.9 (b).
- Beyond the first local buckling point, up to approximately 560kN / 8.4mm, the panel exhibited local buckling shapes in the panels in between the frames and the

stiffeners, with increasingly smaller wave lengths as shown in the representative figure 4.9 (c).

Approximately at 560kN / 8.4mm, global buckling failure was expected. The central stiffener buckled into a sinusoidal shape, one half of it shall move upward the other half downwards in z – direction. This is shown also in 4.9 (e).

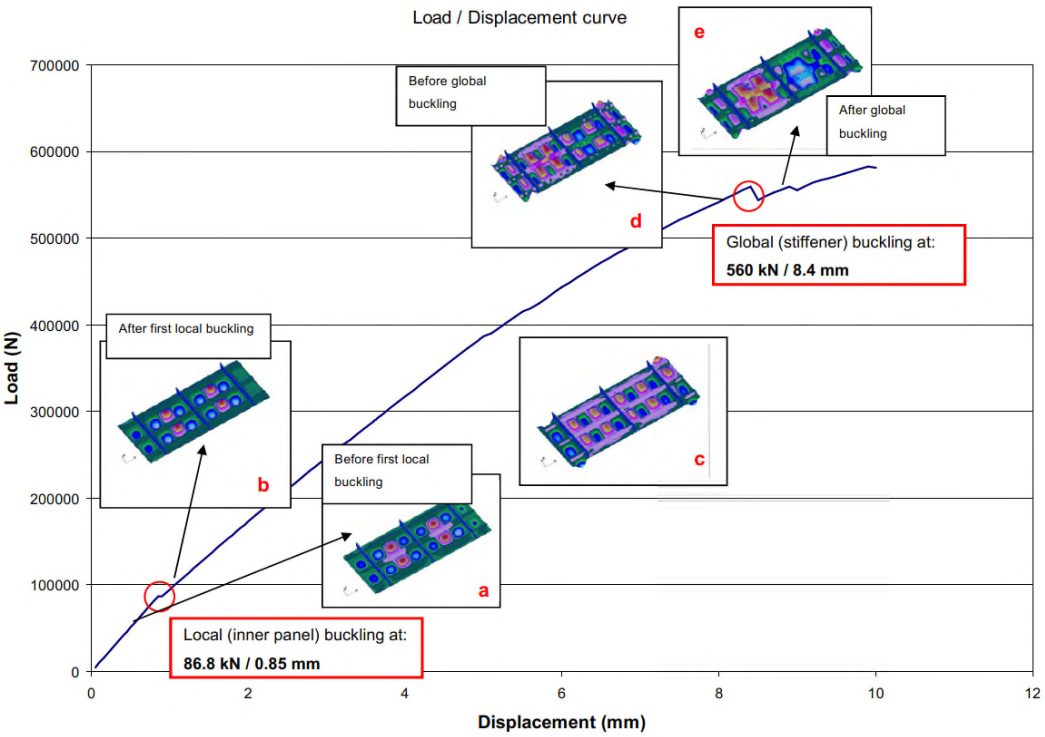

Figure 4.8: Predicted load displacement curve with pictorial representations of the deformed FE model and legends describing the state of deformation

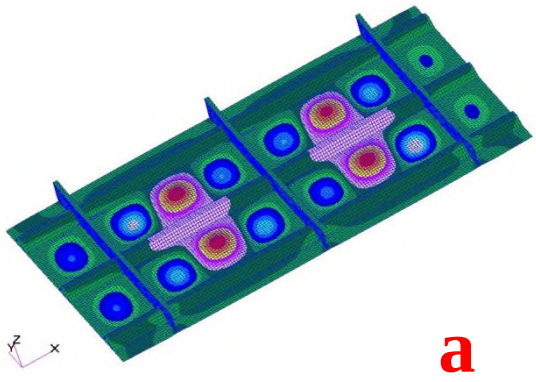

a. Pre- local buckling deformation shapes up to **86.8 kN / 0.85 mm**

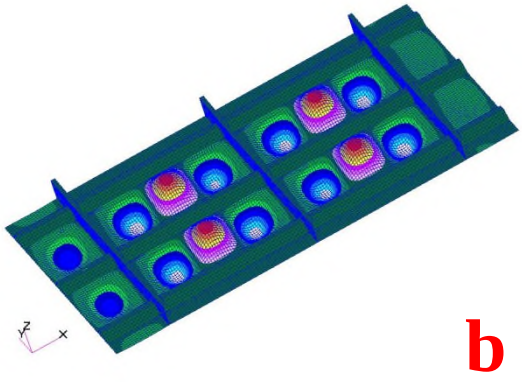

b. Local buckling deformation shape at **86.8 kN / 0.85 mm.** Panel buckling in between frames and stiffeners

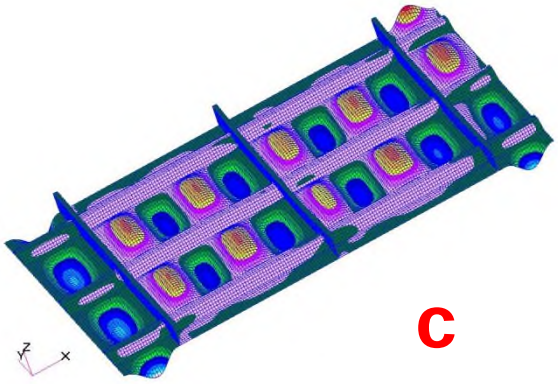

c. Local buckling deformation shapes from **86.8 kN / 0.85 mm** up to **560 kN / 8.4 mm**. Panel buckling with decreasing the shape wave length

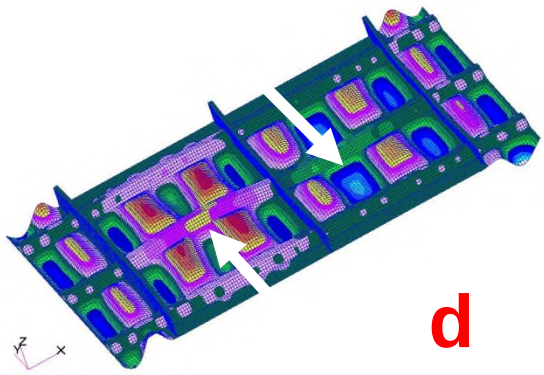

d. Global buckling initiation just before **560 kN / 8.4 mm**.

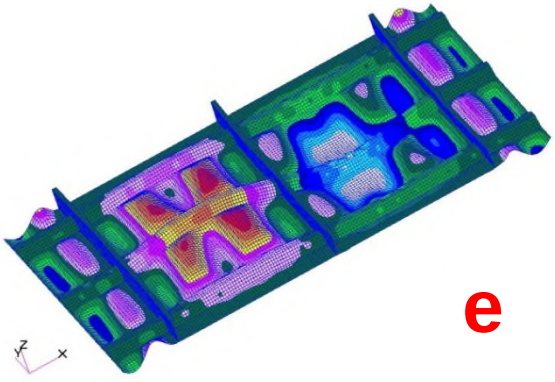

e. Buckled stiffener and most probably destruction of panel just after **560 kN / 8.4 mm**.

Figure 4.9: Total displacement fringe plots at various stages of compression loading

The afore mentioned elastic stability results were overlaid with the maximum strain criterion. It was important to monitor the stain levels in the process because a premature material failure in the deformation process shown if figure 4.9(a)-(e) would alter the sequence of failure events. Maximum / minimum fiber strain criteria were used in order to give an insight in the composite panel strength during the test. Lamina strength properties degradation due to matrix cracking was not considered, in order to keep the analysis simple. The fibers were expected to break in tensile mode at 15.000 με and in compression within a range from 8.000 to 10.000 με due to fibre kinking. Fringe plots at 10.000 με are displayed below.

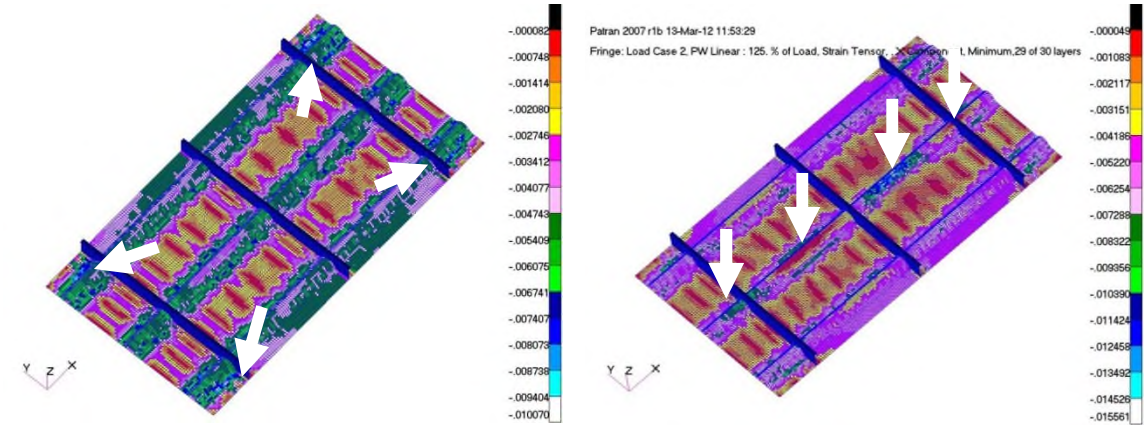

a) Maximum compressive strains along the fiber direction are at a level of 10.000 με at 500 kN / 7.1 mm

b) Maximum compressive strains along the fiber direction are at a level of 15.000 με close to the vicinity of global buckling i.e. 560 kN / 8.4 mm

Figure 4.10: Maximum and minimum allowable strains.

Maximum tensile strains were not expected to be reached, unless the panel was to be driven beyond the global buckling mode at 560 kN, were the middle stiffener would bent in a sinusoidal format and cause tension failure in the positive part of the beam under bending. Since global instability seemed to be a rather catastrophic failure mode, the structure wouldn't have any substantial structural element left the bypass the load, global buckling and tensile failure would take place simultaneously.

Well before the 560 kN global buckling mode, at 460 kN / 6.2 mm, the maximum allowable compression stresses were to be reached. It was then anticipated that failure will initiate at this point. The most loaded areas starting from up to **460kN / 6.2mm**, were the stringers overlap to the skin as shown in figure 4.10 a). The maximum allowable compression strain, resulted in the following failure load prediction, shown in figure 4.11 below. It was anticipated that failure will initiate at 460 kN and the panel would not have been able to go past the load of 560 kN.

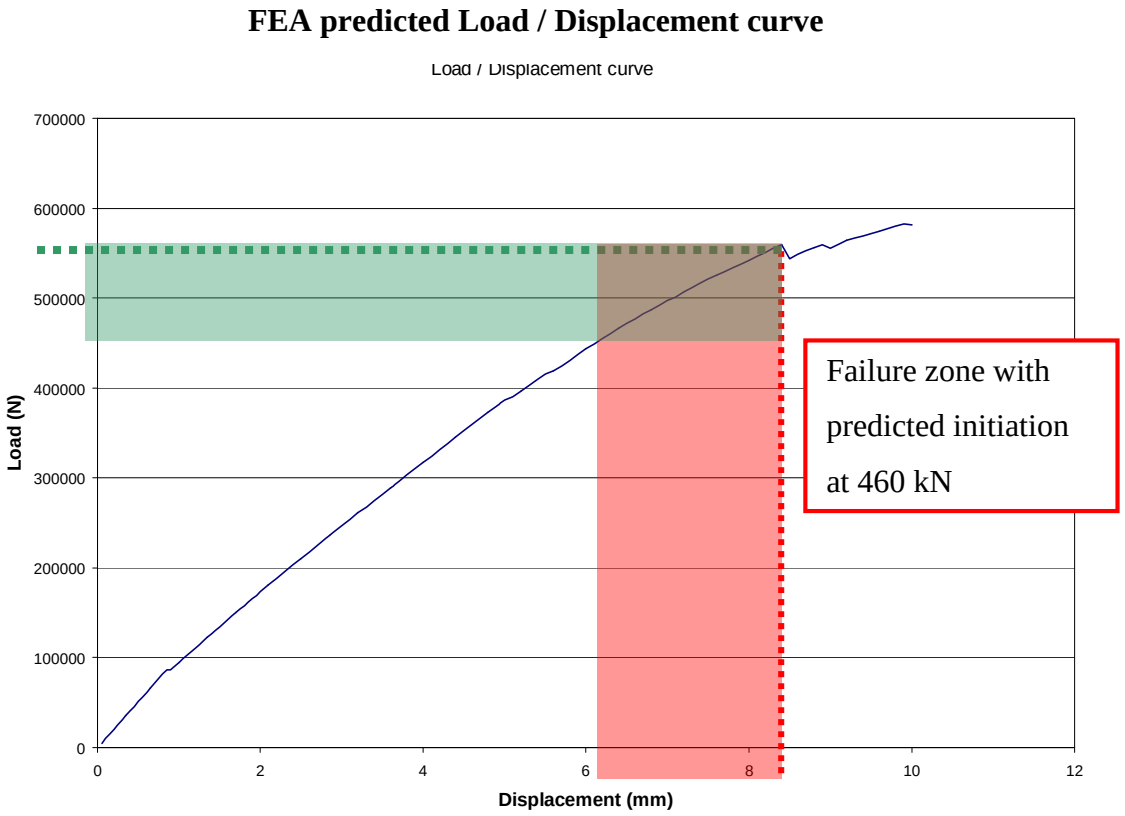

Figure 4.11: Maximum and minimum allowable strains.

4.3.2 Test results and discussion

The test results for the panel under compression are shown in figure 4.12 and 4.13. The actual test utilized our predicted FEA loading and loaded the panel at first up to 400 kN load, retracted to zero and then load again until failure. The actual tested panel **failed at 448N / 7.34mm** displacement of the test machine head displacement.

The numerical prediction in terms of failure was: the level of compression would start to become critical at**460 kN / 6.2 mm** and total panel failure is expected to take place well before**560kN / 8.4mm** where global buckling is expected. The most loaded areas up to **460 kN / 6.2 mm**, were the stringers overlap to the skin shown in figure 4.12 a). If the point of global buckling was to be reached i.e. approximately at **560kN / 8.4mm**, the fiber strains immediately will rise to the failure value and the middle stiffener will be shuttered. So although our main supposition was that the panel will survive the initial minor damages at approximately **460 kN / 6.2 mm,** this was actually not the case and catastrophic failure of the complete panel initiated at one of these spots, progressed to the complete panel failure, shown in figure 4.12 b) and c). First ply failure location, initially considered not able to cause catastrophic failure of the complete panel. In the test situation, the damage initiated at this position, progressed throughout the panel, causing total failure.

Disregarding the fact that we initially assumed that the damages caused at **460 kN / 6.2 mm** stage would not have been enough to progressively fail the complete panel, the error in the prediction of the failure compressive load in terms of loading was:

Error (%) in terms of total loading capacity = (460 - 448) / 448 = **2.7 %**

The strength had not been accurately assessed in terms of load since there has been stiffness deviations between the FEM and the actual panel discussed previously.

In terms of total panel compressive displacement, the error in the prediction was:

Error (%) in terms of total displacement = (6.2 – 7.1) / 7.1 = **12.7 %**

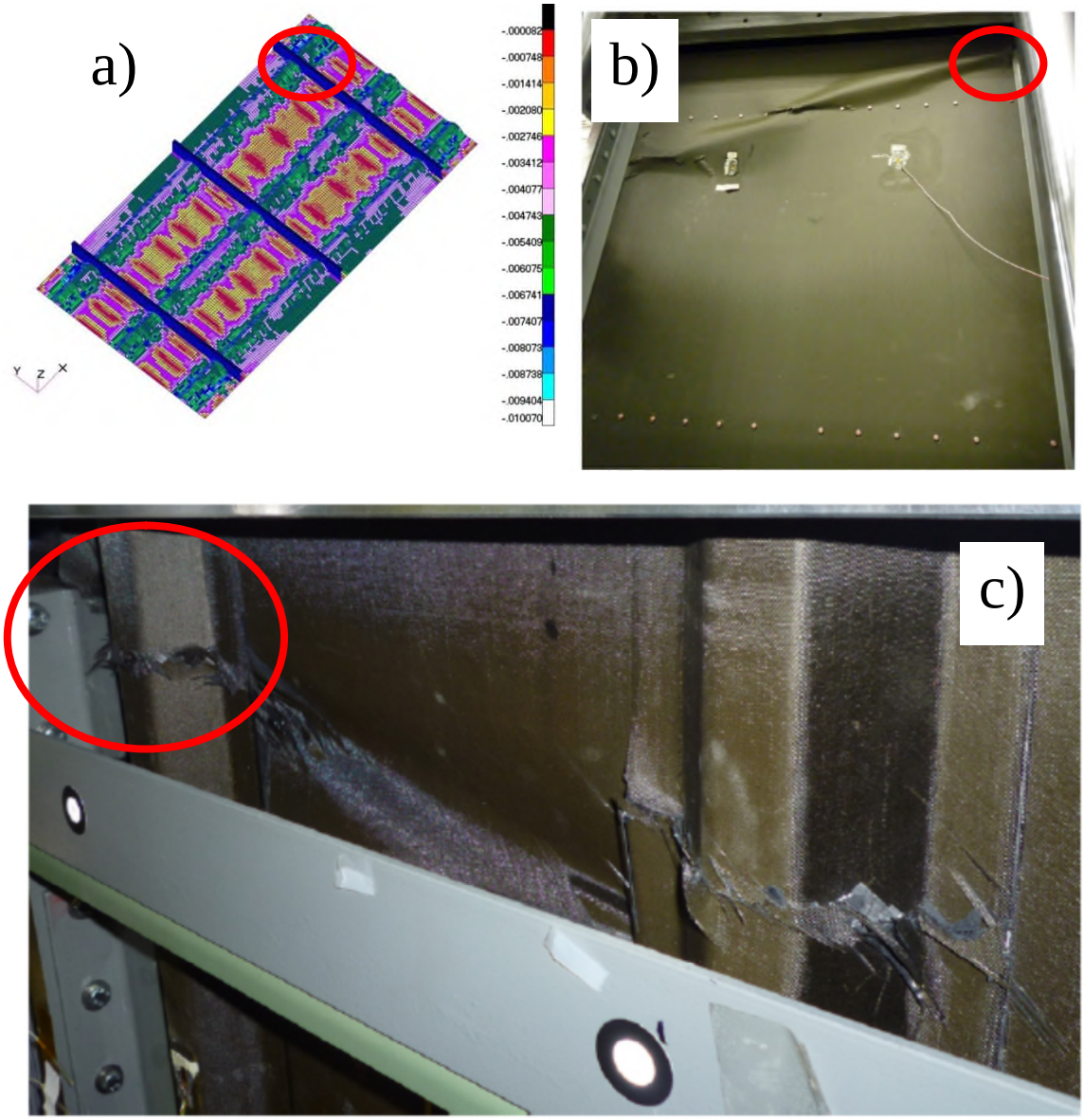

Figure 4.12: a) Numerically predicted location of reaching minimum allowable fiber strains, b) and c) locations on the actual panel tested

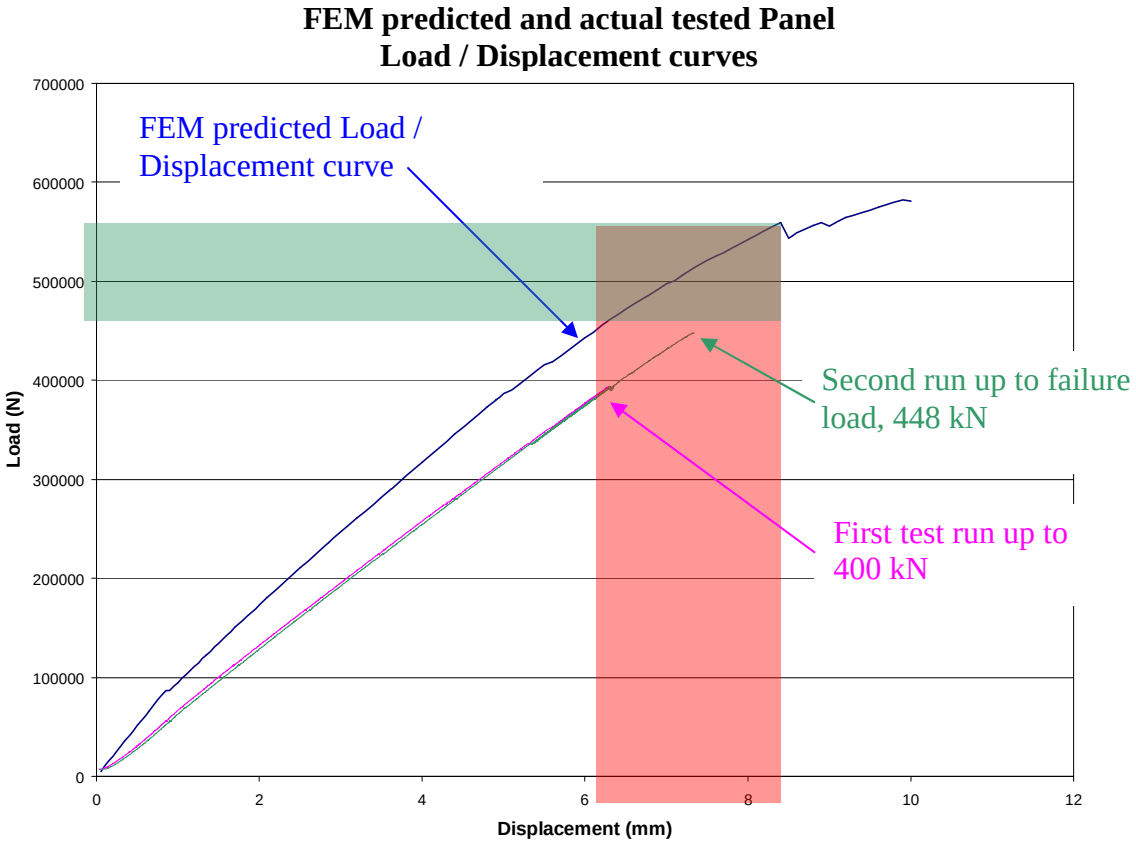

Figure 4.13: FEA load displacement curve superimposed by the testing ones and with the failure zone prediction

The results were further analyzed in regards of the following distinctive deviations:

- The stiffness variation between the analysis and test
- The initial augmented compliance exhibited during the test
- The first local buckling mode occurrence in terms of load and displacement

4.3.3 Variation in the stiffness observed between test and numerical simulation

A striking effect observed upfront in the testing was that the stiffness of the panel showed higher stiffness in the numerical simulation than in reality. This was obvious since the tangent line to the curves that represent the stiffness in each case, was

slightly larger for the FEA model and for smaller loads, whereas for larger loading, the stiffness becomes more or less the same. This effect is shown in figure xx

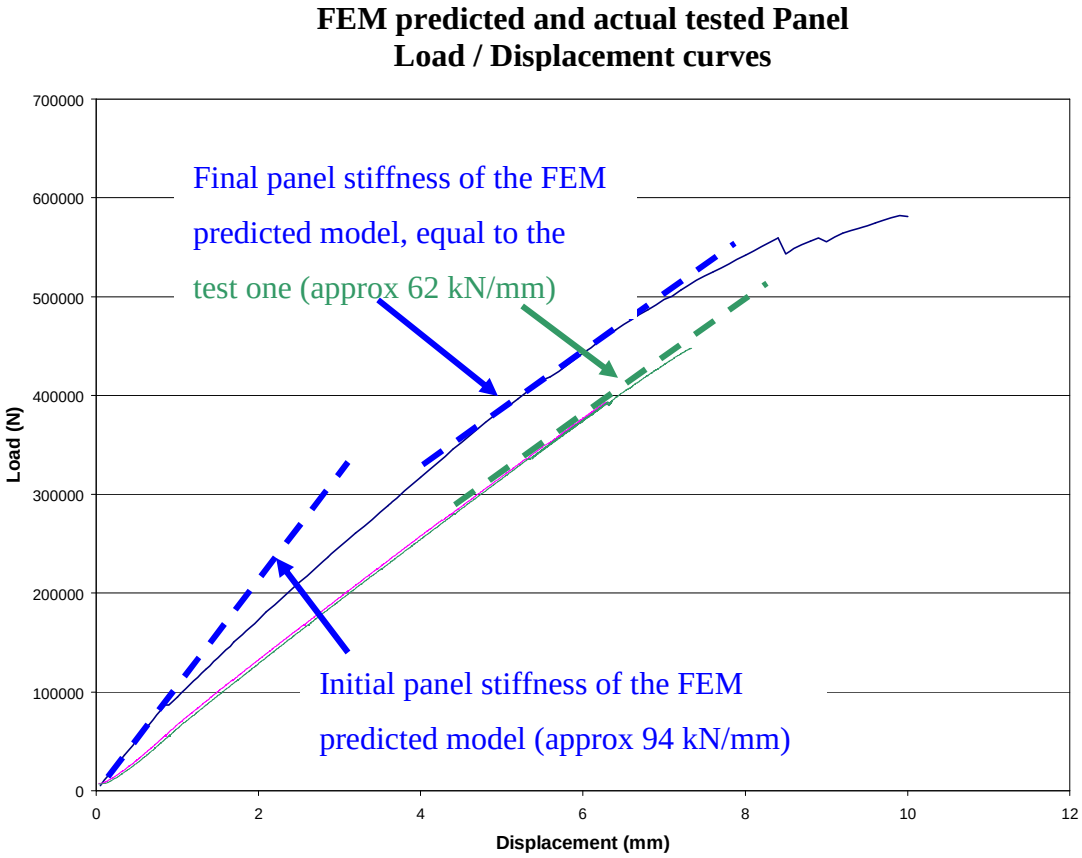

Figure 4.14: Variation in the stiffness of the panel between numerical simulation and testing

The test results indicated that the actual part has a more or less unchanged stiffness throughout the experiment. On the other hand the FEM model, lowers its stiffness after the bays give in to buckling failure and practically contribute less and less to the panel stiffness only via a (continuously reducing with larger force) “effective length” to the major stiffeners.

A simple hand calculation of the panel stiffness can be performed, assuming the panel to be three major springs in parallel in compression. The springs can be assumed to be the skin part, the stiffener part and the part were skin and stringers are overlaid. Every spring shall represent the different composite layup properties:

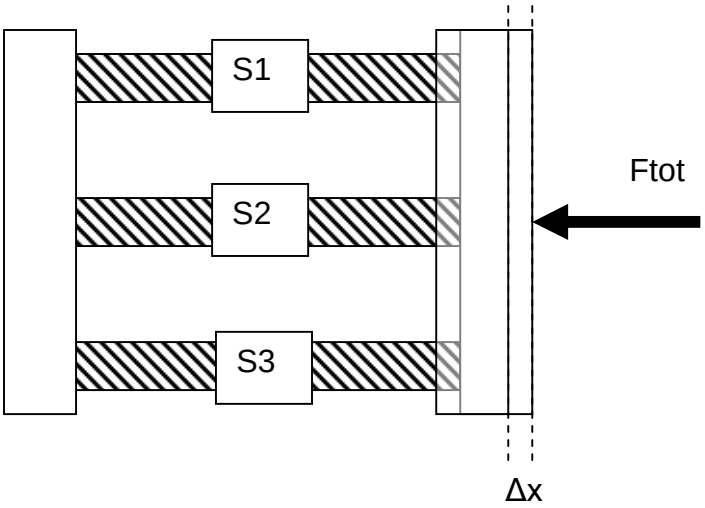

Figure 4.15: Variation in the stiffness of the panel between numerical simulation and testing

With:

$$F1 = S1 \times \Delta x, \quad S1 = E1 \times A1 / L$$
$$F2 = S2 \times \Delta x, \quad S2 = E2 \times A2 / L$$
$$F3 = S3 \times \Delta x, \quad S3 = E3 \times A3 / L$$

Total load: $Ftot = F1 + F2 + F3$

Total panel stiffness: $Stot = S1 + S2 + S3$

- S1, S2, S3: the stiffness of the skin, stiffener and skin + stiffener layup respectively
- E1, E2, E3: the elastic modulus for the composite laminates of the skin, stiffener and skin + stiffener layup respectively
- A1, A2, A3: the areas in panel section occupied by the composite laminates of the skin, stiffener and skin + stiffener layup respectively
- L: the length of the panel, 1650 mm
- F1, F2, F3: the respective reaction forces to the total load

Using CLT analysis, the following moduli of elasticity can be assumed for the different parts of the panel:

E1 = 57000 MPa, A1 = (790.86 x 2) mm^2 => S1 = 54642 N/mm
E2 = 89700 MPa, A2 = (325.77 x 1.5) mm^2 => S2 = 26565 N/ mm
E3 = 71000 MPa, A3 = (109.08 x 3.5) mm^2 => S3 = 16428 N/ mm

The result was that for the total stiffened panel, the stiffness should be: Stot = 97635 N/ mm, that is for a Δx=1 mm motion of the compression head, an Ftot = 97635 N is expected, which agrees with the FEM model. So by CLT analysis of composite laminates, the initial tangent curve of the FEM prediction is correct (actual value of the FEM model is 94822 N for 1 mm of compressive motion).

The stiffness that is produced by the stiffeners alone, following the same calculation approach is close to 59363 N/mm (neglecting the stiffness of the bays)

The fact that the actual panel tested did not change its stiffness character even after bay first local buckling has occurred, suggested that the bays did not considerably contributed to the panel compression stiffness throughout the experiment. This result leads us to the thought that imperfections in the perfect geometry assumed by the FEA were present in the test. Minor or major geometry deviations from the pure flatness of the panel or the eccentricity in which the bays are loaded in compression, does not allow the bays to be load carrying elements as in the case of the perfectly straight geometry of the FEM environment. Another reason for this could as well be the initial panel deformation caused by thermal stresses as a result of the curing process.

With larger loads, where also in the FEM the bays are also buckled, the FEM stiffness comes to match to the actual test one.

4.3.4 The initial augmented compliance exhibited during the test

Another issue to be discussed considering the inconsistency of the results is that during the test, there is a certain compression head displacement needed in order for the test article to fully engage to compression. It has to be stated that the displacement measured during the test, was the displacement of the crosshead at the location of the top of the panel. The reason for this initial panel behavior was that at the load application points which were practically the edge of the panel, local material crushing

might have taken place. Another indication of this assumption was that the second test up to ultimate loading (green curve) had been relatively displaced with respect the first test (pink curve)

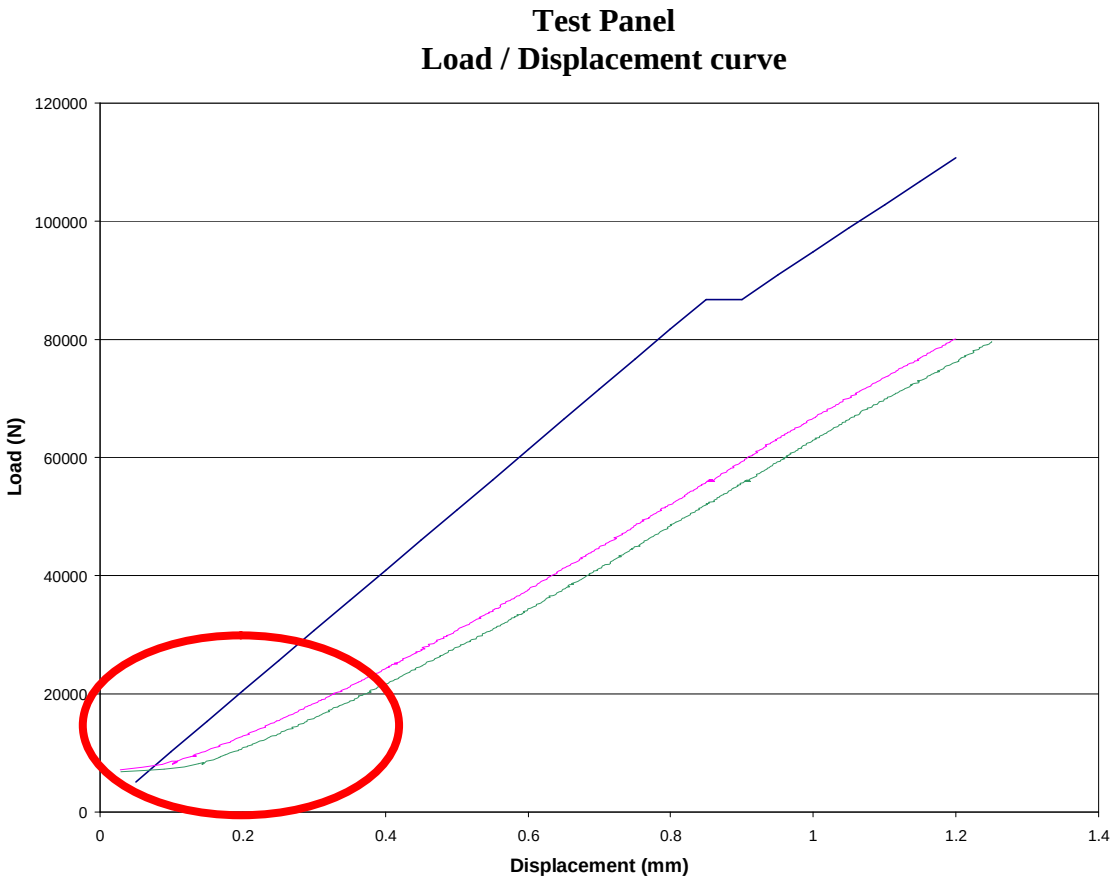

Figure 4.16: Variation in the stiffness of the panel between numerical simulation and testing

4.3.5 First local buckling mode

The panel first local buckling was of a major interest. Post buckling shapes and higher mode shapes than the first one shall not be cross referenced with the FEM model results.

The sensors embedded on the bays of the panel indicated the buckling load.

The measured strain test results have indicated that there are indications of a first buckling mode close to 54 kN:

Strain gauges reading. Approximate location on the panel of the strain gauge indicating buckling

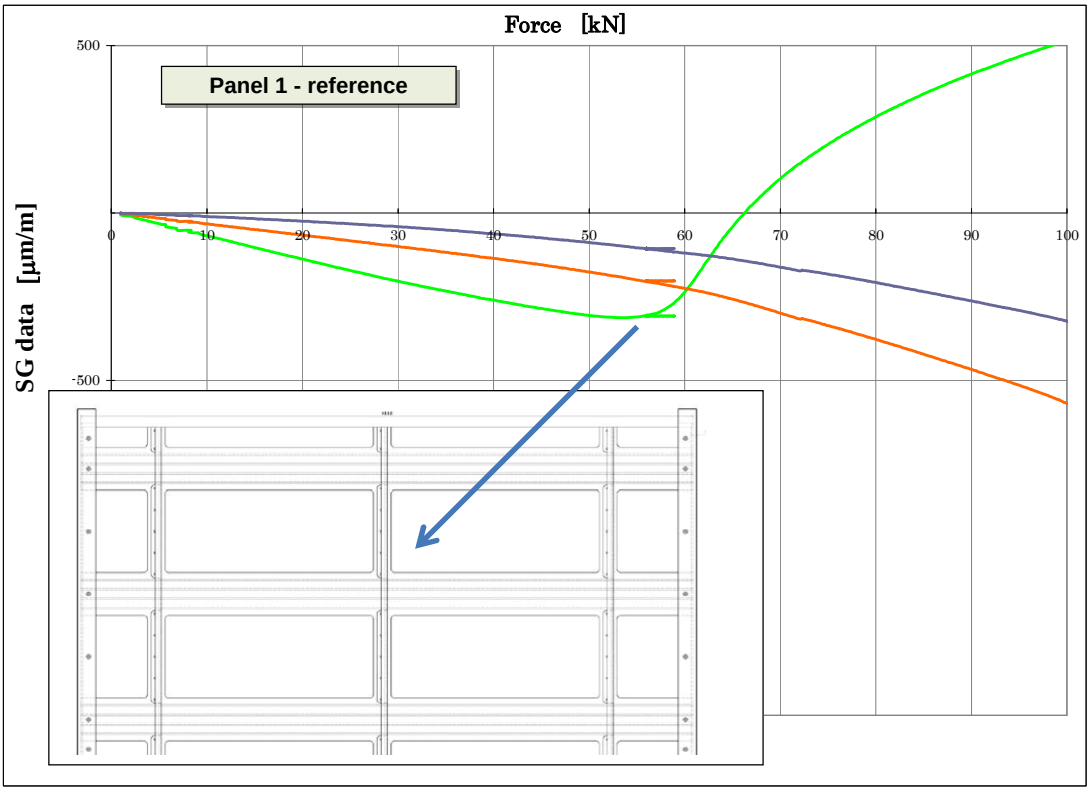

Figure 4.17: Change in the sign of strain measured at the specified location, indicating the elastic instability location, i.e. the initiation of the local buckling mode

Depending on the exact location of the strain gauge and on the sequence of bay local buckling, the initial local bay buckling triggering from the gauges ranges from 54 kN up to 62 kN.

Error (%) in terms of first buckling mode (SOL105) = (58.4 – 54) / 58.4 = **7.6 %**

Geometric nonlinear analysis, did not predict the first buckling mode so accurately in terms of applied load as the eigenvalue analysis did, but as the following diagram suggests, the solution sequence retrieved the correct displacement.

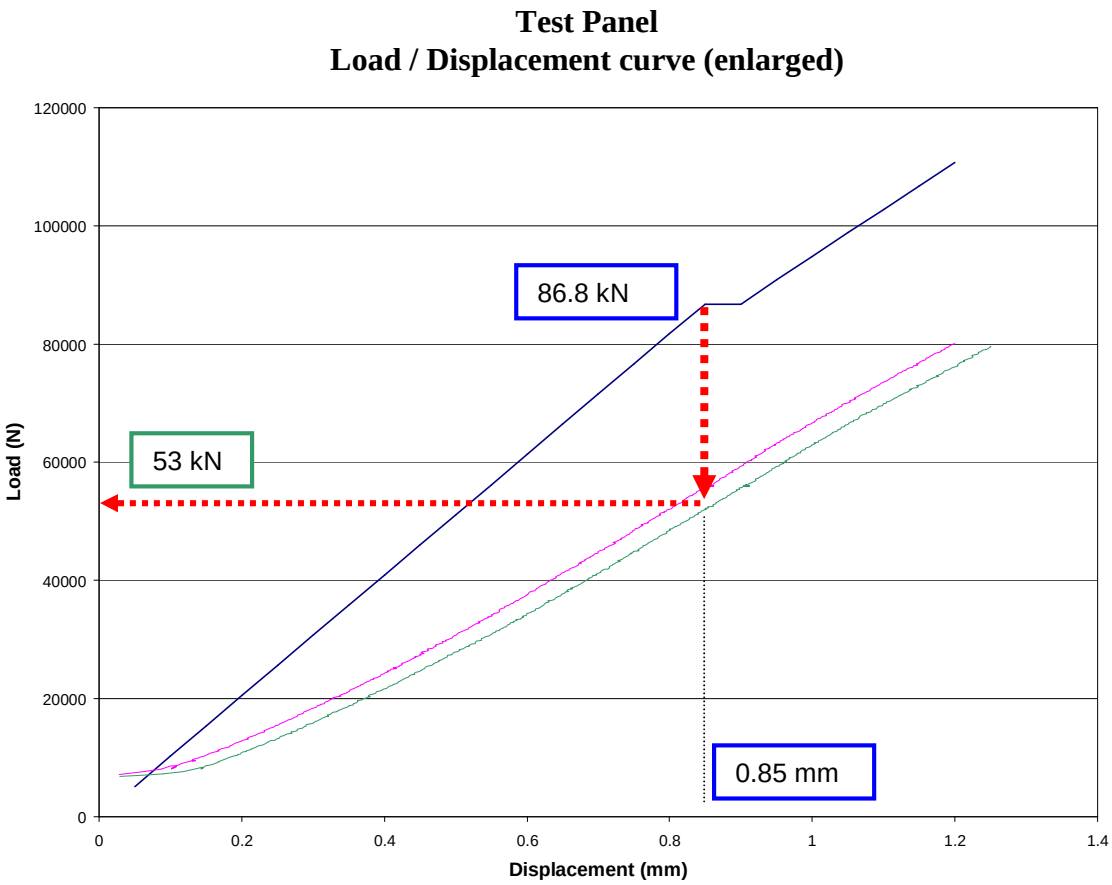

Figure 4.18: Geometrically nonlinear analysis did not pick up the buckling load correctly in terms of loading, but in terms of displacement it the approximation was better

Because the panel in the FE space is purely straight, it shows its first buckling mode at 86 kN, while with the eigen value analysis, we observe that actual instability can start at 58.4 kN. We reserve this value as the most critical one as the initiation of local buckling.

4.4 Artificially damaged panels

Along with the pristine panel, two panels were manufactured and damages were inflicted upon them in a controlled way. Figure 4.19 from ref [2], displays a schematic representation of the damages and figure 4.20 a picture and the respective C-scan image. Figure 4.21 presents VID damage.

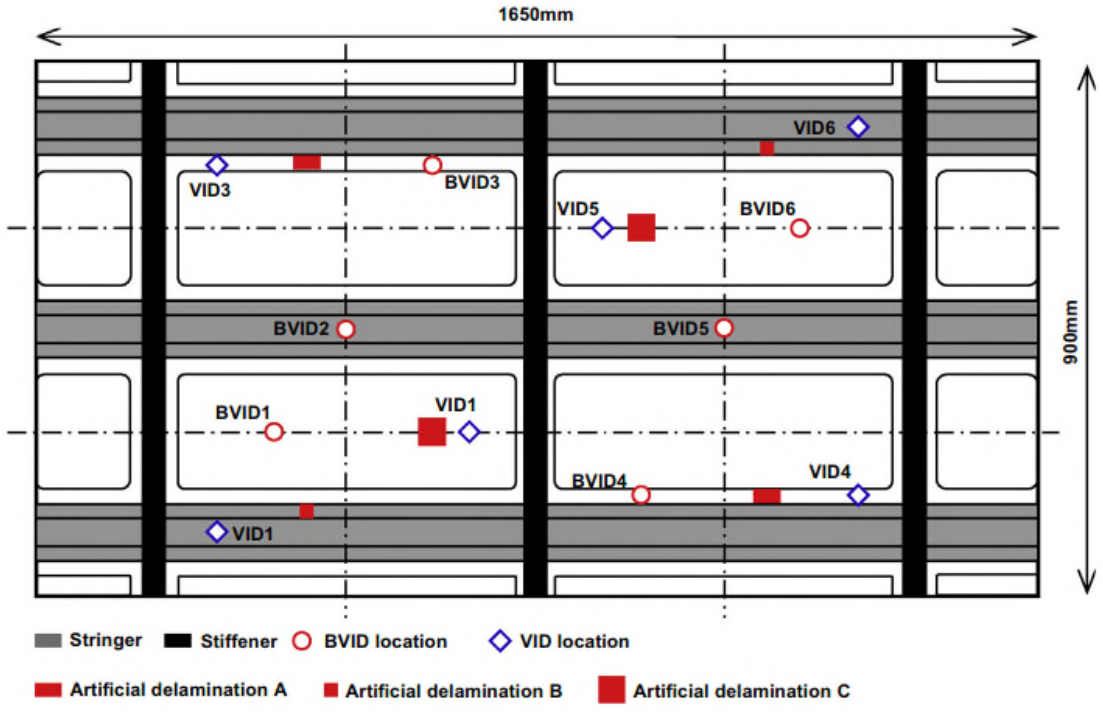

Figure 4.19: Schematic representation of artificially induced damages n the damaged panels of the study ref [2]

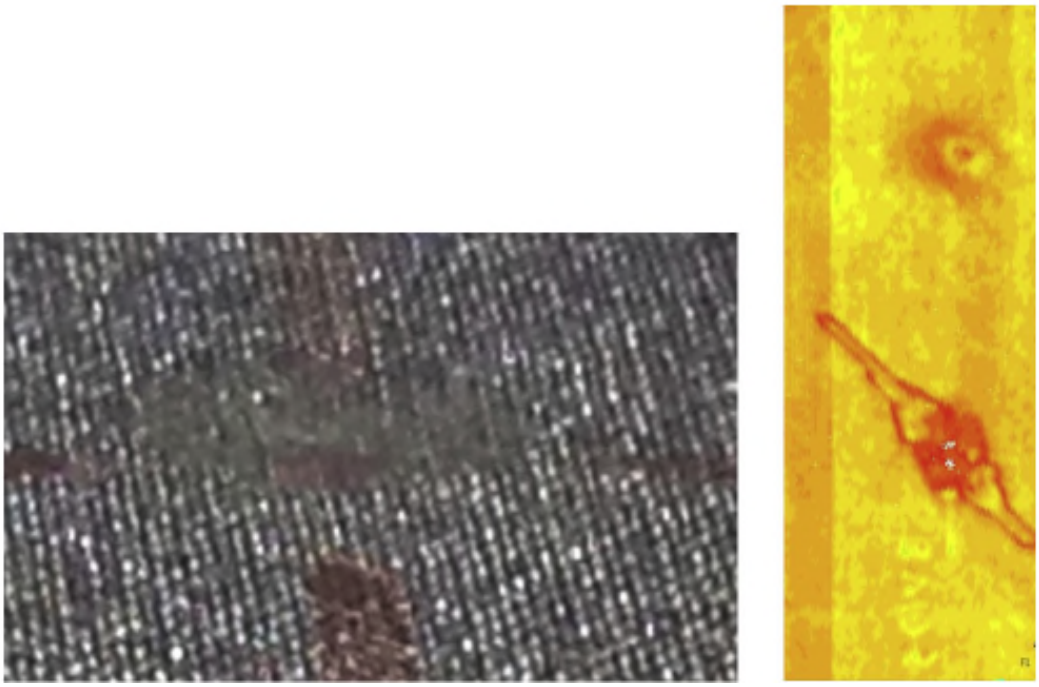

Figure 4.20: Picture and the respective C-scan image of a BVID artificial damage ref [2]

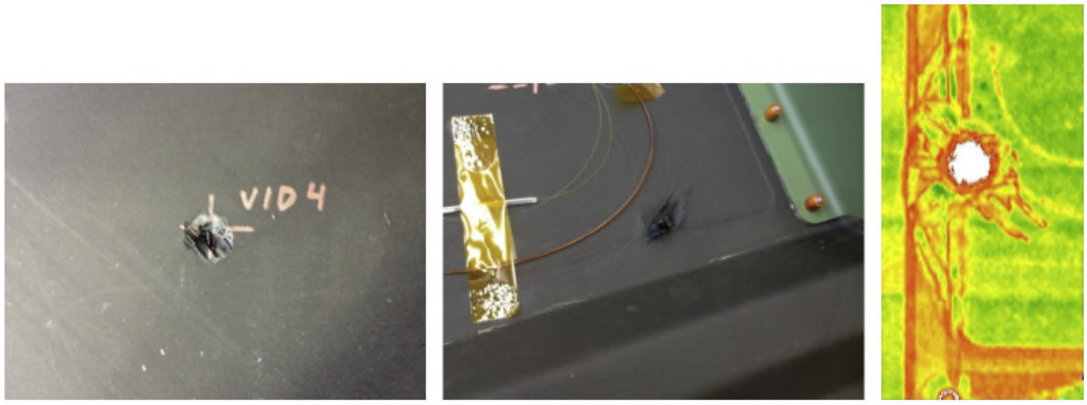

Figure 4.21: Picture and the respective C-scan image of a VID artificial damage ref [2]

At that point in the study, the effect of the damages were not successfully employed in the numerical simulations, hence there was no prediction of the ultimate failure loading for these panels by numerical means. The reason for presenting these images was to indicate the need for simulating the effect of damage in the failure progression of the component. Subsequent information presented in chapter six will elaborate in that field.

4.5 Other current research in the field

Similar research studies are available in the public domain. The authors of ref [9] presented a similar study performed in smaller scale of only one stiffener. It was mentioned that the initial deformation shape of the component, maybe due to residual thermal stresses, was of high importance and it would be decisive on the failure progression of the component. The researchers of the investigation acquired the full 3D initial shape of the component prior to testing as shown in figure 4.22, ref [9] and its correlation with numerical results shown in figure 4.23, ref [9]. A similar study had been conducted from the author of this thesis, shown in figure 4.24. The simulation was not successfully implemented into further numerical steps because of the problem faced in incorporating the metallic frames onto the distorted panel

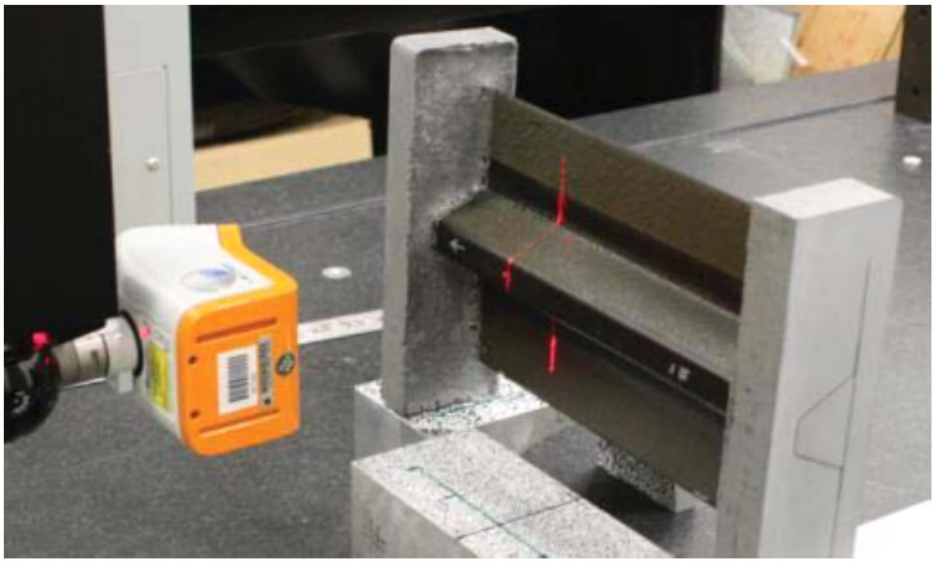

Figure 4.22: Measuring the exact shape of the component prior to testing ref [9]

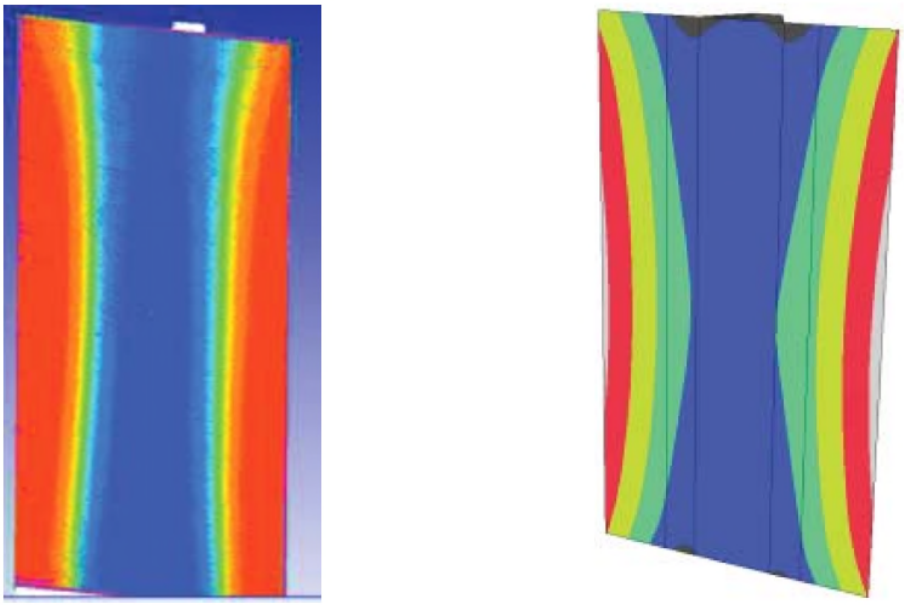

Figure 4.23: Correlation of the measured deformation shown in figure 4.22 and the FE simulations with residual thermal stresses ref [9]

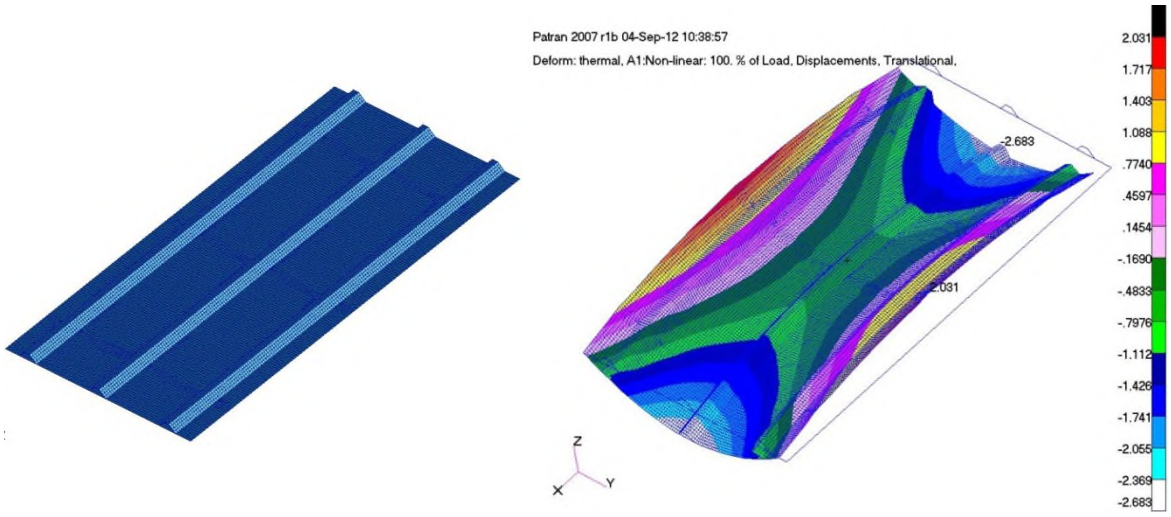

Figure 4.24: Residual thermal stress nonlinear analysis for the panel under investigation in this thesis

In figure 4.25, the numerical simulation of the component is shown with damage propagation characteristics. In figure 4.26, the experiment is shown and in figure 4.27, digital image correlation results at the back face showing failure progression.

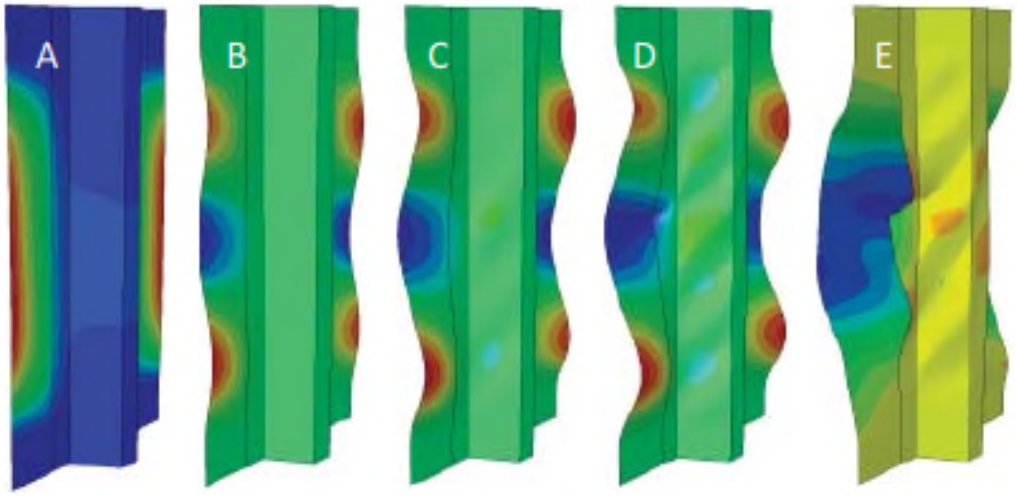

Figure 4.25: Numerical simulation of the failure under compression of the structure presented in [9]. Damage progression is numerically simulated

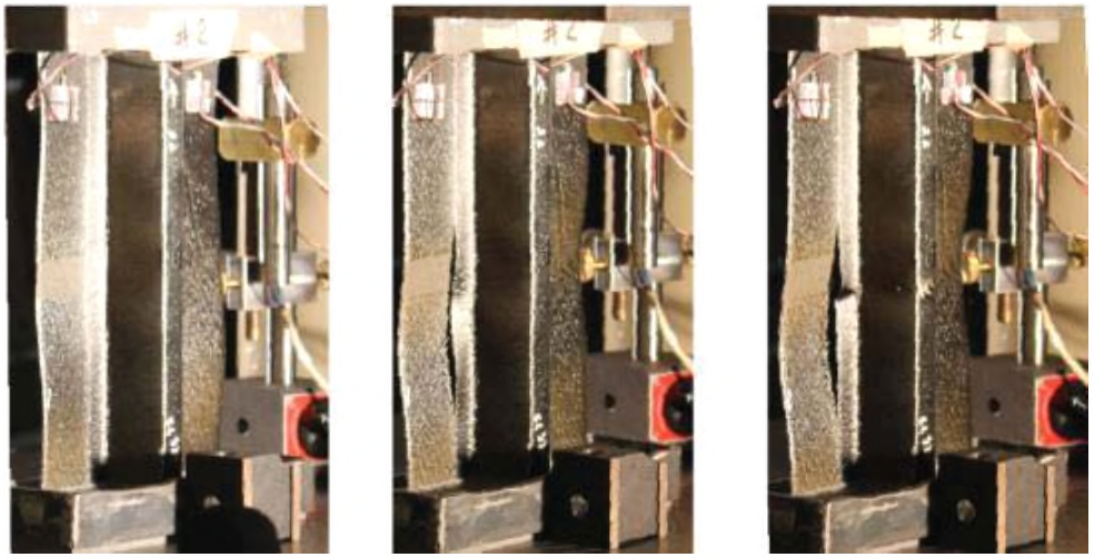

Figure 4.26: Pictorial sequence representation of the experimental procedure until component failure ref [9]

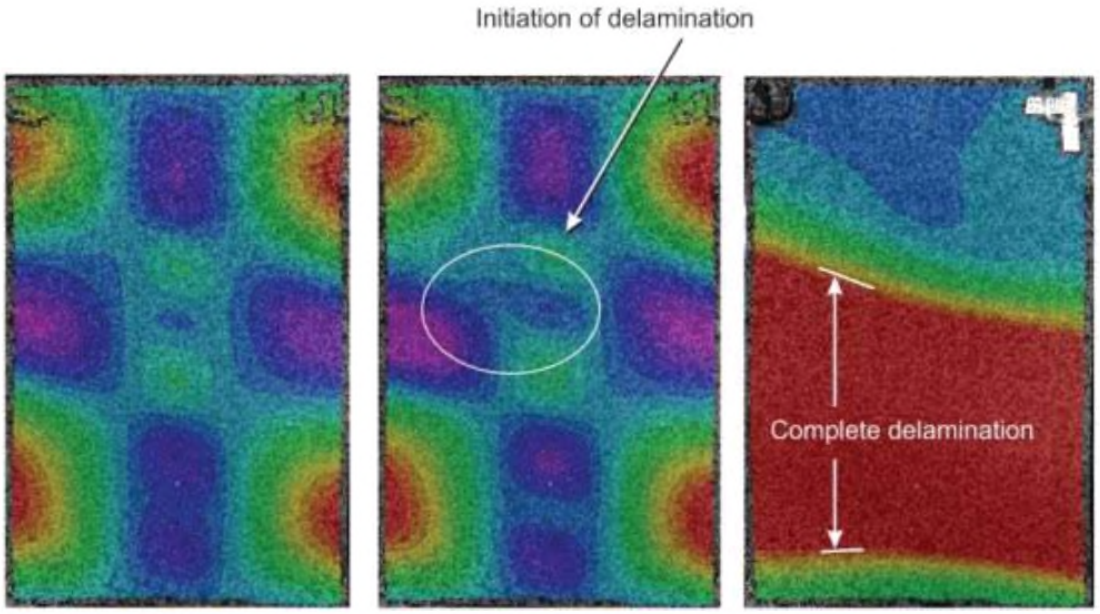

Figure 4.27: DIC pictorial sequence representation of the experimental procedure until component failure ref [9]

The intent of presenting figures 4.25 up to 4.27 was to show that numerical representation of damage is employed for the analysis of component at that level. The level of correlation was not reported in the reference.

Another interesting comment made in [9], is that initial deformation shapes greatly affect the damage progression phenomena, since at a certain defect location it is important if the subsequent buckling shape will act to open or close the delamination. This is represented in the figure below:

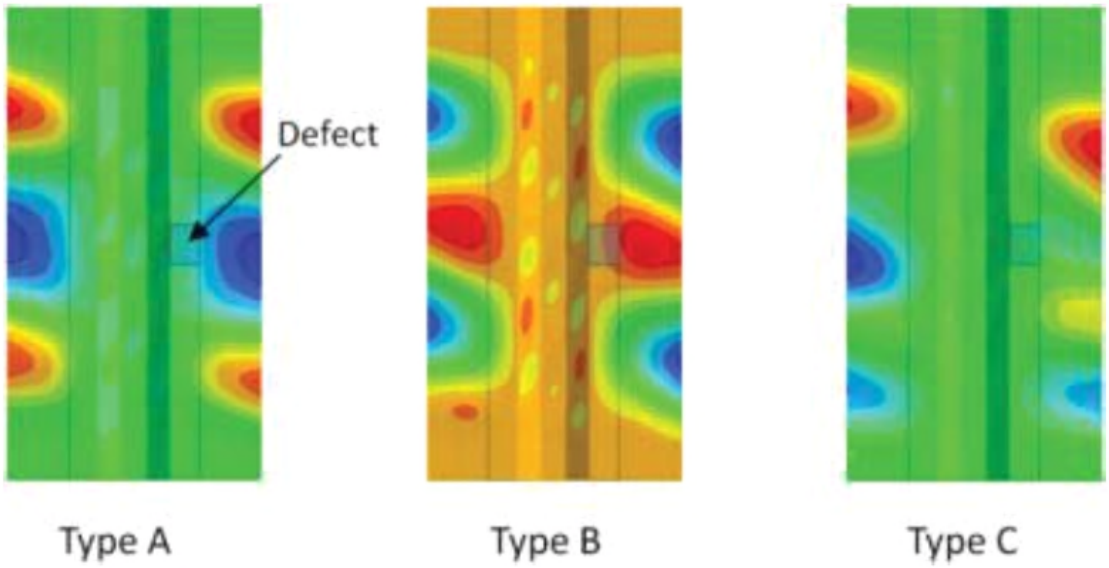

Figure 4.28: Initial deformation shapes are important for the failure succession [9]

4.6 Summary and key points of chapter four

- Numerical analysis was employed in an optimization analysis successfully
- The compression test until failure of an undamaged panel was modelled numerically and the results were benchmarked against testing.
- The actual test panel responded to loading as if only the stiffeners were taking up the load
- The first buckling mode was correctly predicted using eigenvalue analysis
- There is a need for modelling the progressive damage if virtual representation of testing has to be generated

- Initial imperfections to the panel shape either caused by dimensional variances or due to thermal stresses are vital for tracing correctly the load displacement curve
- The most important failure mechanism for damage on composite stiffened panels is to inflict damage from impact

4.7 References in chapter four

[1] EASA, European Aviation Safety Authority (2010). AMC 20-29: Acceptable Means of Compliance - Composite Aircraft Structure. EASA, Germany.

[2] K.I. Tserpes, V. Karachalios, I. Giannopoulos, V. Prentzias, R. Ruzek Strain and damage monitoring in CFRP fuselage panels using fiber Bragg grating sensors. Part I: Design, manufacturing and impact testing. Composite Structures 107 (2014) 726–736

[3] NASTRAN Quick Reference Guide, MSC Software Corp., Newport Beach, CA, 2012.

[4] G.D.Swanson, L.B.Ilcewitz, T.H.Walker 'Local design optimization for composite transport fuselage crown panels', Boeing Commercial Airplane Group Seattle, WA

[5] Geon-Hui Kim, Jin-Ho Choi, Jin-Hwe Kweon 'Manufacture and performance evaluation of the composite hat-stiffened panel'. Composite Structures 92 (2010) 2276-2284.

[6] J.F.M Wiggenraad, P.Arendsen 'Design optimization of stiffened composite panels with buckling and damage tolerance constraints', NLR-TP-98024

[7] C.Mittelstedt, M.Beerhorst 'Closed-form buckling analysis of omega-stringer-stiffened composite panels considering periodic boundary conditions'. Composite Structures 88 (2009) 424-435

[8] Dassault Systèmes. Tutorials in Buckling, Postbuckling, and Collapse Analysis with Abaqus, 2014

[9] Rose C, Davila C, Leone F. Analysis methods for progressive damage of composite structures. NASA/TM-2013-218024

Chapter 5

"Damage on composite airframe structures from low velocity impact"

In the previous chapter, it was discussed that airframe structures made of composite materials have to show compliance with the Airworthiness strength requirements whilst they contain certain levels of *representative damage*. This requirement is specifically applicable to polymer composite laminated structures for various reasons; even by using the most modern and up-to-date toughened fibre/epoxy material systems, along with their current manufacturing and application methods applicable, it has been recognised that these structures cannot be defect free. Defects are inherited to the structure basically throughout the complete material lifecycle prior to manufacturing, during production, storage, handling, while manufacturing and during operation and maintenance of the airframe. It has been deemed necessary and this is engraved within the Airworthiness requirements that composite structural airframes have to show compliance with the strength specifications whilst containing a certain level of defects representative to the structure and to its operational lifecycle and to demonstrate they tolerance of a certain level of accidental damage under the service loads. This so-called damage tolerance requirement is mandatory for passenger aircraft.

Amongst the various damages inflicted on a composite material airframe component, it has been acknowledged that damage due to low velocity impact can be a very serious one. The reason is that impact damage from low velocity impacts can be untraceable / undetectable to visual inspection. A more severe impact damage that could potentially generate a major structural discontinuity as a puncture or a hole can be seen in routine inspections and subsequently being repaired. Impact damages from low velocity impacts can leave no external trace to the internal damage they contain underneath the surface. These damages can be equally severe; they can be expanded to a

larger damage under operational loads and can potentially cause an unexpected collapse of a bigger subassembly, mostly when subjected to compressive loading.

In chapter five, an experimental study in the field of low velocity impact of fibre polymer specimens is presented. Following the analysis of the experimental results an informed design decision is explained at a certain stage of the design cycle. The chapter's main theme revolves around testing procedures, result evaluation and design decision making.

5.1 Introduction: The importance of Impact Damage in the airframe sector

Impact damage is being classified as one the most important damage mechanisms on composite laminated structures. Impact damage on fibrous reinforced polymers used in the aerospace sector has attracted the interested of many researchers and it has been the topic of discussion in countless research publications [39]. Means of assessing the quality of produced composite structures as well assessing the level of damage and other discrepancies inflicted during the production process can be put in place by stringent quality control procedures and inspections at the manufacturing stage. It is only later on, during service, where composite structures will be called to fulfil their structural mission within hostile, strength degrading environments. From all the various damaging phenomena, the foreign object impact is of great importance.

There are mainly two fundamental elements of interest in the structural response of composite material airframes under impact: the first is the way impact energy will be absorbed and the second is the remaining strength of the structure after the impact event.

Foreign object impact damage has been categorised in terms of energy as well as according to the product of mass and velocity of the object impacting the structure. The reason for the classification in terms of energy stems from the fact that a part of the energy the impact is going to be absorbed by the structure and the object in terms of elastic energy, some of it will be absorbed into the various energy consuming fracture mechanisms in the process and even some of it will be restored into a bouncing back kinetic energy. Mass is of importance since for the same impact energy, a larger mass will impact with a lower velocity, hence the structural reaction will be close to quasi static. Impacting with a smaller mass of the same energy, the velocity has to be bigger and the dynamic response of the structure will come into play. Hence, energy is not the only parameter for categorizing impact behaviour. In this chapter low velocity impact events are investigated where the dynamic structural response is not important. Usually these are the impact cases with masses close to 1kg and total energies of less than 50J. Within such a category, the simulations of tool drop events or runaway debris could be assumed.

When an impact event causes damage to a composite structure, chances are that this process will leave visible marks that could be identified by visual inspection. Certainly the damage extend is larger than the visual assessment of the damage, but inspections procedures can be initiated for the complete assessment of the damage in the vicinity. The key element in the above statement is that the damage could be traced even by a visual inspection. More critical are the damages that cannot be traced by visual inspections, the so called Barely Visible Impact Damages (BVID). In the case of metallic materials, plastic deformation and the generation of punctures will expose the location of the damage event. Composite materials do not deform significantly prior to fracture. An impacted site can fail in multiple ways during the impact event, but at the end of it, its original outer shape to resemble very closely the undamaged state. The subtleness in their appearance to the naked eye is the reason for the aerospace sector to take into account BVID damages in the design, testing and certification procedures. Basically composite structures need to prove their ability to fulfil their mission requirements while containing BVID and VID damages.

In the study presented in this thesis, there has not been contribution to knowledge in the field of numerical analysis of impact events. Instead, the contribution was performed though an experimental survey presented in the following chapter.

Relating the importance of impact damage with the certifications specifications, in AMC 20-29 [41], is mentioned under the paragraph for proof of static strength: *"It should be shown that impact damage that can be expected from manufacturing and service, but not more than the established threshold of detectability for the selected inspection procedure, will not reduce the structural strength below ultimate load capability. This can be shown by analysis supported by test evidence, or by a combination of tests at the coupon, element, sub-component and component levels. The realistic test assessment of impact damage requires proper consideration of the structural details and boundary conditions. When using a visual inspection procedure, the likely impact damage at the threshold of reliable detection has been called barely visible impact damage (BVID). Selection of impact sites for static strength substantiation should consider the criticality of the local structural detail, and the ability to inspect a location. The size and shape of impactors used for static strength*

substantiation should be consistent with likely impact damage scenarios that may go undetected for the life of an aircraft. Note that it is possible for some designs to have detectable impact damage and still meet static strength loads and other requirements without repair."

5.2 Impact damage and CAI strength of a composite material with fire retardant properties

5.2.1 Introduction

Aerospace structural development had always been driven by new materials that are being developed for performance and function. The material characterization presented in this article was motivated by the consideration of applying a special woven fibre composite material system to a conceptual aircraft vehicle, due to its peculiar fire retardant matrix characteristics. The composite under investigation was to be utilized in a location, where its fire retardant properties presented an opportunity for fulfilling the airworthiness bottle-neck design specifications. Apart from the fire self-extinguishing character that had to be demonstrated for the certification, strength, stiffness and damage tolerance requirements of the material had to be met, therefore assessed. The response of this new material system, due to its peculiar syntactic core matrix, to low velocity impact and compression after impact residual strength was the subject of the below presented investigation. Following, in the literature review section, a short summary of important research findings that are relevant to our investigation are presented. The intention is to draw the boundaries of the technological domain of our work. In section three our research input is exhibited and in section four we presented our contribution which lies in the proposed method of manipulating the results that helped with our design decision making process.

5.2.2 Literature review

Woven carbon fibre reinforced plastics (CFRP) have a better drape ability and are able to be morphed into complex double curvature shapes more effectively than conventional aerospace unidirectional (UD) material systems [1]. Although overall laminate stiffness and strength are somewhat lower for woven comparing to UD laminates [2], the former offer greater flexibility for producing highly complex shapes and present opportunities for lowering the manufacturing cost [1]. The material fabric under investigation is shown in Fig.5.1.a) while the micro-graph in Fig.5.1.b), depicts a section through the cured laminate. The mechanical properties of the material as provided by the manufacturer [3, 4] were inferior in terms of lamina strength and stiffness (0^o tensile strength approximately at 292 MPa, 0^o tensile stiffness approximately at 38 GPa) as opposed to the more widely used aerospace woven materials [2]. The design decision favoured this material system on the basis of its fire retarding and flame self-extinguishing properties. The inherent inferiority of the material system in terms of laminate strength and stiffness was addressed and overcame in the design process by employing slightly thicker laminated structural components.

The airworthiness design specifications for this vehicle were to follow similar guidelines to [5]. Under those specifications, structural strength and stiffness requirements were met. Damage tolerance had to be demonstrated as well; therefore within the current study the response to low velocity impact loading and compression after impact (CAI) strength of representative test articles of the structural parts were investigated. The major concern during the investigation was the response of the two phase pigmented epoxy matrix material and the synergy of it with the woven carbon fibre weave in order to provide with an acceptable resistance level to impact loading and with adequate strength under compression had an impact event occurred.

On the impact behaviour of unidirectional versus woven CFRP materials

The impact damage imprint of low velocity impact onto woven CFRP laminates via the various damage mechanisms employed to absorb the impact and the effect of these damages upon the structural life of the material [6-8], produce a more favourable result than the one caused upon similar fibre and matrix UD material systems [9-12].

Low velocity impact damage and post-impact strength in composites have been investigated extensively during the last 40 years, especially for the aerospace grade carbon fibre epoxy composites [13-17]. The majority of the experimental research for the predictive capability of resistance to impact damage, damage extends and residual strength after impact was mainly focused and formulated around UD laminate composite materials [18-21]. For the unidirectional composites the damage phenomena and mechanism are well understood and models based on the strength degradation and fracture mechanics have been developed for predicting the damage initiation and propagation.

Analytical prediction of impact damage and post impact performance of woven composite laminated structures is a more difficult task to perform than for UD materials. Fracture mechanisms and failure sequences are documented from observations [6-8] but parametric analytic formulations for predicting the impact performance have not attained yet the maturity level of the unidirectional ones. Impact performance indicators for the laminates tested herein will be presented in the format of experimental observations. Current research effort in terms of prediction is mainly on the improvement of the numerical model efficiency and accuracy in order to develop computer based tools for material selection in structural design. Up-to-date numerical computations consolidate the composite material mechanical and failure properties of either a UD or a woven layer into the properties of a three dimensional finite element generating a mesoscale representation of the laminate. The computational capacity needed to capture the microstructural woven pattern and the assorted individual damage mechanisms during an explicit numerical event is not widely available as of yet.

On the matrix material and inter-laminar interface importance

It was anticipated early during the study that the fire-retardant particles dispersed into the matrix would affect the laminate impact performance. Impact and post impact phenomena are dominated by the inter-laminar fracture toughness properties of the matrix material [22]. Many authors have addressed the issue of assessing and even enhancing the fracture toughness response to impact loading and the subsequent resistance to CAI. For example by using different matrix thermosetting or thermoplastic

materials [23] or by applying veils which are other layered materials within the laminates [24, 25] or even by applying metallic materials in the form of titanium pins in the transverse direction [26]. The major concern in our study was the fracture toughness properties of the two phase epoxy material matrix with the interspersed pigments.

On the fracture toughness of woven CFRP materials

Amongst the many material properties and loading parameters influencing the impact damage response of a CFRP laminate, Mode-II fracture toughness (G_{IIC}) plays a fundamental role especially in the process of delamination progression under Mode-II inter-laminar shear. The other important material parameter that influences mostly the CAI strength is Mode-I fracture toughness (G_{IC}) since the delamination progression within layers under compression resembles a crack opening Mode-I fracture process. It is recognized that the fracture toughness values required for the engineering investigation of delamination propagation in CFRP laminated structures, although matrix dominated [22], they depend on number of other factors such as the type of fibres, fibre volume fraction, manufacturing process, interphase regions between the matrix and the fibre and many more. This being the reason why fracture toughness values are interrogated by testing composite layered specimen and not by using methods that test purely matrix materials. The engineering/scientific community has been successful so far in generating reliable testing procedures to quantify inter-laminar fracture toughness for unidirectional composites under Mode-I [27] and Mode-II [28]. These methods, when employed within the limitations specified, are capable of producing repeatable results with a small scatter. Unfortunately, when woven fabrics are tested to the above specifications, due to the peculiarity provided by the woven fibre architecture to the split surface morphology, run-arrest type of propagation is experienced most of the times rather than slow stable crack propagation [27, 28]. Run-arrest type of crack propagation, induce dynamic effects and the test standards do not address these implications [27, 28]. Other peculiarities that could be experienced while testing woven CFRP materials are the branching of the delamination away from the mid-plane through matrix cracks in off axis plies and the varying toughness measurements due to encountering richer or poorer pocket areas of resin. All these

implications generate a much greater scatter in the fracture toughness test results [29-31].

The current standards of fracture toughness testing methods in Mode-I and Mode-II crack opening, assume unidirectional test specimens, thus test results characterize the fracture toughness in the 0/0 inter-laminar interface. Although the above mentioned testing procedures have been applied to other type of specimens with various interface arrangements [31], it can be argued that reliable and widely acceptable testing methods are not available as of today for measuring the toughness values of for example for the 0/45 inter-laminar interface fracture toughness [29].

The final complication of this study was that the woven CFRP material system contained pigments of another substance interspersed within the epoxy matrix. The matrix was practically a two phase substance and delamination was expected wander about in between the matrix phase where cohesive type of failure within the epoxy would be mixed with an adhesive type of failure between the matrix and the pigments.

Summarizing

- Woven CFRP laminates do not exhibit the strength and the stiffness values of UD laminates of a similar fibre-matrix system but they are more damage tolerant in terms of impact loading damage imprint which results in a smaller decrease in the residual compression after impact strength.
- The computational capacity needed to solve finite element explicit numerical simulations to capture the micro-scale failure mechanisms during impact and post impact events is enormous. Numerical predictive solutions of that kind are not available in the public domain yet.
- Amongst the important material properties influencing the impact and CAI processes are the Mode-I and Mode-II fracture toughness values. These are highly depended from the matrix material. Specific testing procedures for measuring those values for woven fabrics and at various angle ply directions do not exist. Tests for other than unidirectional laminates along the major fibre direction are conducted by slightly violating the region of validated applicability of the existing unidirectional testing methods. During the study an approximate value of Mode-II fracture toughness of

the material system was proposed and derived indirectly by using the analytic formulation in [18].

- The main objective of this research was to present the impact damage characteristics and the compression after impact strength of a conceptually applied, fire retardant woven composite laminate.

5.2.3 Experimental methods

Material

VTS243FR/CF3500 [3, 4] is a partially impregnated pre-preg woven composite material manufactured by Cytec. The material system is made of two plies.VTS243FR is a black-pigmented, flame-retarding, epoxy syntactic-core ply. CF3500 is a high strength (12k) woven carbon fibre ply, with a fabric density of 380 g/m^2, twilled in 2 x 2 weave style, Fig.5.1a). The two plies were expected to infuse into one another during the curing process. The system is capable of initial cure temperatures between 65°C and 150°C. Following post-cure, a glass transition temperature of at least 160°C can be achieved [32]. VTS243FR is self-extinguish when tested to ISO3795/FMVS302 [3].

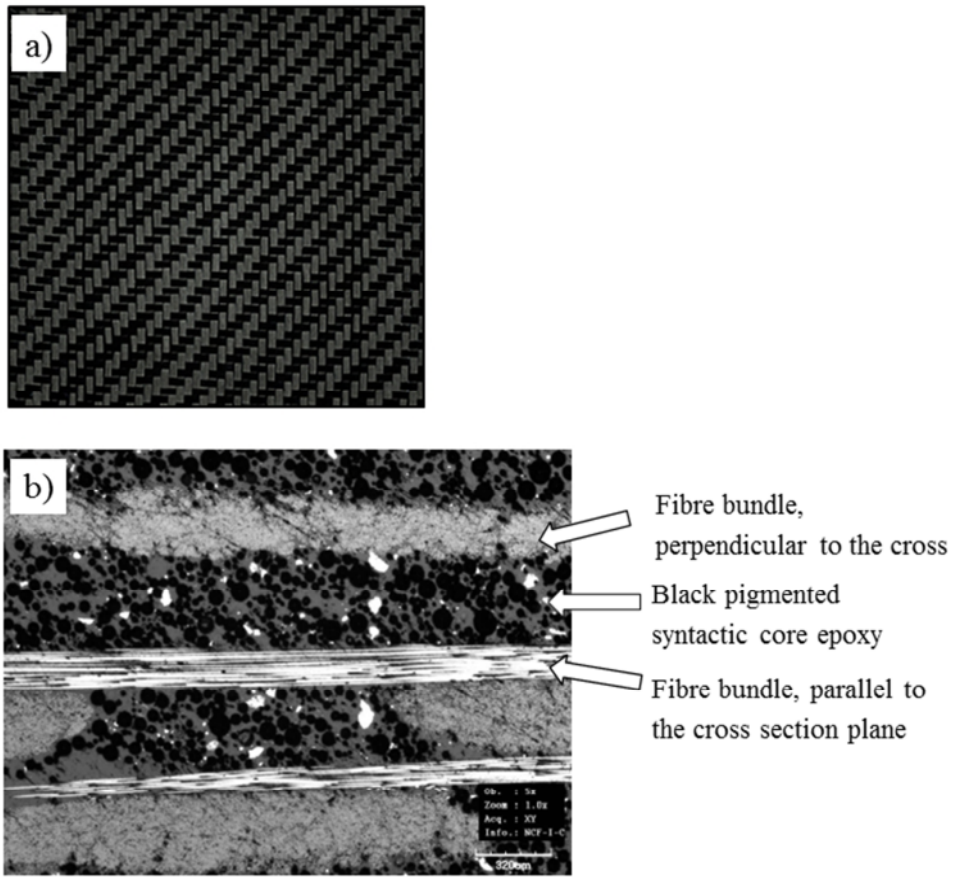

Figure 5.1: a) The 2 x 2 twill weaving pattern of CF3500 woven carbon fibre ply. b)Microscopic image of cross section of cured VTS243FR/CF3500 composite; image scale shown on bottom right: 320 mm

Mechanical properties of cured laminate are lower than that of similar woven composites used in the aerospace industry (0^o tensile strength approximately at 292 MPa, 0^o tensile stiffness approximately at 38 GPa). Cured ply thickness is about 0.79mm and the density is 1.74kg/m^3, [3, 4].

Specimen

One of the objectives of this study was to investigate the effect of different layup on the damage resistance. Two stacking sequences were fabricated, i.e. a quasi-isotropic layup [+/-, 0/90, -/+, 90/0]s denoted as configuration C1, and [+/-, 0/90, 90/0, 0/90]s, configuration C2. Five specimens for each configuration were

produced, 10 specimens overall for impact and CAI testing. The nominal thickness of cured laminate was 6.5 mm.

The material was supplied in a roll form and was stored at -18°C. It was important to thaw the material to room temperature before kitting process takes place for condensation reasons. Thawing process took place overnight at room temperature before the role's packaging bag was opened.

The semi pre-preg was cut into square 340 x 340 mm pieces required for the fabrication of the test specimens. The panels were cured under constant pressure of 627 kPa at elevated temperature of 100 °C for 135 minutes. The temperature increase ramp rate was 0.5 °C per minute and the cooling down rate 1.5 °C per minute. The panels were subsequently post-cured in a pre-heated autoclave for 1 hour at 180 °C to fully develop the material's glass transition temperature. The ramp rate of post curing temperature increase was 0.3 °C per minute and the cooling down rate was 3 °C per minute until 60 °C. After curing, specimens of 100 x 150 mm were cut out of each panel. This dimension is the ASTM standard for impact and compression after impact tests [33, 34].

5.2.4 Test facilities and procedures

Low velocity impact

The impact test procedure adhered to the guidelines [33]. Prior to impact testing, visual and ultrasonic C-Scan observations were made to ensure that no physical damages or delamination were present. Impact test was performed by using the Rosand Instrumented Falling Weight Impact Tester. The striker used for the impact test was blunt with a hemispherical tip. The total mass of the drop weight was 2.2 kg for all the tests. Time histories of the impact force, velocity, acceleration, deflection and absorbed energy were measured and recorded by a computer controlled processor. Five specimens were tested from each configuration at the impact energy levels of 8, 15, 25, 35 and 50 J. Impacted specimens were inspected by ultrasound C-scanning to measure the delamination shape is according to ASTMD7136 [33].

Compression-after-impact (CAI)

The compression test set up was originally designed by Boeing and was later adopted by ASTM D7137 [34]. The machine used was an Avery 600 kN. Compression

loading was induced at a constant head displacement rate of 0.1 mm/min. The load was applied onto the specimens until ultimate failure. The machine was stopped immediately after the specimen failure to allow for the retention of the distortion just before / at failure.

5.2.5 Experimental results and discussion

Impact test

The main focus of this study was to quantify the damage tolerance extends of the fire retardant CFRP material. The synergy of the woven fabric and the matrix was of great importance to the study. Judging from the material mechanical properties published by the manufacturer [3, 4], slightly thicker specimens were designed to counterbalance the slightly inferior mechanical properties benchmarked against other material system candidates. Some of the thickness effects for a different material system were captured in [35]. Amongst the results discussed in [35], a higher peak force is expected for thicker laminates, smaller transverse displacement, increased damage tolerance and shear failure under CAI.

Figure 5.2 presents images of ultrasonically detected delamination damage for the five C1 and five C2 configuration specimens along the various impact energy levels.The maximum damage diameter and area were defined according to[33]. Configuration C1 had bigger damage areas than those of C2, although the maximum diameter was similar at each energy level. The results were used to construct Fig.5.5. It was evident that bigger damage was incurred into the quasi-isotropic layup C1 for the same amount of impact energy.

Impact Energy (J)	8	15	25	35	50
Configuration C1 [+/-, 0/90, -/+, 90/0]s	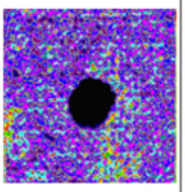	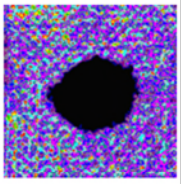	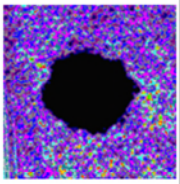	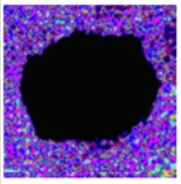	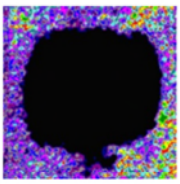
Max Diameter (mm)	30	57	59	85	89
Area (mm²)	688 (circular)	2122 (oval)	2346 (oval)	4504 (oval)	5767 (oval)
Configuration C2 [+/-, 0/90, 90/0, 0/90]s	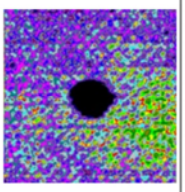	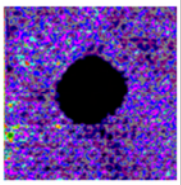	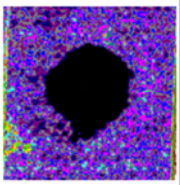	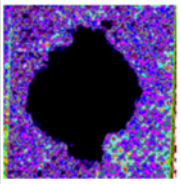	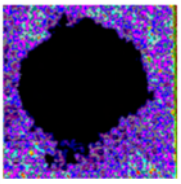
Max Diameter (mm)	29	45	56	79	87
Area (mm²)	550 (oval)	1523 (oval)	2028 (diamond)	3904 (diamond)	4288 (diamond)

Figure5.2: Images of ultrasound detected delamination area for the 10 impacted specimens of two configurations (C1, C2) at various impact energy levels

Impact force versus time histories is shown in Fig.5.3. Figure 5.3.a) depicts the comparison of the two configurations at four impact energies, indicating that C1 and C2 had virtually the same dynamic response at each energy level. Since the response obtained was very similar, only C1 configuration is further presented in Fig. 5.3.b) that depicts all impact energy levels tested in one plot. The quasi-isotropic C1 configuration is stiffer than C2 in terms of transverse deflection. This result was also evident from the stepper initial rise of impact force response versus time shown in Fig.5.3.a). Similarly in Fig.5.4.a), the maximum impact force attained from the C1 configuration is somewhat larger at least for the impact levels of 8 and 15 J. Thus the stiffer in terms of transversal deflection quasi-isotropic layup, resist the impact loading more and a bigger damage was inflicted onto it. Figure 5.3 also shows that generally the two layup configurations responded similarly apart from the 15 J impact case. At that impact energy level, configuration C2 exhibited a distinctly more compliant character, also captured in Fig.5.3.a).

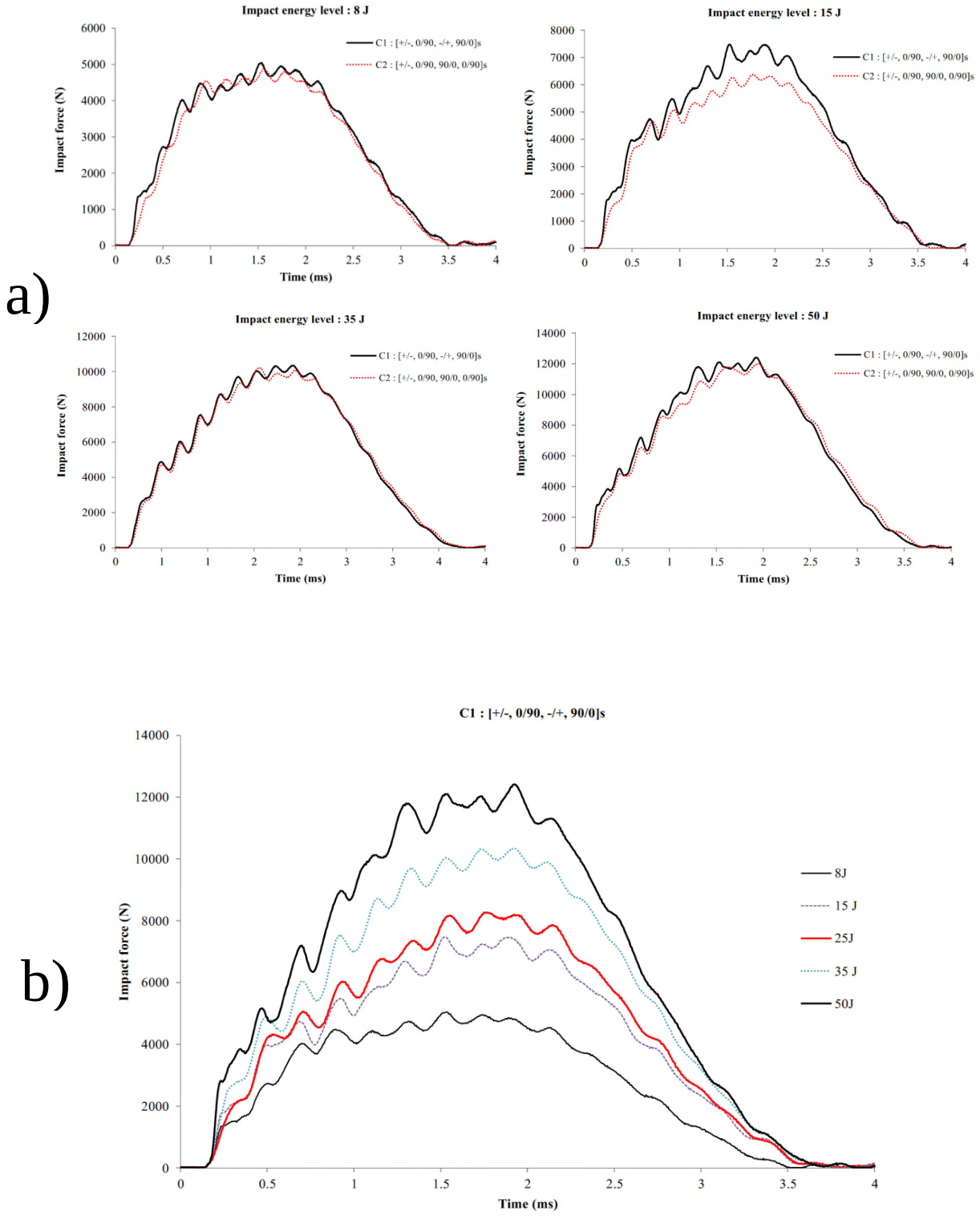

Figure 5.3: a) Impact force versus time histories for the two layup configurations at four impact energy levels: 8J, 15J, 35J and 50J. b) Impact force versus time for configuration C1 at various impact levels

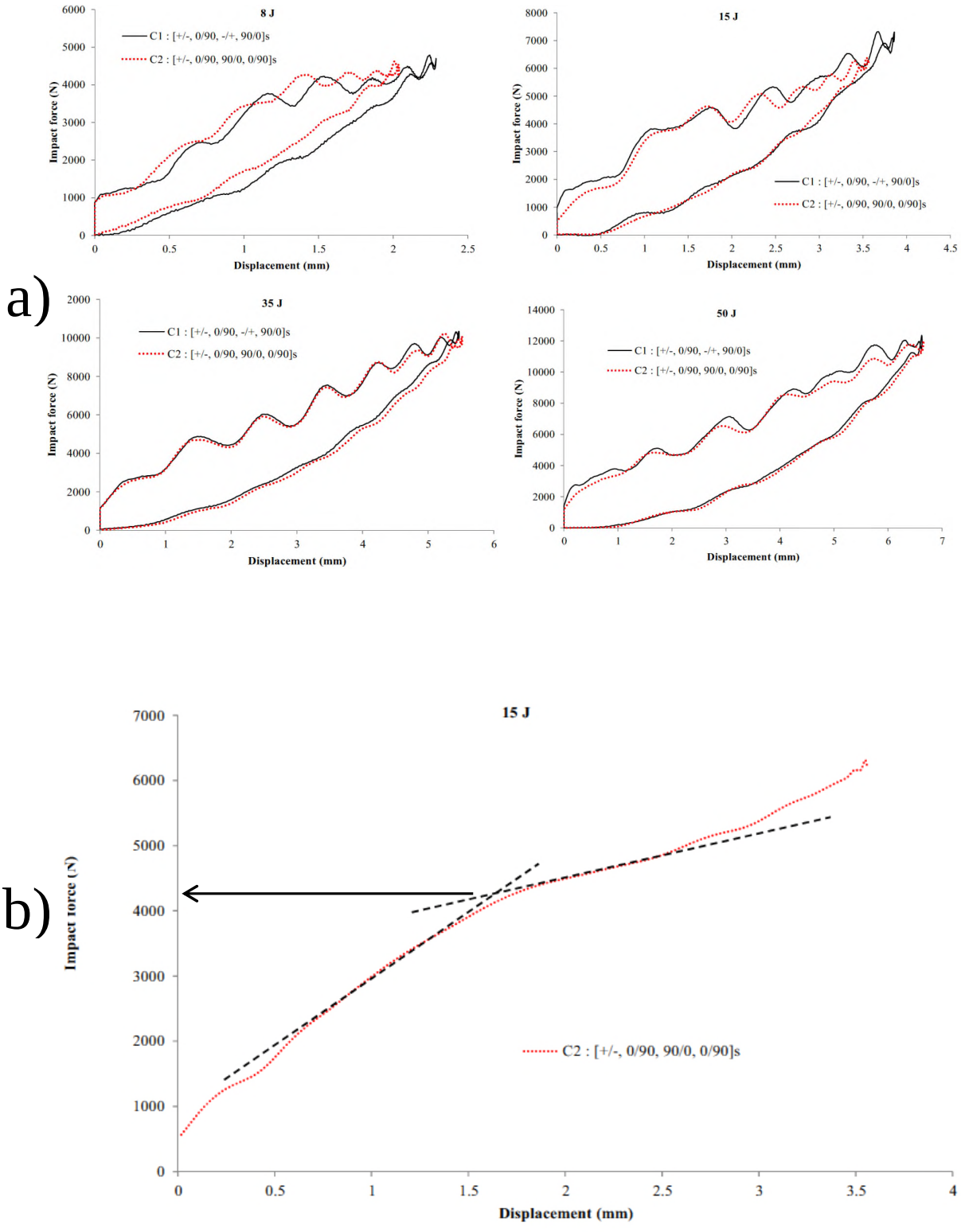

Figure 5.4: a) Impact force versus impactor displacement for the two layup configurations at four impact energy levels. b) Smoothened impact force versus impactor displacement for identifying the critical impact force

An interesting parameter to be investigated during the impact events is the first load drop in the impact force versus time graphs [22]. This first peak point in the graph indicates damage initiation. In our study, even with filtered impact force versus time results a clear picture providing with the first load drop was not able to be produced. Instead, following the suggestions in [19], the impact force versus deflection diagram was further processed by removing the high frequency components from it. The result of the filtered image is shown in Fig.5.4.b). The change in the tangency indicated the change in the laminate stiffness along the transverse direction, which in turn implied the initiation of damage. The first load drop was found to be approximately at 4.2–4.5kN for both layup configurations. This load is often called as the threshold impact force for delamination onset or the critical impact force and is denoted as P_{crit} [20].

As mentioned earlier, Mode-II fracture toughness (G_{IIC}) is an important parameter, amongst many others, for assessing the resistance to impact damage especially the damage initiation. With woven CFRP materials the derivation of G_{IIC} values from tests is a rather tedious task if not impossible to perform. For UD materials, there is a widely accepted analytical formulation which relates the critical threshold values of P_{cr} to G_{IIC} [18] and is shown below (eq.1):

$$P_{cr} = \sqrt{\frac{8\pi^2 E t^3 G_{IIC}}{9(1-\nu^2)}} \qquad (1)$$

In the above equation, E and v are the equivalent Young's modulus and Poisson's ratio of the quasi-isotropic laminate and t is the thickness of the laminate. Reference [22] suggested for equation (1) to be inversely applied in order to estimate G_{IIC} from the values of P_{cr}. It is also suggested that acceptable results were obtained for G_{IIC} values in the case of UD materials related to actual test results. The value of P_{cr} which depends purely on the matrix material system [22] was observed in Figure 5.4.b) to be in the vicinity of 4.2 kN. Following a similar approach and disregarding the rest of the complications of the woven architecture along with the two phase matrix system, an equivalent bulk mode II fracture toughness G_{IIC} was calculated in the range of 300 J/m^2. That result apparently came close to the values presented in [22] for other UD material systems tested which had similar P_{cr} critical threshold values. It needs to be reminded that this bulk

fracture toughness quantification, takes into account all the microstructural behaviour that promote or retard mode fracture, meaning the effect of the pigments and the effect of the woven surface architecture. In [29], it is shown that higher G_{IIC} values are expected for a woven CFRP material system as opposed to a UD of the same material properties for the fibres and matrix. Thus for the material in our study the Mode -II inter-laminar fracture toughness G_{IIC}, resembled more the values exhibited by UD epoxy material systems. The decrease in the expected G_{IIC} can be partly attributed to the two phase epoxy matrix.

Since the first load drop occurred at approximately 4.2 kN, damage in the form of delamination exist for all laminates even at the impact level of 8 J. For the higher impact levels as shown in Fig.5.4.a), the response is more or less the same and most probably other damage modes are present besides delamination. Similarly for the 8 J experiments both configurations responded similarly. The only graph which presented some difference was the one at 15 J level. That can be translated as an indication of triggering the shifting from certain damage modes to include others as well, possibly fibre breakage that occurred for configuration C2 but not for C1.

Figure 5.5 shows the delamination area versus impact energy. Under the same impact energy, the C2 configuration had smaller damage area than that of C1, especially at the higher impact energies of 35-50J.

Delamination area versus peak impact force is shown in Fig.5.6. The two configurations had virtually the same response, except at the higher impact force range of 10-12 kN, in which C2 had approximately 20%smaller damage area.

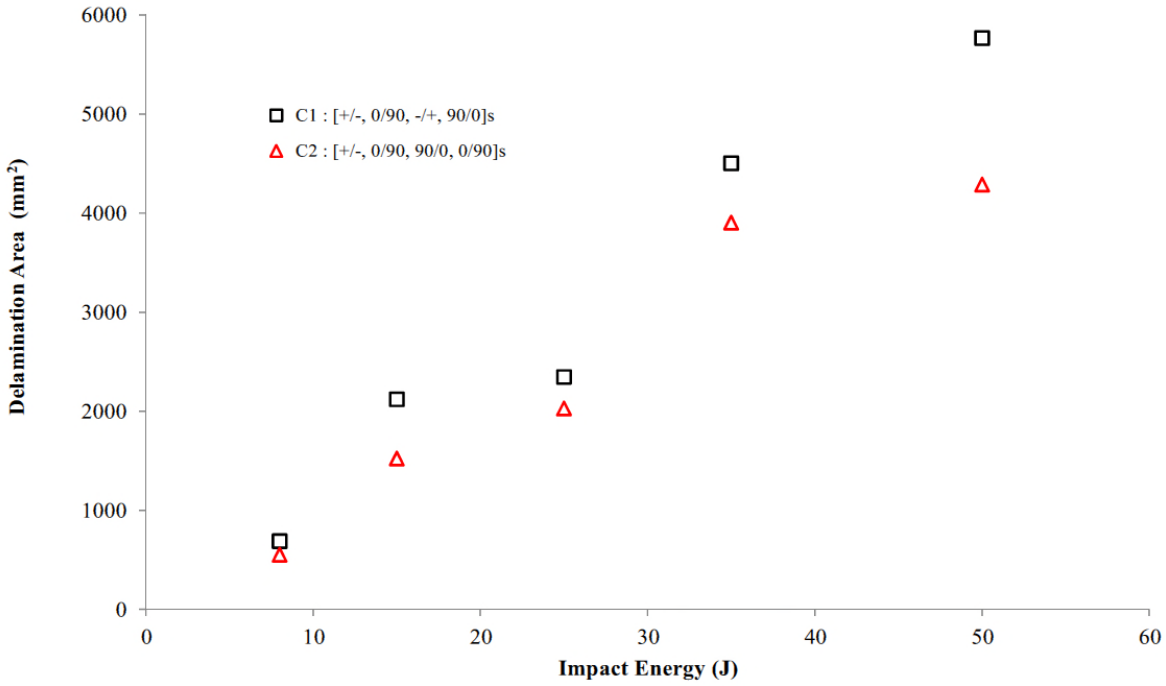

Figure 5.5: Delamination area vs. impact energy for all specimens

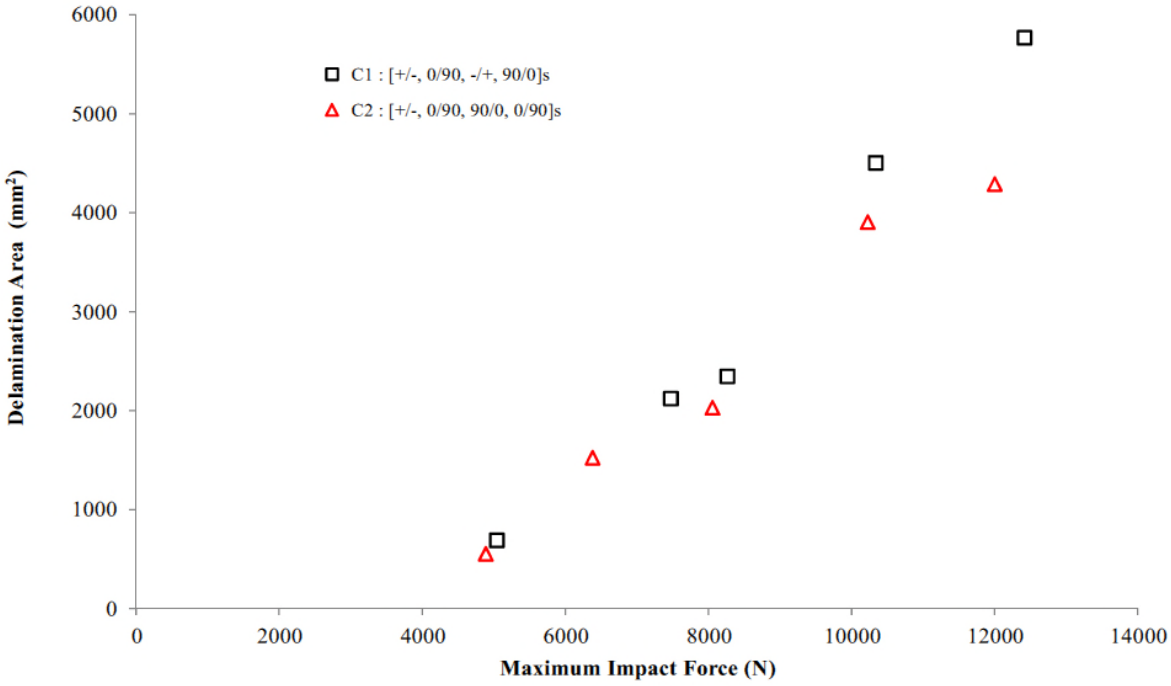

Figure 5.6: Delamination area vs. maximum impact force for all specimens

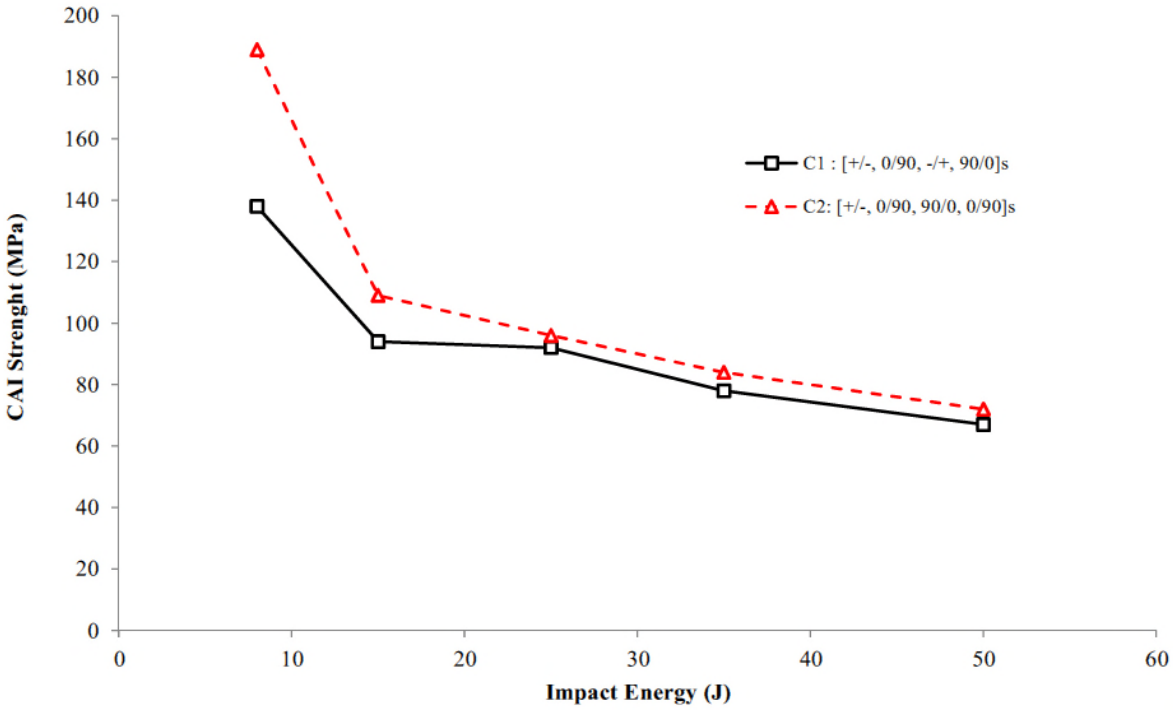

Figure 5.7: CAI strength vs. impact energy for two layup configurations

Microscopic observation

After the impact events, microscopic pictures were taken to inspect the cross-section of impact damaged specimens. Microscopic samples of 10 x 30 mm size were cut off around the impact zone and potted into resin pool of 35 mm diameter and allowed to be hardened and self-cured overnight. Polishing was performed initially by a manual grinder machine, and followed by an automatic grinder. Two of the most representative pictures are shown in Fig.5.8.

Microscopic images revealed that the failure mechanism for impact energy levels below 15 J is mainly due to the internal delamination and matrix cracking; an example of low impact energy is illustrated by in Fig.5.8.a) for the 8 J impact. When the impact energy was beyond 15 J, more damage modes were observed which confirms the transition region captured in Fig.5.4.a), at least for configuration C2. An example the highest impact energy of 50 J is shown in Fig.5.8.b) showing delamination, matrix cracking, and also significant portion of fibre breakage.

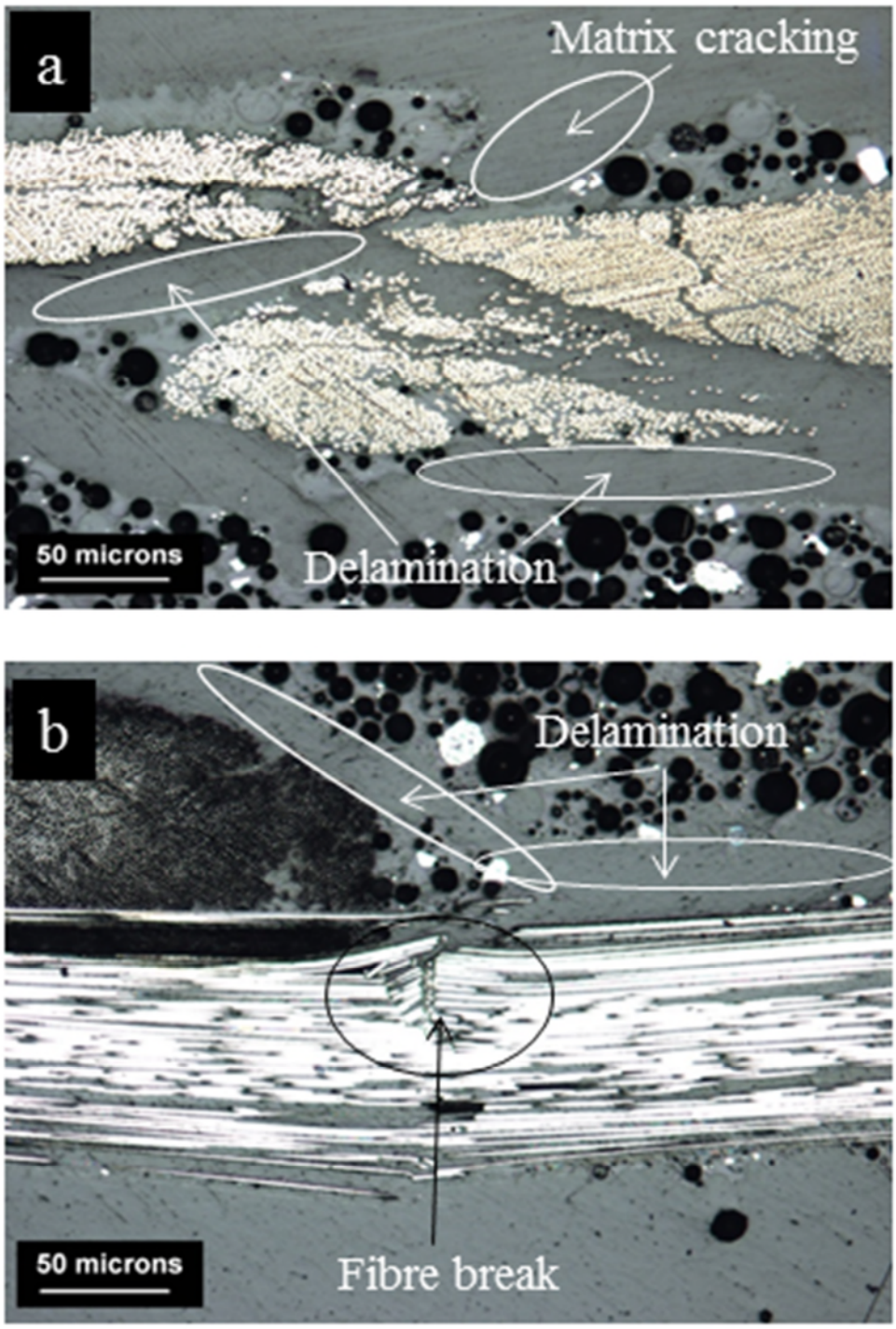

Figure 5.8: Microscopic photo of the C1 specimen: a) 8J impact is mainly delamination and matrix cracking. Damage location shown is near the specimen mid thickness. b) 50J impact revealing multiple damage modes of delamination, matrix cracking, and fibre fracture. Location shown is near the back face of the specimen. Note: grey background is the potting resin

5.2.6 Compression-after-impact

Figure 5.7 shows the CAI strength vs. impact energy for the two lay-up configurations. For impacts below 15Jthe C1 configuration had lower CAI strength because it had suffered larger impact damage (Fig.5.5). However, beyond the 20-25J mark, the CAI strength values of the two configurations were virtually the same despite the C1 specimens having had much larger impact damage area at higher impact energies of 35J and 50J (Fig.5.5). This sign indicated the change of damage/failure mode under the compressive load for higher impact energy discussed in the previous section in the light of microscopic inspections. The strength of the C2 configuration was expected to be greater along the 0/90 plys since more fibres are aligned along these directions. Performing a rough 10% rule Hart-Smith strength estimation, C2 configuration could potentially exhibit 1.33 times higher strength than configuration C1 under tensile loading. Therefore effect on the decrease in the CAI strength if assumed normalized to the actual un-notched laminate strength is more severe for the C2 configuration.
The impactor head punctured barely visible impact type of damage (BVID) on the laminates at energy levels of 8 and 15 J. Above15 J, the damage was fairly visible (VID).

Figure 5.9 shows the cross sections of failed specimens after CAI covering the full range of impact energies. Following observations were made:

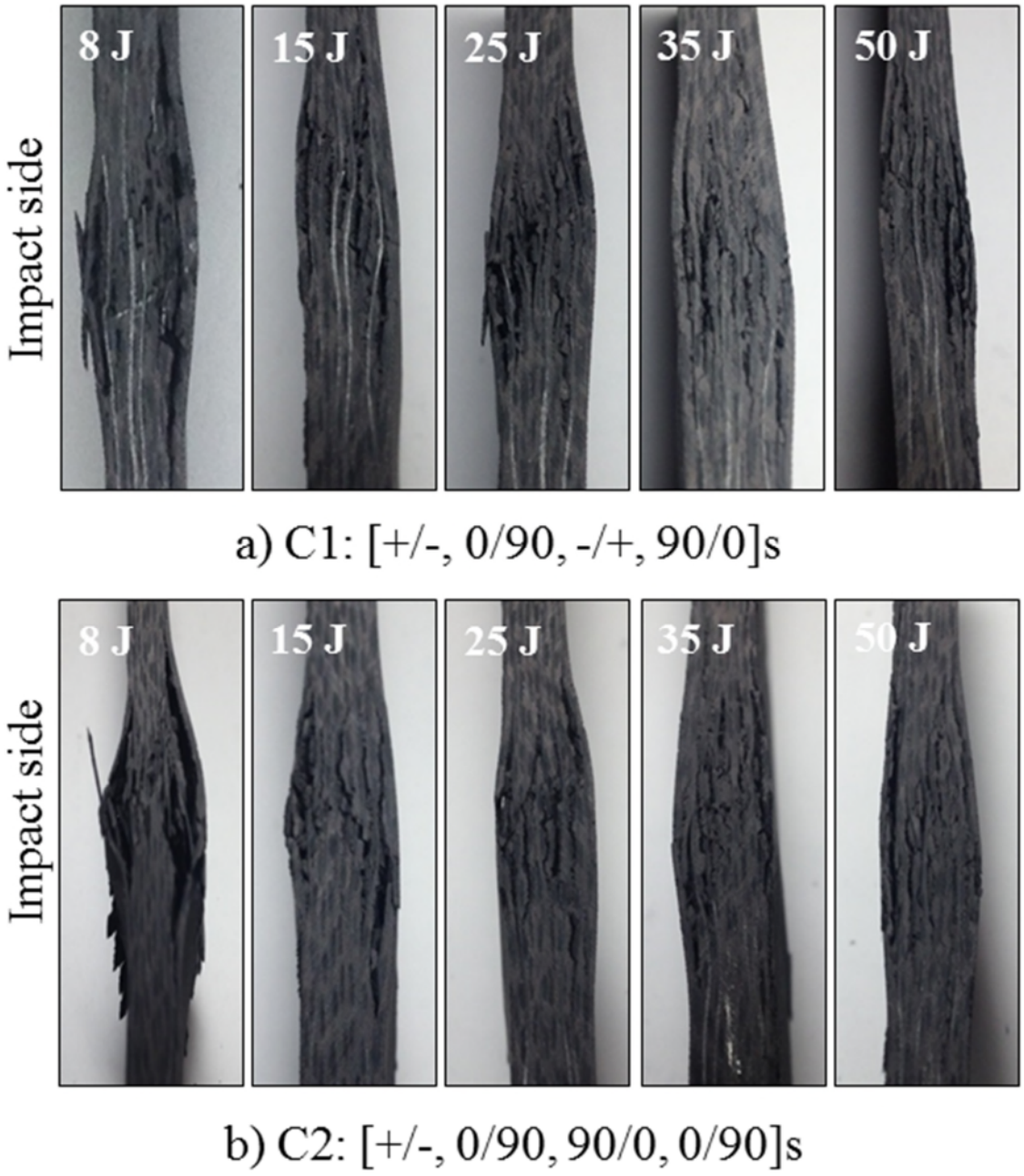

Figure 5.9: Photos of failed specimens after the CAI tests at various impact energy levels. “Pine tree” shaped fracture pattern clearly visible

Since the 8J impact caused the smallest damage area, specimens (both C1 and C2) failed at much higher compressive load in the CAI test comparing to the ones impacted at higher energy levels. The photos of the 8J impact specimens depicted a

clear outer ply mode I delamination and fibre crushing in the main core of the specimen due to the high compressive load.

Configuration C2 exhibited the outer layer delamination at all impact energy levels, which indicated the weaker interface in terms of mode I fracture toughness for the inter-laminar region of adjacent plys having a 45^{o}shift in the orientation

When the impact energy was greater than 8 J, fractured patterns in terms of cracked matrix under shear and broken fibres in a “pine tree” pattern were formed underneath the impactor head. These locations marked the CAI test failure initiation points.

Overall, The laminate CAI strength measured is smaller than most of the commonly used fibre CFRP materials employed currently in the airframe industry [38], where a rather general and rough estimate for impacted laminates with Visible Impact Damage (VID) can average from 200 to 250 MPa in terms of CAI strength levels.

5.2.7 Design decision

The outcome of the study indicates that C1 configuration was preferred over configuration C2. In general the two layups performed similarly at least above a certain impact energy level. Although the damage imprint was larger for C1, the ratio of the decrease in the residual CAI strength to the original un-notched strength was better. Also the quasi-isotropic arrangement can carry variable direction in-plane loading more efficiently. The reasons for the minor difference in impact and CAI response can be attributed partly to fracture toughness properties and partly to the residual thermal stresses arising from the mismatch of the Coefficient of Thermal Expansion (CTE).The more directional configuration C2 had lower curing induced residual stress in the matrix due to less mismatch of the CTE. The C1 quasi isotropic configuration had more inter-laminar regions interfacing +45/-45 to 0/90 layers. On the other hand, for the inter-laminar regions interfacing layers of the same orientation, fibre tows from one layer sit among the bundles of the adjacent layer, effect which greatly enhances the resistance in shear thus affects the mode II fracture toughness.

5.3 Summary and key points of chapter five

- In this section, the third item of our study published was presented shown also in [40]. The study investigated the application of a novel material with fire retardant properties and the effect of its impact and CAI strength properties on the design.
- A new material system has been assessed on its resistance to low velocity impact and in terms of residual strength in post-impact compression. Based on the impact damage size and CAI strength, the test results indicated a design application window for the woven material system for the two selected layup configurations. Two different layup configurations of a woven carbon fibre composite with a fire retardant epoxy matrix were impacted at five energy levels. Impact damage size was measured by ultrasonic C-scan and the subsequent CAI strength was measured by compression load test until specimen failure.
- The material system was more complex in microstructure as opposed to a unidirectional one, taking into account the pigmented epoxy matrix and the woven interlaminar surface architecture. Nevertheless, by the use of the manipulated force-displacement diagrams along with the critical load formula originally conceived for the unidirectional materials, a plausible quantification of “equivalent bulk Mode II fracture toughness” can be assumed.
- The results obtained indicate the usage limitations for this material system, specifically for the two layup configurations tested. The material may be used in certain applications where a major driver for materials selection for the structural location under consideration would be exposure to flame.
- Relating the CAI strength measured by testing to the most commonly used materials in the airframe industry [38], the CFRP material system presented herein would ideally be best utilized in non-critical, non-primarily loaded structural components, whose probable failure during service will not result in the loss of the aircraft.

5.4 References in chapter five

[1] Niu M C Y. Composite Airframe Structures. Hong Kong Conmilit Press Ltd 1995

[2] Reddy J N. Mechanics of Laminated Composites Plates and Shells. Theory and Analysis 2e. London, CRC Press LLC 2004

[3] Cytec Industrial Materials 2012. VTS243FR, Derby: Cytec.

[4] Cytec Industrial Materials 2012. BPS240 Format 1, Derby: Cytec.

[5] EASA. Certification specifications and acceptable means of compliance for large aeroplanes CS-25. Amend 15

[6] Kim JK, Sham ML. Impact and delamination failure of woven-fabric composites. Compos Sci Technol 2000;60: 745-761

[7] Gerlach R et al. In plane and through the thickness properties failure modes, damage and delamination in 3D woven carbon fibre composites subjected to impact loading. Compos Sci Technol 2012; 72: 397-411

[8] LLorca J et al. X-ray micro-tomography analysis of the damage micro-mechanisms in 3D woven composites under low velocity impact. Composites Part A 2013; 45:49-60

[9] Olsson R. A review of impact experiments at FFA during 1986 to 1998.FAA TN 1999-08, 1999

[10] Davies GAO, Hitchings D, Zhou G. Impact damage and residual strengths of woven fabric glass/polyester laminates. Composites Part 1996;27A:1147-56

[11] Kim J-K, Leung LM, Lee SWR, Hirai Y. Impact performance of a woven fabric CFRP laminate. Polym Compos 1996;4:549-61

[12] Siow YP, Shim VPW. An experimental study of low velocity impact damage in woven fiber composites. J Compos Mater 1998;32:1178-2020

[13] Richardson MOW, Wishheart MJ. Review of low velocity impact properties of composite materials. Composites Part A 1996;27A:1123-31

[14] Cantwell WJ, Morton J. The impact resistance of composite materials - a review. Composites 1991; 22: 347-62.

[15] Abrate S. Impact on composite structures. Cambridge: Cambridge University Press; 1998.

[16] Hancox NL. An overview of the impact behaviour of fibre reinforced composites. In Reid SR, Zhou G, editors. Impact behaviour of fibre reinforced composite materials and structures. CRC Press, Woodhead Pub. Ltd.; 2000.

[17] Davies GAO, Olsson R. Impact on composite structures. Aeronaut J 2004; 108:561-563

[18] Davies GAO, Zhang X. Impact damage prediction in carbon composite structures. Int J Impact Engng 1995; 16: 149-170

[19] Schoeppner GA, Abrate S. Delamination threshold loads for low velocity impact on composite laminates. Composites Part A 2000;31:903-915

[20] Davies GAO, Hitchings D, Wang J. Prediction of threshold impact energy for onset of delamination in quasi-isotropic carbon epoxy composite laminates under low-velocity impact. Compos Sci Technol 2000;60:1-7

[21] Atas C., Sayman O. An overall view on impact response of woven fabric composite plates. Compos Struct 2007;82:336-345

[22] Irving P E, Cartie D D R. Effect of resin and fibre properties on impact an dcompression after impact performance of CFRP. Composites Part A 2002: 33; 483-493

[23] B. Vieille, V.M. Casado, C. Bouvet. About the impact behaviour of woven ply carbon fiber reinforced thermoplastic and thermosetting composites - a comparative study. Compos Struct 2013;10:9-21

[24] Kuwata M, Hogg P J. Interlaminar toughness of interleaved CFRP using non-woven veils: Part 1. Mode-I testing. Composites Part A 2011: 42; 1551-1559

[25] Kuwata M, Hogg P J. Interlaminar toughness of interleaved CFRP using non-woven veils: Part 1. Mode-II testing. Composites Part A 2011: 42; 1560-1570

[26] Zhang X, Hounsow L, Grassi M. Improvement of low-velocity impact and compression-after-impact performance by z-fibre pinning. Compos Sci Technol 2006; 66: 2785-2794

[27] ASTM D5528. Standard test method for Mode-I interlaminar fracture toughness of unidirectional fibre reinforced polymer matrix composites. American Society for Testing and Materials, 2007.

[28] ASTM D6671.Standard test method for mixed Mode-I Mode-II interlaminar fracture toughness of unidirectional fibre reinforced polymer matrix composites. American Society for Testing and Materials, 2007.

[29] Paris I, Minguet P J, O'Brien K T. Comparison of delamination characterization for IM7/8552 composite woven and tape laminates. Composite Materials: Testing and Design. ASTM 2003; 372-390

[30] Ogasawara T et al. Interlaminar fracture toughness of 5 harness satin woven fabric carbon fibre/epoxy composites. Adv Compos Mater 2012;45-56

[31] Wang Y, Zhao D. Characterization of interlaminar fracture behaviour of woven fabric reinforced polymeric composites. Composites 1995; 26:115-124

[32] Cytec Industrial Materials 2012. Autoclave Processing - Lay Up and Bagging Guidelines, Derby: Cytec.

[33] ASTM D7136. Standard test method for measuring the damage resistance of a fibre reinforced matrix composite to a drop-weight impact event. American Society for Testing and Materials, 2007

[34] ASTM D7137. Standard test method for compressive residual strength properties of damaged polymer matrix composite plates. American Society for Testing and Materials, 2007

[35] Naik N K et al. Impact and compression after impact characteristics of plain weave fabric composites: effect of plate thickness. Adv Compos Mater 2004; 12:261-280

[36] Fuoss E, Straznicky P, Poon C. Effects of stacking sequence on the impact resistance in composite laminates. Part 2: predication method. Compos Struct 1998; 41:177-186

[37] Aktas A, Aktas M, Turan F. The effect of stacking sequence on the impact and post impact behaviour of woven/knit fabric glass/epoxy hybrid composites. Compos Struct 2013; 103:119-135

[38] DOT/FAA/AR-10/6. Determining the fatigue life of composite aircraft structures using life and load enhancement factors, 2011

[39] G. Davies, P. Irving. Impact, post impact strength and post impact fatigue behaviour of polymer composites. Chapter in book: Polymer composites in the

aerospace industry. Edited by P.E. Irving and C. Soutis. Woodhead publishing 2015

[40] Ioannis K. Giannopoulos, Efstathios E. Theotokoglou, Xiang Zhang. Impact damage and CAI strength of a woven CFRP material with fire retardant properties. Composites Part B: 91 2016, 8-17

[41] EASA, European Aviation Safety Authority (2010). AMC 20-29: Acceptable Means of Compliance - Composite Aircraft Structure. EASA, Germany.

<*Page intentionally left blank* >

Chapter 6

"Micromechanics of fibre reinforced polymers"

In the following chapter, the topic of micro-mechanical analysis in the application field of fibre reinforced polymers mechanical response is introduced along with a limited exhibition of the role, the importance and the potential of these studies to the future airframe structural development.

Currently, the usage of fibre polymers in the airframe industry is showing increasing trends. The current airframe engineering marvels of the civil transport aircrafts, are using carbon/glass reinforced polymer materials that account for more than 50% of the total volume of the structure. Along with these increasing material usage trends, there is a constant increase in the virtual modelling and prototyping, meaning the usage of numerical methods for eliminating part of the costs in the design of the product life cycle. Examples in the numerical modelling implementation for structural strength prediction, has been shown in the previous chapters. Airworthiness requirements are strict in that regard by not allowing structural certification to take place purely based on numerical analyses. Nevertheless, the ability and knowledge, the know-how growth in terms of utilizing such methods from the design organizations is factored in the testing plans imposed by the authorities for structural compliance verification and the total number of testing articles can be greatly reduced. Various industrial key players are currently discussing and they are actually paving the way to the so called *Virtual Certification* approved methods, which could potentially lead to cheaper, more reliable and faster produced airframe products.

In the previous sections, the numerical performance and capabilities in the strength prediction using finite element software, was shown in the case of the compression of a stiffened panel, the results were discussed, correlated with other similar research in the field and the current limitation faced were exposed. It was shown that the trend in the airframe structural virtual testing has to come through the microstructural details of it

since compliance with the strength requirements has to be shown for a damaged component. The items that need to be addressed for proper numerical simulations are the damage mechanisms initiation and propagation at the micro scale of the fibrous polymer structures. Numerical models that contain material description at the micro level are confined to describe response at the level of a single or an array of fibres in the so called RVE models, the Representative Volumetric Element models. Full specimen or component numerical simulations are performed by using finite element RVE models were the microstructural behaviour of damage is explored and the materials' response is subsequently engulfed within larger elements. Current research resources are spent towards better numerical *micro-scale* modelling at the RVE level in order to better describe the strength of fibrous polymers by describing damage initiation and damage propagation events as well as towards the appropriate methods in *meso-scale* translation of the microscale events by engulfing the micro level response into a less computationally expensive numerical simulation.

The knowledge domain in the micromechanical analyses for fibrous polymers is vast and the author studies addressed only a small fraction of it related to static and dynamic moduli properties derivation. Research from other sources published form various authors is also exhibited and discussed in order to forecast future trends in the field and result to the final conclusions of the chapter.

6.1 Introduction to the Micromechanical analysis of Fibre Reinforced Polymers

Fibre Reinforced Polymer (FRP) composites are making use of the properties of their individual constituents to result in materials with enhanced properties. The scale that exposes the heterogeneity in the material has given rise to analyses set at the level where fibres and matrix can be assumed as different continuum materials. Micromechanical investigations can be represented at the smallest practical modelling scale, where fibres and matrix are modelled as separate material phases. The dimensions of the fibre embedded in polymer matrix systems practically is the controlling parameter that dictates the scale were mechanical properties and fracture events can be studied.

Practical applications for structural analysis of composite material structures are performed at a mesoscale level, where that the composite material is assumed in a continuum anisotropic material domain. In the aerospace sector, structures made of composite materials are mostly in the form of laminated layered shells. Mesoscale analysis is referencing the mechanical properties of the individual plies which have resulted from tests. Classical Lamination Theory (CLT) is the example of such a theory, subjected to some assumptions and aimed at deducting the thermo-mechanical response of a multidirectional laminate comprised from a set of individual layers were the properties of the material at the layer level are known.

Analyses at the micromechanical level are aimed at interrogating the material mechanical performance by modelling the composite constituents with their properties separately and not as a continuum. Some examples of analysis of the sort can be the derivation of the elastic properties based on different constituent properties, of a different microstructural arrangement and the fracture sequencing event occurring at the micro scale.

As discussed in the previous chapters, amongst the many contributions, micromechanical analysis can help to better understand the damage initiation and propagation processes at the micro-structural level. Hence, it can be used for the validation of failure theories and for generating better approximations to the continuum damage fracture behaviour. The behaviour exhibited at the micro level can be then fed

through the larger CDM models at the mesoscale in order to derive a full scale structural response.

6.2 Aims of the chapter

The chapter is aimed at presenting the author's contribution in the field of micromechanical analysis. The contribution in the field is related mainly with the elastic moduli predictions under static and/or dynamic loading and the role of the interphase region between the fibres and the matrix. It is also aimed at presenting current advances in the field of micromechanical analysis and their relation to strength prediction, studies which are published in the public domain.

6.3 Investigations at the micromechanical level

The previous chapters of this thesis, prelude to the need of investigating the mechanical properties and response of fibrous composite materials at the microscale in order to further analyse the response at the meso and subsequently at the macro scale.

Analyses at the micromechanical level have been conceived early on in the design of fibrous reinforced polymer composite structures, stemming mainly from the property inhomogeneity between the two major material phases, being the fibre and the matrix. The simplest conceptual analyses can be regarded as the formulations relating the mechanical properties of the composite to the individual constituent's contribution depending on the volume fraction. For example, formulations relating the modulus of elasticity or the strength of the composite with the fibre volume ratio of the participating constituents can be regarded a form of micromechanical analysis. Many derivatives of such property formulation calculations exist in the literature, each one of them taking into consideration and proposing a novel set of parameters to be taken into account.

The next level of analyses which augments the complication in the problem formulation is sought with the solution of two dimensional displacement fields similar to the ones shown in figure 6.1. Making use of specially selected micromechanical model representation, symmetry in the model and the applied loading the displacement fields in the model could be solved even with analytical methods.

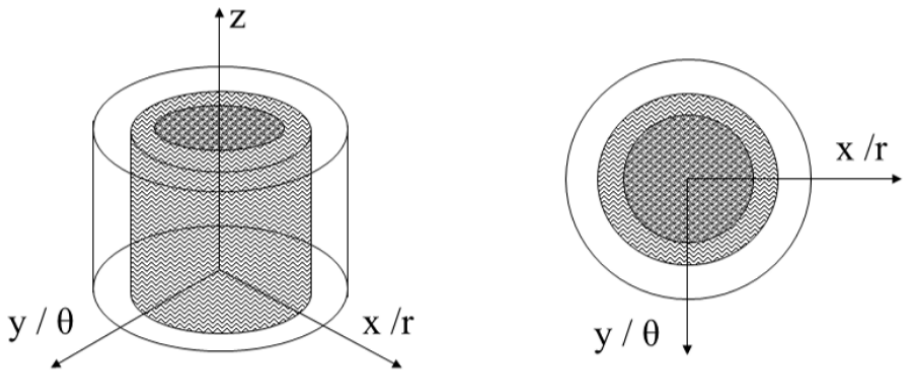

Figure 6.1: Representation of a composite material by assuming coaxial cylinders representing each material phase. Assuming a model structure of the sort along with axisymmetric loading and boundary conditions, the displacement field problem can be addressed by analytical methods as well

Analyses at the micromechanical level, are making use of continuum domains designed as such in order be representative of the structure and the properties of the material modelled and in order to help the analytical/computational solution scheme. In that regards, the so called *Representative Volumetric Elements, (RVEs)* have been have been conceptualized, where the material constituents are modelled in a proper way so that the response of the RVE at the microscale can be extrapolate to a structural response. The model shown in figure 6.1 is a RVE representing a fibre being the central cylindrical domain with two coaxial cylinders representing the interphase and the matrix. When the problem description increases in complexity, the solution of the displacement field in a micromechanical model can be solved only by numerical methods. Finite element analysis provides the means for solving complex displacement fields in strangely shaped domains assuming progressive damage as well. Some examples of RVE representations are shown in the figures below:

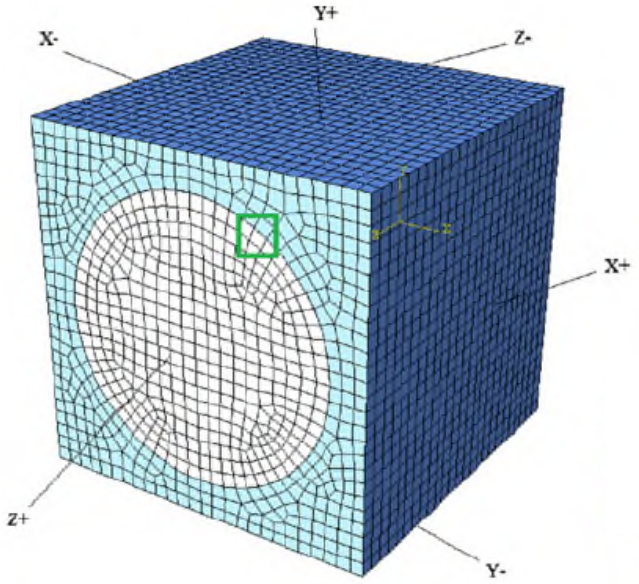

Figure 6.2: RVE representation for studying the elastic properties in composite under incomplete adherence with the matrix, according to the authors of [1]

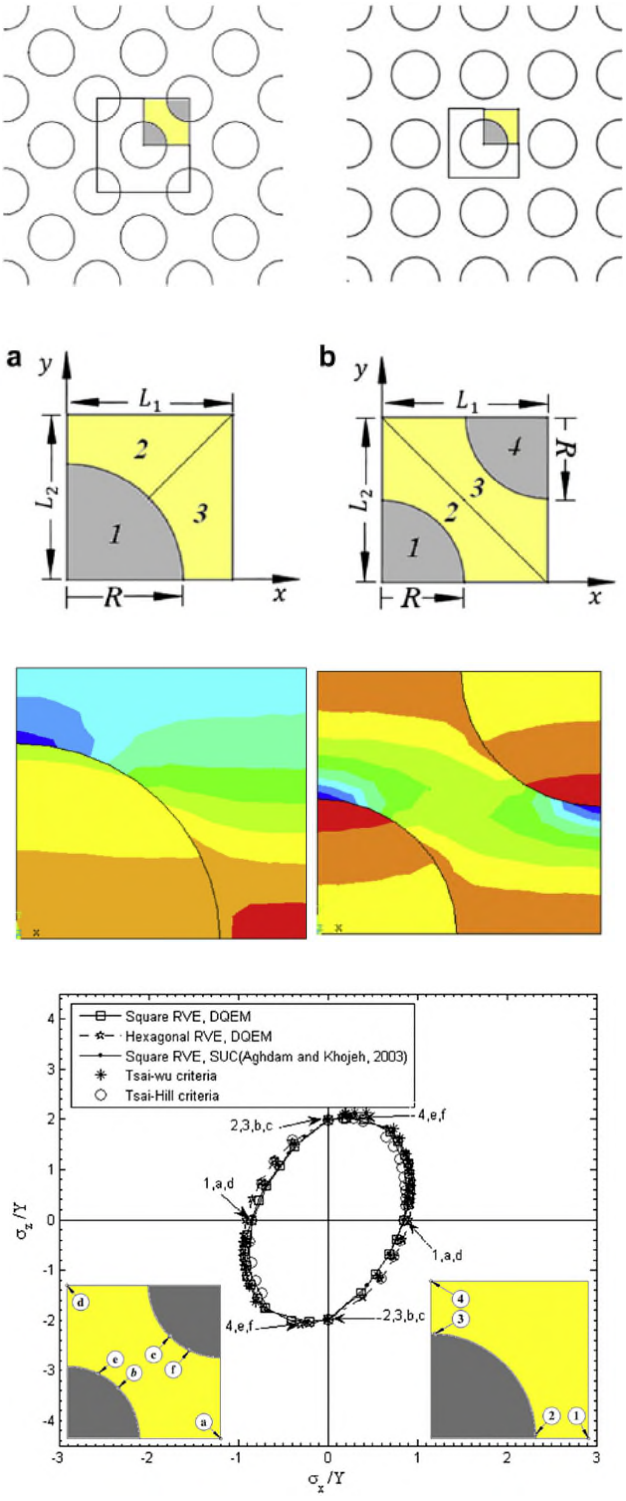

Figure 6.3: Hexagonal vs square assumed array of fibres in a composite, their RVE representations for studying stresses and provide with insight into the effect of the representation in the failure envelope, according to the authors of [2]

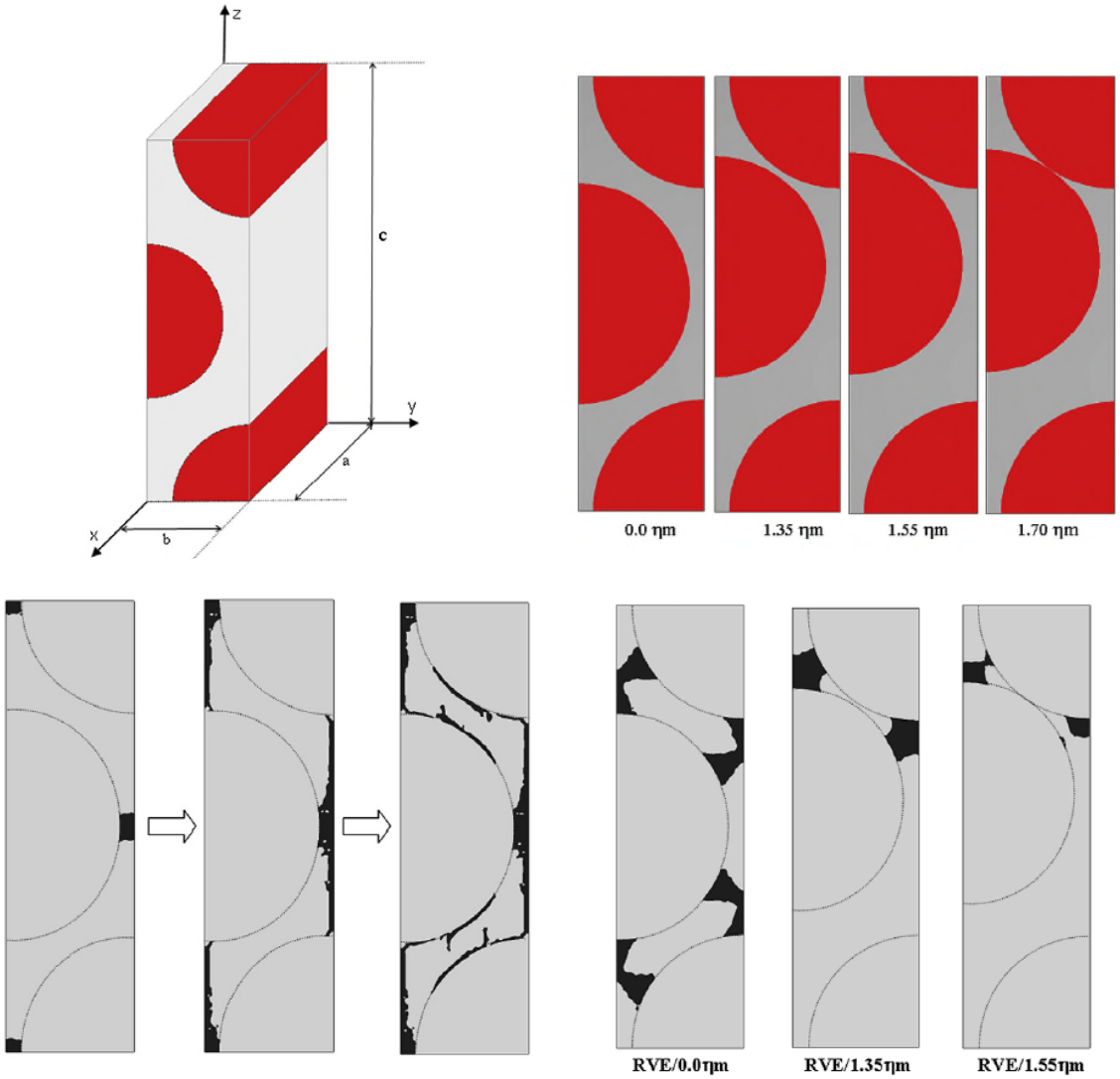

Figure 5.4: RVE representations for studying damage initiation and propagation depending on the proximity of the fibres according to the authors of [3]

In the following sections, the author's contribution to the micromechanical analysis knowledge domain will be presented which is related with the numerical derivation and the correlation with test and analytical results of the elastic properties of a fibrous reinforced polymer with the assumption of the interphase region existence in between the fibre and the matrix. There is also a numerical investigation presented regarding the dynamic response and the correlation with test and analytical results.

Finally, important proceedings from other authors in the field are presented and discussed.

6.4 The role of the interphase in the elastic properties in a fibre reinforced polymer: introduction and description of work

Found experimentally and being reported in the literature, a third material phase can be assumed in a fibrous reinforced polymer material between the fibre and the matrix. A simplistic representation of it is shown in figure 6.1. The role of the interphase is very important since it is where stress transfer between the two phases takes place. It has also been reported that depending on the interphase properties, providing a weak or a strong bond between the matrix and the fibres, different response is exhibited at the structural level. In the context of the thesis and published also as a journal [4] and conference articles [5], the effects of the interphase on the mechanical properties of the composite material was studied. Investigations were performed in micromechanical models as the one shown in figure 6.1.

The problem statement was that the elastic properties of the interphase could be modelled by the representative functions shown in figure 6.5:

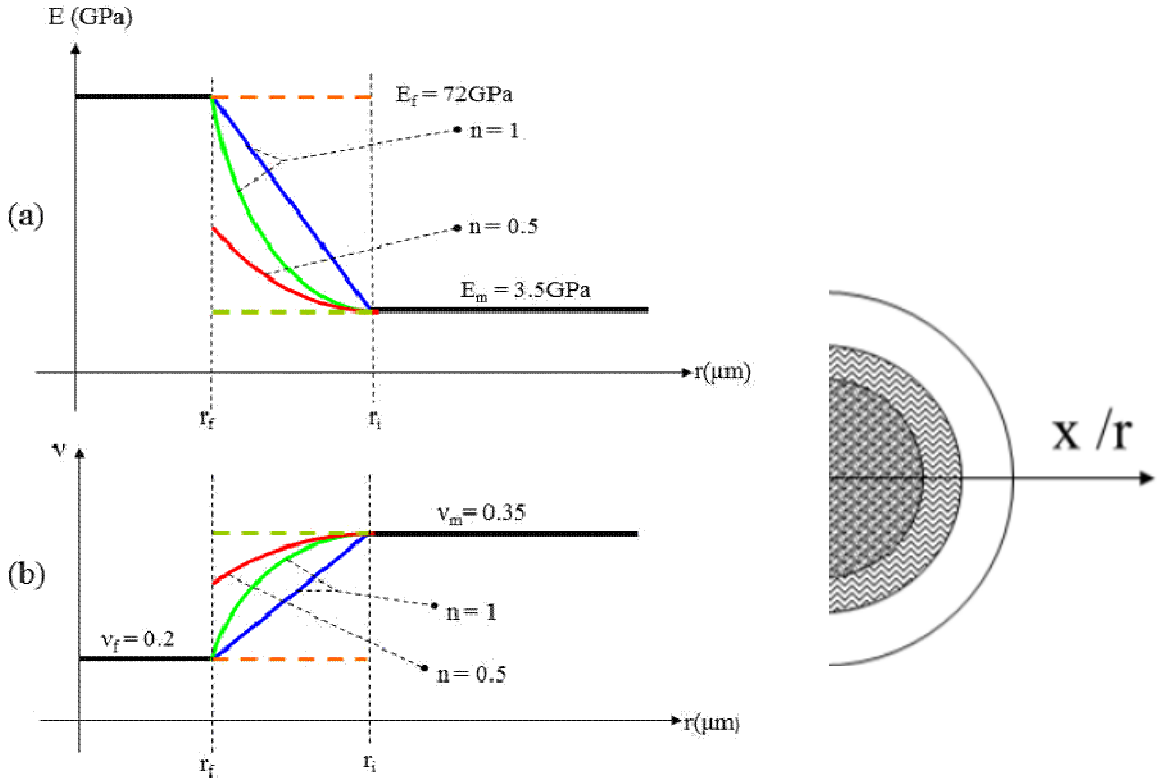

Figure 6.5: Modulus of elasticity and Poisson's ratio variation along the radius

In order to model the variation of the properties properly, a high fidelity region was designed in terms of element presented in figure 6.6. In figure 6.7, the variation of the interphase radius size is depicted for various fibre volume ratios.

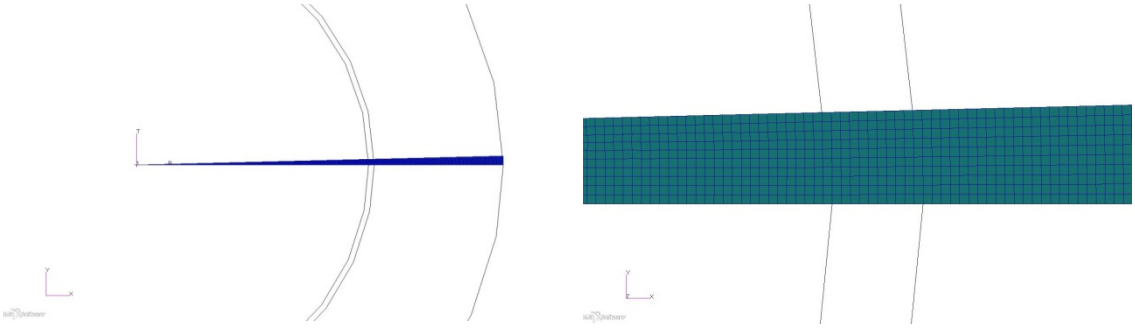

Figure 6.6: Modulus of elasticity and Poisson's ratio variation along the radius

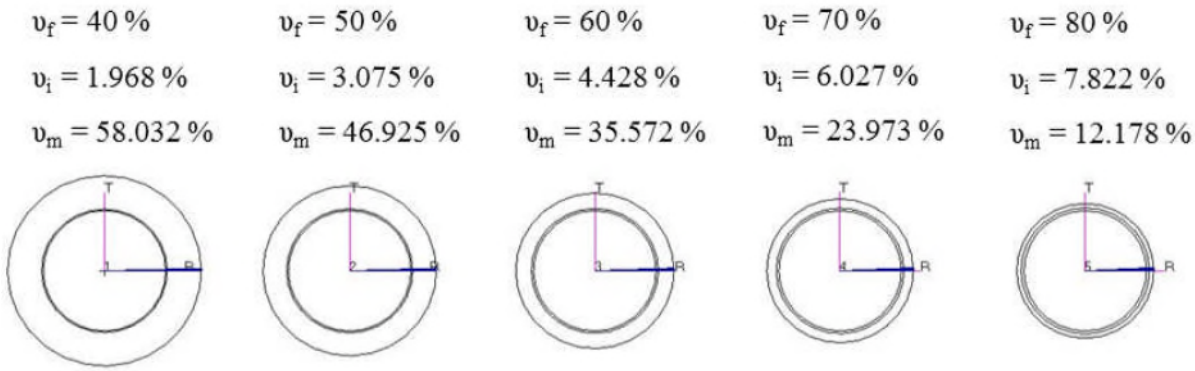

Figure 6.7: Modulus of elasticity and Poisson's ratio variation along the radius

6.4.1 The role of the interphase in the elastic properties in a fibre reinforced polymer: results from the study

The results of the study which were then correlated with analytical and experimental methods are shown in the figures 6.8 and 6.9. References shown on the figures are the ones in [4].

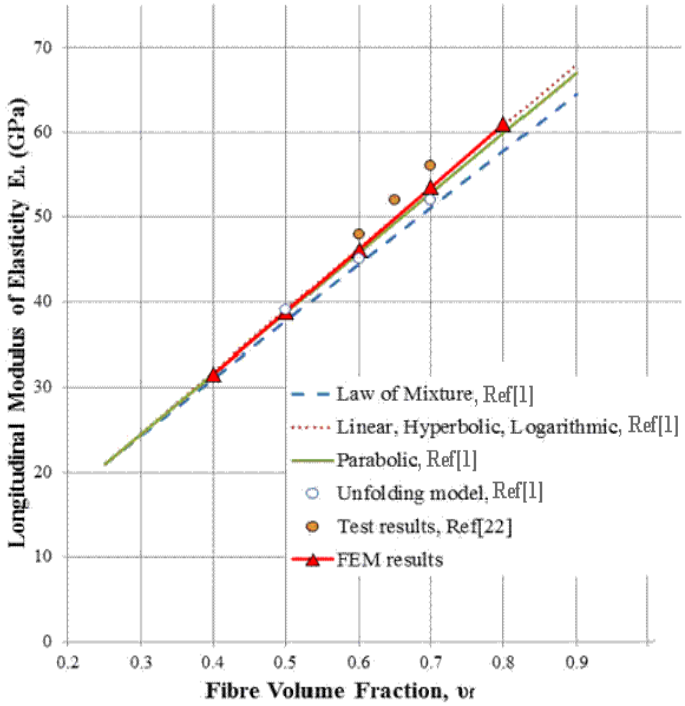

Figure 6.8: Longitudinal modulus of elasticity variation for different fibre volume ratios. References shown on the figures are the ones from the respective article [4]

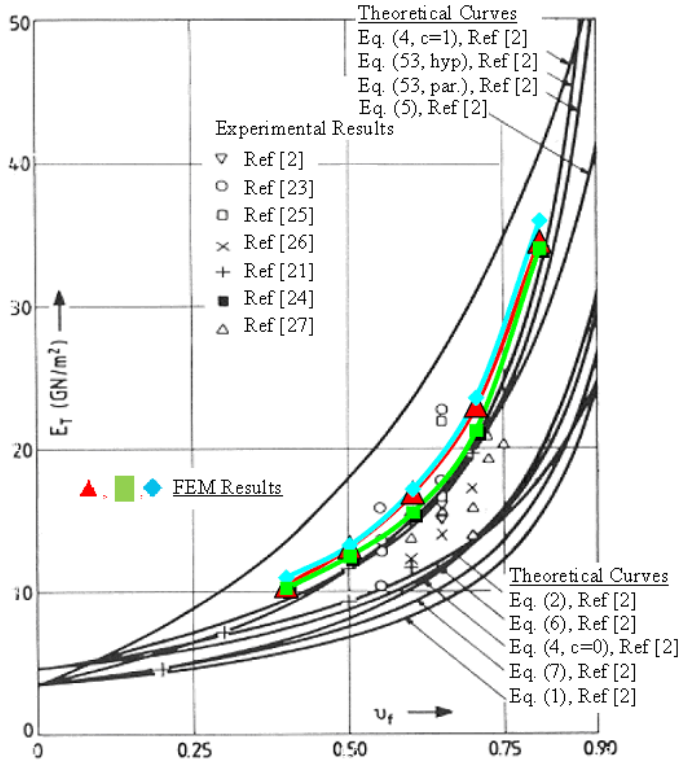

Figure 6.9: Transverse modulus of elasticity variation for different fibre volume ratios. References shown on the figures are the ones from the respective article [4]

The numerical study showed good correlation with the analytical and experimental results in the cases of the longitudinal elastic modulus. For the transverse elastic modulus, where there was a relatively large scatter in the results from various authors and in terms of analysis and testing, the numerical simulations sketched out the predicted values of the modulus. The effect of the property distribution along the interphase in the radial sense was deemed as insignificant parameter and that it will not affect the global results significantly in relation to the scatter provided in the results from the rest of the predictive methods and tools.

6.4.2 Research highlights in the field by others

As mentioned in the introductory part of the thesis, within the thesis and where is deemed necessary, contribution to knowledge from other researchers will be exhibited

in the form of a small but representative selection of research studies published in certain knowledge field. Following that introduction, it is worthwhile presenting an effort in the estimation of the mechanical properties of stochastically distributed computational domains, shown in ref [6]. In that article, the authors presented an algorithm for modelling the statistic nature of the fibres, which they imply is affecting the global properties by a considerable amount. The stochastic model generated, represents a transverse section of a unidirectional fibre polymer composite, shown in figure 6.10.

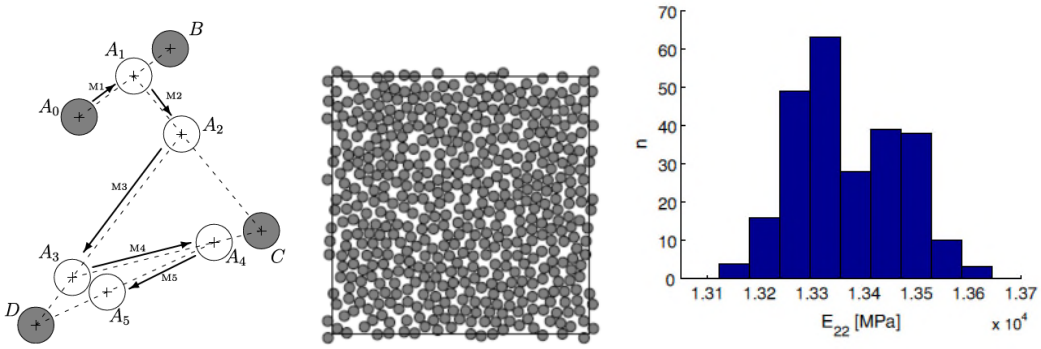

Figure 6.10: Algorithm of generating stochastic fibre distributions within a matrix for different fibre volume ratios. Size of the stochastic representation domain, large enough for capturing the behaviour. Distribution of the transverse modulus of elasticity for various stochastically generated models

6.5 Dynamic response of FRP in the transverse direction

The mechanical properties in the transverse direction attract the interest of the research community as shown in the previous sections. Transverse properties are matrix dominated. The microstructural representation of fibrous polymer sections, exhibits the complexity in the computational domain and prelude to the coupling of various elements and responses for deriving properties in that direction.

In the numerical study presented in this section, study which was presented in a conference and shown in ref [7], the dynamic response of micro-mechanically modelled unidirectional fibre reinforced composites was investigated. The aim was to use numerical analysis for providing with an insight to the material properties that would be used for initial assessment of the dynamic response of composite materials. Assumption to the investigation was the known dynamic response of the matrix material in terms of its tangent and loss moduli, which were evaluated through dynamic mechanical analysis testing and therefore treated as an input to our numerically simulated problem. Consequently, composite fibre materials made of glass fibre and epoxy matrix modelled with finite elements and tested in dynamic numerical solution sequences. The results of the analyses were the prediction of the tangent and loss moduli of the composite material. The results were correlated with analytical and experimental studies. The modal behaviour of the material was numerically investigated as well in an effort to describe the structural damping properties in terms of fibre volume content.

6.5.1 Storage and loss moduli of fibre reinforced epoxy composites

Dynamic Mechanical Analysis (DMA) is an experimental set of testing methods generally employed for extracting polymer material property information. Information like the material storage and loss modulus curves can be extracted by the use of these methods. DMA is more often conducted on specimens where load or displacement is applied at a constant frequency, while the testing temperature is varied. The opposite technique is also applicable, i.e. keeping the specimen temperature constant and varying the applied loading testing frequency. The storage and loss modulus curves of the material are used for the approximation of the polymer material Glass Transition Temperature (Tg) which is an important parameter for understanding the polymer material behaviour and its usage spectrum.

Structural applications employing polymer composite materials are in the need of high material stiffness, high damping and large utilization spectrum in terms of environmental temperature exposure. Unfortunately, polymer materials generally are not used beyond the temperature region of the Tg, so it is quite advantageous to use polymer matrices with high glass transition temperatures. Polymer materials with high Tg's, are generally very stiff with low fracture toughness and low structural damping. Thus material scientists are compromising some properties in order to achieve acceptable overall material response. Nanomaterials are employed in this sense in order to augment the original polymer matrix base mechanical behaviour. Another example of DMA testing is to test polymer matrix fibrous composites specimens in order to verify the application range of the composite material upon specific structural applications.

Micromechanical analysis can be assumed as an idealized material modelling practice. Application of it on fibre reinforced composites was found to be a useful tool for material property extrapolation to the macro-material scales. Using the modelling methods of micromechanics and the techniques of Dynamic Mechanical Analysis, the dynamic response of polymer materials or composite polymer materials can be approximated. The current study employed dynamic finite element analysis in order to extract a glass / epoxy fibrous composite dynamic material properties using as an assumption only the known dynamic response of the polymer matrix.

Another interesting characteristic that we set out to investigate was the effect of the variation in the storage and loss moduli due to temperature on a composite material due to the variation of these properties in the matrix. In the problem statement the response of the epoxy matrix was given and it is represented in figure 6.11.

A numerical study was performed and the results for it were correlated with analytical and experimental ones.

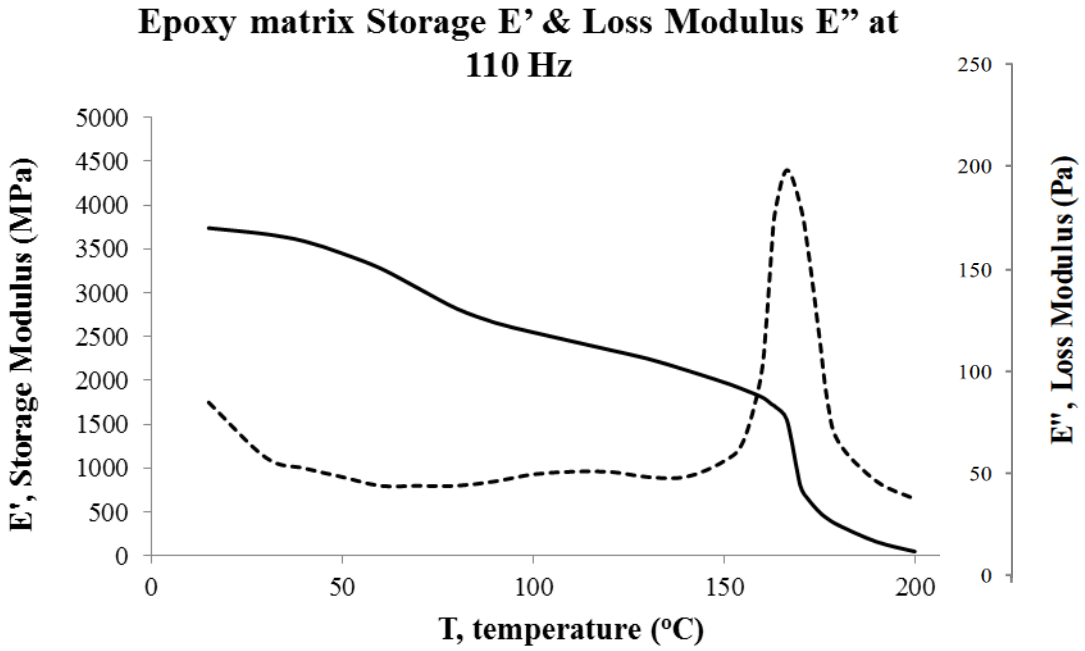

Figure 6.11: Storage and loss modulus for the epoxy matrix, measured at 100 Hz.

The numerical model use for conducting our investigation is shown in figure 6.12:

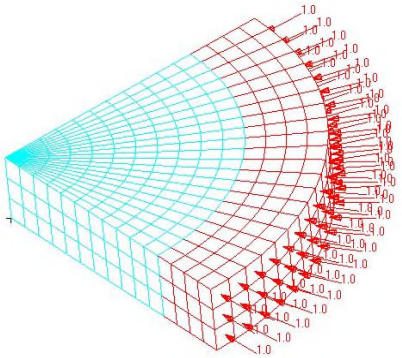

Figure 6.12: Numerical model representing the RVE of figure 5.1. Assumed loading in the transverse direction is shown and the frequency of load application was 110Hz. The epoxy matrix property variation was modelled according to figure 6.11

6.5.2 Storage and loss moduli of fibre reinforced epoxy composites: Short summary of results

The numerical results and their correlation with experimental ones and the analytical predictions are shown in figures 6.13 and 6.14:

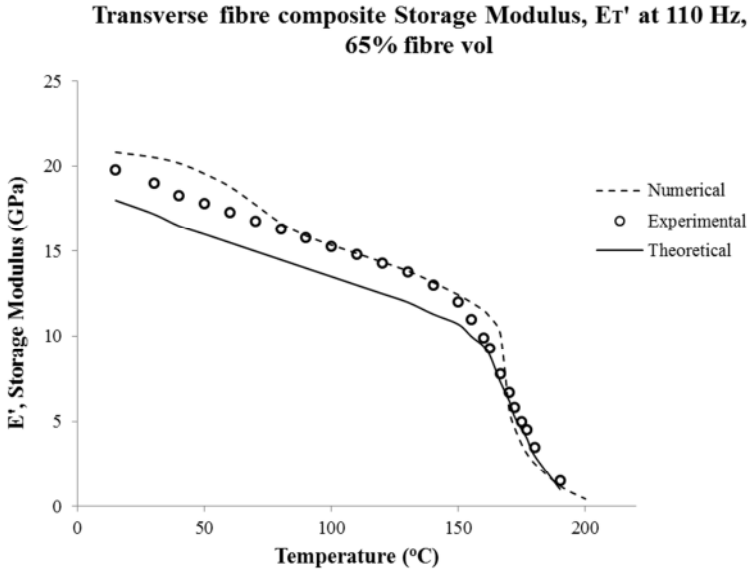

Figure 6.13: Correlated Storage Modulus curves

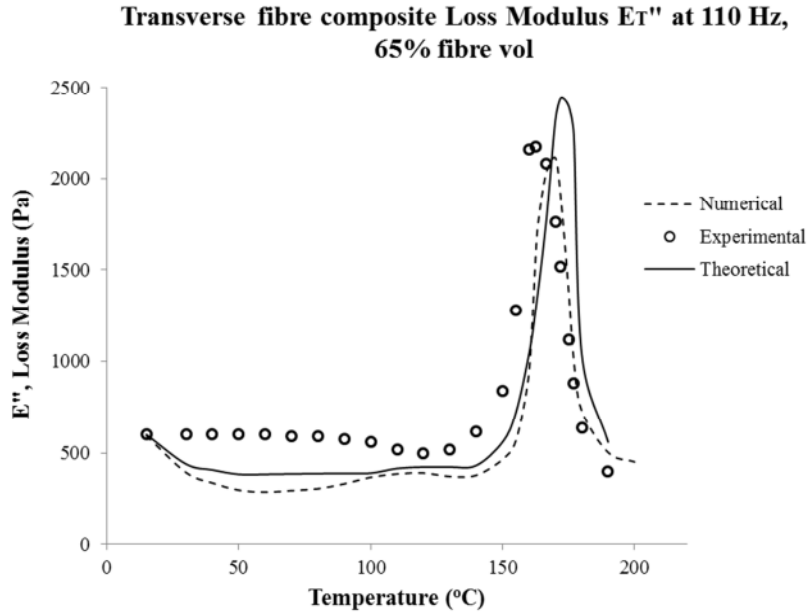

Figure 6.14: Correlated Loss Modulus curves

6.5.3 Storage and loss moduli of fibre reinforced epoxy composites: discussion and conclusions

Numerical analysis results from the temperature sweep DMA, showed that for higher fibre volume content, the composite material was proportionally stiffer. Similarly, the loss modulus of the composite material exhibits higher values. Those results were anticipated since the tanδ of the epoxy material, where δ represents the phase difference between load and the response is constant. The levels of the storage and loss moduli at various temperatures were approximated. Figures 6.13 and 6.14 show the correlation between the numerical results of the current study, to the experimental and analytic results of [8]. The differences between these results can be attributed to the approximation efficiency of the numerical model, to variations in values from the actual testing set up and to the approximating assumptions that led to the analytic study of the problem [8]. The difference in the peak value of the loss modulus in terms of actual loss modulus value as well as the temperature of occurrence indicates the dependence of the tested epoxy material properties to other factors and processes within the test that simple finite element procedure was not able to capture with great accuracy.

The additional effect of numerically modelling the interphase region as a separate domain in between the fibre and the matrix was investigated separately. It was hard to make any assumption for the domain size where the interphase region resides, since there was no information in the literature on the domain's variance according to temperature, especially in the vicinity of the glass transition temperature of the epoxy. As a rough approximation, the existence of an interphase domain to our two phase material, would give rise to a stiffer composite material, thus its response could be approximated and bounded by simulations of a slightly larger in fibre volume content composite.

Micromechanical modelling and numerical analysis could be used to generate rough approximations to the dynamic response of unidirectional fibrous composites, assuming that the dynamic response of the matrix and the fibre material are known. Fibre and matrix materials and properties could be mixed along with the assorted fibre volume ratios in the composite and their dynamic response to be calibrated accordingly. Such an investigation could potentially provide insights to the designing of suitable

materials specifically tailored to certain applications were specific dynamic response characteristics are expected. Numerical results that can be utilized for the designing purposes are the storage and loss moduli, their mapped variations with temperature as well as the material modal damping at various frequency levels.

6.6 Strength prediction in the micromechanical modelling scale

The following section of the thesis is aimed at presenting published research in the field of micromechanical analysis strength prediction of fibre reinforced polymer composites. According to the author's opinion, a short bur representative selection of articles presenting key concepts in the fields is presented and their findings discussed and correlated with the aim of the thesis.

Mentioned in chapter four, numerical modelling of damage at the micromechanical level, can potentially provide with a lot of insightful results that can be used subsequently in lower fidelity larger structural representation models.

6.6.1 The strength at the interphase between fibre and matrix

As a first step for assessing the strength of a fibre reinforced composite material, the strength of the fibres and the matrix alone have to be assessed. This task is a rather straightforward one to perform and there are standard testing methods available for the characterization of the strength of each phase in a composite material. It has been reported in the literature that a major contributor to the performance of the composite is the performance of the interphase. Understanding the fracture behaviour at the interphase is key for progressing to the next level of an array of 3D fibre modelling. The representative article to be used for making a case according to that phenomenon is shown in ref [9]. A study of the effect of surface treatment on the interfacial fracture toughness between a fibre and matrix was presented there. In the study it was explained that for the overall performance, is very critical to maintain both strong adhesion at fibre–matrix interface and high interfacial fracture toughness. In figure 6.15, a selection of pictures form [9] depicts the major concepts of the analysis.

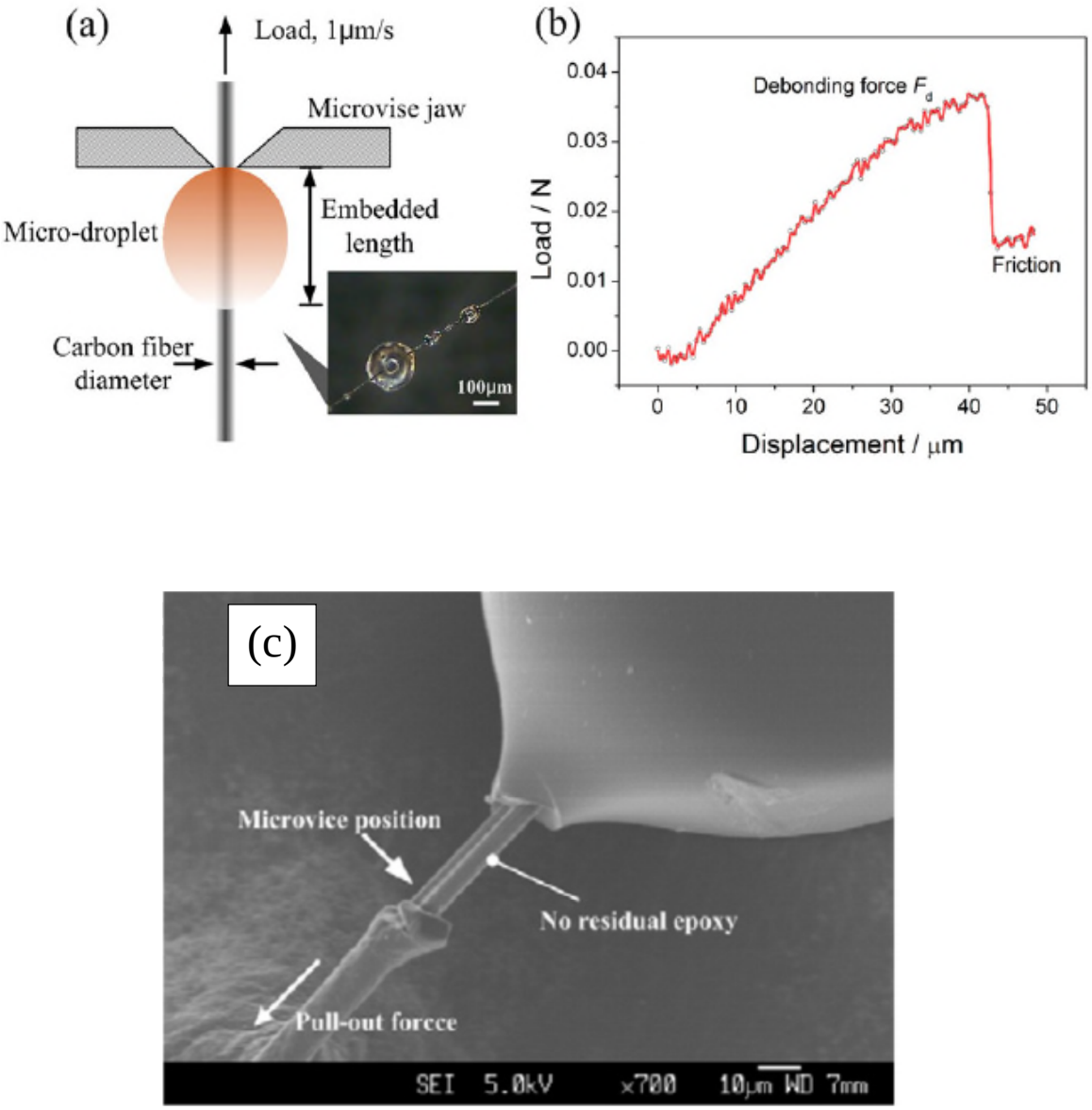

Figure 6.15: a) Micromechanical testing for deriving the bond force between a single fibre from its matrix, b) a graph showing the load vs displacement measured from the test and c) a micrographic representation of the process

Micromechanical testing at a single fibre level can provide with the description of the fracture process at the boundary between fibres and matrix. This test is representative of a fibre pull out event and more related to tensile failure along the fibre direction. The results of such a study can be used for extrapolating the behaviour of the interface at different at different loading modes.

6.6.2 Modelling fracture at the interphase between fibre and matrix

As a next step to the micromechanical testing investigation in the fracture parameters of the fibre matrix interface, numerical studies of single fibre models can provide with some further insights to the process. A representative work related is shown in reference [10] where the authors presented a study in the debond onset and propagation in mixed mode in the case of a single fibre subjected to a biaxial remote loading. The following figure 6.16 is representative of their study:

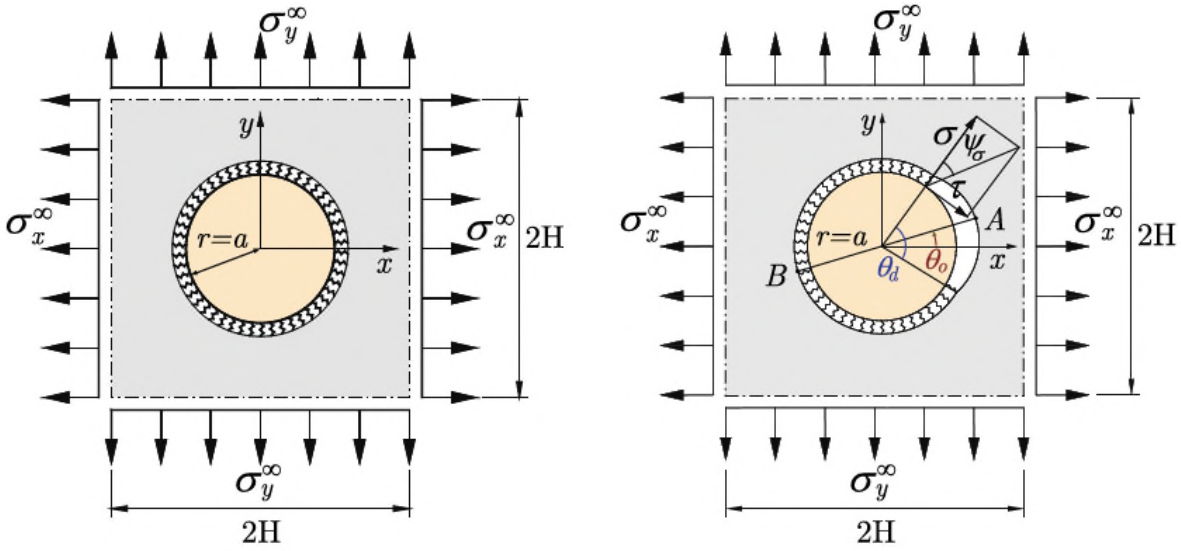

Figure 6.16: Example of micromechanical modelling and investigation in the fracture process at the interphase [10]

6.6.3 Modelling fracture in a statistically distributed array of fibres: Fracture toughness in the transverse direction

The authors of reference [11], presented a micromechanics damage model which examined the effect of fibre–matrix debonding and thermal residual stress on the transverse damage behaviour of a unidirectional carbon fibre reinforced epoxy composite. They investigated the weak versus strong fibre–matrix interface in the presence of thermal residual stress. The micromechanical model was subjected to multiple loading cycles and it was shown to provide novel insight into the microscopic damage accumulation that forms prior to ultimate failure, clearly highlighting the different roles that fibre–matrix debonding and matrix plasticity play in forming the macroscopic response of the composite. Such information is vital to the development of accurate continuum damage models, which often smear these effects using non-physical material parameters. Representative figures from their study are displayed in figures 6.17 and 6.18 below:

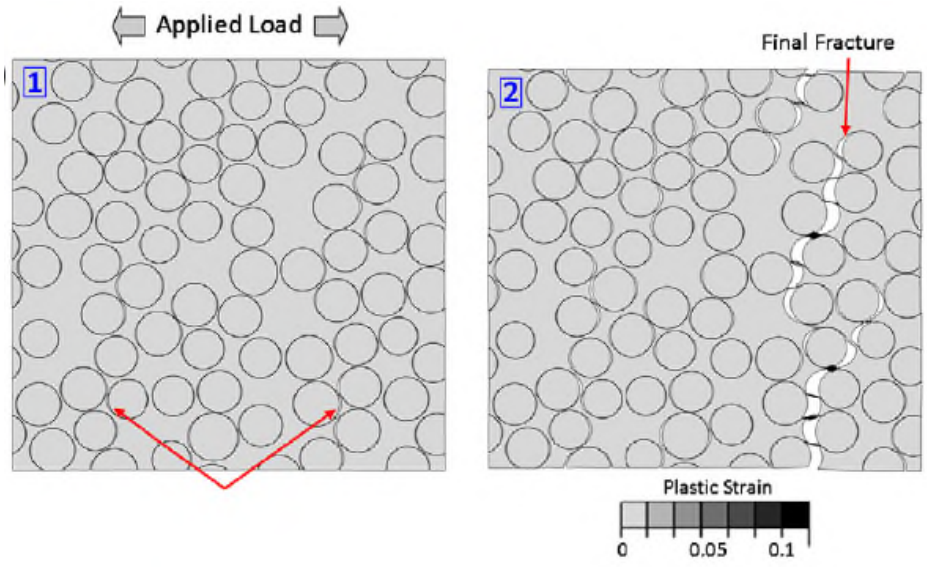

Figure 6.17: Example of micromechanical modelling and investigation in the fracture process using a statistically distributed fibre array RVE, matrix with plastic response and cohesive interface elements [11]

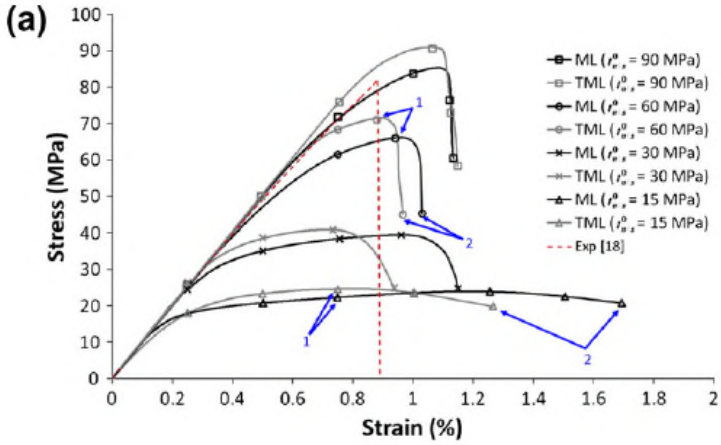

Figure 6.18: Example load displacement curves that could result from the micromechanical model shown in figure 5.17. The response can be fed through continuum damage modelling analysis at a mesoscale level [11]

A similar study was presented by the authors of reference [12], shown in figure 6.19:

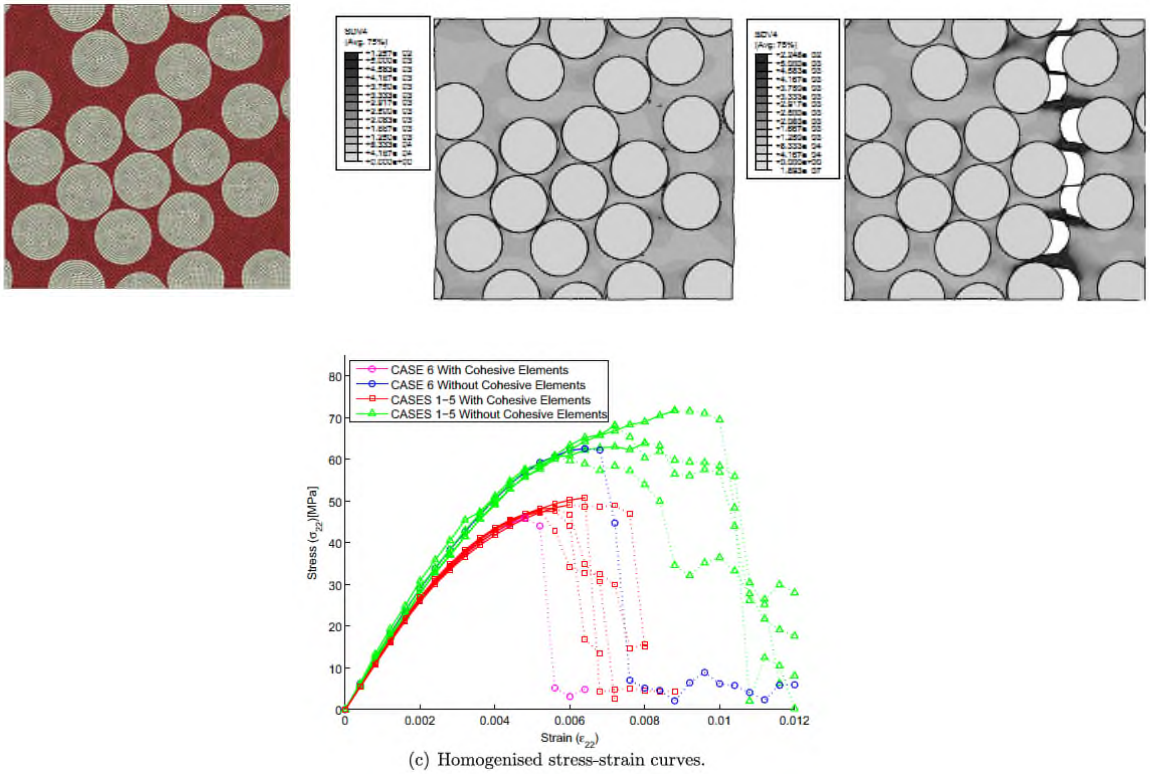

(c) Homogenised stress-strain curves.

Figure 6.19: Micromechanical model and fracture character in the transverse direction by the authors of [12]

6.6.4 Modelling fracture in a statistically distributed array of fibres: Failure envelopes

Other interesting applications of the statistically distributed fibre RVEs, in the case that damage initiation and progression is numerically modelled are the investigations in the failure surfaces of composite materials. Figure 6.20, depicts the failure surface drawn from numerical FEA studies [13]. Currently of the sort are only 2D, hence investigations are confined to 2D failure theories.

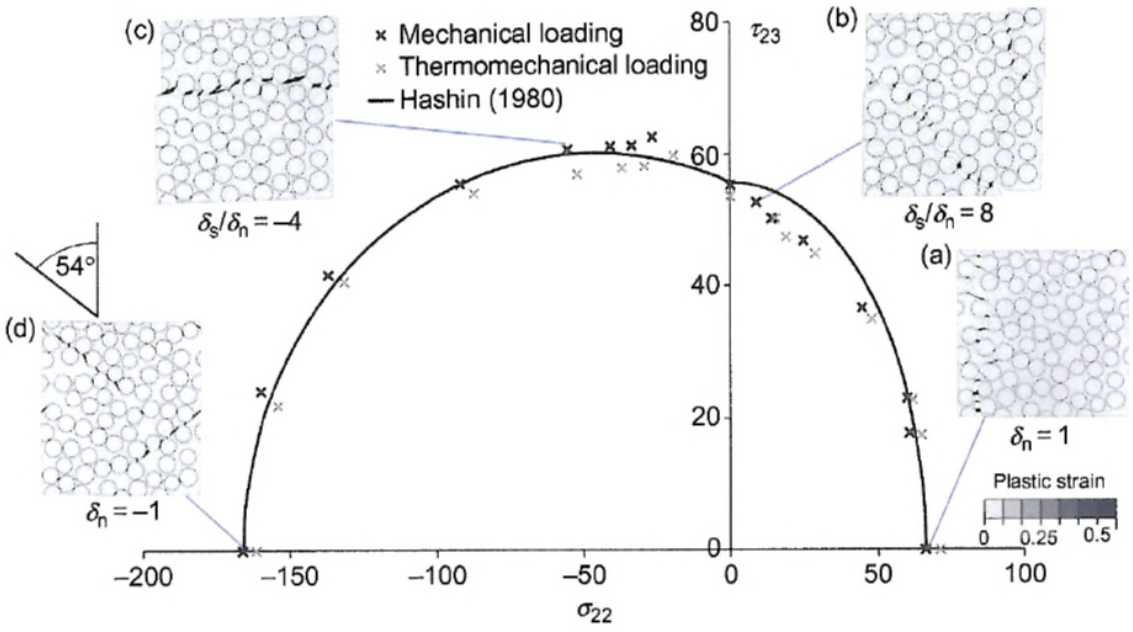

Figure 6.20: Failure surface investigations from fracture processes simulated in a 2D numerical micromechanical model [13]

6.6.5 Fracture toughness along the fibre direction

An interesting experimental study in the derivation of fracture toughness values along the fibre direction of a fibre reinforced polymer was presented by the authors of [14].

In that article, *the fracture toughness associated with fibre tensile failure and compressive fibre kinking in a T300/913 carbon-epoxy laminated composite are measured using compact tension and 'compact compression' tests respectively. The specimen strain fields were monitored using a digital speckle photogrammetry system during the tests. The damage present in the specimens after the tests was investigated using C-scan and optical and scanning electron microscopy.* Figures 6.21, 6.22, 6.23 and 6.24 below, are depicting the process and the assorted results:

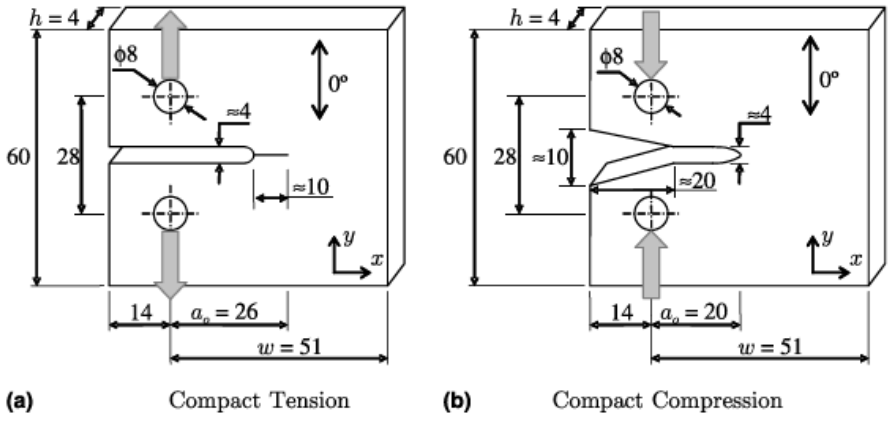

Figure 6.21: CT and CC specimens for the experimental derivation of fracture properties along the fibre direction [14]

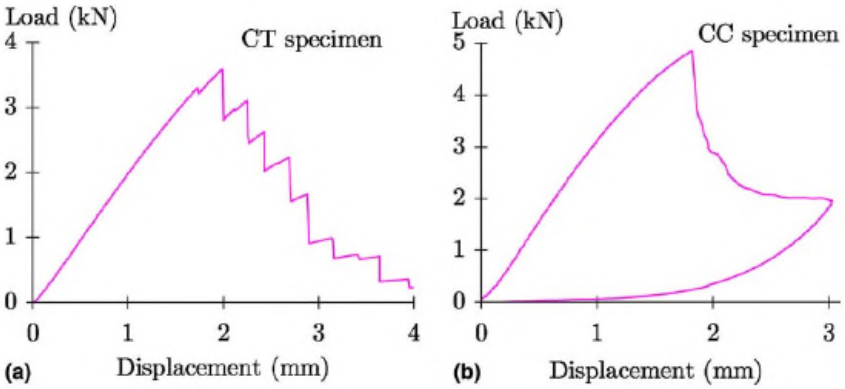

Fig. 5. Typical load vs. displacement curves for a (a) CT and (b) CC specimens.

Figure 6.22: Representative load displacement curves from the experimental derivation of fracture properties along the fibre direction [14]

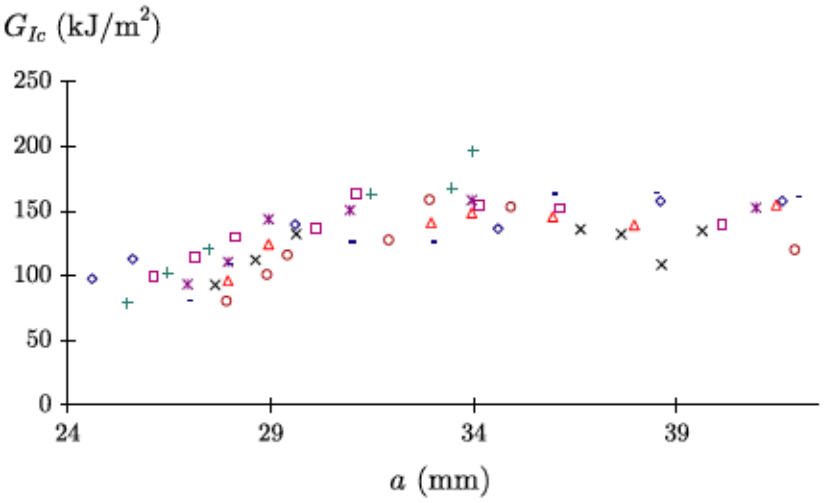

Figure 6.23: Fracture toughness values in tension from testing of various specimens [14]

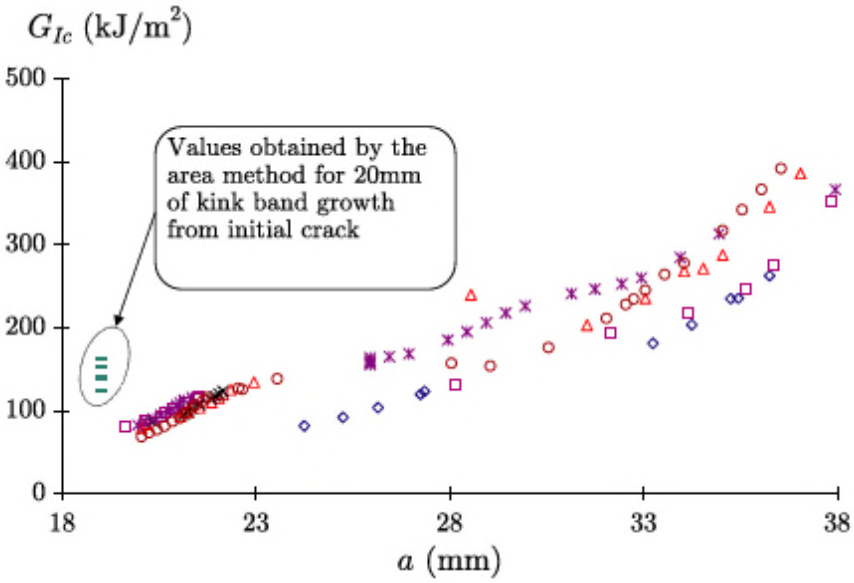

Figure 6.24: Fracture toughness values in compression from testing of various specimens [14]

Fracture toughness results similar to the ones measured in the article [14] can be utilized in CDM modelling but with the restriction mentioned in chapter six.

Reference [15], present an analytical prediction of fracture toughness in tension. Relevant numerical modelling and simulations in that area has not been presented in open literature as of today.

6.7 Summary and key point of chapter six

- Derivation of the elastic properties of a fibre reinforced polymer in the presence of an interphase was successfully implemented for static and dynamic behaviour.
- Computational resources needed to proceed with a numerical investigation of strength in the presence of the interphase are computationally prohibiting. Symmetry in the model cannot be utilized and the model has to be three dimensional. Investigation in the micromechanical strength proceeded with presenting the findings from other researchers in the field. In the demonstrated examples, the interphase is only modelled as a boundary and not as a domain with varying mechanical properties.
- Numerically predicting the failure strength of a composite material structure is a task requiring large computational resources. Numerical micromechanical modelling is a fast growing field of engineering which can effectively be used to bridge the gap between micro and mesoscale modelling, by feeding the results generated from the microscale to models generated in the meso scale. In real practise, there is large gap that needs to be bridged between the numerical analyses at the microscale with the numerical models whose results can be used for substantiating the strength requirements for certifications reasons.
- The micromechanical models are making use of huge computational resources as well. Even today, mostly 2D representations of fibre reinforced composites are present, employing fracture and damage behaviour. It is expected that in the near future, 3D models simulating the 3D tomography image shown on figure 6.25 will be analysed.

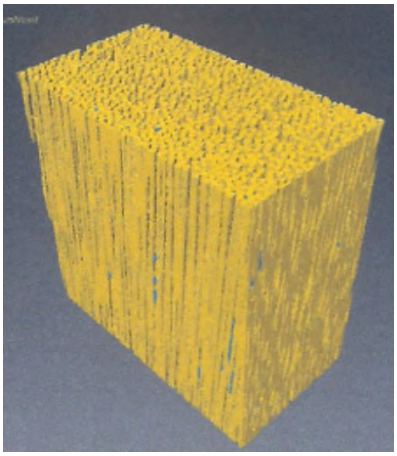

Figure 6.25: Tomography showing the complexity in a potential 3D numerical model with statistical distributed fibres and damage modelling [13]

- Deriving property values at the micro level, is a very tedious task. Special equipment is needed. Some of the answers posed from the engineering community, like the fracture toughness between a fibre and the matrix in modes I, II and III are still pending

6.8 References in chapter six

[1] Reinaldo Rodríguez-Ramosa et all. Different approaches for calculating the effective elastic properties in composite materials under imperfect contact adherence. Composite Structures 99 (2013), 264–275

[2] M. Bayat, M.M. Aghdam. A micromechanics-based analysis of effects of square and hexagonal fibre arraysin fibrous composites using DQEM. European Journal of Mechanics A/Solids 32 (2012) 32e40

[3] A.R. Maligno, N.A. Warrior, A.C. Long. Effects of inter-fibre spacing on damage evolution in unidirectional (UD) fibre-reinforced composites. European Journal of Mechanics A/Solids 28 (2009) 768–776

[4] E. Sideridis, E.E. Theotokoglou & I. Giannopoulos (2015): Analytical and computational study of the moduli of fiber-reinforced composites and comparison with experiments, Composite Interfaces,

[5] Efstathios E. Theotokoglou*, Emilio Sideridis, Ioannis.Giannopoulos. Analytical and computational solution of moduli and fracture offiber reinforced composites. 20th European Conference on Fracture (ECF20).Procedia Materials Science 3 (2014) 880 – 885

[6] A.R. Melro, P.P. Camanho, S.T. Pinho. Generation of random distribution of fibres in long-fibre reinforced composites. Composites Science and Technology 68 (2008) 2092–2102

[7] Efstathios E. Theotokoglou, Ioannis Giannopoulos, Emilio Sideridis. Analytical, experimental and numerical approach of storage and loss moduli of fibre reinforced epoxy composites. 20th International Conference on Composite Materials Copenhagen, 19-24th July 2015

[8] P.S. Theocharis, G. Spathis, E. Sideridis. Elastic and viscoelastic properties of fibre reinforced composite materials. Fibre Sci & Technol 1982; 17:169-181

[9] ChenWang, Xianbai Ji, Anish Roy, Vadim V. Silberschmidt, Zhong Chen. Shear strength and fracture toughness of carbon fibre/epoxy interface:effect of surface treatment

[10] M. Muñoz-Reja, L. Távara , V. Mantic, P. Cornetti. Crack onset and propagation at fibre–matrix elastic interfaces under biaxial loading using finite fracture mechanics. Composites: Part A(2015), article in press

[11] T.J. Vaughan, C.T. McCarthy. Micromechanical modelling of the transverse damage behaviour in fibre reinforced composites. Composites Science and Technology 71 (2011) 388–396

[12] A.R. Melro, P.P. Camanho, F.M. Andrade Pires, S.T. Pinho. Micromechanical analysis of polymer composites reinforced by unidirectional fibres: Part II – Micromechanical analyses. International Journal of Solids and Structures 50 (2013) 1906–1915

[13] C.T. McCarthy, T.J. Vaughan. Micromechanical failure analysis of advanced composite materials.Chapter in: Numerical modelling of failure in advanced composite materials, edited by P.P Camanho and S.R. Hallet. Woodhead publishing 2015

[14] S.T. Pinho, P. Robinson, L. Iannucci. Fracture toughness of the tensile and compressive fibre failure modesin laminated composites Composites Science and Technology 66 (2006) 2069–2079

[15] S. Pimenta. Fibre failure modelling. Chapter in Numerical modelling of failure in advanced composite materials, 2015, edited by P.P Camanho and S.R. Hallet

< Page intentionally left blank >

Chapter 7

"Summary of conclusions and future works"

Mentioned also in the introductory part of the thesis, extensive conclusions and summaries were presented within each chapter in great detail. Chapter seven is presenting a summary of conclusions at a higher level, concisely tailored for higher level decision making. Thus, the most important results of the study are presented herein in short, in relation to the main aims and objectives of the thesis regarding the static strength of fibrous polymer composite airframes:

- Compliance with Airworthiness certification requirements suggests large and expensive material and structural qualification programs in order to certify the strength in structures made of fibrous polymer composites. In order to diminish the costs associated with the coupon/component testing strength verification, experience in the application of numerical methods such as the FE method has to be further accumulated within the engineering community. Currently, airframe structures cannot be certified solely based on numerical or other types of analysis methodologies.

- Certification requirements will never get rid of the testing verification component embedded in the directives/legislation. Success in the field of numerical strength substantiation will be measured in terms of reducing the breadth in the testing requirements to the minimum acceptable level by the Airworthiness authorities. Experience accumulated in the field of numerical modelling and success stories of good correlation in the prediction results versus testing is the way forward.

- Approved analyses methodologies for strength substantiation that have been proven to produce acceptable using metallic material structures, have to be re-evaluated when analysing structures made of fibrous polymer composite materials.

- Finite element analyses are successfully employed in parametric design studies and can be used in order to generate general structural response trends. They are also used in analyses that show appropriate levels of results correlation with testing. The cost of the testing program required to prove the compliance with the airworthiness specifications could much reduced with the advancement and in-depth understanding in the numerical modelling of damage and damage progression in composite airframes. To date, progressive failure analysis models for large subassemblies is not possible. Simulations at coupon level have a high computational cost and are not deemed reliable enough for ascertaining strength substantiation. Modelling composite structures with initial imperfections, damage initiation and damage propagation successfully with good level of correlation with testing results is the way forward.

- Composite airframe structures unavoidably are going to be impacted by foreign objects within their lifecycle. Foreign object impact damage is one of the major threats to composite structures. Small scale damage modelling and damage progression has been successfully implemented and the results show good correlation levels. There is still more work that needs to be done for proper numerical simulation of the damage events from impact in terms of defect inherited on the structure and in terms of residual strength. Currently, industry relies on test results for certifying structural response to foreign object impact events and damage.

- Micromechanical analyses have shown great potential to analysing the fracture process in the microscale, necessary result for mesoscale modelling. Micro mechanical analyses are in the need of specialized input like fracture values at the fibre/matrix interface scale, matrix plastic behaviour etc., which a rather tedious task to derive by testing. Generation of 3D models with statistical damage distribution and progressive failure capabilities is yet to be seen. The correlation of the micro

modelling simulation results with testing is an essential towards model verification but testing in micro scales poses a lot of challenges